The role of SOSTDC1 in interactions between myeloma and cells of osteoblast lineage

Thesis submitted for the Degree of Doctorate of Philosophy by

Zahra Fahimeh Faraahi

Department of Human Metabolism

Medical School

University of Sheffield

Submitted April 2014

Acknowledgment

"You think because you understand 'one' you must also understand 'two', because one and one make two. But you must also understand 'and'."

― Rumi

I wish to start this acknowledgment by declaring my gratitude to my supervisors Professor Peter Croucher and Dr Colby Eaton. I am grateful to you **Peter** for funding my PhD and giving me the opportunity to live my dream. I am particularly grateful to experience working with someone as passionate about research as you. **Colby**, I cannot tell you how blessed I feel to have had you as a mentor, supervisor and friend. Your kindness, humour, encouragement and unwavering belief in me can only be compared to a light at the end of a dark tunnel. I would also like to extend my gratitude to **Clive Buckle**, the students and staff of the Department of Human Metabolism for their invaluable input and support. I would particularly like to thank **Juhi** and **Anava** for their warm friendship and immense kindness. I will miss our midnight office pizza fests, 5pm coffee breaks and endless laughter.

I would like to dedicate this Thesis to my Pedar Ahmad and Maman Farzaneh. I aspire to be like you **Pedar** and to make you proud. You have set the bar so high in terms of being passionate and successful at what you love to do that even if I am halfway there, I am content. **Mamanam**, why does it always seem that nothing is possible without you? Thank you for always loving me and believing in me all my life. Most of all, thank you both for always telling me to aim for an A* so that I would at least achieve a B. I am grateful to you my sweet sisters **Sara** and **Mahya** for just being you and making me laugh even when I thought I couldn't.

And of course, I would like to acknowledge you my darling **Mohammad Danesh**. You are the very meaning of love and support. I have no words that could describe how grateful and proud I am to have had you stand by my side. I love that you say 'my success is your success'. I love that you are always calm when I am not. I love that your world revolves around me and my needs. I want to acknowledge that you spent what seems like a lifetime encouraging me to achieve my dreams even if it meant putting yours on hold. Asheghetam my wonderful man. Finally but foremost, thank you Lord, just because the possibilities are endless when I have you.

Declaration

The work presented in this thesis funded by the Leukaemia and Lymphoma Research (LLR), UK blood group charity. The work presented in this thesis was carried out by the candidate, with the following exceptions: 5T33MM and 5TGM1 cells were kindly provided by **Dr Claire Edwards** from the University of Oxford; Work with 5TMM series mice in the animal house was performed by **Dr Shelly Lawson** and **Dr Julia Hough**; Processing of tissue samples for immunohistochemistry was performed by the Bone Analysis Laboratory and facility at the Medical school; Flow cytometric cell sorting was carried out in the Flow cytometry core facility in the Medical School with the assistance of **Mrs Susan Newton** and **Mrs Kay Hopkinson**.

Summary

Multiple myeloma (MM) is characterised by destructive bone disease, mediated by an increase in osteoclastic bone resorption and impaired osteoblastic bone formation (Boise, Kaufman et al. 2014) The canonical Wingless-type (Wnt) and bone morphogenic protein (BMP) signalling pathways have both been implicated in the osteoblastogenesis (Chen, Deng et al. 2012, Kim, Liu et al. 2013). Data from our group in Sheffield (unpublished) show that SOSTDC1 is upregulated in the bone marrow (BM) of mice with osteolytic bone disease associated with myeloma. It is unclear whether SOSTDC1 regulates signalling in bone directly and which cells in the BM express SOSTDC1. We hypothesise that SOSTDC1 disrupts Wnt and BMP signalling in bone and is expressed by both myeloma cells (MC) and osteoblast (OB) progenitors as a result of direct MC/OB contact.

In the first part of the work presented in this thesis, I characterised the murine OB progenitor model *in-vitro* establishing that these cells differentiated exponentially between day 8 and 15 of culture. I then assessed the effect of SOSTDC1 in OB progenitor differentiation in the presence of activated BMP and Wnt signalling. I showed that Wnt3a, BMP2 and BMP7 stimulated OB progenitor differentiation and downstream signalling of the Wnt and BMP pathways. Recombinant human SOSTDC1 (rhSOSTDC1) protein reduced the Wnt and BMP-induced differentiation/signalling in OB progenitors on a protein and gene level. This effect was observed in early differentiation, indicating that the inhibitory effect of SOSTDC1 on Wnt/BMP-induced signalling is specific to osteoprogenitors rather than mature OB. I also showed rhSOSTDC1 had the highest affinity for BMP7 out of the BMP2, BMP7 and Wnt-receptor LRP-6, interactions tested.

In the second part, I assessed whether OB progenitors and 5TMM myeloma cells produced SOSTDC1 and sought to determine the distribution of SOSTDC1 in MC/OB progenitor cultures and co-cultures. SOSTDC1 was detected in MC but not OB progenitors and that SOSTDC1 was upregulated in both myeloma and OB progenitors following direct OB/MC contact in co-cultures. SOSTDC1 protein was also detected *in-vivo* in myeloma-infiltrated bone sections. Blocking SOSTDC1 *in-vitro* using an antibody specific to SOSTDC1 reversed the suppression of OB progenitor differentiation. Taken together from these results, I conclude that targeting SOSTDC1 may reduce the osteolytic bone disease observed in MM.

Table of Contents

List of Figures

Chapter 4

Chapter 5

Chapter 6

List of Tables

Chapter 1 - Introduction

1.1 Multiple Myeloma

Multiple Myeloma (MM) is a B-cell malignancy characterised by clonal proliferation of plasma cells (Egan, Shi et al. 2012). MM accounts for more than 10% of haematological cancers and accounts for approximately 1% of all cancer-related deaths in Western countries (Kyle and Rajkumar 2008). Myeloma is the 17th most common cancer in the UK (2011), accounting for around 1% of all new cases. In males, it is the 15th most common cancer (2% of the male total) and the 17th in females (1%). The latest statistics showed that in 201,4,792 new cases of myeloma were diagnosed in the UK. From this total 56% were men and 44% were women, resulting in a male:female ratio of 12:10 for the incidence of myeloma (Cancer Research UK 2014). In the United States, it is expected that by the end of 2104 over 24 000 new cases of MM will be diagnosed resulting in approximately half of these individuals to die (Siegel, Ma et al. 2014).

In most cases, MM develops from a Monoclonal Gammopathy of Undetermined Significance (MGUS), a premalignant stage of clonal plasma cell proliferation displaying no obvious symptoms. Over 3% of the over 50 population will carry MGUS and 1% will develop myeloma or other related malignancies. Smouldering Multiple Myeloma (SMM) is another type of this disorder found in some patients who present with clinically recognisable symptoms of MM accompanying a more advanced premalignant stage (Mahindra, Hideshima et al. 2010).

The acronym CRAB summarizes the typical clinical manifestations of MM: hypercalcemia, renal insufficiency, anaemia, and bone lesions (International Myeloma Working 2003). The CRAB features of MM can be used to distinguish between active, symptomatic MM and its precursor states MGUS and smouldering myeloma. The distinction is relevant not only for classification and diagnosis, but also for therapy: CRAB symptoms are critical for deciding when to initiate antineoplastic therapy, as asymptomatic cases of MM do not obtain survival benefit from treatment (Kyle and Rajkumar 2007). Beyond the usual CRAB symptoms, patients with MM can present with other relevant clinical manifestations including hyperviscosity syndrome, neurologic impairment from spinal cord compression, nephrotic syndrome or other signs of amyloidosis, cryoglobulinemia, recurrent infections, extramedullary involvement of various organs, and other complications. MM patients can be diagnosed only by chance,

in asymptomatic patients, often when tested for annual examination by primary care physician (Talamo, Farooq et al. 2010)..

MM is the most common cancer to involve the skeleton with 80–90% of patients developing bone lesions during the course of the disease (Hameed, Brady et al. 2014). The bone lesions in myeloma are purely osteolytic and are associated with severe and debilitating bone pain, pathologic fractures, hypercalcemia, and spinal cord compression, as well as increased mortality (Terpos, Berenson et al. 2010). It is estimated that 20% of MM patients present with pathologic fractures, 40% develop a fracture in the first year after diagnosis, and up to 60% develop pathologic fractures over the course of their disease. Additionally, patients with pathologic fractures have a 20% increase in mortality when compared to patients without pathologic fractures (Saad, Lipton et al. 2007). The bone destructive lesions can be extensive and severe and bone pain, frequently centred on the chest or back and exacerbated by movement, is present in more than two-thirds of patients at diagnosis (Sezer 2009).

The increasing evidence highlighting the crucial role of tumour cells and the bone microenvironment in the pathogenesis of myeloma has created novel targets for the therapy of myeloma bone disease (Fowler, Edwards et al. 2011). The tightly controlled physiological process of bone metabolism can be disrupted by various genetic and environmental factors. These include factors related to the onset of age, menopause hormone related changes, drugs, mechanical loading and secondary diseases leading to bone disorders (Feng and McDonald 2010). Disruptions in the interaction and regulation of the various osteotropic cytokines and hormones involved in maintaining the bone formation/resorption balance can result in irregular bone turnover cycles (Rodan and Martin 2000).

Treatment of myeloma bone disease requires management of both the underlying malignancy and the increased bone destruction and suppressed new bone formation. Until the 1990s, there were few advances in the treatment of MM the disease and a result myeloma was deemed incurable with a median survival of 2-3 years. The introduction of high-dose melphalan and autologous bone marrow (BM) transplantation towards the end of the 1990's was a major breakthrough in MM therapy and saw improvements in patient survival (Attal, Harousseau et al. 1996). A decade later saw the introduction of highly

active agents including Thalidomide and bortezomib did not target DNA damage and subsequently, immunodulatory drugs (IMiDs) and proteasome inhibitors. The combinations of these novel agents resulted in positive responses to treatment in the majority of myeloma patients and are now routinely used for the treatment of newly diagnosed myeloma followed by stem cell transplant (Lonial and Boise 2013). Bone disease is managed with a combination of bisphosphonate therapy, localized radiation, (for control of bone pain, treatment of impending fractures or solitary plasmacytomas) and kyphoplasty, vertebroplasty, or surgery (Hameed, Brady et al. 2014). Taken together, the overall survival of myeloma patients has improved with 20-30% of patients surviving for >10 years (Boise, Kaufman et al. 2014).

Bisphosphonates, potent inhibitors of bone resorption, currently remain the standard therapy of MM-related bone disease. Bisphosphonates slow the progression of lytic bone disease, preventing the development of new pathologic fractures and improving bone pain. (Zhang, Chang et al. 2012, Terpos, Roodman et al. 2013). There is also some *in-vitro* evidence to suggest that bisphosphonates have a direct anti-myeloma effect (Avcu, Ural et al. 2005). However, there are now thought to be complications associated with bisphosphonate therapy associated with osteonecrosis of the jaw (ONJ), with reports of 1.6–11% of myeloma patients developing ONJ (Van den Wyngaert, Huizing et al. 2007). Importantly, bisphosphonates cannot restore bone formation and lytic lesions do not heal even in patients in prolonged remission. These evidence highlight the need for the development of anabolic agents, which could potentially reverse osteolytic bone disease and reverse the loss of skeletal integrity at sites of previous bone destruction in MM patients (Hameed, Brady et al. 2014).

1.2 Bone remodelling

The skeleton is a sophisticated metabolically active structure that functions to protect major organs, supports locomotion and stature and is involved in maintaining plasma calcium homeostasis (Crockett, Rogers et al. 2011). Bone is composed of various components including minerals (most of which are calcium), phosphates, proteins and bone cells (Strewler 2001). The cells of the bone are osteoclasts (OC), osteoblasts (OB) and osteocytes. OC are giant multinucleated cells often containing between two and ten

nuclei and are responsible for the removal of bone through the process of bone resorption. These cells are mobile and morphologically structured to maintain optimal contact with the bone's mineralised surface. OC precursors have a haemopoietic origin and are derived from monocyte-macrophage lineage. OC progenitor cells are recruited from haematopoietic compartments and proliferate and differentiate into mature OC cells (Vinholes, Coleman et al. 1996).

OB cells are responsible for bone formation and normally attach to the surface of bone in a monolayer (Vinholes, Coleman et al. 1996). OB cells are derived from mesenchymal stem cells (MSC), which undergo differentiation to become pre-osteoblasts. The pre-osteoblasts further differentiate to become matrix synthesising OB (Vinholes, Coleman et al. 1996). OB are located on a narrow area of newly produced organic matrix known as an osteoid seam and regulate formation of un-calcified matrix (osteoid). Osteoid mainly comprises type I collagen, and subsequently mineralises to become bone (Karsenty, Kronenberg et al. 2009). The basophilic cytoplasm of OB cells produce alkaline phosphatase (ALP), an enzyme involved in bone mineralization, and hormones that target the bone itself (Ducy, Schinke et al. 2000). In addition, OB produce both type I collagens and non-collagenous proteins (Vinholes, Coleman et al. 1996) including osteopontin, osteonectin, osteocalcin, fibronectin, decorin, bone sialoprotein (BSP) and traces of others (Strewler 2001). Following active bone formation, some OB cells become embedded within the bone matrix where they differentiate into osteocytes.

In order to maintain its multitude of functions during vertebrate life, bone is under continual adaptation. These adaptations areregulated through the two distinct mechanisms of bone modelling and remodelling. Bone modelling involves the coordinated yet independent processes of bone formation and bone removal at different anatomical locations (Raggatt and Partridge 2010). Once bone becomes mature, it is continuously renewed to ensure microfractures are repaired and calcium homeostasis is maintained though the remodelling process. The tightly regulated process of remodelling involves the removal and replacement of measurable bone packets (bone structural units) at the same anatomical location consistent with an activation, resorption and formation order of activity (Robling, Castillo et al. 2006). The process of bone remodelling involves resorption by OC and is followed by matrix formation via OB activity (**Figure 1.1**) (Feng and McDonald 2010). The molecular mechanisms and cellular activity involved in

remodelling are closely coordinated which ensures that the bone resorption-formation sequence is carried out at a mutual location thus sustaining bone mass (Raggatt and Partridge 2010).
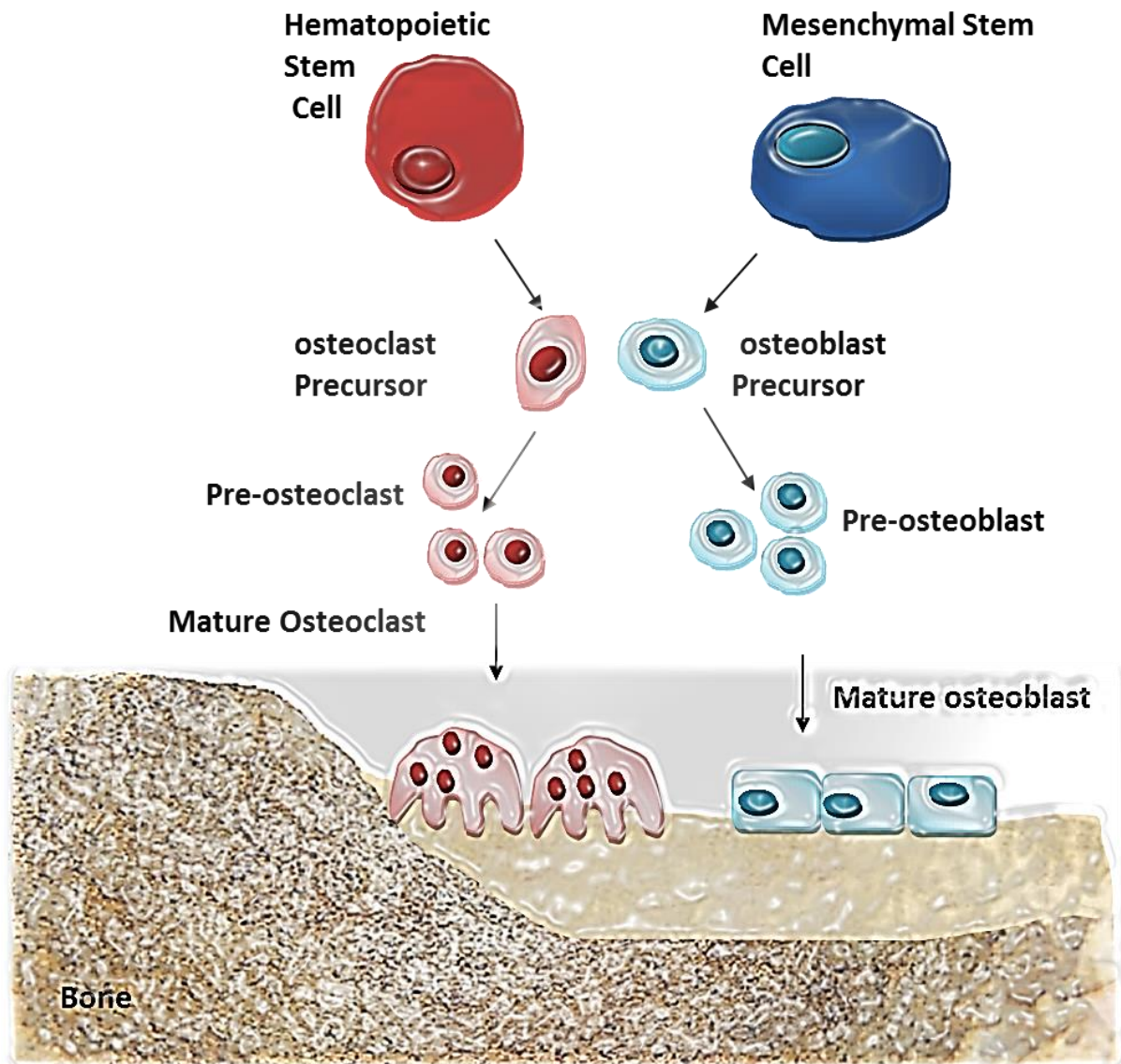
Figure 1.1- Bone remodelling: *Mature osteoclasts (OC) are recruited to the bone target site. Mature OC originates from haemopoietic precursor cells, which differentiate into pre-OC and then further differentiate into mature OC. Mature OC remove bone during bone resorption phase of bone remodelling. Once the resorption process is complete, OC undergo apoptosis and mature osteoblast (OB) cells are recruited to the site. Mature OB originate from Mesenchymal Stem Cells (MSC), that undergo differentiation to become pre-osteoblasts, and subsequently matrix synthesising OB responsible for bone formation (Vinholes, Coleman et al. 1996).*

1.2.1 Regulation of bone resorption

The remodelling process occurs in different parts and at different times of the skeleton asynchronously, highlighting the importance of locally generated and regulated factors in ensuring effective communication mechanisms between the cells involved (Henriksen, Karsdal et al. 2014). Osteoclastogenesis is predominantly regulated by the expression of cytokines which are produced by MSC and their derivative OB in response to pro-resorption stimuli, and regulate OC formation, activation, and function (Vaananen, Zhao et al. 2000). The role of the cytokine macrophage colony-stimulating factor (M-CSF) in osteoclastic activity has been demonstrated using mice deficient in M-CSF, which develop osteopetrosis characterised by significant reduction in OC number (Tanaka, Takahashi et al. 1993). M-CSF functions through interaction with its receptor colony stimulating factor 1 (c-fms) located on the OC. The c-fms is a transmembrane tyrosine kinase receptor that activates tyrosine kinase (Src). Both c-fms and Src are required for osteoclastogenesis and the differentiation of OC precursors (Aeschlimann and Evans 2004).

The recognition of the RANKL-RANK/OPG system in bone biology first brought to light in 1997 in a paper by Simonet et al (Simonet, Lacey et al. 1997). Receptor activator of nuclear factor-kappa B (RANK) also referred to as TRANCE Receptor, is a Type I membrane protein expressed on OC, which is activated upon adhesion to its ligand receptor activator of nuclear factor-kappa B ligand (RANKL). RANKL is a member of Tumour Necrosis Factor (TNF) family and is a key cytokine that operates as a system to maintain the bone resorption and bone formation cycle, ultimately sustaining skeletal integrity. RANKL couples to the soluble decoy receptor osteoprotegerin (OPG) expressed on OB progenitor cells and MSC. OPG competes with RANK for RANKL binding. RANKL-RANK interaction promotes differentiation of monocytic precursor cells to octeoclastic lineage (Kohli and Kohli 2011).

Studies demonstrate osteotropic factors and hormones such as PTH, 1,25-Dihydroxyvitamin D3 $(1,25(OH)_2D_3)$, interleukin-11 (IL-11), interleukin-1β (IL-1β), TNF-α or prostaglandin E_2 (PgE_2) promote RANKL expression in OB/stromal cells. Also PgE_2 has shown to suppress OPG expression, whereas oestrogens up-regulate its expression (Hofbauer, Khosla et al. 2000). Cytokines IL-11 and leukaemia inhibiting

factor (LIF) have also shown evidence of stimulating bone resorption through induction of OC differentiation (Girasole, Passeri et al. 1994). *In-vitro* studies have shown that other cytokines such as interleukin-4 (IL-4) and interferon-gamma (IFN-γ) inhibit OC differentiation. Transforming growth factor β (TGF-β) has a more complicated role in that it suppresses the proliferation of OC precursors and bone resorption (Roux and Orcel 2000).

1.2.2 Regulation of Bone Formation

Bone formation is activated through a series of complex cascades involving the proliferation of MSC and formation of matrix that subsequently becomes mineralised. When bone resorption is terminated, bone formation is activated in the resorption lacunae, mediated by local factors produced during the resorption mechanism. The release of local factors by bone during resorption results in the inhibition of OC function, coupled with induction of OB activity. The OC release factors that have inhibitory effects, thus enhancing OB function. On completion of the OC-induced resorption cycle, the OC produce proteins that are substrates for OB adhesion. *In-vitro* studies show resorbing bone produce chemotactic factors for OB-like cells (Suda, Takahashi et al, 1999). OB proliferation is activated following the formation process. Although the exact mechanism is unknown, growth factors and proteinases including TGF-β, insulin-like growth factor -I (IGF-I), IGF-II and plasminogen activators, have been implicated in OB proliferation. Other autocrine and paracrine presenting factors that stimulate OB proliferation and are sequestrated in bone matrix include fibroblast growth factors (FGF) and platelet-derived growth factor (PDGF). *In-vitro*, these growth factors appear to prevent OB apoptosis (Suda, Takahashi et al. 1999, Raggatt and Partridge 2010).

1.2.3 The Role of Wnts in Osteoblast Differentiation

An important pathway implicated in postnatal bone formation is the canonical Wingless-type (Wnt) signalling pathway. Components of the Wnt pathway have been shown to effect OB proliferation, function and survival. Members of the Wnt protein family are a large group of soluble glycoproteins formed from a combination of two homologous genes: the wingless (Wg) gene and the Int gene. The Wg gene was initially identified owing to a recessive mutation in Drosophila melanogaster causing defects in the wing and haltere (Sharma and Chopra 1976). The Int genes were established as vertebrate genes located close to sites of mouse mammary tumour virus (MMTV) (Rijsewijk, Schuermann et al. 1987) resulting in overproduction of a Wnt genes (Nusse 2008).The Wnts are secreted glycoproteins involved in a range of biological processes including embryogenesis, organogenesis (Yavropoulou and Yovos 2007) and tumour formation. The central role of the Wnts in OB development is well documented. The Wnts initiate cell signalling by interacting with receptor complexes consisting of low-density lipoprotein receptor–related protein 5/6 (LRP5/6) and frizzled (Fz) G-protein-coupled receptor (Zhong, Zylstra-Diegel et al. 2012). As a result, molecular groups are formed, stimulating nuclear production of transcription factors via activation of various intracellular signalling cascades (Kikuchi 2003). The mutation of LRP5 can lead to osteoporosis-pseudoglioma syndrome, characterised by childhood onset of osteoporosis and loss of vision (Gong, Slee et al. 2001). Alternatively, there are gain of Wnt function mutations such as G171V in LRP5, which lead to increased bone mass (Little, Recker et al. 2002).

The canocnical Wnt signalling involves stabalisation of β-catenin (**Figure 1.2**), which aids transcription of genes controlled by lymphoid enhancer-binding factor 1/T cell–specific transcription factor (LEF/TCF) enhancers (Hens, Wilson *et al.* 2005). There is evidence that Wnt/ β-catenin signalling is a physiological response to mechanical loading (Robinson, Chatterjee-Kishore et al. 2006) and is involved in the repair of bone fractures (Chen, Whetstone et al. 2007). Adhesion of Wnt glycoproteins to Frizzled/LRP 5/6 complex stimulates phosphorylation of Dishevelled (Dsh) and LRP 5/6. Dsh and LRP 5/6 bind to Axin and prevent activation of a 'destructive' protein complex consisting of adenomatous polyposis coli protein (APC), glycogen synthase kinase-3β (GSK-3β) and serine/threonine kinase (CK1γ). Inhibition of the APC/GSK-3β/CK1γ complex, prevent

β-catenin loss. β-catenin is free to translocate to the nucleus and interact with LEF/TCF transcription factors to stimulate specific gene transcription (Westendorf, Kahler et al. 2004).

Extracellular Wnt antagonists are produced naturally and impair OB function, suppressing bone formation. The soluble Wnt antagonist family members are sub-categorised into the secreted Frizzled-related proteins (sFRPs) and the dickkopfs (Dkks), each group specific in its Wnt-related function. sFRPs directly adhere to Wnt to block receptor binding, whereas Dkks inhibit Wnt receptor complex activity via adhesion to the Wnt co-receptors LRP5/6 (Pearse 2006).
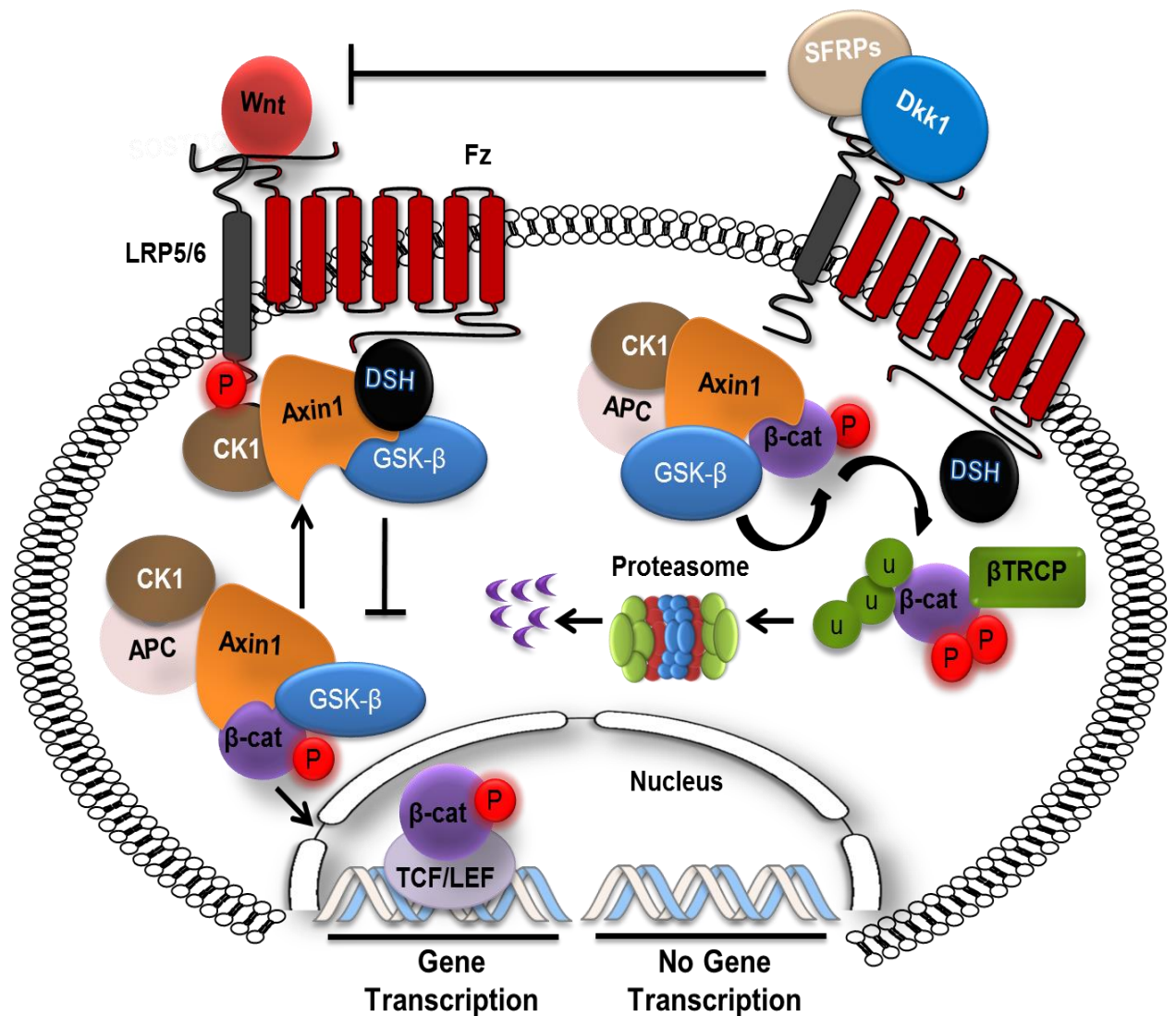
Figure 1.2 - The proposed mechanism of the canonical Wnt signalling pathway.
Axin and DSH are key proteins that bind to Wnt receptor complexes and result in the inhibition of the 'destructive' protein complex constituting of APC/GSK-β/CK1. β-catenin is stabilised in the cytoplasm and translocates into the nucleus, where it interacts with LEF/TCF transcription factors. When Wnt signalling is inhibited, β-catenin is phosphorylated by the APC/Axin/GSK-3β and subsequently relocated to the proteasome where it is degraded. Soluble Wnt antagonists such as Dkk1 and SFRPs block the interaction between Wnt ligands and their receptors suppressing osteoblast differentiation .

1.2.4 The Role of BMPs in Osteoblast differentiation

As an extensive subgroup of the TGF-β family, the bone morphogenic proteins (BMPs) play an important role in embryogenesis by targeting the genes involved. Originally associated with bone formation by Wozney *et al* (Wozney, Rosen et al. 1988), the BMPs are now known to be exhibit a broad spectra of biological activities in various tissues, including blood vessels, heart, kidney, neurons, liver, lung cartilage and bone (Miyazono, Kamiya et al. 2010, Chen, Deng et al. 2012). Furthermore, after birth, BMPs regulate the pathophysiology of several diseases including osteoporosis, arthritis, renal diseases, pulmonary hypertension and cancer (Walsh, Godson et al. 2010).

Once TGF-β is released from the bone following resorption, and exposed to OB precursors, OB cells undergo proliferation. As TGF-β exposure is brief, proliferating cells differentiate and then express BMPs. BMPs are produced in the bone marrow (BM) and adhere to their corresponding receptors, which in turn results in the production of the transcription factor Runt-related transcription factor 2 (Runx2) also referred to as core-binding factor-1 (Cbfa1). Runx2/Cbfa1 is expressed on OPG cells and plays an essential role in the differentiation of OB cells from stromal cells of the BM, or MSC of the connective tissue. Of the 16 BMPs identified, BMP2 through to BMP7 and BMP9 primarily mediate MSC differentiation into OB (Chen, Deng et al. 2012)

BMP signalling occurs through activation of Smad proteins (**Figure 1.3**). Extracellular BMPs bind to type I and type II ligand-specific receptors. BMPs bind with a stronger affinity to type I and type II receptor heteromeric complexes. Upon binding of the BMP to a receptor heteromeric complex, the type I receptor becomes phosphorylated by the constitutively active serine/threonine kinase of the type II receptor. The Smad proteins are downstream intracellular messengers and are subdivided into receptor-mediated Smads (R-Smads), the common mediator Smad (C-Smad) and the inhibitory Smads (I-Smads). Smad1, 5 and 8 are R-Smads, which are phosphorylated by activated receptor complexes and are ligand specific. Smad4 is the C-Smad and forms a complex with the R-Smads once they have been activated by the type I receptor. The Smad complex translocates to the nucleus where it binds directly or indirectly (through BMP-binding partners) to specific promoters sequences within BMP target genes and regulates gene transcription (Varga and Wrana 2005). Although the mechanism by which the BMPs target genes is

not entirely understood, the Indian hedgehog (Ihh) gene has been identified as a BMP signalling target. Evidence of PTH and PTHLH regulation mediated through Ihh, which in turn maintains chondrocyte hypertrophy, has been determined in past studies (Seki and Hata 2004).

In addition to the expression of tissue-specific BMP molecules and their associated cell surface receptors, BMP signalling is also tightly regulated by a family of soluble, extracellular secreted BMP antagonists. The relationship between BMP and their antagonists controls a variety of cellular processes including establishment of the embryonic dorsal–ventral axis, formation of neural tissue, development of joints in the skeletal system and brain neurogenesis. BMP antagonists function through direct interaction with BMP molecules and are characterized by their ability to block the action of BMPs through direct binding, stopping the BMPs from binding their receptors (Walsh, Godson et al. 2010). BMP antagonists are characterised by their ability to prohibit BMP signalling and include the Cerberus and DAN (CAN) family of proteins that include Cerberus and Gremlin (Pearce, Penny et al. 1999, Yeung, Gossan et al. 2014), Twisted gastrulation, Chordin and Crossveinless (Oelgeschlager, Larrain et al. 2000, Forsman, Ng et al. 2013) and Noggin (Tylzanowski, Mebis et al. 2006). Uterine sensitization-associated gene-1 (USAG1) (Kiso, Takahashi et al. 2014) and Sclerostin are also more recently characterised BMP antagonists expressed in the kidneys and bones, respectively (Kiso et al. 2014; Krause et al. 2010b). The timing and concentration of BMP and their antagonists is essential to normal developmental processes. Modifications to the levels of BMP and BMP-antagonist can result in deformities in bone, limb and kidney formation, highlighting their role in the progression of human diseases including cancer (Walsh, Godson et al. 2010).
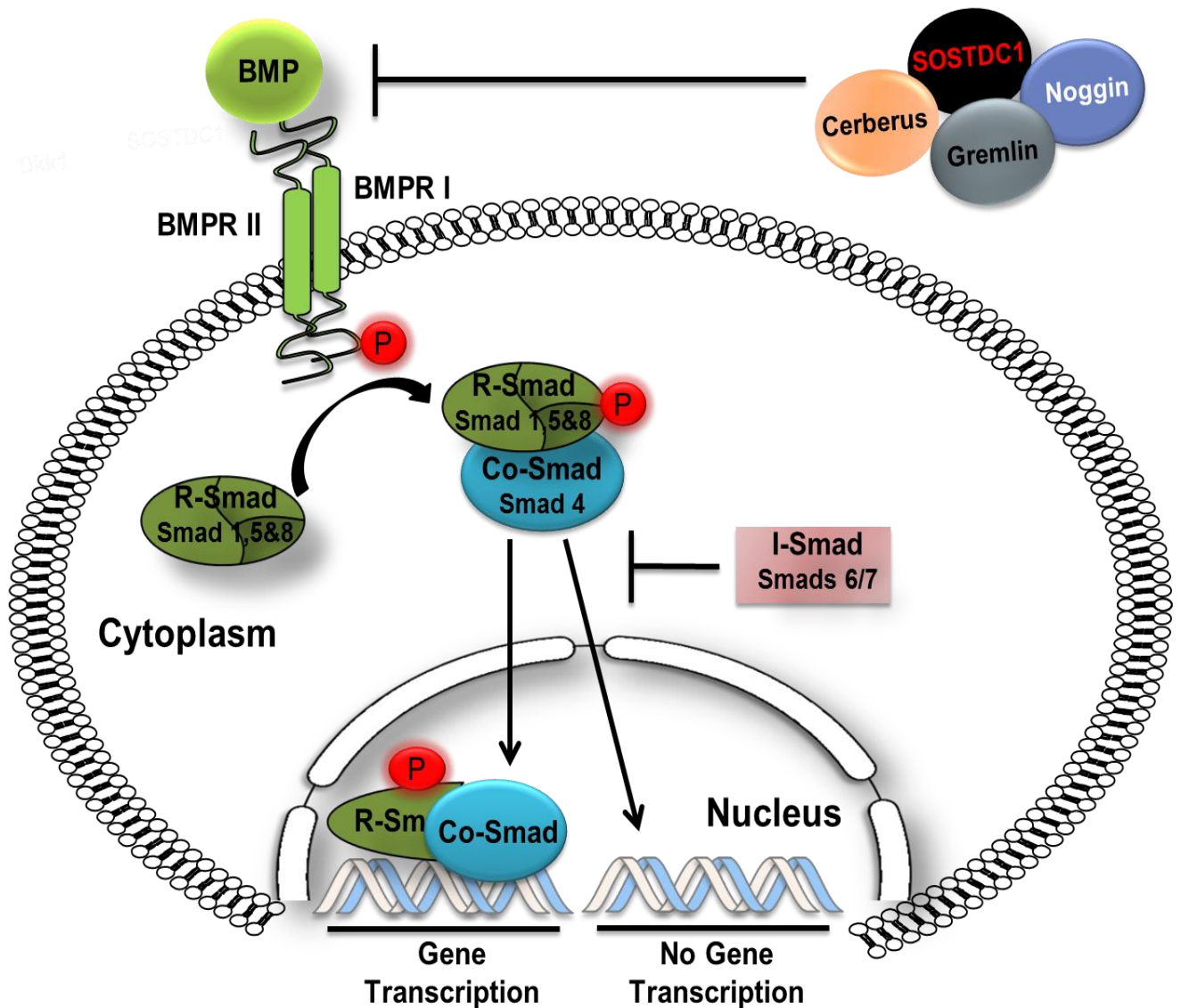
Figure 1.3 - BMP-dependent Smad phosphorylation: *BMP ligands bind to the* BMP heterotetrameric receptor complexes activating signalling through type II-receptor-mediated phosphorylation of the type I receptor on the GS domain. This induces *phosphorylation of regulatory Smad 1,5&8. The co-Smad 4 forms a new complex with the phosphorylated Smad 1,5&8 proteins. This newly formed pSFmad 1,5&8/Smad 4 complex translocates into the nucleus where it binds to transcription factors/enhancers and regulates gene expression necessary for the differentiation of osteoblasts. BMP signalling is both extracellularly modulated (e.g., Noggin, SOSTDC1, Gremlin) and intracellularly modulated (e.g I-Smads).*

1.3 Dysfunction of bone remodelling in MM: Cellular and molecular mechanisms

Reduced formation of bone resorbing or forming cells, an increase in resorption or formation activity and abnormal mineral crystal formation, are all characteristic of disruptions in bone remodelling, which inevitably result in diseases such as Paget's and osteoporosis (Russell, Mueller et al. 2001). The osteolytic and osteoblastic features of these diseases are characteristic of secondary tumours within the skeleton. Metastasis of the bone is the third most prevalent form of metastatic disease and most commonly results from tumours within the breast, prostate, thyroid, lung, bladder, kidney and MM (Chiang and Massague 2008). MM differs to bone disease occurring in other cancers, as the resorption of bone is not followed by further formation, and OB activation is reduced. Histomorphometric analysis of bone from patients with advanced MM shows a lack of bone formation within lesions, coupled by an increase in OC number at resorption sites. In addition, levels of bone resorption markers, including carboxyl-terminal telopeptide of type I collagen and tartrate-resistant acid phosphatase are elevated (Roodman 2009).

The OC and OB activity that occurs during infiltration of MM through the marrow does not follow through when the disease advances. The coupling interaction between up-regulated osteoblastic activity and increased bone resorption was initially reported in 1991 by Bataille *et al.* They showed that this interaction occurs during early stages of MM, secondary to MGUS, and osteolytic disease does not develop in patients that maintained increased OB activity (Bataille, Chappard et al. 1991). Based on the observations that there is increased osteoclastic bone resorption coupled with decreased osteoblastic bone formation in myeloma bone disease, research has focused on OC and, more latterly OB activity.

As reviewed by Fowler and Edwards et al, more recent research in MM bone disease has targeted the influence of other BM cell types, including immune cells, MSC and bone marrow stromal cells (BMSC) to determine potential therapeutic targets (Fowler, Edwards et al. 2011). The 'seed and soil' theory first described by Paget outlined the mechanisms existing between cancer cells and the bone microenvironment, where bone is the preferable soil in which cancer cells are seeded and go on to flourish. Growth factors within mineralized bone matrix are activated in the local microenvironment. Their release stimulates the physiological mechanisms between OC and OB (Guise and Mundy 1998).

In MM these mechanisms are disrupted, leading to aggressive bone disease in approximately 80% of patients (Yaccoby 2010).

1.3.1 Dysfunction of bone resorption in MM

Generation of OC activating factors by myeloma cells or the BM microenvironment can potentially result in the excessive bone resorption activity observed in MM. These factors function through mutual regulatory pathway involving RANKL/RANK (Roux and Mariette 2004). Myeloma cells may express RANKL, while OPG binds both surface and soluble RANKL inhibiting OC development and bone resorption. Mouse 5T33MM myeloma model has been utilised to determine OPG-mediated changes in the local bone microenvironment and their effect on tumour activity/progression (Vanderkerken, De Leenheer et al. 2003). Inhibition of the RANK/RANKL-OPG interaction interferes with the progression of myeloma within bone and may reduce tumour growth and increase patient life span (Roux and Mariette 2004).

Myeloma cells bind to BMSC via coupling of vascular cell adhesion molecule-1 (VCAM-1) expressed on stromal cells and the $\alpha 4\beta 1$ integrin VLA-4 located on the surface of MM cells. The interaction between MM cells and BMSC stimulates production of RANKL, OC activating function (OAF) cytokine activity and M-CSF and at the same time inhibits OPG production (Pearse 2006). Therefore the role of RANKL in MM has mainly been researched on OPG, peptidominetics, anti-RANKL antibodies and soluble receptor constructs as targets (Buckle, Neville-Webbe et al. 2010). RANKL/RANK deficient mice and those with over-expression of OPG present a reduction in OC activity resulting in ostopetrosis, abnormal increased hardening of the bones (Dougall, Glaccum et al. 1999). OPG deficiency and excessive RANKL activity in mice has been linked to osteoporosis, although the mechanisms responsible are not clear (Mizuno, Amizuka et al. 1998). Evidence indicates that the crucial events in osteoclastic resorption in MM not only occur due to deregulation of the RANKL/OPG coupling (Brounais, Ruiz et al. 2008), but also through the various cytokines with OAF activity produced by MM cells and cells of the microenvironment. The OAFs that primarily mediate osteoclastogenesis are TNF, IL-1, IL-6 and specific chemokines including macrophage inflammatory protein-1α (MIP-1α),

macrophage inflammatory protein-1β (MIP-β) and stromal derived factor-1α (SDF-α) (Roodman 2004).

Production of MIP-1α, hepatocyte growth factors (HGFs) up-regulate OC precursor proliferation and differentiation (Terpos and Dimopoulos 2005). HGF and the HGF receptor (c-met) are found on myeloma cells and promote OC activation, epithelial cell proliferation and angiogenesis. HGF increases IL-11 expression on OC-like cells and both IL-1 and TGF-β1 disrupt HGF activity on IL-11 (Seidel, Lenhoff et al. 2002). The cytokine VEGF is expressed on myeloma cells and increases osteoclastic bone resorption and survival, as it adheres to its OC receptor VEGFR-1. Studies have shown that in M-CSF deficient mice, VEGFR is expressed as a substitute for OC recruitment. In addition, the cells increase IL-6 expression from stromal cells in response to the increased levels of VEGF (Dankbar, Padro et al. 2000).
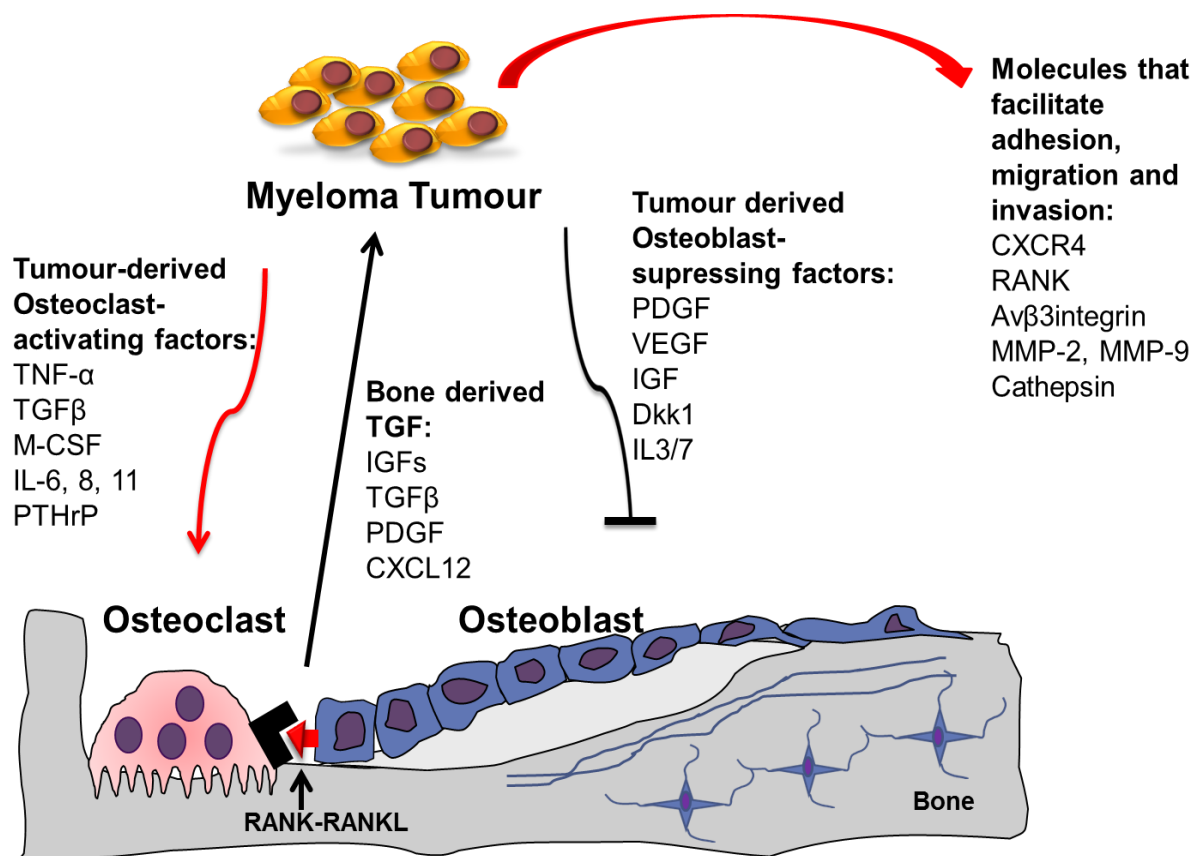
Figure 1.4 – Myeloma vicious cycle: *MM cells interact with OB precursors inducing RANKL, OAF and M-CSF. Tumour-derived osteoclast activating factors upregulate OC precursor differentiation and osteoclastic resorption. Tumour-derived osteoblast supressing factor inhibit OB differentiation . RANKL/OPG ratio favours RANKL, promoting OC activity.*

1.3.2 Dysfunction of Bone Formation in MM

Based on the literature, it can be deduced that our understanding of the suppression of bone formation in myeloma disease is poor. Recently, animal models have been used to further investigate the pathways and molecules involved in the mechanisms responsible for the suppression of bone formation. Although a number of molecules have been implicated in these mechanisms, there is a lack of functional data supporting an underlying role. In myeloma patients, abnormalities in osteoprogenitors and the production of OB inhibitors by both myeloma cells and myelomatous bone microenvironment cells results in a reduction in osteoblastogenesis. In MM the osteolytic lesions arise in close proximity to the tumour, indicating that in addition to the soluble factors that regulate osteoblastogenesis suppression, the close contact between myeloma cells and MSC also influence bone remodelling (Yaccoby 2010).

The importance of the transcription factor RUNX2/Cbfa1, in the formation and differentiation osteoblastic cells has to date been established. RUNX2 interacts with other transcription factors including osterix, to activate the bone formation process. The activation of Runx2/Cbfa1 in human BMSC and osteoblastic cells induces the expression of the OB markers collagen I, ALP, and osteocalcin during OB differentiation (Giuliani, Rizzoli et al. 2006). The potential involvement of Runx2/Cbfa1-mediated transcription in MM-induced OB inhibition has previously been reported (Giuliani, Colla et al. 2005). Giuliani et al showed that blocking Runx2/Cbfa1 activity in human osteoprogenitors in myeloma-osteoprogenitor co-cultures resulted in myeloma-induced inhibition of OB differentiation in long-term bone marrow culture determined by a decrease in ALP, osteocalcin, and collagen I (Giuliani, Colla et al. 2005).

The concept that myeloma-OB cell contact induces a detrimental effect on the differentiation of OB has been demonstrated in Giuliani et al findings showing that when stimulated by myeloma cells, MSC reduced expression of Runx2 through cell surface molecules VLA-4 and VCAM-1. Their data strongly suggests that the effect of myeloma cells on Runx2/Cbfa1 activity is primarily mediated by cell-to-cell contact between myeloma and osteoprogenitor cells (Giuliani, Colla et al. 2005). It has previously been reported that direct contact between human myeloma and OB-like cells results in the inhibition of osteocalcin production in OB-like cells (Barille, Collette et al. 1995). In

addition, other adhesion molecules appear to be involved in the inhibition of osteoblastogenesis by human myeloma cells. For example, Neural Cell Adhesion Molecule (NCAM)-NCAM interactions between myeloma and OB-like cells decreased osteoid and bone matrix production by osteoblastic cells *in-vitro* (Griffiths and Ling 1991). Based on these reports, regardless of the molecular interaction, it would appear that myeloma-OB interaction is linked to the development of osteolytic bone disease in myeloma.

There is mounting evidence indicating OB differentiation is inhibited by factors secreted by myeloma cells including Wnt-signalling inhibitor Dkk1 (Tian, Zhan et al. 2003), sFRP-2 (Oshima, Abe et al. 2005), IL-7 (Standal, Abildgaard et al. 2007) and HGF (Lee, Chung et al. 2004) and by microenvironmental cells within myelomatous bone (e.g. IL-3) (Ehrlich, Chung et al. 2005). In the past decade, extensive research on myeloma-produced soluble inhibitors of Wnt ligands has been carried out. Data implicates the critical inhibitory role of Wnt in MM bone disease. These implications have been strengthened by *in-vitro* studies that determine the impact of Wnt in the formation of bone (Tian, Zhan et al. 2003, Oshima, Abe et al. 2005).

The relationship between Dkk1 and inhibition of OB activity has been established. Tian *et al* analysed ALP activity of C2C12 MSC treated with BMP2 in human MM patient samples with high Dkk1 levels. The findings determined the inhibitory function of the patients BM plasma and recombinant human Dkk1 on the cells ALP activity (Tian, Zhan et al. 2003). More recent *in-vivo* studies using 5T2MM murine myeloma model in the investigation of Dkk1 inhibitory effects on osteolytic lesions, show that administration of 5T2MM cells into C5BL/KaLwRjj mice leads to osteolytic bone lesion formation consistent with increased OC number, decreased OB numbers and reduced bone mineralisation. Although no effect was seen on OC number, treatment of 5T2MM cell with anti-Dkk1 antibody increased both mineralised surface by 28% and rate of bone formation by 25% (Heath, Chantry et al. 2009). These findings are consistent with the earlier studies by Tian *et al* using neutralising anti-Dkk1 antibodies on BM plasma in C2C12 cells (Tian, Zhan et al. 2003), in that suppressing Dkk1 promotes bone formation and is therefore an effective therapeutic target for preventing development of myeloma induced osteolytic bone disease (Heath, Chantry et al. 2009).

Other Wnt antagonists including sFRP-2 and sFRP-3 have been identified during MM related transcript screening. Although analysis of MM cell lines and primary samples showed evidence of SFRP-2 expression, the link between sFRP-3 and MM has yet to be established (Pearse 2006). *In-vitro* studies by Oshima *et al* on MC3T3-E1 and human BM-derived MSC, suggest that recombinant mouse S2FRP-2 in the presence of BMP-2, inhibits ALP activity and mineralisation. Similar to Dkk1, anti-sFRP-2 antibodies expressed neutralising effects on the myeloma cells (Oshima, Abe et al. 2005). Taking into consideration the role of Wnts in osteoblastic activity, Wnt antagonists may be responsible for the mechanism in which MM affects OB and OC function (Glass, Bialek et al. 2005, Holmen, Zylstra et al. 2005).

As the most abundant cell in the bone, we have extensive knowledge of the biology of osteocytes (Bonewald 2011). However, the contribution of osteocyte cells to MM development and progression in bone remains unclear. Osteocytes produce molecules that modulate bone formation and resorption (Xiong, Onal et al. 2011). Recently, the Giuliani group showed that the osteocytes life span is compromised in MM patients with bone lesions (Giuliani, Ferretti et al. 2012). They also showed that MM cells affect the osteocyte transcriptional profiles, resulting in the upregulation of RANKL and increasing osteoclastogenesis. Patients with active MM also have increased levels of osteocyte-produced circulating sclerostin, a potent inhibitor of bone formation (Brunetti, Oranger et al. 2011). Therefore, understanding the role of osteocytes in mechanisms associated with MM bone disease could provide important new therapeutic strategies that target MM-osteocyte interactions (Delgado-Calle, Bellido et al. 2014).

1.3.3 MM Models

The development of effective MM drug therapy is required for the development of biological systems for pre-clinical evaluation of potential therapeutic molecules and for better understanding of the disease (Mitsiades, Anderson et al. 2007). Most established human myeloma cell lines (HMCL) are derived from the advanced or extramedullary phases of MM and are obtained from BM, peripheral blood, ascites or pleural effusion. HMCL have revealed many of the molecular and biological aspects of myeloma including the complicated cytokine network influencing angiogenesis and the growth of plasma cells (Moreaux, Klein et al. 2011). RPMI 8266 and Y-266 were the first MM cell lines which were established in the in the 1960s (Matsuoka, Moore et al. 1967; Nilsson, Bennich et al. 1970). In the following twenty years, an estimated 112 MM cell lines have been described since in the literature The availability of the HMCL has also meant that the function of the target genes of chromosomal translocations and the activity of novel candidate therapeutic agents can be investigated (Seidl et al., 2003; Bergsagel and Kuehl, 2005). However, the establishment of HMCL are rare and samples are usually derived from patients who have end-stage disease. This means that the cells retain oncogenic abnormalities found at the time of isolation and are only partially reflective of the heterogeneity found in MM patients (Chiron, Surget et al. 2012). In addition, the clinical, immunophenotypic, cytogenetic and cell culture features of the majority of these HMCL are either partially characterized or, in some cases, have not been described at all (Drexler and Matsuo 2000).

An animal model that accurately reflects human myeloma and takes into account the protective nature of BMSC would be powerful in defining the efficacy of therapeutic agents *in-vivo*, and accelerate the drug development process. A number of different animal models are currently used to study myeloma, and these include the severe combined immunodeficiency (SCID)-hu/rab xenograft model and the Radl 5TMM models (Fryer, Graham et al. 2013). Several mouse models of MM bone disease have been developed exhibiting OB suppression (Hjorth-Hansen, Seifert et al. 1999; Vanderkerken, Asosingh et al. 2003; Epstein and Yaccoby 2005). Recently Italian scientists Pierfrancesco Tassone and bioengineer Filippo Causa devised the Xenograft model using HMCL (Calimeri, Battista et al. 2011in which, small cylindrical plastic scaffoldings punctured with pores are used as a substitute for human bone. The purified

MM cells (CD138+) from human BM aspirates are injected into the artificial bone scaffolds and the whole structure implanted under the skin of immune-deficient mice. Once the human MM cells start interacting with the artificial bone, it is possible to study the interaction between the MM cells and BM (DeWeerdt 2011).

The 5T series are another MM mouse model in which the MM cells can be transferred between syngeneic mouse models. In the Radl 5T murine model, young mice are injected with myeloma cells, which originated spontaneously in aged C57BL/KaLwRij mice. Originally, the well characterised 5T2MM and the 5T33MM cell lines derived from these elderly C57BL/KaLwRij mice where used to study the mechanisms associated with myeloma cell-BM homing, myeloma tumour interaction with the bone microenvironment and to assess novel anti-MM therapies (Radl, De Glopper et al. 1979; Radl, Croese et al. 1988). Both the 5T2MM and 5T33MM models were characterised by the MM cell infiltration restricted to the BM and spleen. The main difference between the two models was that only the 5T2MM cells caused the osteolytic disease observed in the long bones of patients with MM. In a further development of the model, *in-vitro* sub-clones of the 5T33MM model were established, and subsequently named the 5T33MMvt and the 5TGM1MM cells. It was found that mice intravenously injected with 5TGM1MM cells developed MM disease (Asosingh, Radl et al. 2000). The 5TGM1 cells have since also been labelled with green fluorescent protein (GFP) and luciferase for *in*-vivo imaging in MM studies. Despite the advantages of the syngeneic 5TMM models, one major limitation is their dependency on the specific C57BL/KaLwRij mouse strain (Vanderkerken, Asosingh et al. 2003). Both the Xenograft and 5T series models show suppression of OB activity and bone formation, coupled with OC activation in the MM-infiltrated BM. These models have been important in determining which molecules modulate bone lesion formation, induced by MM, and in helping to evaluate novel therapeutic approaches aimed at reversing osteolytic bone disease in MM patients.

1.4 The role of novel SOSTDC1 in Wnt and BMP signalling in osteoblasts

Sclerostin domain containing 1 (SOSTDC1) is also known as SOSTL (Sclerostin-like) due to its homology with the SOST gene (Brunkow, Gardner et al. 2001). Expression of SOSTDC1, also referred to as uterine sensitisation-associated gene-1 (USAG-1), Ectodin and Wise in the literature, has been demonstrated in various tissues including surface ectoderm of the posterior axis, branchial arches, hair follicles, rat endometrium, vibrissae, mammalian tooth cusps, developing testis, interdigital tissues and the kidneys (Lintern, Guidato et al. 2009). SOSTDC1 was originally isolated as a secreted molecule by a functional screen of chick cDNA library of embryonic cells. SOSTDC1 (referred to as Wise in this study) altered the antero-posterior character of neutralised Xenopus animal caps, stimulating Wnt signalling (Itasaki, Jones et al. 2003). In other studies, SOSTDC1 was isolated from a functional screen of specifically expressed rat endometrium genes sensitised to implantation, and named USAG-1 (Simmons and Kennedy 2002). The protein was again identified, this time called ectodin, as a mouse and human cDNA encoding antagonist of BMP for mouse pre-osteoblastic MC3T3-E1 cells (Laurikkala, Kassai et al. 2003).

Within the literature, reports suggest that SOSTDC1 and its orthologs modulate Wnt signalling and inhibit BMP activity. Data implicates that SOSTDC1-Wnt signalling is regulated via interactions with Wnt co-receptor LRP6 and SOSTDC1 induced BMP inhibition is regulated via adhesion to BMP ligands (Lintern, Guidato et al. 2009). The SOSTDC1 protein is very likely structured to form a three looped cystine knot (Avsian-Kretchmer and Hsueh 2004) and binds to LRP5/6 through one of these loops. SOSTDC1 deletion construct lacking this loop domain, still bind BMP4 and inhibit BMP signals. BMP4 does not disrupt SOSTDC1-LRP6 interaction, implicating separate domains for binding. The information that we now have in relation to the interactions of SOSTDC1 with the BMP family members, LRP6 and its molecular characteristics, has given some perspective into the proteins' multifunctional existence on a molecular level (Lintern, Guidato et al. 2009).

There is evidence of SOSTDC1 inhibitory effect on BMP in the dental ectoderm, where SOSTDC1 expression is seen to suppress BMP2 and BMP7 activity. Mice deficient in SOSTDC1 (referred to USAG-1 in this study) display altered tooth morphology and

increased tooth growth (Laurikkala, Kassai et al. 2003). In other studies, SOSTDC1 is seen to inhibit BMP2, -4, or -7 induced bone differentiation in a mouse myeoblast cell line (C2C12) (Yanagita, Oka et al. 2004). More recent research in tooth development, demonstrates the importance of SOSTDC1 expression in mesenchyme-epithelial tooth formation. Munne *et al* investigated SOSTDC1 induction of mouse incisors and determined SOSTDC1 an antagonist of BMP signalling mesenchymal induced tooth formation. Munne *et al also* show that reductions in dental mesenchyme in SOSTDC-1 deficient incisors result in development of additional *de novo* incisors resembling those that develop from activated Wnt signalling. In this study the inhibitory role of Dkk1 is determined as preventing additional incisor development, thus implicating BMP and Wnt signalling inhibition promotes the inhibitory function of tooth mesenchyme (Munne, Tummers et al. 2009, Munne, Felszeghy et al. 2010). In a similar study by Ahn *et al*, SOSTDC1 is shown to suppress of tooth cells via inhibition of LRP5/6–induced Wnt signalling. SOSTDC1 suppression up-regulates Wnt signalling, consequently tooth buds in toothless regions proliferate and result in tooth development (Ahn, Sanderson et al. 2010).

In Wnt/β-catenin mediated hair follicle regeneration, SOSTDC1 is seen to express an inhibitory role. SOSTDC1 is repressed by nuclear receptor co-receptor Hairless (HR) in progenitor keratinocytes consistent with the timing of follicle regeneration (Beaudoin, Sisk et al. 2005). Other data suggest SOSTDC1 function in the inhibition of Wnt antagonists; Wnt1, Wnt3a and Wnt10 (Yanagita, Oka et al. 2004, Beaudoin, Sisk et al. 2005). There is little data on the role of SOSTDC1 on osteoblastogensis and bone disease. In one recent study on Chinese women, a common variation in the SOSTDC1 gene was associated with increased bone mass (He, Yue et al. 2011). In earlier *in-vitro* studies, SOSTDC1 was seen to inhibit BMP2, -4, or -7 induced bone differentiation in a mouse myoblast cell line (C2C12) (Yanagita, Oka et al. 2004). Although this data is limited, it does provide a rational for studying the potential role of SOSTDC1 in the dysfunction of osteoblastogenesis.

There is evidence of crosstalk between Wnt and BMP signalling in MSC (Bennett, Longo et al. 2005) and pre-osteoblasts (Bain, Muller et al. 2003, Mbalaviele, Sheikh et al. 2005). Data has shown that the loss of BMRP-1A results in increased levels of Wnt signalling in OB cells, correlating to an increase in bone mass (Kamiya, Ye et al. 2008). Findings from

other studies suggest that BMP4/BMP6 and Wnt1/3 regulate OB differentiation through a GSK3β-dependent but β-catenin-independent mechanism.(Fukuda, Kokabu et al. 2010). Although this data is indicative of a dependency of the BMP and Wnt signalling in OB, the underlying mechanisms are poorly understood. The role of SOSTDC1 in Wnt-BMP dependent signalling has not been reported in OB differentiation. Understanding the molecular mechanisms associated with SOSTDC1-modulated Wnt-BMP signalling crosstalk in OB is a novel understanding which could produce new therapeutic targets in osteolytic bone disease.

1.5 SOSTDC1 expression in cancer: Could SOSTDC1 have a role in MM?

Although data are limited, there is evidence that SOSTDC1 can regulate cell activity through BMP and Wnt signalling pathways within cancer of the breast and kidney (Blish, Wang et al. 2008, Clausen, Blish et al. 2010). Findings from numerous studies show that both BMP and Wnt signalling are modulators of breast cancer (Alarmo, Rauta et al. 2006, Alarmo, Kuukasjarvi et al. 2007). Studies by Clausen *et al* into SOSTDC1 secretion and BMP/Wnt signalling in breast cancer cells, link decreased SOSTDC1 expression to increased tumour size. Intriguingly, this group showed that SOSTDC1 modulated Wnt and BMP signalling very selectively in that within breast tissue, SOSTDC1 increased Wnt3a signalling, reduced BMP7 signalling and had no significant effect on BMP2 signalling (Clausen, Blish et al. 2010). This data suggests that SOSTDC1, through its ability to regulate Wnt or/and BMP signalling, may contribute to the development of breast cancer. Similarly, the function of SOSTDC1 as a potential tumour suppressor has also been implicated in Wilms paediatric renal tumour development. The gene encoding SOSTDC1 is proven relevant to tumour activity consistent with evidence that the protein is down-regulated in adult renal cancer and regulates BMP and Wnt signalling activity (Blish, Clausen et al. 2010).

The evidence indicating that SOSTDC1 modulates tumourgenesis in breast and rental cancer suggests that SOSTDC1 could play a similar role in other cancers. There is currently no evidence to show that SOSTDC1 has any role in MM or bone disease secondary to MM. As mentioned previously there are a few well characterised molecules known to be involved in osteoblastic suppression secondary to MM (Alarmo, Rauta et al.

2006) including Dkk1 which is perhaps the best characterised (Pinzone, Hall et al. 2009). As mentioned previously over-expression of Dkk1 has been associated with MM bone disease and the use of anti-Dkk1 neutralizing Ab has demonstrated a pro-anabolic effect with associated anti-myeloma activity *in-vivo* (Heath, Chantry et al. 2009). Nevertheless, data shows that Dkk1 is not detectable in all serum samples obtained from MM patients (Tian, Zhan et al. 2003). The Dkk1 absence from MM clones that still expressed morphological characteristics of OB dysfunction suggest other MM-mediating factors may exist (Pearse 2006).

In the search to identify other molecules that that could have a potential causal role in the suppression of osteoblastogenesis in MM, our group identified *SOSTDC1* (data unpublished), as a gene that was highly upregulated in the 5T2MM C5BL/KaLwRjj mice compared to naïve animals using Affymetrix GeneChip™ technology (**Figure 1.5 A**, ****P<0.002*). The expression of *SOSTDC1* in 5T2MM compared to naïve mice was further confirmed using TaqMan™ gene expression assays (**Figure 1.5 B**). This compelling data coupled with reports highlighting the role of SOSTDC1 in Wnt and BMP signalling modulation encouraged the rational that SOSTDC1 may have a key role in the suppression of osteoblastogensis in MM. Targeting SOSTDC1 could be the ideal therapy for the reversal of osteolytic bone disease in MM, specifically in cases where patients do not exhibit elevated levels of Dkk1.

A

B
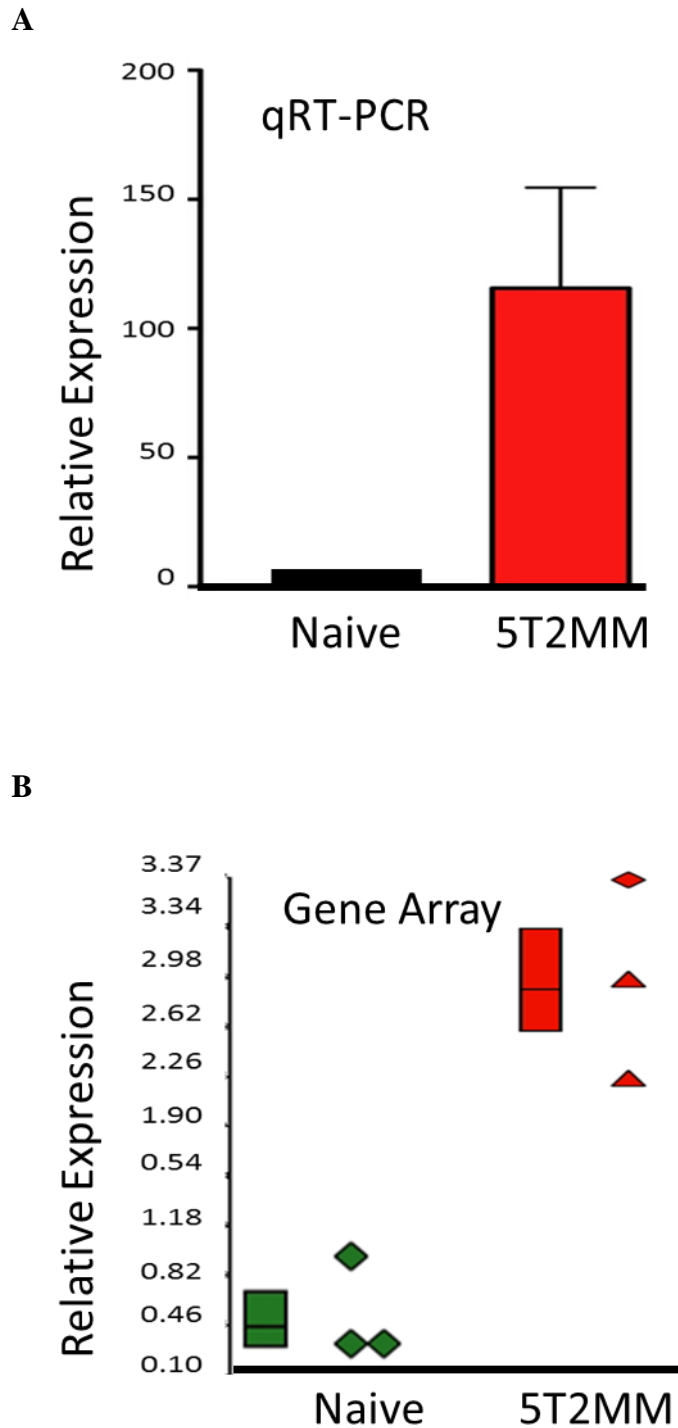
Figure 1.5 – SOSTDC1 was detected in 5T2MM myeloma model and not detected in naïve C5BL/KaLwRjj mice: *SOSTDC1 was significantly upregulated in the 5T2MM mice compared to naïve animals, determined by Affymetrix GeneChip™ technology (A) and TaqMan™ gene expression assays (B) (Buckle et al, data unpublished).*

1.6 Overall aims and objectives of the study

1.6.1 Aims

To date, there has been no evidence of work investigating the role of SOSTDC1 in the suppression of bone formation in myeloma. Determining the effect of SOSTDC1 on OB differentiation and proliferation *in-vitro* is key to understanding the role of this novel protein in myeloma-induced suppression of bone formation and perhaps bone resorption. Our recent data (unpublished) suggest a putative role for SOSTDC1 protein in Wnt signalling modulation, resulting in suppression of bone formation. Following array analysis and using experimental models of myeloma bone disease, we suggest that SOSTDC1 may be a modulator of Wnt signalling in MM. The regulatory role of SOSTDC1 has been implied in BMP signalling in other tissues (Ahn, Sanderson et al. 2010, Blish, Clausen et al. 2010, Clausen, Blish et al. 2010), and BMPs are known to have a regulatory role in bone development (Chen, Deng et al. 2012). This provides the rational for investigating the effect of SOSTDC1 on Wnt and BMP signalling in differentiating OB cells at various stages cell development.

There have been recent reports of evidence of Wnt-BMP crosstalk in pre-osteoblasts, providing some insight into the role of other antagonists such as Sclerostin and noggin (Itasaki and Hoppler 2010). The potential regulatory role of SOSTDC1 in Wnt-BMP signalling in OB differentiation may be another target for osteolytic bone disease therapy in myeloma. Interestingly, there is no data in the literature to suggest that either myeloma cells, osteoblasts or cells in the BM actually express SOSTDC1. Here, I aim to determine whether the 5TMM series of mouse myeloma models and differentiating OB progenitor cells do produce SOSTDC1 both *in-vitro* and *in-vivo*. In MM disease, there is a link between increased suppression of osteoblastogenesis and myeloma-OB interaction (Chen, Orlowski et al. 2014). In this study I wanted to further investigate a potential role for SOSTDC1 in myeloma-OB interaction using an *in-vitro* co-culture system. The overall aim of this study is to provide insight into the molecular mechanisms involved in SOSTDC1-regulated Wnt-BMP signalling and establish the conditions required for SOSTDC1 expression myeloma bone disease.

1.6.2 Objectives

This study will address the hypotheses of '**SOSTDC1 suppresses OB progenitor differentiation'** and '**myeloma cells express SOSTDC1 and promote SOSTDC1 expression in OB progenitors'.**

The hypotheses will be tested by addressing the following objectives:

1 To determine the proliferation, differentiation and mineralisation profile of murine OB progenitors in culture.

2 To determine the effect of SOSTDC1 on Wnt and BMP-induced differentiation, mineralisation and downstream intracellular signalling in differentiating OB progenitors *in-vitro.*

3 To determine a modulatory role for SOSTDC1 in BMP-Wnt signalling crosstalk in differentiating OB progenitors *in-vitro.*

4 To determine whether the 5TMM series myeloma cells and differentiating OB progenitors produce SOSTDC1 *in-vitro* and *in-vivo.*

5 To determine the optimal conditions under which SOSTDC1 in produced in a myeloma and OB contact dependent microenvironment.

Chapter 2 – Materials and Methods

All equipment, chemicals and solutions used in this research were assessed for health and safety precautions (Control of Substances Hazardous to Health (COSHH). All appropriate safety measures were used, including latex examination gloves and laboratory coat (Kimerley-Clarke).

2.1 Cell culture

Cell Culture Equipment	
IITEM	**SUPPLIER**
Haemocytometer - depth 0.1mm, 1/400mm^2	Hawksley
Cell culture flat bottom plates – 6, 12, 24, 48& 96	Corning® Costar®
Nunc™ cell culture treated flasks with filter caps – T25cm3, T75cm3, T175cm3	Nalgene, Nunc Ltd.
BD Falcon™ centrifuge tube – 15ml, 50ml	Fisher Scientific
Cryovials, 1.5ml	Nalgene, Nunc Ltd.
Bjoux tubes (5, 15, 15, 50ml)	Starstedt
Eppendorph tubes (0.05 abd 1.5ml)	Starstedt
Cell scrapers	Nalgene, Nunc Ltd.
GPR centrifuge	Beckman Coulter
Microcentrifuge	IEC Micromase
Water bath	Fisher Scientific
Vortex mixer	VLP® Scientifica
Heater Thermomixer Comfort	Eppendorf
Z2 counter	Bechman Coulter Inc.
Coulter Counter	Beckman Coulter Inc.
Syringe filters, 25mm	Acrodisc® Pall® Life Sciences
BD Sterifill SCF™ syringe	BD Biosciences

Cell Culture Reagents

ITEM	SUPPLIER
Minimum Essential Media (MEM) -Alpha + GlutaMAX	Gilbco[TM], Invitrogen
Roswell Park Memorial Institute (RPMI) 1640 (1x)+ GlutaMAX	Gilbco[TM], Invitrogen
Dulbeccos Modified Eagle Medium (DMEM) + GlutaMAX	Gilbco[TM], Invitrogen
Keratinocyte-SFM Medium (Kit) with L-glutamine, EGF, and BPE	Gilbco[TM], Invitrogen
MEM Non-Essential Amino Acids (NEAA) x100	Gilbco[TM], Invitrogen
Sodium pyruvate	Gilbco[TM], Invitrogen
Fetal calf serum (FCS)	PAA Laboratories
Penicillin: streptomycin solution (PenStrep)	Gilbco[TM], Invitrogen
Fungizone® Antimycotic 250µg/ml amphotericin B and 205µg/ml sodium deoxycholate	Gilbco[TM], Invitrogen
Phosphate buffered saline (PBS)	Sigma-Aldrich
0.05% Trypsin EDTA (0.53mM)	Sigma-Aldrich
Collagenase I	Sigma-Aldrich
Hank's Balanced Salt Solution (HBSS)	Gilbco[TM], Life Technologies
Ethylenediaminetetraacetic acid (EDTA)	Sigma-Aldrich
L-ascorbic acid	Sigma-Aldrich
β-glycerophosphate disodium salt hydrate	Sigma-Aldrich
Trypan blue	Sigma-Aldrich
Dimethyl sulphoxide (DMSO)	Sigma-Aldrich
70% Industrial methylated spirits (IMS)	Fischer Scientific

All cell culture procedures were carried out within microbiological class II safety cabinets (Walker, UK), using sterile equipment. Media were always filtered and warmed to 37°C prior to cell treatment. All cell cultures were incubated in a humidified atmosphere at 37°C and 5% CO_2.

2.1.1 Osteoblast progenitor cell culture

Osteoblast cultures were prepared with a modification of the method of Ecarot-Charrier et al (Ecarot-Charrier, Glorieux et al. 1983). Mouse primary osteoblast (OB) progenitor cells were isolated from the calvarial bones of 2 to 4 day old C57BLKaLwRij mice, (Harlan, UK) using Collagenase I digestion (**Figure 2.1**). Typically, 12-15 dissected calvarial bones were cut into small pieces using a scalpel and placed in 50ml BD falcon™ tubes containing 3ml of 1mg/ml Collagenase I digestion solution and placed in a water bath at 37°C on a shaker for 10 minutes. The Collagenase I solution (fraction 1) was then removed and the calvaria submerged in 3ml of fresh Collagenase I solution. The calvaria were incubated for 30 minutes at 37°C with the fresh Collagenase I solution and the cells collected (fraction 2). The solution containing fraction 2 were transferred to a new 15ml BD falcon™ tubes. The calvaria bone cells were washed with 7ml of PBS and centrifuged at 1000 RPM for 5 minutes. The supernatant containing the cells added to fraction 2. The calvaria bone cells were incubated with 4μM EDTA solution for 10 minutes at 37^oC (fraction 3).

The calvaria were washed in 7ml Hank's Balanced Salt Solution (HBSS) and the wash added to fraction 3. 3ml of fresh Collagenase I solution was added to the calvaria and incubated for 30 minutes at 37^oC (fraction 4). The solution collected from calvarial cell cultures from the fraction 4 digestions containing were centrifuged at 250g RPM for 5 minutes and re-suspended in standard Minimum Essential Medium (MEM) alpha containing 10% fetal calf serum (FCS), 1% Streptomycin (PenStrep) (100 units/ml Penicillin/100 μg/ml) and 1% Fungizone Antimycotic (250μg/ml amphotericin B /205μg/ml sodium deoxycholate). MEM-Alpha and all its constituents will be referred to as standard MEM-Alpha media unless specified otherwise. OB progenitor cells were cultured in 7ml of MEM -Alpha in T25cm^2 culture flasks for a minimum of 2 days until the cells were 70-80% confluent and ready for use. All experiments using OB progenitors were carried out with cells that had been passaged up to an including passage 4.
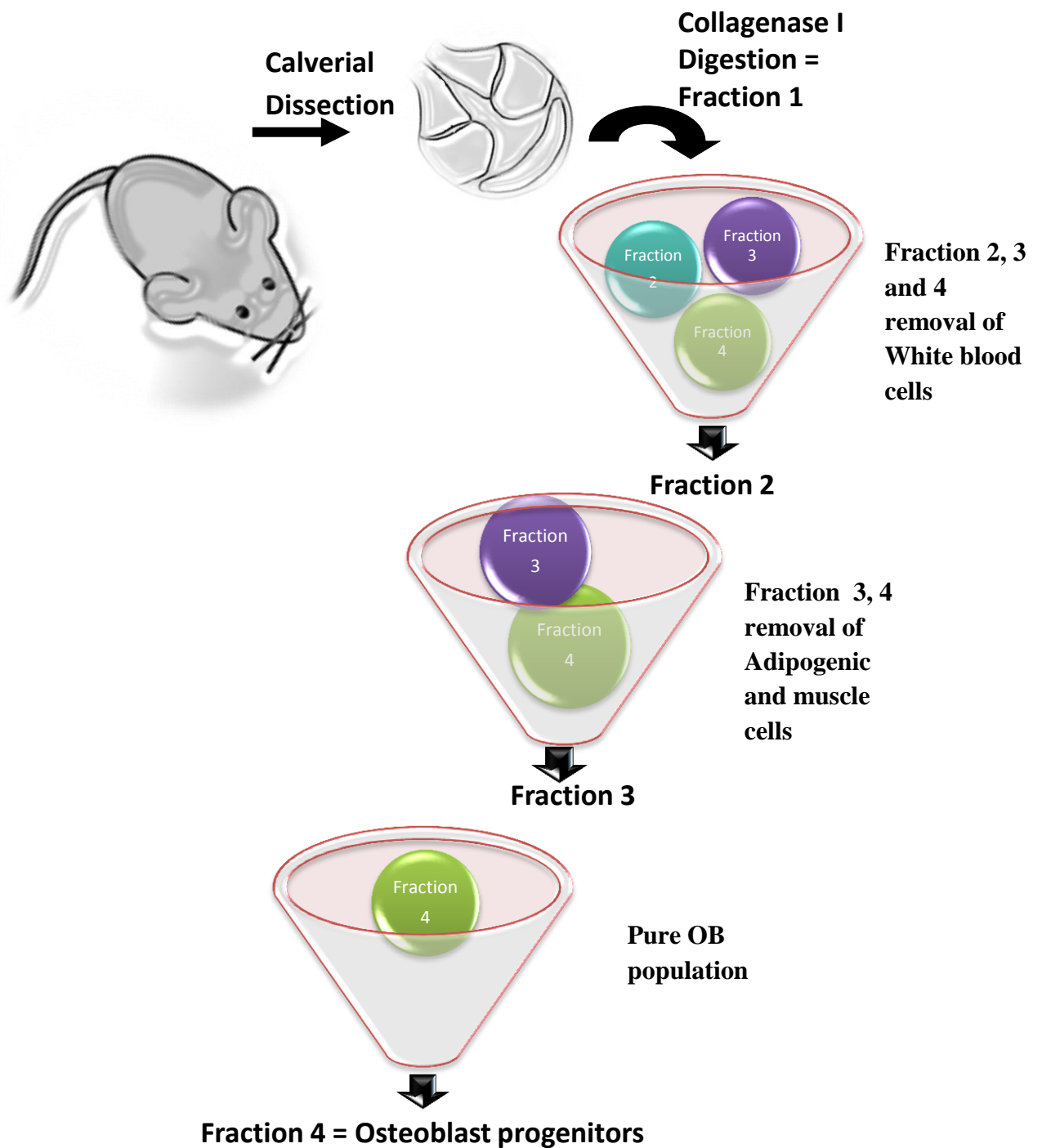
Figure 2.1 - Calvarial osteoblast isolation: *Osteoblast progenitor cultures were derived from the calvaria of neonatal C57BLKaLwRij mice using Collagenase I digestion in 4 stages (fractions) of digestion.*

2.1.2 Cell Lines

2.1.2.1 5TMM myeloma Series

The 5TMM myeloma series of cell lines were used as their features *in-vivo* are highly similar to human disease wherein they home and grow in the Bone Marrow (BM), as well as causing osteolytic bone disease. The 5TGM1MM murine multiple myeloma (MM) cells were derived from the 5T33MM murine myeloma cells (Fowler, Mundy et al. 2009). Both 5TGM1MM-GFP and 5T33MM-GFP myeloma cells were kindly provided by Claire Edwards at The University of Oxford, UK.

The 5T33MM-GFP or 5TGM1MM-GFP cells were resuspended in 200µl PBS and injected via tail vein into 17-19 weeks old female C57BL/KaLwRijHSD (C57BLKaLwRij) mice at a cell density of 2 x10^6. At the same time naïve mice were injected with PBS and used as tumour-negative controls. The growth of myeloma tumour was via the measurement of human Igλ in murine serum monitored by enzyme-linked immunosorbent assay (ELISA) (Human Lambda ELISA Kit; Bethyl Laboratories Inc). The assay was carried out as per the manufacturer's protocol. Briefly, 100µl of standard or serum was added to designated wells and the plate incubated at room temperature for 1 hour. Next, 100 µl of anti-Lambda detection antibody was added to each well and incubated at room temperature for 1 hour. Proteins were incubated with 100µl of HRP Solution for 30 minutes followed by the addition of 100µl of TMB Substrate in the dark at room temperature for 30 minutes. The reaction was stopped by adding 100µl of Stop Solution to each well. The absorbance was measured on a plate reader (Spectramax M5, Sunnyvalet) at a 450 nm wavelength.

5T33MM and 5TGM1MM mice developed myeloma within 6-12 weeks of inoculation. At the first signs of illness (36 days 5T33MM-bearing mice and 21 days for 5TGM1MM-bearing mice) animals were sacrificed by injection of pentobarbitone. In sterile conditions, the femora and tibiae were dissected free of soft tissue and the bone marrow of the animals were flushed out with 1000µl PBS. The cell suspension was mixed with 3ml Roswell Park Memorial Institute (RPMI) medium and slowly overlaid onto 4ml of a Lymphoprep™ (Ficoll gradient). The cells were centrifuged at 400g for 20 minutes without any brakes. The mononuclear layer of cells were collected and washed twice in RPMI media. Isolated 5T33MM or 5TGMMM cells were then cultured in a T25 flask

containing 3 ml of RPMI medium with the following additive; 10% FCS, 1% PenStrep, 1% sodium pyruvate and 1% NEAA. Cells were then sorted using a murine CD138 kit (Milteny Biotec) according to manufacturer's instructions. Cell were cultured for 2 days and then frozen as outlined in **section 2.1.4**. All *in-vivo* animal work requiring an animal-handling licence including the paraprotein ELISA and 5TMM cell isolation from the bone was kindly performed by Dr Shelly Lawson.

2.1.2.2 SAOS2 cells

Human osteoblast-like SAOS2 cell were purchased from American Type Culture Collection (ATCC®). SAOS2 cells are particular useful for the study of molecular mechanisms associated with OB differentiation due to their OB-like phenotype. SAOS2 cells were cultured in T75 flasks containing 12 ml of Dulbeccos Modified Eagle Medium (DMEM) + GlutaMAX medium with the following additive; 10% FCS, 1% PenStrep, 1% sodium pyruvate and 1% NEAA. SAOS2 cells were passaged or frozen when not required for experimental purposes, as outlined in **sections 2.2.2** and **2.2.3**, respectively.

2.1.2.3 Human Kidney Epithelial (HK-2)

Human Kidney Epithelial (HK-2) cells were purchased from ATCC®. HK-2 cells are immortalised proximal tubule epithelial cells isolated from normal adult human kidney. HK-2 cells express SOSTDC1 and were used in experiments as a positive control for SOSTDC1 production. HK-2 cells were maintained in Keratinocyte-SFM media containing L-glutamine. Keratinocyte-SFM was supplied with prequalified human recombinant epidermal growth factor 1-53 (EGF 1-53) and bovine pituitary extract (BPE). The Keraticonyte media was supplemented with 30 μg/ml of BPE, 0.2 ng/ml rEGF, 10% FCS, 1% PenStrep, 1% sodium pyruvate and 1% NEAA. The HK-2 cells were passaged or frozen when not required for experimental purposes as outlined in **sections 2.2.2** and **2.2.3**, respectively.

2.1.2.4 Endothelial STR-10 cells

Human endothelial STR-10 cells were purchased from ATCC®. The SRT-10 cells were maintained in DMEM supplemented with 10% FCS, 1% PenStrep, 1% sodium pyruvate and 1% NEAA. STR-10 cells were passaged or frozen when not required for experimental purposes as outlined in **sections 2.1.2** and **2.1.3**, respectively.

2.1.3 Cell passage and routine counting using a haemocytometer

OB progenitor cultures and cell lines were maintained in their standard media and passaged when cell confluence had reached 70-80%. All media was removed from T25, T75 or T175 flasks and discarded. Adherent cells were washed with sterile PBS to remove debris and remaining media, and 0.05% trypsin was used to re-suspend the adherent cells. The volume of trypsin used to detach cells from the culture surface was dependent on the size of flask i.e.0.5ml for T25, 1.5ml for a T75 and 3ml for T175. 10ml of media was added to the trypsinised cells to neutralise the effect of trypsin. Cell suspensions were transferred into a BD Falcon™ tubes and centrifuged at 1000 RPM for 5 minutes. Non-adherent cells were transferred directly into the BD Falcon™ tubes and also centrifuged at 1000 RPM for 5 minutes to pellet cells. The supernatant from cell pellets were discarded and the cells re-suspended in 10 ml of fresh media. Approximately 1/5 or 1/10 dilution of the cells (dilution depended on the cell density and speed that was required for cell growth in preparation for an experiment) were placed in fresh flasks containing media and maintained in culture at 37℃ and 5% CO_2. Cells were routinely passaged every 2-4 days when they became approximately 70-80 % confluent.

Routine cell counting was performed on passaged cells prior to the set-up of experiments or freezing down of cells, using the Neubauer haemocytometer. The Neubauer haemocytometer has 4 large squares consisting of 16 smaller squares, each with a volume of $0.1mm^3$. Each of the 4 large squares of the haemocytometer, with a cover slip in place, represents a total volume of 0.1 mm^3 (1.0mm X1.0mmX 0.1mm) or 10^{-4} cm^3 (**Figure 2.2**). The marked grid within the counting chamber allowed for the number of cells to be estimated. 10μl of this cell suspension was mixed with 10μl of 0.4% trypan blue solution in a 1:1 ratio and inserted into the counting chamber of the haemocytometer. The number of cells in each of the 4 squares was counted manually using a counter. The number of cells counted was divided by 4 to equate the average number of cells per grid. The calculated result was then multiplied by 2 to account for the dilution factor of adding trypan blue and then multiplied by the total volume of the large square; x 10^{-4} cm^3. Since 1 cm^3 is equivalent to approximately 1 ml, the final value obtained was representative of the total number of cells per ml. The final number of cells/ml was used to calculate the volume of cell suspension required to seed the desired number of cells with a fresh flask.

For example:

To calculate the number of cells in a 5ml cell suspension:
Total number of cells counted in 4 squares: 56 cells
Average number per square: 56/4 = 14
X2 to account for the addition of trypan blue: = 14 x 2
28 x 10,000 (volume of each large square 10-4 cm3) = 280,000 cells/ml
= 280,000 cells/ml x 5ml
= Total of 1,400,000 cells in 5ml

Each 4x4 square

= 0.1mm³ or 0.1µl
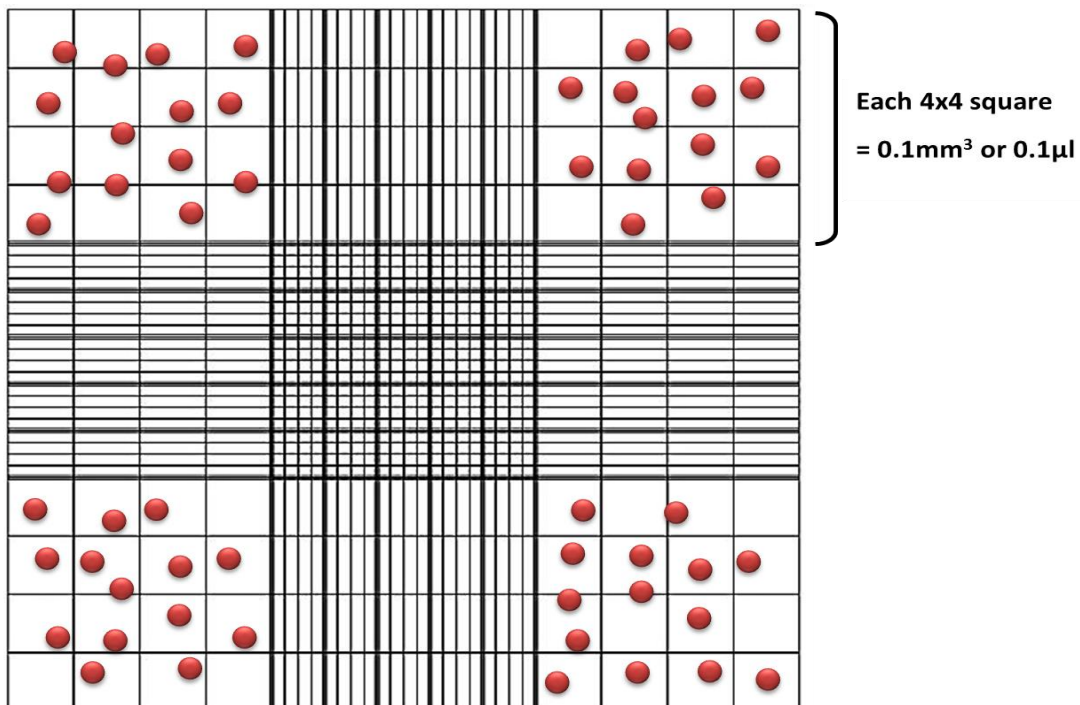
Figure 2.2 - Cells were counted using a Neubauer haemocytometer: *The haemocytometer comprises 4 large squares consisting of 16 smaller squares, each with a volume of 0.1mm³. Each individual square from the 16 squares has a volume of 0.00625 mm³. Therefore each of the 4 large squares of the haemocytometer represents a total volume of 0.1 mm³ (1.0mm X1.0mmX 0.1mm) or 10-4 cm³.*

2.1.4 Cell counting using Coulter Counter

The Coulter Counter technology is used for determining the number and size of cells in a suspension. Similar to the flow cytometer, the cell suspension is passed through a small aperture and cell number/size assessed by changes in the electrical conductance within the aperture. The coulter count was performed as described by Wood et al (Wood, Requa et al. 2007). Cells were harvested from culture surfaces using 0.05% trypsin as outlined in **section 2.13** and centrifuged at 1000 RPM for 5 minutes in 50ml BD Falcon™ tubes. The supernatants were removed and cells were resuspended in 10ml of isotonic solution. The cell suspensions were transferred to plastic cuvettes and the cuvette was inserted in the sample holder of the counter. The counter sampled 500µl of cell suspension per run and recorded the cell number and modal size. A threshold on the counter was set to only consider cells with a diameter of between 10 to 30µm. The cell number within each sample was counted 3 times in consecutive analysis. The average of these 3 readings was then multiplied by 20 to account for the dilution factor (0.5ml samples from 10ml). The final value calculated was the estimated total number of cells within the cell suspension.

2.1.5 Freezing and thawing of cell cultures

Cells were frozen down and maintained in liquid nitrogen until required for experimental purposes. OB progenitor cells were frozen down between 0-3 passages and cell lines were frozen down between 2-10 passages to be used when required. Briefly, adherent cells were washed with sterile PBS and 0.05% trypsin was used to re-suspend the adherent cells. Media was added to the tryspinised cells to neutralise the effect of trypsin. Cell suspensions from adherent or non-adherent cultures were transferred into the BD Falcon™ tubes and counted using a haemocytometer as described in **section 2.1.3**. Following cell counting, $1x10^6$ cells per sample were centrifuged at 1000 RPM for 5 minutes at room temperature. Each sample was resuspended in 1 ml of 10% dimethyl sulphoxide (DMSO) diluted in 90% FCS (10µl of DMSO and 90µl of neat FCS). The cells were transferred into cryovials and placed immediately into a Cryo 1℃ freezing container. The freezing container was transferred to a -80°C freezer over-night and the vials were placed in liquid nitrogen for long-term storage.

When cells were required, they were removed from the liquid nitrogen storage and immediately agitated at 37^oC in a water bath to aid efficient thawing. The cells were transferred into BD Falcon™ tubes containing 10 mL of pre-warmed standard media and centrifuged at 1000 RPM for 5 minutes. On discarding of supernatant, the pellets were re-suspended in fresh medium and harvested into fresh, sterile flasks. Cell pellets were usually re-suspended into T75 flasks at a cell density of $1x10^6$ cells in ~12ml of media and maintained in culture at 37℃ and 5% CO_2.

2.2 Osteoblast progenitor differentiation using osteogenic media

OB progenitors were counted using a haemocytometer as outlined in **section 2.1.3** and cultured in plates or flasks in standard MEM-Alpha media. OB progenitor cultures were differentiated as reported by Ecarot-Charrier et al (Ecarot-Charrier, Glorieux et al. 1983). Briefly, isolated OB progenitors were incubated at 37°C and 5% CO_2 for 72 hours, to allow the cells to adhere to the culture surface in optimal conditions. Standard MEM-Alpha osteogenic media was prepared containing; 4% FCS, 1% PenStrep, 10mM β-glycerol and 50μg/ml L-ascorbic acid (vitamin C) according to **Table 2.1**. The β-glycerophosphate was prepared to a stock solution of 1000mM diluted in distilled water and L-ascorbic acid was prepared in a stock solution of 50mg/ml in distilled water. The β-glycerophosphate and L-ascorbic acid stock solutions were aliquoted and stored at -20ºC until use. On each occasion, the osteogenic media was prepared fresh and filtered prior to use using 25mm syringe filters. All future references made to standard osteogenic media refer to media prepared as outlined in this section unless stated otherwise.

Preparation of Osteogenic Media		
INGREDIENT	Final Concentration	Volume from Stock (ml) to make 500ml of osteogenic media
L-ascorbic acid	10mM	5
β-glycerophosphate	50μg/ml	0.5
Alpha-MEM + GlutaMAX	Neat	470
Penstrep	1%	5
Fungizone	1%	5
FCS	4%	20

Table 2.1 - *Preparation of standard MEM-Alpha osteogenic media.*

Standard MEM-Alpha media was removed from the OB progenitor cultures and cells were washed once with PBS. The PBS was aspirated from the cells and osteogenic media was added in a volume specific to the size of the well within the culture plates or size of the culture flasks, as specified in **Table 2.2**. OB progenitor cultures were differentiated in osteogenic media for up to 4 weeks. Osteogenic media from OB progenitor cultures were discarded and replaced with fresh media every three days.

PBS Wash Volumes	
Cell Culture Plate	**Volume of PBS, per well or flask**
96 well plate	100 μl
48 well plate	250 μl
24 well plate	500 μl
6 well plate	1.5 ml
T25cm Flask	7 ml
T75cm Flask	10 ml
T175cm Flask	20 ml

Table 2.2 - *Volume of PBS used to wash each well or flask prior to media change.*

2.3 Alkaline phosphatase activity

Alkaline phosphatase Assay	
ITEMS	**SUPPLIER**
p-Nitrophenyl phosphate (pNPP)	Sigma Aldrich
1.0mg/ml PNPP, 0.2 M Tris buffer	
0.1% Triton - 5µl of Triton X into 5ml of PBS	Sigma-Aldrich
Plate reader Spectramax M5	Sunnyvale

The p-Nitrophenyl phosphate (pNPP) is a soluble substrate used for the detection of alkaline phosphatase (ALP) activity. ALP hydrolyses colourless pNPP to a yellow coloured product, which is determined by reading the absorbance (OD) at 405. ALP activity was assayed according to the method of Kumegawa (Kumegawa, Hiramatsu et al. 1983) with adaptions outlined by Gartland *et al* (Gartland, Rumney et al. 2012). ALP assays were carried out on differentiated cells cultures in 96 well culture plates at a cell density of 6000cell/cm^2. Briefly, the cell supernatant was removed from each well and the cells were gently washed twice with PBS, avoiding detaching the cells. Cells were then permeabilised with 20µl of 0.1% Triton with agitation on a shaker for 20 minutes at 200 RMP at room temperature. At the same time, one tablet of pNPP and one of Tris buffer were added to 20ml of distilled water and dissolved with agitation on a shaker for 20 minutes at 200 RMP and at room temperature. Next, 200µl of pNPP was carefully added to each well and immediately analysed for ALP using SoftMax Pro software on a plate reader. ALP was determined by taking OD readings at A405 every 5 minutes for up to 90 minutes using the Beer-Lambert law (**Figure 2.3**). To maintain uniformly across biological experimental repeats, the most linear part of ALP curve was used to calculate the ALP activity of the cell cultures within each well. The ALP values were normalised to DNA contents (ng/ml) by PicoGreen analysis as outlined in **section 2.4,** taking into account dilution factors.

A

B
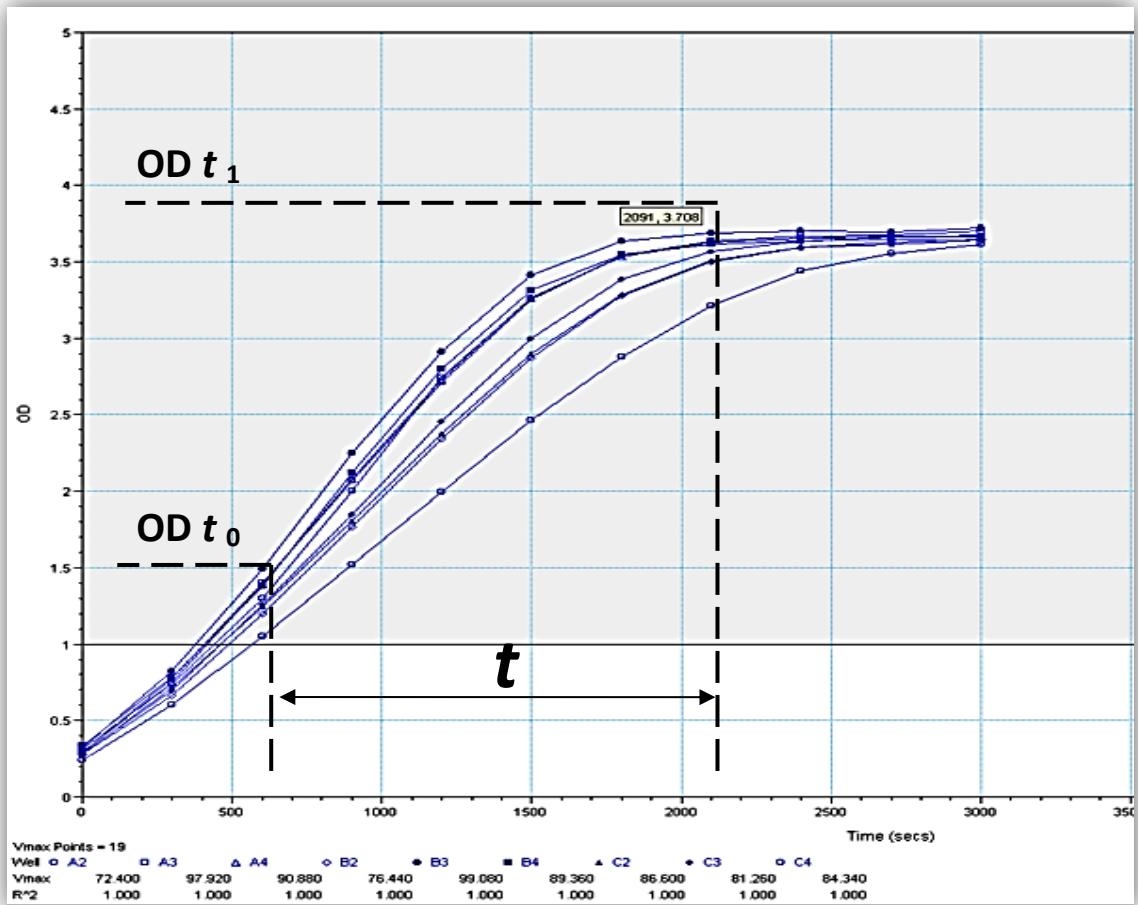
$$U = \frac{(ODt_1 - ODt_0) \times V}{t \times \varepsilon \times}$$

U = ALP activity (nmol Pi per min).
OD t_1 = absorbance at 405 nM of sample at the end time point.
OD t_0 = absorbance at 405 nM of sample at start (background).
V = volume in microlitre of sample and reagent in well that is measured.
t = reaction time in min.
e = 17.8 m L/nM/cm for p NPP.
l = path length of light in cm (specific to the plate reader which is 0.639).

Figure 2.3 - Alkaline phosphatase analysis: *(A) The ALP was determined by taking absorbance (OD) readings at A405 every 5 minutes for up to 90 minutes. The OD values at the most linear part of the ALP curves were used to calculate the ALP activity (**U**). (B) ALP activity was calculated using Beer-Lambert Law.*

2.4 Pico Green assay

ITEM	SUPPLIER
PiocoGreen Reagents	
Quant-iT™PicoGreen®dsDNA reagent	Invitrogen
Lambda DNA standard	Invitrogen
X20 TE buffer; 200mM Tris-HCl, 20mM EDTA, pH 7.5 1 ml X20 diluted in 19 ml of PBS	Invitrogen
0.1% Triton X	Sigma-Aldrich
Plate reader Spectramax M5	Sunnyvale

PicoGreen® double-stranded DNA (dsDNA) quantitation reagent is a fluorescent nucleic acid stain used to quantify dsDNA and is used as a surrogate for cell number. PicoGreen analysis was performed according to the protocol outlined by Gartland *et al*. Picogreen assays were carried out on cells cultures in culture plates at a cell density of 6000cell/cm^2. Media from cell cultures was discarded and the cells were gently washed twice with 200μl of PBS, avoiding detaching the cells. Cells were then permeabilised with 20μl of 0.1% Triton with agitation on a shaker for 20 minutes at 200 RMP at room temperature. A 2μg/ml dsDNA standard solution was prepared from a stock of 100 μg/ml dsDNA supplied with the PicoGreen kit. 8μl of the 100μg/ml was diluted in 392μl of 1X TE buffer in a 1 ml eppendorf tube. Increasing concentrations of 0, 50, 100, 200, 400, 600, 800 and 1000ng/ml of dsDNA standard were prepared in a fresh 96 well plate, using appropriate volumes of 1X TE buffer and the prepared 2μg/ml dsDNA standard (**Table 2.3**). Next, 50μl of the unknown permeabilised samples were transferred into the 96 well culture plate, and 50μl of 1X TE buffer was added to these samples. 100μl of 1:200 dilution of PicoGreen reagent was added to each standard and unknown sample and placed on a shaker at room temperature for 5 minutes in the dark. Quantitation of DNA was determined by exciting samples at 485nm and detecting fluorescence emission intensity at 530nm using the plate reader.

Plate well	Final DNA Concentration (ng/ml)	Volume of 2 µg/ml DNA standard (µl)	Volume of X1 TE Buffer (µl)
A1 +A2	0	0	100
B1+ B2	50	2.5	97.5
C1 + C2	100	5	95
D1 + D2	200	10	90
E1+ E2	400	20	80
F1 + F2	600	30	70
G1 + G2	800	40	60
H1 + H2	1000	50	50

Table 2.3 - *Preparation of dsDNA standard curve for PicoGreen analysis.*

The fluorescence readings were exported into an Excel template and used to generate the linear regression analysis with coefficient of determination (R^2). The concentration (ng/ml) of DNA for unknown samples were extrapolated from the standard curve linear regression using the formula **Y = *a* + *b*X;** where each point on the line has a **Y** value that is calculated by multiplying the point's **X** value by '***b***' (slope of the line) and then adding '**a**' (distance of the line's intercept). The line of best fit was plotted through 0 at the intercept (**a**=0). The R^2 was used as a measure of the consistency of prepared standard dilutions. The extrapolated concentration of the unknown '**X**' was multiplied by 4 to account for the dilution factor of the DNA within each well (100µl of PicoGreen reagent + 50µl TE for every 50µl of DNA sample) (**Figure 2.4**).

	Known DNA Standard (ng/mL)							
	0	**50**	**100**	**200**	**400**	**600**	**800**	**1000**
Fluorescence	6	68	122	217	430	627	817	961
	5	62	112	212	408	597	771	930
Average	5	65	117	215	419	612	794	946
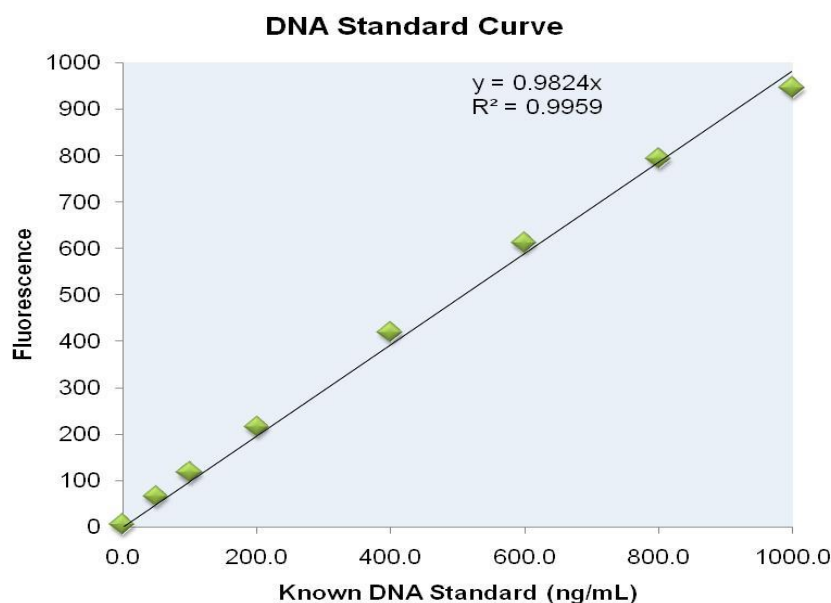
For example:

The DNA contents (ng/ml) of unknown samples with a fluorescent reading of 500 can be determined using the above calculated linear regression data from the standard curve:

$Y = a + bX$
$Y = 500$
$a = 0$
$b = 0.982$
$X = 500 / 0.982$
$X = 509.2$ ng/ml

Final concentration of unknown sample taking into account the dilution factor:
$= 509.2 \times 4$
$= 2039$ ng/ml

Figure 2.4 - Cell DNA contents were determined using PicoGreen analysis: *PicoGreen® double-stranded DNA (dsDNA) quantitation was used to quantify the concentration of total dsDNA (ng/ml) of unknown samples. DNA for unknown samples were extrapolated from the DNA standard curve using the linear regression formula $Y = a + bX$.*

2.5 Mineralisation

Osteoblasts produce an extracellular collagenous matrix that subsequently becomes mineralised by hydroxyapatite deposition (Coelho and Fernandes 2000, Jiang, et al 2013, McQuillan, et al 1995). Ascorbic acid promotes collagen secretion and serves as a cofactor for prolyl hydroxylase which catalyses the hydroxylation of proline residues, integral to the stability of the collagen triple helix (Franceschi, et al 1994, Murad, et al 1981). Ascorbic acid also upregulates osteoblastic ALP and osteocalcin genes expression (Franceschi, et al 1994, Rickard, et al 1994). Inorganic phosphates initiate mineralisation by providing a source of phosphates to OB cells for the formation of hydroxyapatite.

OB progenitor mineralisation was assessed using Alizarin red staining, an anthraquinone dye that binds to mineral deposits as confirmed by energy dispersive X-ray spectroscopy (Chang, et al 2000). OB progenitors were seeded in 48 well plates at a cell density of $6000cm^2$ and cultured in 250μl per well of standard MEM-alpha media for 72 hours. OB Cultures were differentiated in standard osteogenic Alpha-MEM media containing 4% FCS for up to 21 days. Osteogenic media was replaced from the OB cultures every 3 days. Mineralisation was assessed on various time points throughout differentiation. On these time points, the OB cultures were washed with 500μl of PBS and fixed in 100% ethanol for 1 hour on ice. To stain for mineral deposits, the wells were washed with PBS and incubated with 1% Alizarin red stain for 20 min on an orbital shaking platform. Excess stain was washed water until water ran clear. Stained cultures were also washed once with 200μl of 95% ethanol and plates air-dried overnight. The culture plates were scanned on a flatbed scanner and the percentage area of mineralisation per well was quantified using ImageJ (http://imagej.nih.gov/ij/). Values were expressed as a percentage response of the control.

2.6 Cell protein extraction

Cell protein extraction	
ITEM	**SUPPLIER**
Mammalian cell lysis buffer kit	Sigma-Aldrich
Protease inhibitor cocktail	Sigma-Aldrich
Phosphatase inhibitor cocktail 2	Sigma-Aldrich

Protein was extracted from cultured cells for protein quantification and subsequently western blotting analysis. Mammalian cell lysis buffer was prepared according to **Table 2.4**; 1ml of mammalian cell lysis buffer was prepared and 1/100 dilution of protease inhibitor cocktail was added immediately prior to cell lysing procedure. For phosphorylation studies, 1/100 dilution of phosphatase inhibitor cocktail was also added to the lysis buffer. Cells were initially counted to establish cell number using the haemocytometer counting protocol outlined in the method **section 2.1**.**3**.

Mammalian cell lysis buffer	
INGREDIENT	**Quantity**
Mammalian cell lysis buffer (kit): 5X buffer Tris-EDTA 5X Deoxycholic acid sodium salt 5X Igepal CA 630 5X Sodium dodecyl sulphate (SDS) 5XSodium chloride	1ml
Protease inhibitor cocktail	10µl
Phosphatase inhibitor cocktail 2: Sodium orthovanate Sodium molybdate Imidazole	10µl

Table 2.4 - *Preparation of mammalian cell lysis buffer.*

Media containing non-adherent cells were transferred into BD Falcon™ tubes and cells pelleted by centrifugation at 2000 RPM for 3 minutes. Media was removed from the cell pellets and pellets resuspended in 1ml of ice cold PBS. The PBS solution containing resuspended cells were transferred into 1.5ml eppendorf tubes and cells centrifuged for 1000 RPM for 5 minutes. PBS wash was removed from cell pellets. Lysis buffer was added to cell pellets and the cell/lysis buffer solution vortexed for 2 minute to ensure membranes had sheared. The volume of lysis buffer added was dependent on the number of cells counted before seeding. Generally for every 500,000 cells, 100µl of lysis buffer was added to the cell pellets. After the vortex mix, eppendorfs containing cells/lysis buffer were placed on ice on an orbital shaker and agitated at 500 RPM for 30 minutes.

Adherent cells cultured in 6 well culture plates containing adherent cells were placed on ice and the media removed carefully and quickly as to not disturb the cells. Cells were washed once with 1ml of ice cold PBS and lysis buffer added one well at a time. Based on proliferation assays, it was estimated that following cell seeding at a density of 6000 cell/cm^2 and at around 8 days in culture, each well within a 6 well plate contained approximately between 400,000 to 500,000 cells. 100µl of lysis buffer was added to each well and adherent cells were scraped off well surface using a plastic cell scraper one well at a time. The lysed cell solutions were transferred into 1.5ml eppendorfs and vortexed for 2 minute to ensure membranes had sheared. Samples were placed on ice on an orbital shaker and agitated at 500 RPM for 30 minutes.

Cells cultured in large T75 flasks were detached from the plastic surface by trypsination and resuspended in 1ml of ice cold PBS and counted using a haemocytometer as outlined in method **section 2.1.3**. Cell suspensions were transferred into 1.5ml eppendorf tubes and cells centrifuged for 1000 RPM for 5 minutes. PBS wash was removed from cell pellets and lysis buffer added. The volume of lysis buffer added to the cell pellet was dependent on the number of cells counted before seeding; in general the T75 flasks containing proliferating cells that were cultured for 8 days contained approximately 1.5×10^5 cells and were therefore lysed with 300µl of lysis buffer. Eppendorfs containing cell/lysis buffer solution were vortexed for 2 minute to ensure membranes had sheared and placed on ice on an orbital shaker and agitated at 500 RPM for 30 minutes.

Cell lysates were centrifuged at 13,000 RPM for 15 minutes at 4°C to remove any cell debris from the protein solution. The purified protein containing supernatants were transferred into fresh eppendorf tubes and the pellets discarded. A small volume (10-20µl) of lysate was retained to perform protein assay and the remnants aliquoted to avoid protein degradation as result of freeze thawing. Protein lysate aliquots were either stored at -20°C or diluted in Laemmli buffer in preparation for western blotting (**section 2.8**).

2.7 Bicinchoninic acid protein quantification assay

Bicinchoninic acid protein assay	
ITEMS	SUPPLIER
Mammalian cell lysis buffer	Sigma-Aldrich
7.5 % Bovine serum albumin (BSA)	Sigma-Aldrich
Bicinchoninic acid (BCA) solution	In-house
Copper (II) sulphate solution (4%)	Sigma-Aldrich
Plate reader Spectramax M5	Sunnyvale

Bicinchoninic acid (BCA) protein assay was performed to measure the concentration of protein in each sample. Copper ($Cu^{2}+$) ions were added to the sample and consequently reduced to $Cu^{1}+$ ions by the peptide bonds in the protein. As a result, the greater the amount of protein in the sample the greater the amount of $Cu^{1}+$ ions present. Two molecules of BCA chelate with each $Cu^{1}+$ ions and result in a green to purple colour product that strongly absorbs light at 563nm wavelength. At higher temperatures of around 37°C to 60 °C, peptide bonds stimulate the formation of the reaction product (Olson and Markwell 2007).

BCA was prepared by diluting Copper II sulphate ($CuSO_4$) 1:50 in BCA (for one 96 well plate, 250μl of $CuSO_4$ was added to 12.25ml of BCA). A stock solution of 1000μg Bovine Serum Albumin (BSA) was prepared from 7.5% BSA; 10μl of 7.5% BSA was diluted in 740μl of distilled water. Next, 7.4% BSA and cell lysis buffer were combined to obtain 1000, 800, 600, 400, 200, 100 and 0μg/ml of BSA as outlined in **Table 2.5**. 10μl of each BSA concentration was added to duplicate columns A and B on a 96 well culture plate. Unknown samples were diluted with lysis buffer and 10μl of each sample was also added to duplicate columns on a 96 well plate.

BSA standard curve for BCA assay		
BSA Concentration **(µg)**	**BSA Volume** **(µl)**	**Lysis Buffer Volume** **(µl)**
1000	10	0
800	8	2
600	6	4
400	4	6
200	2	8
100	1	9
0	0	10

Table 2.5 - *Preparation BSA standards ranging from 0 to 1000µg for the BCA assay.*

200µl of BCA/Copper II sulphate solution was added to each well. BCA assay was performed at 37°C in an incubator for 30 minutes. Colour change was quantified on a plate reader and values extrapolated standard protein solution. The absorbance was read at 562nm using a plate reader (Spectramax M5) and compared to the standard curve. Values from the standard curve were exported into Graphpad software (Prism V5) and un-known values extrapolated. Calculated values gave a standard amount of protein per sample (mg/ml). Based on the concentrations calculated, all protein samples within an experiment were diluted with lysis buffer to same concentration so limit any variability as a result of protein loading during western blot analysis.

2.8 Western blot

Western blotting	
EQUPTMENT	**SUPPLIER**
Mini PROTEAN electrophoresis system	Bio Rad
Mini Trans-blot cell	Bio Rad
Filter paper	Sigma-Aldrich
Kodax Biomax MS film	Sigma-Aldrich
Gel Doc XR+ System and the Quantity One software	Bio Rad
GS-710 Calibrated imaging densitometer	Bio Rad
Curix 60 film processor	Curix, AGFA

REAGENT	SUPPLIER
Molecular weight marker	Bio Rad
ß Mercaptorethanol	Sigma-Aldrich
Glycerol	Fisher
Bromophenol blue	National Diagnostics
ProtoGel resolving buffer - 0.4 M Tris-HCl, 0.1% SDS, pH 8.8	National Diagnostics
ProtoGel stacking buffer 1.0M Tris-HCL pH6.8	Life Sciences
Sodium dodecyl sulphate (SDS)	Sigma-Aldrich
30% Acrylamide	Geneflow, LTD
Ammonium persulfate (APS)	Sigma-Aldrich
TEMED	Sigma-Aldrich
Bovine serum albumin (BSA)	Sigma-Aldrich
SuperSignal*West Dura chemiluminescent substrate	Thermo-scientific
Methanol	Sigma Aldrich
Ethanol	VWR International
Skimmed milk powder	Marvel
0.05% PBS Tween	In-house
PBS tablets	Oxoid
Tween X20	VWR International

Western blotting is a technique used to identify and locate proteins based on their ability to bind to specific antibodies against these proteins. The proteins within a sample are separated using polyacrylamide gel electrophoresis (PAGE), where polyacrylamide gels and buffers are loaded with sodium dodecyl sulfate (SDS). SDS-PAGE maintains polypeptides in a denatured state once they have been treated with strong reducing agents to remove secondary and tertiary structures and allows separation of proteins according to their molecular weight.

2.8.1 Sample preparation

Protein samples (either recombinant protein or cell lysate) were mixed with 5X Laemmli buffer, one part buffer and four parts sample, in 0.5ml eppendorf tubes according to **Table 2.6**. Protein sample and buffer solutions were mixed by vortex and briefly pulsed in a microcentrifuge. Protein samples were denatured for 5 minutes at 96^{0}C on a hot block. Boiled samples were maintained on ice until the gel loading stage. Denatured protein samples were aliquoted into 0.5ml eppendorfs and frozen at -20°C.

5X Laemmli loading buffer	
INGREDIENT	**Quantity**
SDS	2g
0.5M TrisHCl pH 6.8+ 0.4% SDS	2.13ml
ß Mercaptorethanol	2.56ml
Glycerol	5.0ml
Bromophenol blue	0.1g

Table 2.6 - *Preparation of 5X Laemmli loading buffer*

2.8.2 SDS-PAGE and protein migration

For each experiment, two SDS gels were prepared constituting of a separating gel layer and stacking gel layer. The separating gel ingredients were combined in a 50ml BD Falcon™ tube according to **Table 2.7** and TEMED was added last to initiate the polymerisation reaction. The combined ingredients were mixed by vortexing the separating gel solution for 1 minute. Immediately the separating gel was cast between two glass plates. To maintain an even gel level and inhibit gel dehydration, 70% ethanol was added covering approximately 0.5cm of the top of the separating gel. Once the separating gel had set, all traces of the ethanol were removed by washing the gel three times using distilled water. All traces of water were removed by inserting a flat resorbing paper between the casting classes.

Separating gel		
INGREDIENT	**12%**	**10%**
Volume (ml)		
Distilled water	3.35	4.05
Resolving buffer	2.5	2.5
10% SDS	0.1	0.1
30% Acrylamide	4.0	3.3
10% APS	0.05	0.05
TEMED	0.05	0.05

Table 2.7 - *Preparation separating gel solution for 1 gel.*

The ingredients for the stacking gel were combined according to **Table 2.8**. TEMED was added to the stacking gel solution last, and the solution mixed by vortex for 1 minute. The stacking gel solution was poured immediately to the top of the separating gel and 8, 10 or 15 plastic tooth combs were inserted between the casting glass plates into the separating gel to create wells for loading of protein samples. The gels were allowed to set completely, usually requiring 15-20 minutes and the combs were removed.

Stacking gel	
INGREDIENT	**Volume (ml)**
Distilled water	6.1
Stacking buffer	2.5
10% SDS	0.1
30% Acrylamide	1.3
10% APS	0.1
TEMED	0.01

Table 2.8 - *Preparation stacking gel solution for 1 gel.*

The glass casting plates were placed into an electrophoresis tank. The central portion of the tank were the gel was placed, was filled with cold X1 running buffer and the buffer allowed to overflow into the tank to ensure bubbles did not interfere with the electrophoresis. Each tank required approximately 1 Litre of buffer. Each gel was loaded with 5-100µg of protein sample and 5µl of a 10-250kD horse radish peroxidase (HRP)-conjugated molecular marker was pipetted into the first (and sometimes last) lane of each gel. For the migration of proteins, samples were run through the stacking gel for 45-60 minutes at 60 Volts per gel at room temperature and further run through the separating gel for a further 60-120 minutes at 100 Volts.

10 X Running buffer *100ml added to 900ml distilled H_2O for X1 working solution*	
INGREDIENT	**Amount**
Distilled water	500ml
0.25M Tris	15.13g
0.2M Glycine	75.05g
1% SDS	5g

Table 2.9 - *Preparation of 1 litre of 10X running buffer.*

2.8.3 Transfer

Following protein migration, the stacking gels were cut off from the remainder of the gel and discarded. The separating gel was carefully dislodged from the glass pane. An arrangement constituting of a scouring pad, two pieces of cellulose blotting paper and a piece of polyvinylidene fluoride (PVDF) membrane previously soaked in methanol for 20 seconds, were placed within an open transfer cassette. The gel was placed onto the PVDF membrane (marker facing top left of membrane). The PVDF membrane was cut slightly on the left upper corner to indicate the position of the first lane containing protein sample. The PVDF membrane was sandwiched with another two pieces of cellulose blotting paper and a scouring pad. The cassette was closed firmly and placed into an electrophoresis tank. The tank was then filled with 1 Litre of 1X transfer buffer, prepared according to **Table 2.10**. The transfer buffer was kept cool using an ice pack, which was placed at one side of the tank. A magnetic stirrer was also placed in the centre of tank to distribute the temperature within the tank and also stir the buffer solution. Membranes were blotted at 70V for 60-70 minutes (depending on the size of the protein) at 4ºC in a cold room.

10 X Transfer buffer *100ml added to 900ml distilled H_2O for X1 working solution*	
INGREDIENT	**Amount**
Distilled water	500ml
20% Methanol	100ml
0.25M Tris	15.13g
0.2M Glycine	75.05g

Table 2.10 - *Preparation of 1 litre of 10X transfer buffer.*

2.8.4 Blocking and immunological detection

Each membrane was removed from the transfer cassettes and placed in 20ml of 5% milk blocking solution for 1 hour on an orbital shaker at room temperature. Probing with primary antibody varied depending on the antibody being used. Primary antibody was added in the membrane blocking solution and either incubated overnight at 4ºC or for 2 hours at room temperature. Each membrane required at least 10ml of primary antibody solution to be submerged completely and evenly in flat square polystyrene containers. The primary antibody was removed and the membrane was washed 3 times in 0.05% PBS-Tween, for 20 minutes per wash on an orbital shaker at room temperature. Next, membranes were incubated with secondary antibody prepared in 5% milk for 1 hour on an orbital shaker at room temperature. Membranes were washed again with 0.05% PBS-tween X3 20 minute washes.

0.05% PBS-Tween washing buffer	
INGREDIENT	**Quantity**
Distilled water	2L
PBS tablets	20 Tablets
Tween X20	1ml

5% Milk blocking solution	
INGREDIENT	**Quantity**
Skimmed milk powder	5g
0.05% PBS Tween	100ml

Table 2.11 - *Preparation of 0.05%PBS-Tween washing buffer and 5% milk blocking solution.*

The detection method for protein is dependent on the enzyme to which the secondary antibody is conjugated. HRP is the most common enzyme used in western blotting, and the substrate used for detection is known as chemiluminescent substrate (**Figure 2.4**). For visualisation of bands, the membranes were incubated in the dark for 5 minutes with Supersignal West Dura chemiluminescent substrate made from equal volumes of peroxidase and enhancer mixed together. Blots were developed in a dark room on photographic paper using an automated film processor. Protein bands on X-ray films were inspected using the GS-710 Calibrated imaging densitometer and the Quantity One software.
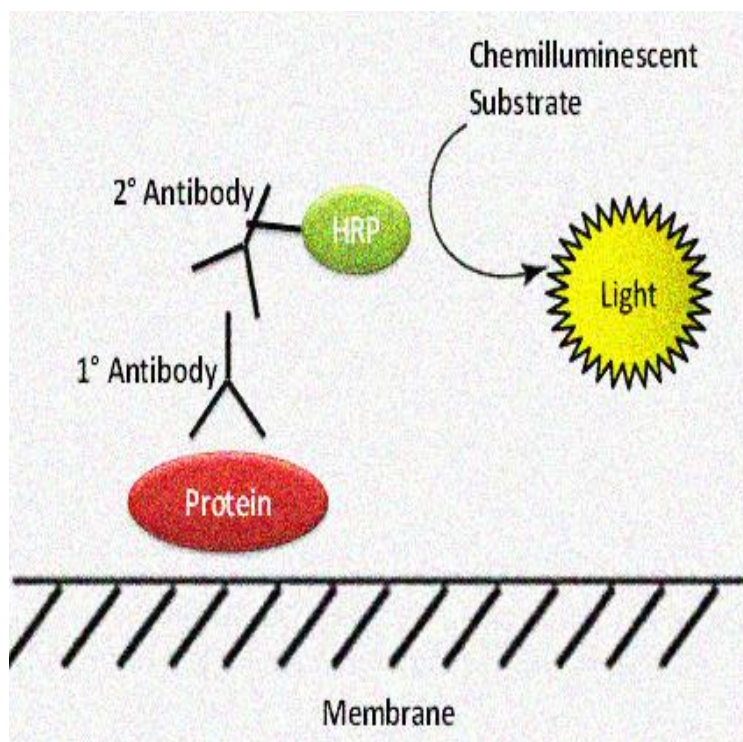
Figure 2.5 - Diagrammatic representation of immunological protein detection using chemiluminescent substrate in western blot: *Anti-antigen IgG antibody binds to its specific antigen which is bound to the blot. The species-specific secondary HRP-conjugated antibody binds to the protein-primary antibody complex. A HRP chemiluminescent substrate is introduced to the complex which is bound to the blot, and the emitted X-ray light is captured on film.*

2.8.5 Membrane stripping

Antigens on the membranes were 'stripped' of their primary and secondary antibody complexes using a mild stripping buffer according to the Abcam® protocol. Membrane stripping was performed for the detection of multiple proteins on the same blot, for instance a protein of interest and a loading control. In brief, the stripping buffer was prepared according to **Table 2.12** and adjusted to pH 2.2. Each membrane was incubated with 10ml of stripping buffer for 10 minutes on an orbital shaker. The buffer was discarded and the membrane washed twice with 10ml of PBS followed by one wash with 0.05% PBS Tween. The membrane was then blocked in 5% milk solution as outlined in **section 2.8.4**.

Stripping buffer	
INGREDIENT	**Quantity**
Distilled water	1 L
Glycine	15 g
SDS	1 g

Table 2.12 - *Preparation of 1 litre of mild stripping buffer.*

2.9 Flow cytometry

Flow Cytometry	
ITEM	**SUPPLIER**
Formalin solution	Sigma Aldrich
Bovine serum albumin (BSA)	Sigma-Aldrich
FACS perm buffer	BD Phospflow
Triton X	Invirtrogen
BD Falcon™ round bottomed flow cytometry tubes	BD Biosciences
BD FACSCalibur™ platform and Cell Quest software	BD Biosciences

Flow cytometry is a quantitative method used for the analysis of various parameters including cell surface expression, detection of intracellular molecules and characterisation of different cells types within a heterogeneous cell population. Flow cytometry enables simultaneous analysis of single cells by measuring the fluorescence intensity produced by fluorescent labeled antibodies that are specific for the molecule of interest. Cells are pushed through a fluidic system in a monolayer and several prisms and lenses direct a laser light to the cuvette where it intercepts with the cells. It is at this point that the information associated with the fluorescence and scatter of each individual cell can be obtained. Light scattered in the forward direction is collected by the Forward Scatter Channel (FSC) photodiode and provides information on the cells relative size. Light measured at a 90° angle to the excitation beam of the laser is collected by the Side Scatter channel (SSC) photomultiplier tube (PMT) and is used as a measure of the relative granularity of the cell. Fluorescent light associated with a cell is detected by individual fluorescence channels (FL). The data generated is either plotted in a single dimensional histogram or in a two-dimensional dot plot or in some cases, in three dimensions. Based on fluorescence intensity, the regions on plots can be separated using subset extractions or 'gates'.

Flow cytometry was used to determine the presence of specific proteins in cells cultures. Cells were seeded at a density of 6000cm^3/ml in T25 or T75 flasks. Media was removed from the cell cultures. The cells in T25 flasks were washed with 5ml of ice cold PBS and cells cultured in T75 flasks were washed with 10ml of ice cold PBS. Adherent cell cultures were detached from the plates or flask surface by trypsinisation as outlined in **section 2.1.3.** Adherent cells were resuspended in 1ml of ice cold PBS in 1.5ml eppendorfs, transferred to 1.5ml eppendorfs and chilled on ice. Non-adherent cell cultures were centrifuged at 2000 RPM for 3 minutes and the supernatant discarded. The cell pellets were resuspended in 1ml of ice cold PBS in 1.5ml eppendorfs and chilled on ice.

The cell pellets resuspended in PBS were centrifuged at 2000 RPM for 3 minutes on a bench-top microcentrifuge. The supernatant was discarded and cells fixed with 300μl of 4% Formalin per 1x10^5 cells for 10 minutes at room temperature in the dark on a rotator. Cells were washed twice in 1ml of PBS (washing refers to the addition of PBS followed by centrifugation at 2000 RPM for 3 minutes). Cell pellets were re-suspended in 0.1% Triton-X to permeabilise membranes for 10 minutes at room temperature in the dark on a rotator. Cells were washed twice with PBS to remove all traces of fixative and detergent. Cells were then blocked in 10% normal serum originating from the species in which the secondary antibody was produced. The 10% normal serum was made up in 0.5% BSA solution and cell pellets were blocked in 300μl serum per 1x10^5 cells in the dark for 30 minutes at room temperature. Cells were washed twice with PBS. Supernatant was removed thoroughly by inversion on an absorbent paper surface to remove all liquid. Pellets were resuspended in 40μl of X1 Sample Perm buffer and 20μl of this cell suspension was transferred to another tube. Each of the 20μl cell suspensions was incubated with either 100μl of primary antibody or 100μl of isotype control antibody (at the same concentration of as the primary antibody) made up in 3% BSA for 30 minutes in the dark. Cell suspensions were washed twice with PBS ensuring all the liquid was removed completely following the final wash. The cell pellets were resuspended in 100μl of species-specific biotinylated secondary antibody and incubated in the dark for 30 minutes. Cells were washed twice in PBS and 300μl of X1 Sample Perm buffer was added to cells. The cells were centrifuged at 2000 RPM for 3 minutes and re-suspended in 300μl of Sample Perm buffer. Samples were transferred to flow cytometry tubes prior to analysis. Flow cytometric analysis was performed using the BD FACSCalibur™ platform and the data analysed using the Cell Quest software. Cells of interest were sorted through

three modes of scatter plot; FSC vs SSC, single color vs. SSC and a two-colour fluorescence plot. GFP-cells were detected through FL4 fluorescence channel and all other through the FL2 fluorescence channel. Analysis of results was carried out by gating around the viable cells and the presence of the protein of interest was detected through comparison with isotype antibody staining. The threshold for the isotype controls were set at >1% on the scatter plots. The same gating used for the isotype controls were copied and pasted onto the scatter plots of corresponding samples.

2.10 Cell sorting

Flow cytometers are capable of sorting cell populations of purified cells with specific characteristic from mixed cell populations. The stream of cells, which have been passed though the sheath fluid and are required for sorting, are passed through a narrow vibrating orifice. This results in the breakup of the cell steam into droplets containing cells. The period of time between the cells passing through the laser as a stream and then as droplets, is regulated. The cells of interest within the droplets become charged and subsequently flow through high-voltage deflection plates. The charged droplets are deflected appropriately into a collection vessel and any uncharged droplets are disposed into the waste container. Co-cultures were separated into their individual populations using the FACS Aria Cell sorter. Cells were cultured alone or co-cultured with a different cell type. Media was removed from the cells cultured in T25 or T175 and the cells washed once with 5ml or 10 ml of PBS, respectively. Adherent cell cultures were detached from the culture surface by trypsinisation as outlined in **section 2.1.3.** Cell pellets were resuspended in 1ml of PBS. Non-adherent cell cultures were transferred from the culture flasks into BD Falcon™ tubes and centrifuged at 2000 RPM for 3 minutes. The supernatant was discarded and the cell pellets were resuspended in 1ml of PBS. Protein and RNA were isolated from sorted samples as outlined in **sections 2.5** and **2.12**, respectively.

2.11 Immunofluorescent microscopy

Immunofluorescent microscopy	
REAGENTS	**SUPPLIER**
Poly-L-lysine	Sigma-Aldrich
Sterile distilled water	In-house
Formalin solution, neutral buffered	Sigma Aldrich
Triton-X	Invirtrogen
DAPI in mounting reagent	Duolink
Glass cover slips	Menzel-Glasser

Immunofluorescent microscopy is performed to detect the presence of proteins of interest in microbiological samples with the use of a fluorescent microscope. This technique uses the specificity of antibodies to their antigen to target fluorescent dyes to specific biomolecule targets within a cell, allowing the distribution of the target molecules within a sample to be visualised. Immunofluorescence is a widely used example of immunostaining which effectively makes use of fluorophores to visualise the location of the antibodies.

Immunofluorescent microscopy was performed to determine the presence of specific cellular intracellular and extracellular proteins. Non-adherent cells were attached to the surface of culture plates using sterile tissue culture grade Poly-L-lysine polymer reagent. The culture surface was aseptically coated with 1.0 mL/25 cm^2 of the Poly-L-lysine, with gentle rocking to ensure even coating of the culture surface and aspirated after 5 minutes. The culture surface was thoroughly rinsed using sterile tissue culture grade water. The culture surface was allowed to dry thoroughly for 4 hours before introducing cell cultures. Cells were cultured at the same cell density of 6000cm^2 in 8 well slide chambers (BD Falcon^{TM}), 24 or 48 well plates. Media was removed from the adherent cell cultures and the cells washed once with 1ml of ice cold PBS (washing refers to the addition of PBS to

the cell cultures and removal of PBS). The cell cultures were fixed with 4% Formalin for 10 minutes at room temperature in the dark. Cells were washed twice in 1ml of PBS and cell membranes were permeabilised using 0.1% Triton X for 10 minutes at room temperature in the dark. The volume of PBS, fixative and permeabilisation reagent was dependent on the well size/cell density (**Table 2.13**).

Cell culture plate	Volume of PBS, 4% formalin and 0.1 Triton X per well
8 well slide chamber	200µl
24 well plate	500µl
48 well plate	300µl

Table 2.13 - *The volume of PBS, fixative and permeabilisation reagent used in immunofluorescence microscopy were dependent the size of each well within the culture plate.*

Cells were washed twice with PBS to remove all traces of fixative and detergent. Non-specific antigen-antibody binding in cell cultures was minimized by using 10% normal serum diluted in 0.5% BSA solution. The normal serum used originated from the species in which the secondary antibody was produced. Cell cultures were blocked in 10% normal serum in the dark for 30 minutes at room temperature on a shaker. The blocking solution was removed from cell cultures and the cells incubated with a primary antibody specific to the antigen of interest or an antibody isotype control.

Unconjugated antibodies were made up (concentrations optimised) to the required concentrations in 3% BSA solution. Depending on the size of the plate/chamber, cells were incubated with 200-500µl of unconjugated primary/isotype antibody over night at -4°C. Cell cultures using a biotinylated-primary antibody system (no secondary antibody required) were incubated with the antibody for 1 hour at room temperature in the dark. The culture plates were wrapped in parafilm to prevent evaporation and cell dehydration. The cell cultures were washed twice with PBS for 3 minutes on a rotator.

Cell cultures that had been stained with an unconjugated primary/isotype antibody were incubated with biotinylated secondary antibody prepared in 3% BSA for 1 hour at room temperature in the dark on a rotator. The cell cultures were washed twice with PBS for 3 minutes on a rotator. All PBS was removed completely from the cell cultures and one drop of DAPI mounting reagent added to visualise nuclear staining. Slides and wells were mounted with coverslips and cellular staining observed by the Leica DM16000 Inverted microscope and analysed by corresponding AF6000LX software. The DAPI blue staining was visualised through filter cube A4, far-red APC staining visualised though filter cube Y5 and the green staining via the L3 filter. To allow for direct comparisons between the isotype control and positive staining, images were captured at the same exposure, gain and intensity setting within each experiment.

2.12 Immunohistochemistry

ITEMS	SUPPLIER
Ethanol	VWR
Xylene	VWR
Haematoxylin solution	Merck
1% Eosin solution	VWR
Trypsin enzyme digestion kit	Menarini Diagnostics
Formalin solution, neutral buffered	Sigma Aldrich
Hydrogen peroxide 30%	Suprapur®
DAB substrate-chromogen system	Vector
Glass cover slips	Menzel-Glasser
Aperio® ScanScope slide scanner	Leica Biosystems
Microscope DMI4000	Leica Biosystems

Immunohistochemistry

Immunohistochemistry is the technique used for the detection of antigens within cells of a tissue section using the principle of specific antibody-antigen interaction. Immunohistochemical staining is widely used in basic research to establish the distribution and localization of biomarkers in biological tissue. Antibody-antigen interactions can be visualised using an antibody-conjugated enzyme, such as peroxidase, which catalyses a colour-producing reaction. Immunohistochemistry analysis was performed according to Nakane et al (Nakane and Pierce 1966) with protocol modifications proposed by Clausen et al (Clausen, Blish et al. 2011).

In brief, tissue fixation, embedding and processing were performed by our in-house Bone Analysis Laboratory facility. Briefly, tissue sections were fixed in paraformaldehyde (PFA) and decalcified for 7 days, with solution change every 3 days. The tissue sections were processed through graded alcohol solutions ad xylene overnight. Sections were embedded longitudinally in paraffin wax contained in a square mould, according to embedding machine manufacturer's instructions. The tissues were cut in 3µm thick sections at 2 levels 50µm apart, using a rotatory microtome (Leica Microsystems) and

mounted on positively-charged Superfrost®PLUS slides. When required for immunohistochemical analysis, the tissue sections were first de-waxed by immersing the tissues in various solvents solutions in 5 steps for 4 minutes per step; xylene, xylene, 99% ethanol, 99% ethanol, 95% ethanol and 70% ethanol. Tissue sections were hydrated in running water for 2 minutes.

A humid environment was prepared for tissue sections by moistening immunohistochemistry staining slide trays with distilled water. Heat-activated antigen retrieval was performed using 1:3 dilution of trypsin enzyme. The Trypsin was pre-heated in a 37ºC incubator for 30 minutes. Tissue slides were placed in the pre-moistened staining slide trays and 100µl of trypsin placed on each tissue section for 10 minutes at room temperature. Tissue sections were placed in staining racks containing PBS and placed on a rotator for 3 minutes. The PBS was discarded and tissue slides submerged in fresh PBS and washed again for 3 minutes. The tissue slides were removed from the staining racks and returned to the staining tray. The slides were tapped to discard any remaining PBS. A wax isolator pen was used to circle the area around the tissue, creating a reservoir surrounding the tissue.

Tissue sections were incubated with 100µl of 3% hydrogen peroxide for 30 minutes at room temperature. The tissue sections were placed into staining racks containing PBS and washed twice. Sections were placed back in the staining trays and blocked with 100µl of 10% normal serum blocking solution for 30 minutes at room temperature. The species from which the normal serum originated was dependent on the species from which the secondary antibody was produced. Unconjugated antibodies were made up (concentrations optimised) to the required concentrations in 3% BSA solution.

Tissue sections were tapped gently on absorbent paper to remove blocking serum and then incubated with 100µl of unconjugated primary/isotype antibody over night at -4ºC. The tissue sections were placed into staining racks containing 0.05% PBS-Tween. Sections were washed twice for 3 minutes per wash on a rotator. Secondary biotinylated antibody was made up in normal serum to an optimal concentration. Sections were replaced into staining trays and incubated with 100µl of 1:500 dilution of secondary biotinylated antibody. The tissue sections were placed into staining racks and washed twice with 0.05% PBS-Tween for 3 minutes per wash on a rotator. To enhance antibody-

antigen detection, sections were placed back in the staining trays and incubated with 100µl of 1:300 Streptavidin solution for 30 minutes at room temperature. Sections were washed twice with 0.05% PBS-Tween for 3 minutes per wash on a rotator.

Antibody-antigen specific staining was developed with DAB chromogen as per supplied kit; 1 drop of DAB was placed into 1ml of DAB buffer. Tissue sections were incubated with 100µl of the DAB solution for 5 minutes in the dark at room temperature. The tissue sections were placed into staining racks and washed under tap-water for 5 minutes. Tissue sections were counterstained with Gills haematoxylin for approximately 20 seconds and excess stain removed by washing sections gently under running tap water for 2-3 minutes.

The tissue sections were dehydrated in solvent in consecutive steps; 70% ethanol for 12 seconds, 95% ethanol for 12 seconds, 99% ethanol for 12 seconds, 99% ethanol for 12 seconds, xylene for 30 seconds and xylene for 2 minutes. The sections were mounted with DPX and cover-slips and allowed to dry in a ventilated environment. Slides were scanned and images captured using the Aperio® ScanScope slide scanner or an upright light microscope (DMI4000, Leica Biosystems).

2.13 RNA Extraction

RNA Extraction	
ITEM	**SUPPLIER**
ReliaPrep™ RNA cell miniprep system: ReliaPrep™ minicolumns (50/pack) Collection tubes (50/pack) Elution tubes (50/pack) BL buffer Column wash solution (CWE) 1-Thioglycerol (TG) Nuclease-free water Yellow core buffer RNA wash solution (RWA) MnCl2, 0.09M DNase I (lyophilized)	Progema
Molecular-grade isopropanol	Sigma-Aldrich
95% Molecular-grade ethanol	Sigma-Aldrich
Individual PCR tubes, 0.5 ml and 1.5ml	Thermo-Scientific
384-Well standard PCR plates	Thermo-Scientific
Microseal® 'B' adhesive seals	Bio Rad

Prior to RNA extraction, the following reagents were prepared:

DNase I

Lyophilised DNase I was reconstituted with 275µlof nuclease-free water (provided) as indicated on the vial label. The vial was gently mixed by swirling the vial of solution. A total of 3µl of rehydrated DNase I was required per RNA purification. The rehydrated DNase I was stored at –20°C for up to 6 months.

BL-TG buffer

The BL-TG buffer was prepared by adding 325µl of 1-thioglycerol (TG) to 32.5ml of BL buffer. The BL-TG buffer was stored at 2°C–10°C for up to 30 days.

RNA wash solution

RNA wash solution was prepared by adding 60ml of 95% molecular grade ethanol to the bottle containing 35ml of concentrated RNA wash solution and stored at +15°C to +30°C.

Colum wash solution

Column wash solution was prepared with the addition of 7.5ml of 95% molecular grade ethanol to the bottle containing 5ml of CWE. The column wash solution was stored at +15°C to +30°C.

2.13.1 Column based RNA isolation

RNA was extracted from cell cultures using the column-based ReliaPrep RNA cell Miniprep kit. RNA was extracted from adherent cells cultured in multiwall plates or flasks. The media from the cell cultures was removed and the cells washed with ice-cold sterile PBS followed by the addition of BL-TG buffer in a volume that was dependent on the estimated number of cells within each well or flask. RNA shearing was assisted with repeated pipetting of the lysate over the well surface. Non-adherent cell cultures were transferred into BD Falcon™ tubes and centrifuged at 1000 RPM for 5 minutes at room temperature. The supernatant was discarded and the cell pellets were washed in ice-cold PBS followed by the addition of BL-TG buffer in volumes according to **Table 2.14**. Lysates for adherent and non-adherent cell cultures were collected and transferred to PCR-grade microcentrifuge eppendorfs. Isopropanol was added to cell lysates in 1:3 ratios; as an example, cells cultured in 6 well plates were lysed with 250µl of lysis buffer and 85µl of isopropanol was added to the lysed cells. The cell lysate and isopropanol were mixed thoroughly by vortex for ~10 seconds.

Manufacturer recommended wash and lysis volumes for harvesting adherent cells			
Plate/flask	PBS wash volume per well	Volume of BL-TG buffer	Volume of isopropanol
96-well	100 µl	100 µl	35µl
48-well	250 µl	100 µl	35 µl
24-well	500 µl	100 µl	35 µl
6-well	2.0 ml	250 µl	85 µl
T-25	5.0 ml	500 µl	175 µl

Table 2.14 – *The manufacturer recommended wash and lysis buffer volumes used for harvesting adherent cells*

For each sample, a ReliaPrep™ minicolumn was placed into a collection tube and cell lysate transferred to the minicolumn. The lysate was centrifuged at 12,000 RPM for 30 seconds at room temperature. The supernatant was discarded from the collection tube and 500µl of RNA Wash Solution was added to the minicolumn and centrifuged at 12,000 RPM for 30 seconds. The collection tube was removed the supernatant discarded. The RNA sample was DNase treated to remove any genomic DNA contamination. In a sterile tube, 30µl of DNase I solution was prepared by combining 24µl of Yellow Core buffer, 3µl 0.09M MnCl2 and 3µl of DNase I enzyme per sample. The DNase I was mixed by pipetting and 3µl of freshly prepared DNase I solution was transferred directly to the membrane inside the minicolumn. RNA was incubated with DNase I solution for 15 minutes at room temperature.

Next, 200µl of Column Wash solution was added to the minicolumn and centrifuged at 12,000 RPM for 15 seconds. 500µl of RNA Wash Solution was transferred into the minicolumn and centrifuged at 12,000 RPM for 30 seconds and the supernatant was discarded from the collection tube. The minicolumn membrane was washed a final time with 300µl of RNA Wash Solution and centrifuged at 13,000 RPM for 2 minutes. The minicolumn was transferred to a new Elution tube, and nuclease-free water added to the membranes, ensuring the entire surface of membrane was covered with the water provided with the ReliaPrep™ Kit. The volume of water required to elute the RNA was dependent on the original number of cells cultured within the well/flask as recommended

by the manufacturer (**Table 2.15**). The minicolumn was centrifuged at 13,000 RPM for 1 minute. The elution tube containing the purified RNA was stored at –80°C.

Recommended volume of nuclease-free water	
Cell number	**Nuclease-free water**
1×10^2 to 5×10^5	15µl
$>5 \times 10^5$ to 2×10^6	30µl
$>2 \times 10^6$ to 5×10^6	50µl

Table 2.15 – *The addition of nuclease-free water required to elude the purified RNA was dependent on the original number of cells cultured in the well or flask.*

2.13.2 RNA quantification

Nucleic acid concentration and purity were quantified using the NanoDrop-1000 spectrophotometer (Thermo scientific) at an absorbance of 260nM (A_{260}) and 280nM (A_{280}). 1µl of RNA or DNA sample were required for the NanoDrop analysis. The concentration of nucleic acid was determined using the Beer-Lambert law, which calculates the change between light absorbance (**A**), the sample concentration (**c**) the specific extinction coefficient (**ε**) and the length of the pathway the light travels through the absorber (**l**), which is specific for every spectrophotometer:

The Beer-Lambert Law: A = εlc

As an A_{260} reading of 1.0 was equivalent to approximately 40 µg/ml of RNA, the absorbance at 260 nm was used to determine the RNA concentration in an unknown sample. A $A_{260/}A_{280}$ ratio between 1.8 and 2.2 was considered an indicator of 'clean' RNA, which was free from contamination.

2.14 Reverse transcription-polymerase chain reaction (RT-PCR)

Reverse Transcription and PCR

REAGENTS	SUPPLIER
RNAase-free eppendorfs	Alpha Laboratories
DEPC-treated water	Ambion® Life Technologies
100mM DNTP mix	Thermo-scientific
Random primers supplied at 3µg/µl in 3mM	Invirtrogen
Oligo(dT) 20 primer supplied at 50 µM.	Invirtrogen
5X First-strand buffer 375 mM KCl	Invitrogen
0.1M DTT	Invitrogen
RNasIN recombinant RNase inhibitor	Invitrogen
Superscript® III supplied at 200Unites/µl	Invitrogen
End-point PCR primers	Eurofins/MWS
KAPATaq ready mix kit	Kappa Biosystems
Gel Doc XR+ system	BioRad
Quantity One software	BioRad
Taqman gene expression assays	Applied Biosystem
2X Taqman universal master mix	Applied Biosystem
ABI 7900HT Platform	Applied Biosystem
Agarose	Sigma-Aldrich
Tris/Borate/EDTA (TBE) buffer	Applichem
Ethidium bromide	BioRad
Full range100 BP DNA ladder	Norgen
X5 DNA loading buffer	Kappa Biosystems

PCR is the *in-vitro* enzymatic amplification of a specific DNA sequence involving multiple cycles of template denaturation, primer annealing, and primer elongation. In the denaturation stage, the two strands of cDNA are cleaved. A temperature of 94ºC is required to denature the DNA due to the extremely strong stacking interactions and hydrogen bonds between the two stands. In the annealing step, specific oligonucleotide or primers anneal with their specific target sequences in each of the single stranded DNA templates. The annealing temperature typically ranges between 53ºC and 65ºC, depending on the length and guanine/cytosine (G/C) ratio of the primer.

In the final elongation step, thermo-stable Taq polymerase replicates a DNA strand starting from the 3' end of the primer and synthesising new DNA in a 5' to 3' direction. The Taq polymerase is stable and active at high temperatures, typically to temperatures of 72ºC. The PCR process is exponential in that the amplified products from each previous cycle serve as a template for the next amplification cycle. Typically, abundant amplification product is produced following 20 to 40 cycles of PCR. As a result this technique is highly sensitive and effective for detecting specific nucleic acids sequences.

2.14.1 Primer design

Primer pairs were designed through the NCBI/BLAST software and ordered from Sigma Aldrich. Primers were designed on separate exons were possible, were 18-20 amino acids and contained 50% G/C ratio. The sequences of primers were checked by Blast. On arrival, the lyophilised primers were dissolved in DEPC-treated water to obtain a working concentration of 10μM.

Oligo Name	Sequence (5' -> 3')	Melting temperature	Amplicon size
SOSTDC1f	CCGTCATGCTTCTCAGTTTC (20)	65	198 bp
SOSTDC1r	GCTGTCACACTCCAAGGGCC (20)	65	198 bp
GAPDH f	TTGTCAGCAATGCATCCTGC (20)	57	354bp
GAPDH r	GCTTCACCACCTTCTTGATG (20)	57	354bp

Step	Temperature	Time
Hot start PCR-denaturation	T= 95℃	2 minutes
Second denaturation step	T=95℃	1 minute
Primer annealing temperature	hSOSTDC1= 65℃ GAPDH= 57℃	1 minute
Extension	T=72℃	1 minutes
Repeating 35 cycles		
Last extension	T=72℃	5 minutes
Hold at 4℃		

Table 2.16 - *The sequences and the optimal PCR conditions for the reverse and forward primers specific to SOSTDC1 and GAPDH.*

2.14.2 Reverse Transcription and cDNA production

Reverse transcription (RT) is a procedure based on the activity of the reverse transcriptase enzyme to catalyze the conversion of RNA template to complementary DNA (cDNA), required for the process of polymerase chain reaction (PCR) **(Figure 2.5).** Synthesis of cDNA is performed using a short piece of single-stranded DNA known as oligo(dT), which anneals to the stretch of the poly-A tail at the 3' end of most mRNA molecules. Although oligo(dT) primers are highly specific to mRNA, they have the limitation of initiating RT at the 3´ end of the transcript resulting in incomplete cDNA synthesis.
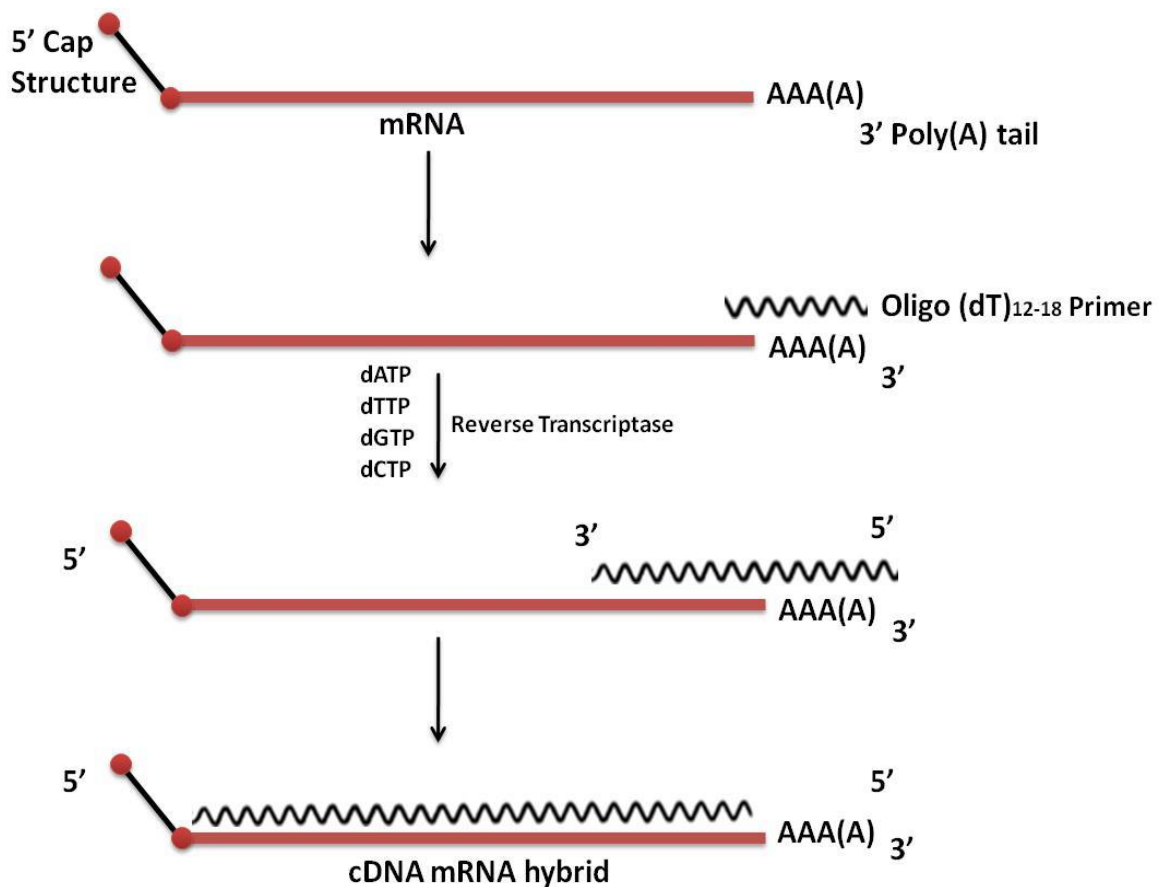
Figure 2.6 - Reverse Transcription (RT) and cDNA production: *Oligo(dT) and random primers can be used in RT to enable higher cDNA yield. Deoxynucleotide triphosphates (dNTPs) and under optimal salt and pH conditions, the RT enzyme extends a primer complementary to the RNA, producing cDNA.*

In all experiments, RNA samples were converted to cDNA using SuperScript III following manufacturer's instruction. Briefly, RNA samples isolated fresh or thawed from the -80°C storage were placed on ice for 20 minutes prior to the RT reaction. The working environment was sterilised using RNase*Zap*® RNase decontamination solution to eliminate RNases and this was followed by sterilisation with 70% ethanol. RNase-free eppendorfs, DEPC-treated water, pipettes and eppendorf racks were placed into a UV hood and irradiated for 20 minutes.

In the RNase-free eppendorfs, 150ng-2µg of total RNA was isolated and quantified as outlined in **Section 2.12.** RNA was prepared in a total volume of 11 µl with DEPC-treated water. For each RNA sample, a corresponding no-RT sample (RT-ve) was also prepared containing no RT enzyme (SuperScript III) to detect any DNA contamination. In addition, for every biological experiment, a no-RNA control was also included, in which DEPC-treated water was substituted for RNA in order to detect any contamination in the water (RT-$H_2$0).

The following were added to 11µl of RNA; 0.25µl of random primers, 0.25µl of oligo (dT), 1.0µl 100mM dNTP and 1.0µl of DEPC-treated water. The reaction was heated to 65°C for 5 minutes on a Thermo Cycler and chilled on ice for approximately 2 minutes. The second part of the RT reaction was prepared in two separate tubes; one tube containing RT Superscript III enzyme and the other containing DEPC-treated water as a substitute for Superscript III. Each cDNA synthesis reactions contained 4µl of First Strand buffer, 1µl of 0.4M DTT, 1µl of RNAseIN and 1µl Superscript III (RT+ve) or DEPC (RT-ve). Each tube containing a total volume of 20µl of RNA/Supercript III or RNA/DEPC-treated water was incubated at 25°C for 5 minutes, 50°C for 60 minutes and inactivated at 70°C for 15 minutes. The synthesised cDNA was stored at -20°C for short period and -80°C for longer term storage.

2.14.3 Polymerase Chain Reaction

Polymerase chain reaction (PCR) is the *in-vitro* enzymatic amplification of a specific DNA sequence involving multiple cycles of template denaturation, primer annealing, and primer elongation. In the denaturation stage, the two strands of cDNA are cleaved. A temperature of 94ºC is required to denature the DNA due to the extremely strong stacking interactions and hydrogen bonds between the two stands. In the annealing step, specific oligonucleotide or primers anneal with their specific target sequences in each of the single stranded DNA templates. The annealing temperature typically ranges between 53ºC and 65ºC, depending on the length and guanine/cytosine (G/C) ratio of the primer.

In the final elongation step, thermo-stable Taq polymerase replicates a DNA strand starting from the 3' end of the primer and synthesising new DNA in a 5' to 3' direction. The Taq polymerase is stable and active at high temperatures, typically to temperatures of 72ºC. The PCR process is exponential in that the amplified products from each previous cycle serve as a template for the next amplification cycle. Typically, abundant amplification product is produced following 20 to 40 cycles of PCR. As a result this technique is highly sensitive and effective for detecting specific nucleic acids sequences.

2.14.3.1 End-point PCR

The traditional PCR method of using agarose gels for the detection of final phase PCR amplification is referred to as End-point-PCR. Products of End-point PCR can be visualized on an ethidium bromide-stained agarose gel. The reaction includes a template (genomic/plasmid DNA and cDNA), forward primer, reverse primer, reaction buffer, magnesium, dNTP mix, and a thermostable DNA polymerase. The forward and reverse primers are specific to a sequence within the template and determine the length of the amplified product. Taq DNA polymerase is the most routinely used thermostable polymerase in amplifications. The concentration of magnesium ions have a direct effect on a range of factors including; enzyme activity, primer annealing, the template melting temperature and primer-dimer formation.

PCR was performed using KAPATaq Ready Mix kit (Kappa Biosystems) following manufacturer's instructions. Primer pairs were designed using the Primer3 software

(http:Frodo.wi.mit.edu/primer3) and ordered from Sigma Aldrich. On arrival, the lyophilised primers were dissolved in DEPC-treated water to obtain a working concentration of 10μM. The PCR reaction mix per cDNA sample comprised; 1-3 μl of cDNA (synthesised from 150ng-2μg of RNA), 2μl of 50mM magnesium chloride, 2μl of 10x NH_4 reaction buffer, 1μl of dNTP mix 10mM, 1μl of 10 μM forward primer, 1μl of 10 μM reverse primer, 1μl of DNA polymerase, 1μl of loading buffer and DEPC-treated water to make up 20μl total reaction volume.

For each experiment, the cDNA was also replaced with DEPC-treated control for one sample and used as a negative control in addition to the RT-ve control (**section 2.14.2**). PCR was performed setting the initial and secondary denaturing temperatures at 95ºC and an elongation temperature of 72ºC according the manufacturer's instructions. The annealing temperature was specific to the melting temperature (T_m) of the primer and was optimised for each primer set.

The annealing and extension steps of PCR were performed for 35 cycles:

Initial denaturation: 95ºC for 2 minutes

Secondary denaturation: 95ºC for 30s
Annealing: 55ºC-65ºC for 30s   } **35 Cycles**
Extension: 72ºC for 1min/kb

Final extension: 72ºC for 2min

2.14.3.2 Agarose gel electrophoresis

The presence of PCR products were verified using agarose-TBE gel electrophoresis. Gel electrophoresis was used to separate PCR productions based on their size (Bp). A 1.5% agarose gel was made by dissolving 1.5g of agarose (Sigma Aldrich) in 1X Tris/borate/EDTA (TBE) buffer. The agarose was dissolved by heating in a microwave for 2 minutes after which ethidium bromide was added to the agarose solution at a dilution of 1:100. A 16 or 32 well comb was placed in the gel plate and the agarose was poured into the gel cast and left to set for approximately 1 hour at room temperature. The set gel was placed in the electrophoresis tank and filled with TBE buffer. The comb was removed carefully from the set gel. 10µl of DNA ladder (full range100 BP Norgen) was loaded into the first well. 5µl of DNA loading buffer was added to 20µl of PCR product in a ratio. Each PCR product was loaded into the agarose gel at a volume of 10µl. The gel ran in TBE at 100V for 30 minutes and DNA fragments were inspected under UV light using the Gel Doc XR+ system and the Quantity One software.

2.14.3.3 PCR product sequencing

PCR products were sent into the DNA sequencing Core Facility housed within the University of Sheffield, Medical School and sequenced to verify *SOSTDC1* expression (http://genetics.group.shef.ac.uk/dna-sequencing.html). Sequencing was performed using the Applied Biosystems' 3730 DNA Analyser. A 10µl of the 100ng/µl PCR product obtained from end-point PCR were initially purified by the Core Genomics Facility to remove excess primers and dNTPs using the Ampure bead purification kit (Beckman Coulter). Sequencing results were analysed using FinchTv software version 1.4.0 and the base pair sequences were assessed for nucleotide similarities to SOSTDC1 using the database on Basic Local Alignment Search Tool (BLAST)®.

2.14.3.4 Real Time quantitative Reverse Transcription-PCR

Real time quantitative RT-PCR (qRT-PCR) enables accurate measurement of products generated during PCR cycles. This technique involves TaqMan oligonucleotide probes have a fluorescent probe (reporter) bound to the 5' end and a 'quencher' molecule attached to the 3' end. During PCR amplification, these probes hybridize to the target sequences in the amplicon. As the polymerase enzyme replicates the TaqMan bound-template, the reported is cleaved due to the polymerase 5'- nuclease activity. The close distance between the reporter and quencher molecule prevents fluorescence from being detected through Fluorescence resonance energy transfer (FRET). The uncoupling of the two molecules results in an increase in fluorescence intensity, which is proportional to the number of the probe cleavage cycles.

Species-specific TaqMan® Assays were used to determine the expression genes of interest. For each gene of interest a 7µl reaction mix was prepared containing; 5µl of TaqMan® gene expression mastermix, 0.5µl TaqMan® Assay and 1.5µl nuclease-free water. 3µl of cDNA template as prepared in **section 2.13.2** and 7µl of reaction mix were loaded into a well in a 384 well PCR plate. Each cDNA sample was loaded in duplicates. The reaction mix was also loaded with 2µl of nuclease-free water instead of cDNA template to detect any contamination in the PCR reaction mix. The plates were sealed using an optical adhesive covers. PCR plates were analysed using Applied Biosystems 7900HT Real-Time PCR system and data analysis performed on the SDS 2.2.1 software. The cycle threshold (CT) value that was measured by the Real-Time PCR system was representative of the number of cycles at which each specific reaction crossed a selected threshold. The CT values were used as a relative measure of the concentration of the template sequences in a sample. The thresholds were positioned to lie in the middle of the linear region of the logarithm amplification plot, in an area where the increasing amplification was exponential. High CT values meant that higher numbers of amplification cycles were required to reach the fluorescence intensity threshold due to lower amount of sample cDNA template.

The baseline of a PCR reaction was set in the SDS 2.2.1 software to remove any background fluorescence. To maintain uniformity across samples, a constant threshold was set at 0.2CT and a constant baseline was also set at 3-15 cycles. Sample replicates were analysed by the ΔΔCT method described by Livak and Schmittgen (Livak and Schmittgen 2001). Relative quantification of gene expression was performed by normalising to β2-microglobulin (*B2M)* and hypoxanthine phosphoribosyl transferase 1 (*HPRTL)* house-keeping genes using the formula; $\Delta CT = CT_{target} - CT_{housekeeping}$. Fold changes in target gene expression were calculated using the ΔΔCT method, in which data are normalised by the $2^{-\Delta\Delta CT}$ function (calculated by taking 2 to the power if ΔΔCT).

TaqMan® assays		
ITEM	**ID**	**SUPPLIER**
Mouse hypoxanthine phosphoribosyltransferase 1 (HPRTL)	Mm00446968-m1	Life Technologies
Mouse β2-microglobulin (B2M)	Mm00437762-m1	Life Technologies
Runt related transcription factor 2 (Runx2)	Mm00501584_m1	Life Technologies
Mouse CTNNB1	mm00483033-m1	Life Technologies
Mouse COL1A2	Mm00483888-m1	Life Technologies

Table 2.17 - *The TaqMan assays specific for genes studied using qRT-PCR in this study.*

2.15 Bio-Layer Interferometry

ITEM	SUPPLIER
BLItz analysis	
Amine reactive 2nd generation (AR2G) Biosensor	ForteBio
96-well, black, polypropylene flat-bottom microplate	ForteBio
NHS/EDC	ForteBio
BLItz® System bioanalyser	ForteBio

Biosensor technology is commonly used the specific and sensitive investigation of biomolecular interactions. The Bio-Layer Interferometry (BLI) developed by ForteBio (www.ForteBio.com), is amongst the well-established biosensor platforms used to evaluate protein/protein interactions in research and routine applications (Wallner, Lhota et al. 2013). The BLI technology used by the BLItz® system provides real-time data on protein interactions. The BLItz® system emits white light down a biosensor, and the light reflected back is then collected by a detector (**Figure 2.6**). The molecule of interest is biochemically bound to the surface of the biosensor, where it forms complexes with partner molecules (analyte). The carboxylated biosensor surface allows covalent coupling of proteins via N-Hydroxysuccinimide (NHS)/ethyl(dimethylaminopropyl) carbodiimide (EDC) mediated amide bond formation. The thickness of the coating on the optical layer affects the reflected wavelengths. The wavelength interference, which is categorised as constructive or destructive, is captured by a spectrometer and is reported in relative intensity units (nm). Changes in the number of molecules bound to the biosensor result in changes or 'shifts' in the wavelength interference which is measured in real time. The interference shifts are a direct measure of the change in optical thickness of the biological layer. Based on these principles, a range of kinetic applications are possible including protein kinetic and affinity characterisation.
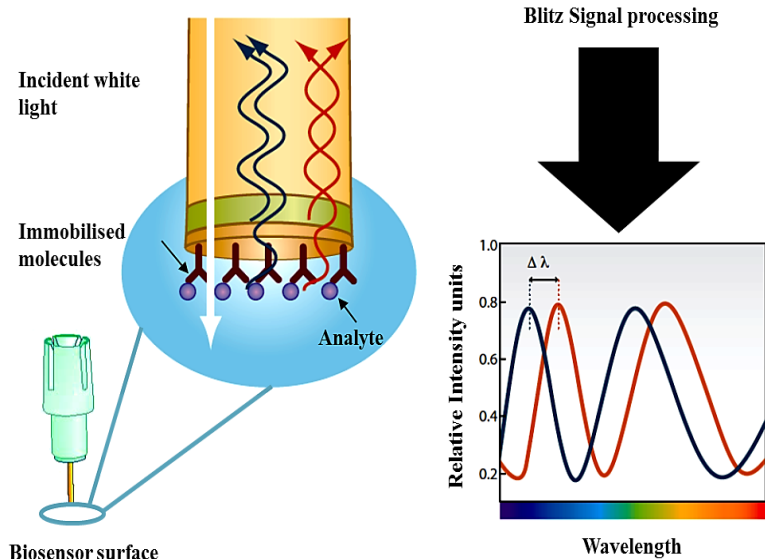
Figure 2.7 – BLItz system: *The BLItz system emits white light down the biosensor, and collects reflected light. Wavelengths interference are constructive interference (blue) or destructive (red). Interference shifts captured by a spectrometer and reported in relative intensity units (nm) and are a direct measure of the change in optical thickness of the biological layer. Image adapted from www.ForteBio.com.*

2.15.1 BLI kinetics

The affinity of one molecule for another is calculated using the association constant (ka) and dissociation constant (kd). The ratio of between the kd/ka gives rise to the affinity constant KD. The ka is defined as the rate of complex formation per second in a 1 molar solution of two reaction partners. The kd (1/s) indicates the stability of this complex. The affinity constant KD is calculated by the ratio of the kd/ka (Katsamba, Navratilova et al. 2006). This relation can be described by a basic equation shown below, where A is the analyte and B is the molecule of interest:
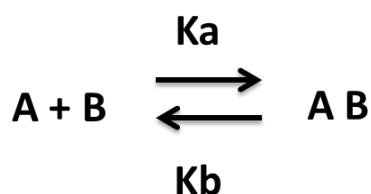
Interferometry data were globally fit to a simple 1:1 Langmuir model (O'Shannessy et al. 1993), calculating the affinities and rate constants (Octet software, Version 6.4,

ForteBio). This model describes a 1:1 interaction where one ligand molecule interacts with one analyte molecule. To produce a complete kinetic prolife for the molecule of interest and its associated analyte, the interaction is measured at multiple analyte concentration (µg/ml) and the data is used for Langmuir model fitting. Ligand-analyte associations were run at an injection period length long enough to observe a curvature of the binding response. The association and dissociation responses were baseline corrected and processed using the Octet Software (Version 6.4, ForteBio). The individual signal responses at each concentration as well as the maximum responses (Rmax) were calculated.

2.15.2 Determining protein-analyte interaction using ARG2 biosensors

A BLI assay involves an equilibrium step, ligand immobilization step, analyte association and analyte dissociation step (**Figure 2.7**). An example of loading conditions and curves for the association of a target protein (termed ligand) and its specific analyte are shown in **Figure 2.7**. The assay was initiated by establishing the equilibration of Amine reactive 2nd generation (AR2G) biosensor tips with PBS buffer to measure the baseline signal (**Step 1**). Biosensors were hydrated for 10 minutes prior to use by inserting the biosensor into 200µl of PBS buffer within a 96-well microplate. Biosenors were activated with EDC/NHS mixture is a tube (**Step 2**). For the immobilisation step, the protein concentrations and loading performance were optimized. Ligand solutions were prepared for the loading step to bring to a concentration of 1–100µg/ml. ARG2 biosensor tips were captured to saturation with the ligand to obtain a loading signal (**Step 3**). Subsequently, an additional equilibration step was applied with buffer to remove the excess ligand and to obtain a constant loading baseline (**Step 4**). In the final dissociation step, the biosensor was 'quenched' with quenching solution (**Step 5**). The sensogram data was collected in real time and presented as binding (nm) affinity at the start of ligand-analyte association and the start of complex dissociation. The measured affinity of the interaction KD (M) between the two proteins was reported by the BLItz Pro™ software.
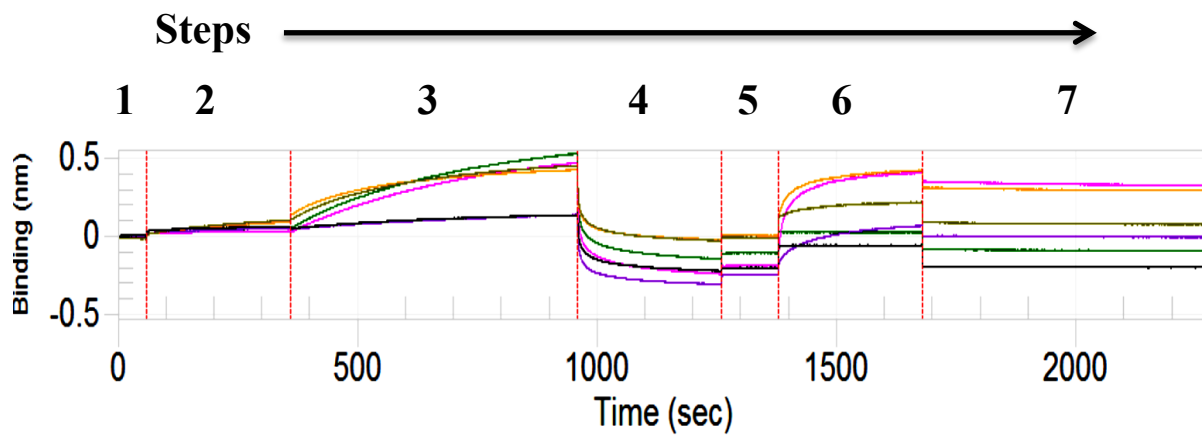
Run Settings		
STEP	**STEP TYPE**	**DURATION**
1	Initial Baseline	60
2	Custom	300
3	Loading	600
4	Custom	300
5	Baseline	120
6	Association	300
7	Dissociation	600

Figure 2.8 – *BLItz system association/dissociation binding curve sensogram and run settings.*

2.16 Statistical analysis

Statistical analyses were performed with the statistical software package, GraphPad Prism 6 version 6.0.4 for Windows. Firstly the data were analysed for normal distribution using the D'Agostino and Pearson normality test. The data were analysed using an ANOVA test (one way analysis of variance) for more than two group comparison. A Holme-Sidak's test was used as post-hoc analysis when ANOVA test was used in normal distribution data. When data not normally distributed, ANOVA test (non-parametric Kruskal-Wallis test) was used for more than two group comparisons. The Dunns test was used as post-hoc analysis when ANOVA test was used in not normally distributed data. For two group comparisons an unpaired student's *t*-test was performed when the data was normally distributed or non-parametric Mann-Whitney test for two group comparisons in cases were data was not normally distributed. Data were considered statistically significant when a p-value was equal to or less than 0.05. Results are expressed as mean ± values of standard error Mean (SEM).

Chapter 3 – *In-Vitro* Characterisation of the Osteoblast Progenitor Model

3.1 Introduction

To study the molecular mechanisms involved in the regulation of osteoblast (OB) differentiation and mineralisation, I wanted to first establish an *in-vitro* culture system using murine OB progenitor cells derived from calvaria primary bone cells, reflecting the different stages of osteogenic maturation from proliferation to differentiation. OB progenitor cells isolated from the calvaria of 2-4 days old neonatal C57BL/*KaLwRij* mouse pups were selected for the optimisation of the *in-vitro* model of osteoblastogensis. These cells have been shown to differentiate into cells with a clear OB phenotype including ALP expression and extracellular matrix mineralisation (Ecarot-Charrier, Glorieux et al. 1983). OB cells are derived from multipontent mesenchymal stem cells (MSC) and regulate the deposition and maintenance of skeletal tissues. The OB phenotype is defined by the genes expressed and the proteins produced by the cells. Characterising the expression of bone-specific genes and proteins provide valuable markers that are characteristic of bone OB phenotype detected *in- vitro* (Del Fattore, Teti et al. 2012).

MSC produce progenitor cells of restricted OB lineage that have the potential to proliferate or continue onto amplification stages where they express specific osteoblastic markers. MSC committed to an osteo/chondro-progenitor lineage become osteoprogenitor cells that subsequently differentiate into pre-osteoblasts, followed by differentiation into active mature OB cells (**Figure 3.1**). Runx2, osterix and β-catenin are essential for OB differentiation. Runx2 plays a fundamental role in directing the MSC to an osteoblastic lineage instead of an adipocytic or chondrocytic lineage. Once MSC have differentiated into pre-osteoblasts, Runx2, osterix and *β*-catenin drive differentiation into immature OB cells that produce bone matrix proteins, suppressing the cells potential to differentiate into the chondrocyte lineage. Runx2 expression prevents the OB cells from developing into osteocytes, maintaining them in the OB phenotype (Komori 2006, Sila-Asna, Bunyaratvej et al. 2007). Mature OB cells synthesize dense cross-linked collagen in addition to other proteins produced in smaller quantities including osteocalcin and osteopontin which make up the matrix of the bone. Mature OB produce calcium and phosphate-based minerals in a tightly regulated manner. These minerals are deposited into the organic matrix forming the dense and strong mineralarised tissue which forms the matrix. OB mineralisation

components such as calcium are commonly used as markers to determine the level of mineralisation using chemical staining (Arnett 2003).

Osteoblastic cells are usually cultured in MEM-alpha or DMEM. Studies have shown that variations in components and their concentrations added to the media can lead in the differences obtained within proliferation and differentiation assays (Coelho and Fernandes 2000). Media additives that have been shown to drive osteoblastic cell function in culture include dexamethasone, $1,25(OH)_2D_3$, β-glycerophosphate and ascorbic acid (Jorgensen, Henriksen et al. 2004). The addition of sscorbic acid to the cell culture media is necessary for the hydroxylation of proline and lysine residues in collagen to synthesis of collagenous extracellular matrix (Takamizawa, Maehata et al. 2004). In the literature 50μg/mL of ascorbic acid is generally the standard concentration used in mouse primary OB cultures and is a sufficient concentration to upregulate proliferation, collagen and ALP expression in these cells. Phosphate substrates are also added to in media and are necessary for matrix mineralisation in primary OB cell cultures. Supplementation of primary OB cell cultures isolated from mice with 5-10 mM β-glycerophosphate leads to spontaneous mineral deposition (Czekanska, Stoddart et al. 2012).

Primary cells isolated from neonatal mice are difficult to isolate and culture routinely. To study molecular mechanisms/signalling in OB cells, fast growing and well characterised OB-like cell lines are commonly used. The Sarcoma osteogenic (SAOS2) cell line was originally derived from the primary osteosarcoma of an 11 year old Caucasian girl in the 1973 by Fogh et al and later determined as possessing osteoblastic features which would be useful as a permanent line of OB-like cells (Fogh, Fogh et al. 1977, Rodan, Imai et al. 1987). The SAOS2 cells present a more mature OB phenotype in comparison to primary OB progenitor cells, making the SAOS2 cells a good model for studying events associated with late OB differentiation stage in human cells (Gundle and Beresford 1995).

It is important to be able to correlate transcription factors, proteins production and mineralisation levels to develop a timetable for OB differentiation (Arnett 2003). In this chapter I selected gene, protein and mineralisation markers that were clearly established markers of OB cell differentiation and analysed these markers across a range of time-points. The primary aim of this analysis was to create a proliferation, differentiation and mineralisation profile for the murine calvarial OB progenitor cultures. This profile could

then be used as the foundations for future experimental design and contribute in the understanding of the molecular mechanisms involved in OB dysfunction.
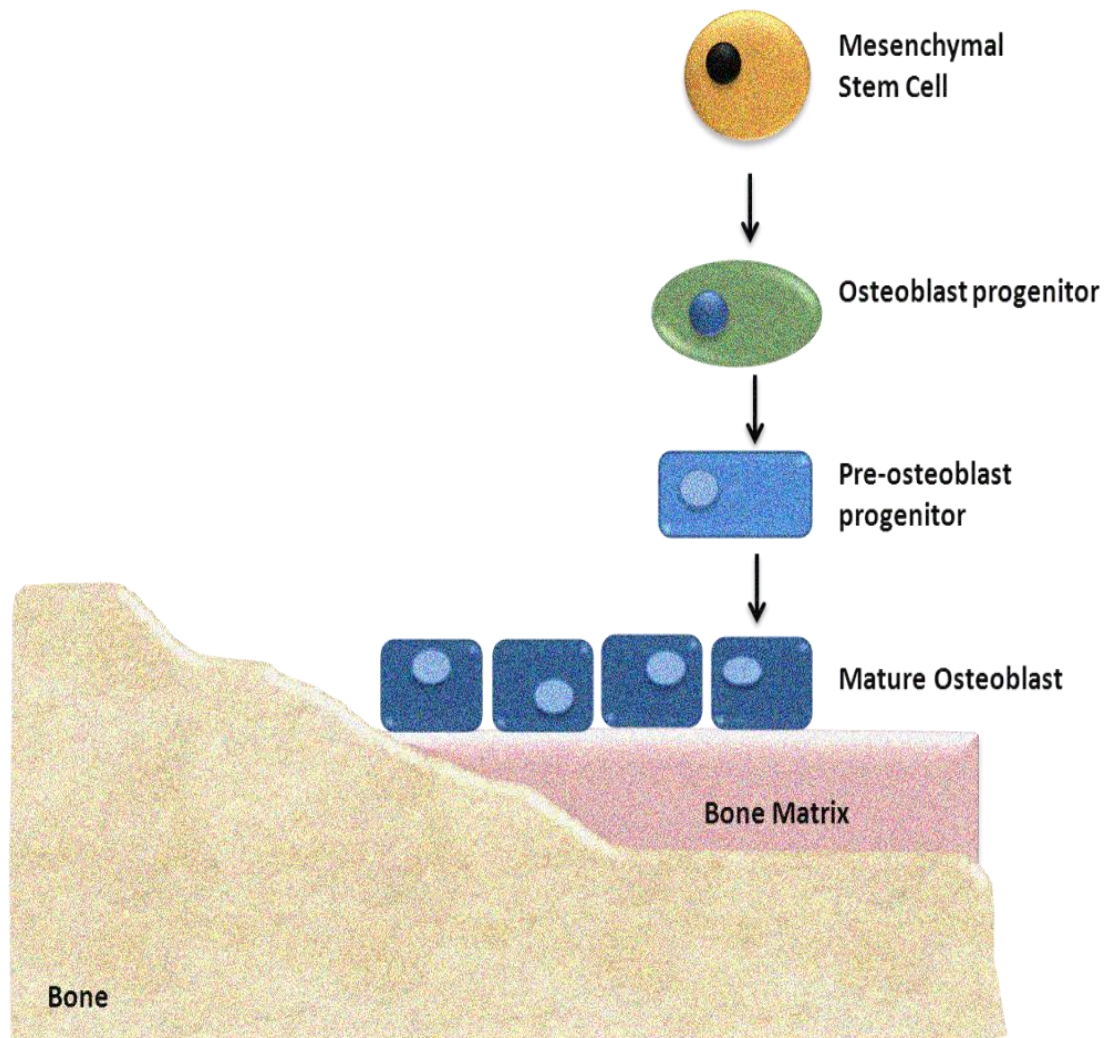
Figure 3.1 - Schematic diagram of the osteoblastogenesis: *osteoblasts arise from MSC which under the required stimuli are driven toward an osteo/chondro-progenitor lineage that then differentiate into osteoblast progenitor cells, followed differentiation into pre-osteoblasts and finally become active, mature osteoblasts. Mature osteoblasts produce calcium and phosphate-based minerals which are deposited into the organic matrix forming the mineralised matrix.*

3.2 Hypothesis and Objectives

3.2.1 Aims

The aim of this study was to characterise an *in-vitro* culture system using murine osteoblast progenitor cells.

To achieve this, the following hypothesis was tested.

3.2.1 Hypothesis

Murine osteoblast progenitor cells differentiate into mature-nodule forming osteoblasts in osteogenic media.

3.2.2 Specific Objectives

To test this hypothesis the following were determined:

Determine the conditions under which osteoblast progenitor cells proliferate, differentiate and mineralise

Determine which differentiation markers are specific to the different stages of osteoblast differentiation

3.3 Chapter specific methods

3.3.1 Assessing the relationship between total cell DNA contents and cell number

PicoGreen analysis of total DNA has been frequently used as a surrogate for cell number (Kumar, Gittings et al. 2010). In my studies investigating ALP activity of OB progenitor cells, the PicoGreen method of determining total DNA contents the cells was to be used as a measure of cell number. PicoGreen and Coulter Counter analysis were used to assess the direct correlation between total DNA contents per cell and cell number, respectively. OB progenitors were used to assess the relationship between total DNA contents and cell number. OB progenitor cells were harvested from a near confluent T75 flask following trypsinisation, pelleted by centrifugation, resuspended in 10ml of PBS and counted using a haemocytometer as described in **section 2.1.3**.12,500 cells were transferred into 15ml BD Falcon™ tubes and counted using a Coulter Counter as described in **section 2.1.4** to verify the haemocytometer count. The 12,000 cells were serially diluted 1:2 to obtain approximate cell densities of 62500, 3125, 1562, 781, 390 and 195 cells.

Using the same batch of OB progenitors, cells of the same densities were also placed into 1.5ml eppendorfs. Cells were centrifuged at 1000 RPM for 5 minutes to pellet the cells. The supernatants were removed and cells lysed with 40µl of Triton-X for 30 minutes at room temperature with agitation. 20µl of the cell lysate was transferred into a well within a 96 well culture plate. The total DNA contents (ng/ml) of the cell populations in the 96 well plates were determined with a PicoGreen dsDNA quantitation kit as described in **section 2.4**. Data from the PicoGreen and Coulter Counter assays were exported to an excel spreadsheet and the linear regression determined.

3.3.2 Determining the optimal FCS concentration in which calvarial osteoblast progenitor cells proliferate and differentiate

OB progenitor cells were obtained from bone cell cultures isolated from the calvarias of 2-4 days old neonatal C57BL/KaLwRij mice using collagenase with the modified time sequential enzymatic digestion described by Bakker et al and outlined in detail in the main method **section 2.1.1** (Bakker and Klein-Nulend 2012). To reduce variability and OB phenotypic modifications, all experiments using OB progenitors were carried out with cells that had been passaged up to an including passage 4. Mouse calvarial OB progenitor cells were harvested from a near confluent flask following trypsinisation. Cells were pelleted by centrifugation and counted using a haemocytometer, as described in **section 2.1.3**.

To determine the optimal growth conditions under which OB progenitors proliferate and differentiate, cells were seeded in 96 well plates at a density of 2000 cells per well. Following a 72 hour period in culture, the OB progenitor cells were carefully washed once with PBS and the media replaced with 100μl of osteogenic MEM-Alpha media containing 0, 0.1, 0.25, 1, 4, 6, 8 or 10 % FCS. Osteogenic Alpha-MEM media containing various FCS concentrations were replaced every three days. ALP analysis which was used as a marker of differentiation in OB progenitors was carried out on day 8, day 11, and day 15 of differentiation. In separate experiments assessing the OB progenitor differentiation in the minimum FCS concentration required (4%) by the cells, OB progenitors were cultured up to day 19 of differentiation. Total DNA content of OB progenitor cultures were also determined with a PicoGreen dsDNA quantitation reagent as outlined in **section 2.4**. Total DNA values were used to normalise ALP activity to total cell DNA content, as described in **section 2.3**.

3.3.3 Assessing *Runx2*, *CTNNB1* and *COL1A2* gene expression in differentiating OB progenitor cells

Runx2, β-catenin and Collagen have been established as gene markers of OB cell differentiation in the literature (Beck, Zerler et al. 2001, Prince, Banerjee et al. 2001, Matsuo, Tanaka et al. 2008, Baron and Kneissel 2013). The expression of *Runx2*, CTNNB1 (gene ecodin the protein for β-catenin) and *COL1A2* (encodes the protein α-1 type I collagen) genes during the differentiation stages of OB progenitors were assessed using qRT-PCR. Mouse calvarial OB progenitor cells were harvested from a near confluent flask following trypsinisation. Centrifuged cell pellets were resuspended and counted using a haemocytometer, as described in the method **section 2.1.3**. OB progenitors were cultured in 6 well culture plates at a density of 57,000 cells per well in standard MEM-Alpha media containing 10% FCS. Cells were differentiated for up to 21 days in standard MEM-Alpha osteogenic media containing 4% FCS prepared according to **section 2.2**. Following a 72 hour period in culture, OB progenitor cells were washed once with PBS per well, and the media replaced with 1.5ml of osteogenic MEM-Alpha media. The osteogenic media on the OB progenitors were replaced every three days. RNA was extracted from the differentiating OB progenitors on day 8, 11, 15 and 21 of differentiation and quantified using a NanoDrop bioanalyser according to **section 2.13**. Following cDNA synthesis from 1000ng of RNA, *Runx2*, *CTNNB1 and COL1A2* gene expression were quantified using qRT-PCR analysis as described in **section 2.14**.

3.3.4 Assessing mineralisation in differentiating osteoblast progenitor cultures

To determine the level of mineralisation in differentiating OB progenitor cells, OB progenitor cells were harvested from a near confluent flask by trypsinisation. Cells were pelleted by centrifugation and counted using a haemocytometer, as described in **section 2.1.3**. Cells were seeded in 48 well culture plates at a density of 5,700 cells per well in standard MEM-Alpha containing 10% FCS. Following a 72 hour period in culture, OB progenitor cells were carefully washed once with PBS per well, and the media replaced with 250μl of osteogenic MEM-Alpha media containing 4% FCS prepared according to **section 2.2**. Osteogenic media in which OB progenitors were differentiating was replaced every three days, for up to 21 days. Mineral deposition was used as a marker of mineralisation in OB cultures and was assessed using Alizarin red staining on days 8, 11,

15 and 21 of OB differentiation as described in **section 2.5**. Percentage area mineralisation of OB cells was quantified per well using ImageJ Software.

3.3.5 Characterisation of differentiated SAOS2 cells culture system

SAOS2 are OB-like cells that have a similar phenotype to primary murine cells and are commonly used in studies in OB studies (Czekanska, Stoddart et al. 2012). The SAOS2 cells have previously been shown to have a mature OB phenotype with high levels of ALP activity (Saldana, Bensiamar et al. 2011). In this study I wanted to establish another *in-vitro* OB-like culture system with a more mature OB phenotype to compare to murine OB progenitor cells. SAOS2 cells were harvested from a near confluent flask following trypsinisation as described in the method section. SAOS2 cells were pelleted by centrifugation and counted using a haemocytometer, as described in **section 2.1.3**. SAOS2 cells were seeded in 96 well plates at a density of 2000 cells per well in 100µl of standard DMEM media containing 10% FCS. Cells were given 48 hours to adhere to the culture surface and DMEM media was removed, washed once with PBS and replaced with 100µl of osteogenic-DMEM media containing 10 mM of β-glycerophosphate and 50 µg/ml of L-ascorbic acid additives as described by Saldana et al (Saldana, Bensiamar et al. 2011). SAOS2 cells were differentiated for 8 days and osteogenic-DMEM media was replaced every three days. ALP analysis of SAOS2 cells was carried out on days 2, 4, 6 and 8 of differentiation. Total DNA content of SAOS2 cells per well were also determined with a PicoGreen dsDNA quantitation reagent to normalise ALP activity to total cell DNA content, as described in **sections 2.3 and 2.4**.

3.4 Results

3.4.1 Total DNA contents within cells determined by PicoGreen analysis correlated with cell number

OB progenitors of various cell densities ranging from approximately 12,500 to 200 cells were counted using the Coulter Counter and this count was compared to the total DNA contents using PicoGreen dsDNA quantitation. The regression analysis between the two sets of data obtained from the PicoGreen and Coulter Counter assay showed that as the number of cells increased, the total DNA contents per cell also increased linearly **(Figure 3.4.1**, R=0.094).
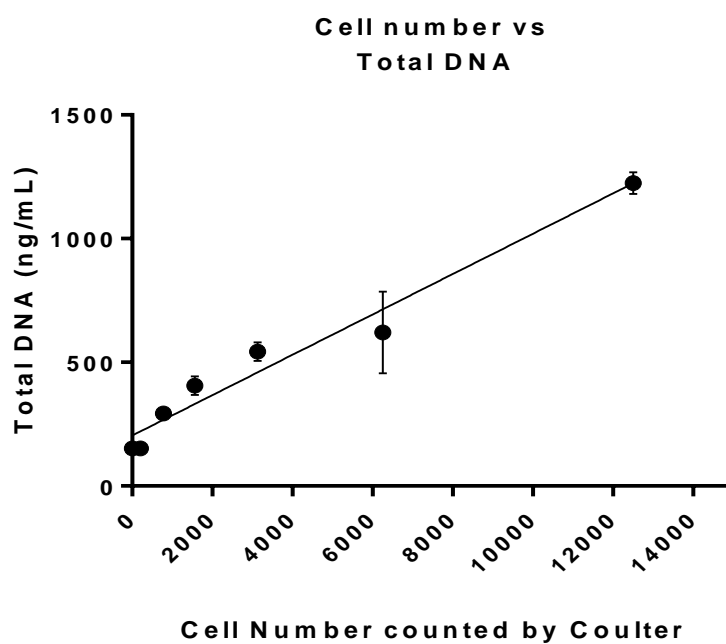
Figure 3.4.1 - Analysis of cell DNA contents correlated with cell number determined by Coulter Counter analysis. *Coulter Counter analysis of cell number showed that an increase in the number of cells correlated with an increase in total DNA contents. N=4 independent experiments, Linear Regression analysis. ***P<0.0001, R=0.092.*

3.4.2 Osteoblast progenitor cells differentiate exponentially from 8 to 15 days in osteogenic media

To establish an *in-vitro* primary cell culture system to utilise in future experiments, I initially established the optimal growth conditions under which OB progenitors proliferated and differentiated. To ensure that the OB progenitor cells used in my studies also behaved comparably to those used in the literature under similar conditions, I first tested the optimal FCS concentration (%) in which OB progenitor cells proliferated and subsequently differentiated. OB progenitors isolated from the calvarias of neonatal pups C57BL/KaLwRij mice were differentiated for up to 15 days in osteogenic media containing various FCS concentrations ranging from 0 to 10 % FCS. ALP analysis of OB progenitors was carried out on day 8, day 11 and day 15 of differentiation and the results normalised to total DNA content of OB progenitor cells per well determined with a PicoGreen dsDNA quantitation assay.

PicoGreen analysis showed that total DNA of OB progenitor cell in culture plate wells increased as FCS concentration increased. The exponential increase in total DNA was evident with as little as 4% FCS up to 10% FCS. By day 15 of differentiation, the total DNA contents of OB progenitors cultured in 10% FCS no longer increased indicated by the plateau phase of the growth curve (**Figure 3.4.2 A**). The ALP analysis of OB progenitors showed that ALP activity was upregulated with increasing doses of FCS during all time points of differentiation, peaking in 10% FCS (**Figure 3.4.2 B**).

Although I showed that the OB progenitor cultures differentiated optimally in 10% FCS, I wanted to carry out future experiments using the minimum dosage of FCS required by the cells. The rational for using a minimum FCS dosage and diluting the concentration of proteins in the FCS, any effects resulting from treatment with exogenous recombinant protein would not be masked. Based on the results in **Figure 2.4.2,** similar experiments were performed in which ALP analysis of OB progenitors cultured in 4% FCS were carried out on day 8, day 11 day 15 and 19 of differentiation. The OB progenitor cells proliferated and differentiated in 4% FCS concentration (**Figure 2.4.2 C, D**). The total DNA of OB progenitor cultures increased exponentially by approximately 40% (~300ng/ml to ~500 ng/ml) from day 4 to day 8 of differentiation. Subsequently, 4% FCS concentration was used in subsequent experiments.
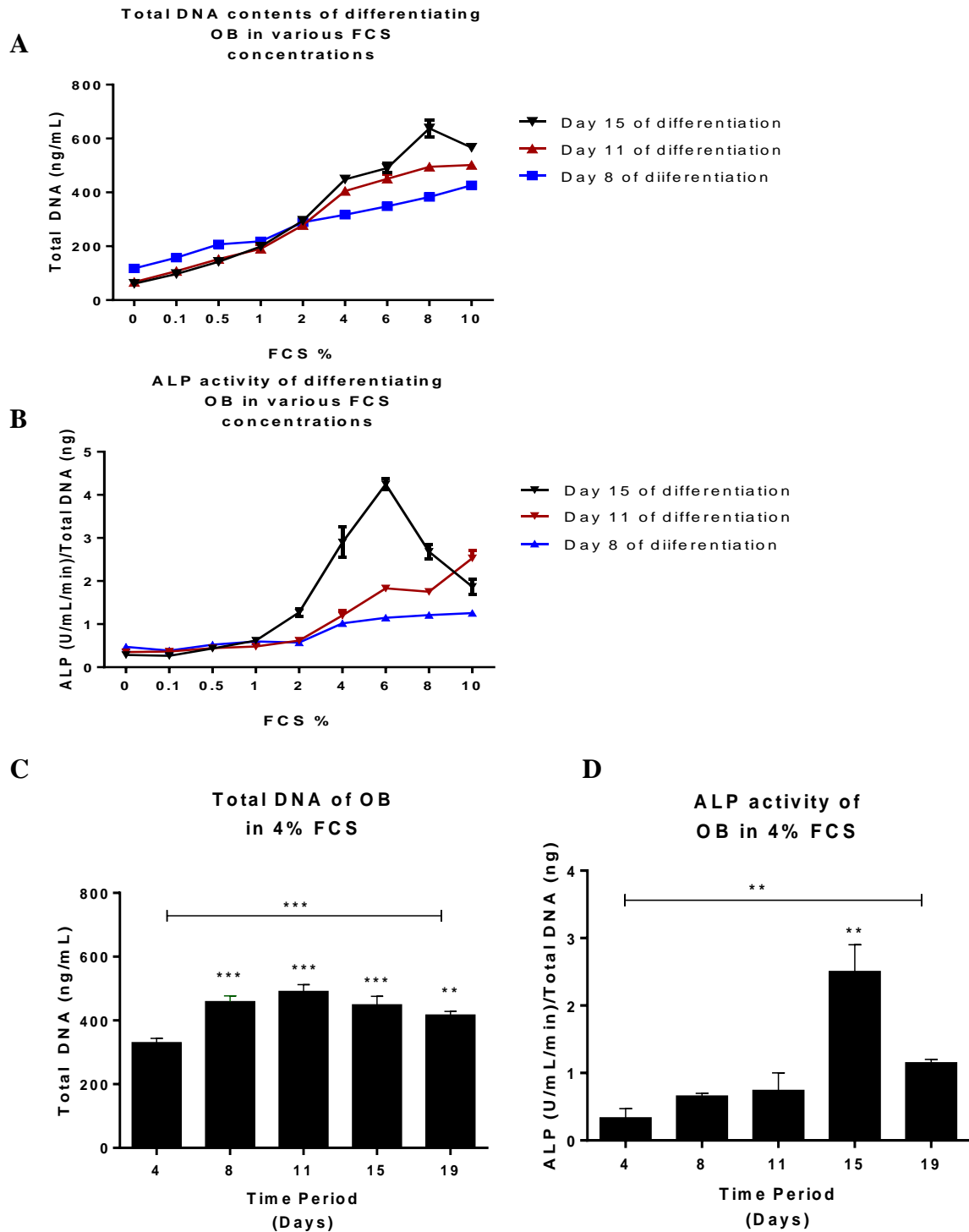
Figures 3.4.2 - Osteoblasts exponentially differentiate in 4-10% FCS from day 8 to day 15 of differentiation: *The optimal FCS concentration (%) in which OB progenitor cells proliferated was determined using PicoGreen analysis of total DNA and the differentiation profile determined using ALP analysis. (A, B) Total DNA increased as FCS concentration increased throughout day 8 to day 15 of differentiation. (C, D) OB progenitors proliferated and differentiated in a minimum concentration of 4% FCS. N=3 independent experiments, One-way Anova. Data are displayed with mean ± SEM. **P=0.01, ***P=0.001.*

3.4.3 *Runx2* and *CTNNB1* gene expression decreased and *COL1A2* expression increased during OB progenitor differentiation

Quantitative RT-PCR was used to assess *Runx2*, *CTNNB1 and COL1A2* gene expression during the differentiation of OB progenitors. Cells were differentiated for up to 21 days in standard osteogenic media containing 4% FCS. RNA was extracted from the differentiating OB progenitors on day 8, 11, 15 and 21 of differentiation. *Runx2, CTNNB1* and *COL1A2* gene expression were quantified using qRT-PCR analysis. The qRT-PCR analysis showed that *Runx2* gene was present at detectable levels on day 8, 11, 15 and 21 of differentiation in OB progenitor cells. The OB progenitor *Runx2* expression was at its highest level on day 8 of differentiation and decreased significantly compared to day 11, 15 and 21 (***$P<0.05$, **Figure 3.4.3 A**).There were no differences between the level of *Runx2* gene expression between day 11 and 21 of differentiation. The *CTNNB1* expression of differentiating OB progenitors was at its highest level on day 8 of differentiation and decreased exponentially until day 21 of differentiation (***$P<0.001$, **Figure 3.4.3 B**). Expression of *COL1A2* gene was detected throughout the various time points of OB progenitor differentiation. *COL1A2* expression did not change between day 8 and day 11 of differentiation, but the expression decreased on day 15 compared to day 8 (***$P<0.001$). Collagen expression of differentiating OB progenitor cells increased on day 21 compared to day 8 (*$P<0.05$) (**Figure 3.4.3 C).**

A
Runx2 expression on Day 8-21 of OB differentiation

B
CTNNB1 expression on Day 8-20 of OB differentiation

C
COL1A2 expression on Day 8-21 of OB differentiation

Average CT values				
	Day 8	**Day 11**	**Day 15**	**Day 21**
Runx2	21.9	22.0	22.9	23.7
COL1A2	18.3	18.4	20.3	20.1
CTNNB1	19.6	20.6	24.4	23.7
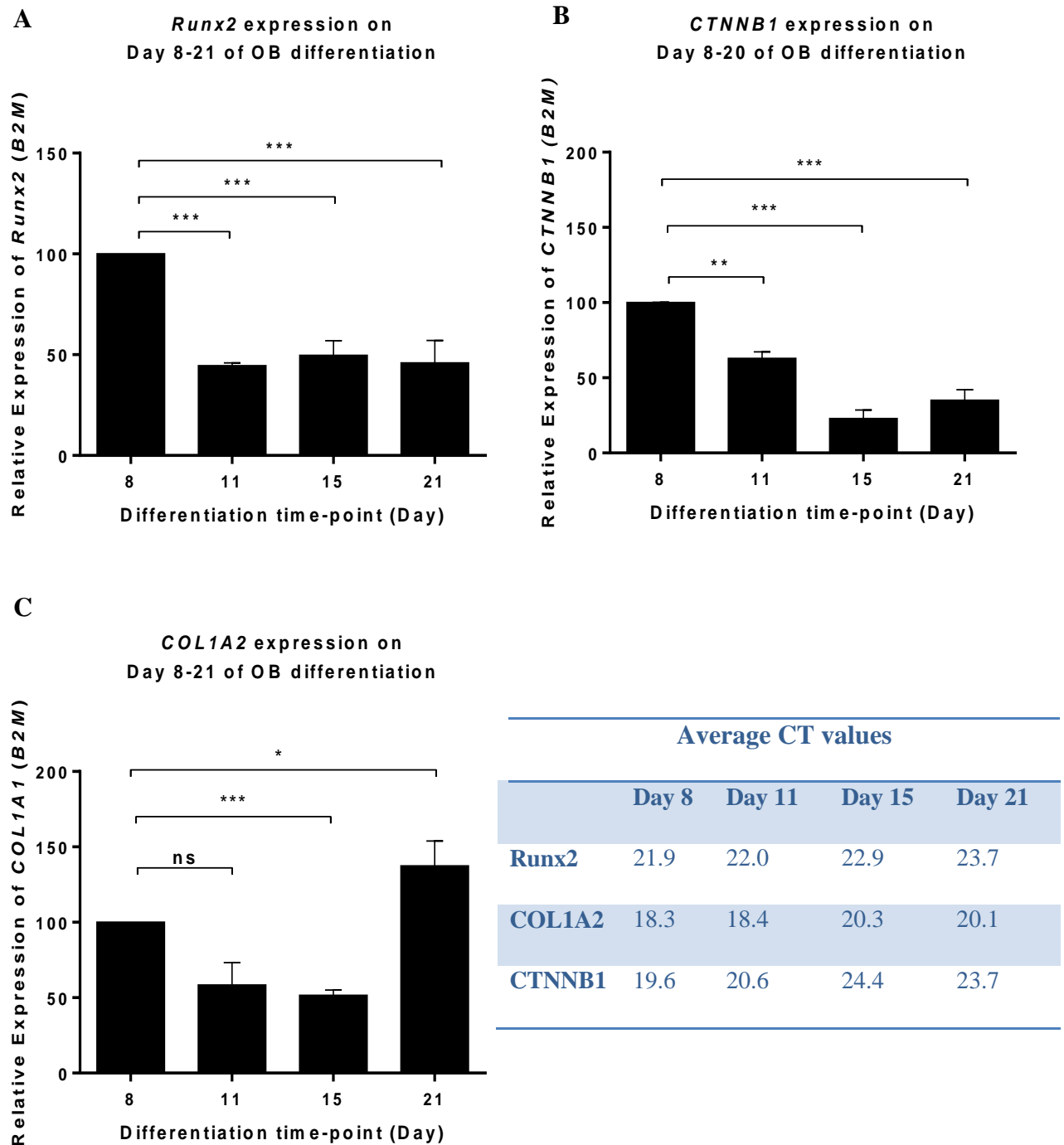
Figures 3.4.3 - *Runx2* and *CTNNB1* expression decreased and *COL1A2* gene expression increased during OB progenitor differentiation: *Runx2, CTNNB1 and COL1A2 gene expression of differentiating OB progenitors were quantified using qRT-PCR analysis and the results normalised to B2M expression and day 8 values. (A) Expression of Runx2 within OB progenitor was present at detectable levels on day 8 and 11 of differentiation and increased on day 15 and 20. (B) Collagen gene expression was detected throughout day 8 to day 21 of OB progenitor differentiation. N=3 independent experiments, Unpaired t test. Data are displayed with mean ± SEM. *P=0.05, **P=0.01, ***P=0.001.*

3.4.4 Osteoblast progenitor cells form visible nodules and mineralise from day 15 of differentiation

To determine the level of mineralisation in differentiating OB progenitor cells, OB progenitors were differentiated in osteogenic media containing 4% FCS and were stained with Alizarin red on days 8, 11, 15 and 21 of OB progenitor differentiation. The percentage area of mineralisation in differentiation OB cells was quantified and normalised to the day 8 values. Alizarin red staining representative of mineral deposition showed that day mineralisation in OB was significant on day 15 and 21 of differentiation (***$P<0.001$). Nodules were visible to the eye on day 15 and 21 of differentiation.
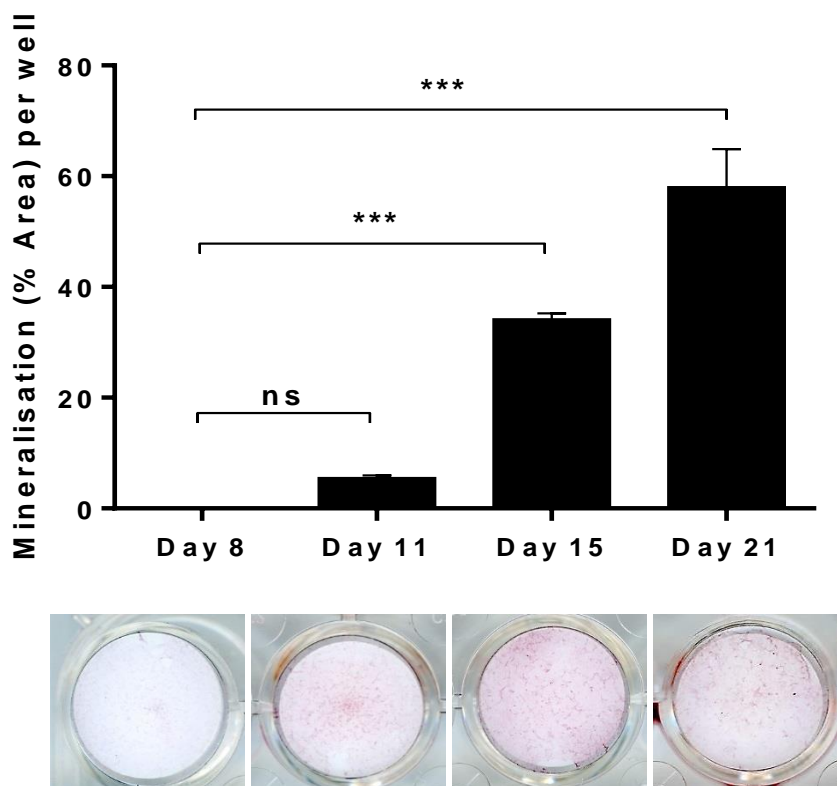
Figure 3.4.4 - Osteoblast mineralisation increased from day 15 to day 21 of differentiation: *OB progenitors were stained with Alizarin red to detect mineralisation on days 8, 11, 15 and 21 of OB progenitor differentiation. The percentage (%) area of mineralisation in differentiating OB cells was quantified using ImageJ Software and normalised to day 8. Mineralisation in OB progenitors was significant on day 15 and 21 of differentiation. Nodules were visible to the eye on day 15 and 21 of differentiation. Graph and image is representative of one experiment from N=3 independent experiments. Unpaired t test. Data are displayed with mean ± SEM. ***$P<0.001$.*

3.4.5 SAOS2 cells had high basal levels of ALP activity, indicative of a mature osteoblast phenotype

SAOS2 cells were differentiated in osteogenic-DMEM media containing 4% FCS for up to 8 days in culture. ALP analysis of SAOS2 cells was carried out on day 2, 4 , 6 and 8 of differentiation and the results normalised to total DNA content of SAOS2 cells per well determined with a PicoGreen dsDNA quantitation assay. Due to a high rate of proliferation, the SAOS2 cells became over-confluent within wells, lifted and died beyond the day 4 time point. PicoGreen analysis showed that total DNA of differentiating SAOS2 cells increased from day 2 up to day 4 of differentiation (**Figure 3.4.5 A**). SAOS2 ALP activity was also upregulated from day 2 to day 4 of differentiation (**Figure 3.4.5 B**).

A   **B**
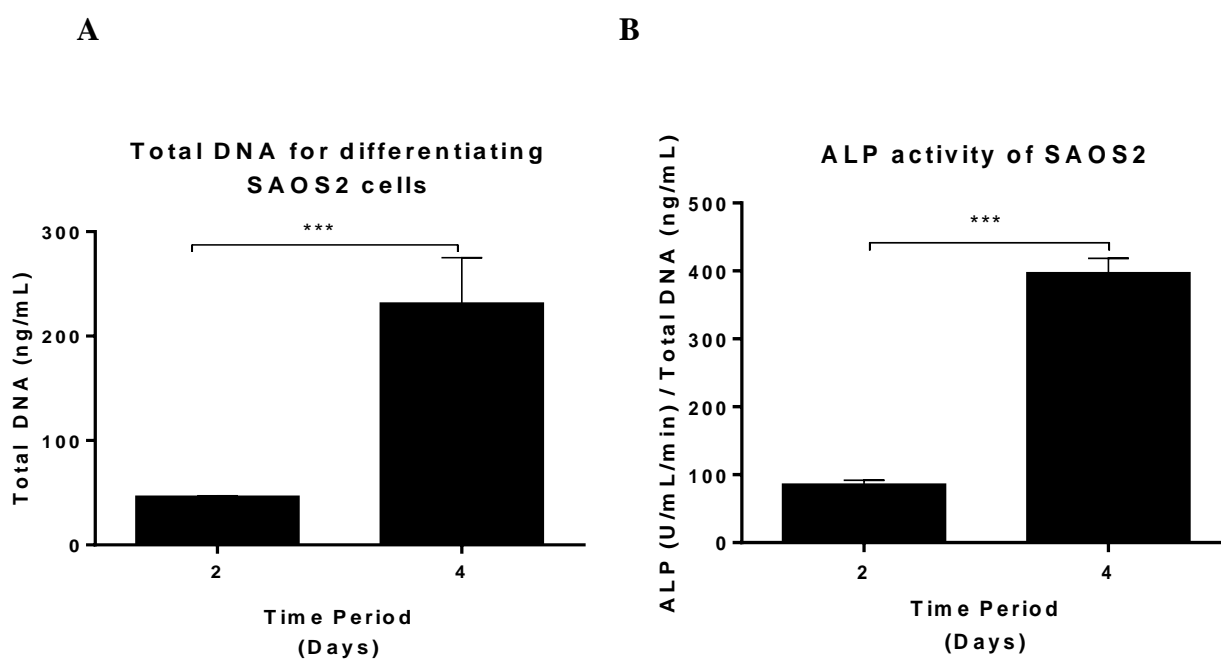
Figure 3.4.5 - SAOS2 cells proliferated and differentiated up to day 4 of differentiation determined by PicoGreen and ALP analysis: *SAOS2 cells were differentiated in osteogenic-DMEM media containing 4% FCS for up to 8 days in culture. ALP analysis was normalised to total DNA contents per well determined with PicoGreen quantitation. (A) The total DNA of differentiating SAOS2 cells increased up to day 4 of differentiation. (B) ALP activity was upregulated from day 2 to day 4 of differentiation. Graph is representative one experiment from N=3 independent experiments. Unpaired t test. Data are displayed with mean ± SEM. ***P<0.001.*

3.5 Discussion

The primary objective of this chapter was to characterise the proliferation, differentiation and mineralisation profile of progenitor cells isolated from calvarial primary bone cultures obtained from neonatal mice. Characterisation and optimising of an *in-vitro* culture system reflecting the different stages of osteogenic maturation using progenitor OB cells was required to understand and validate future experimental data studying the molecular mechanisms involved in regulation of osteoblastogensis. Primary murine cells are commonly used in the bone cell studies as a source of osteoprogenitors as the cells are extracted directly from the bones of animal and there is the possibility of controlling the selection of the donor animals. The disadvantages associated with primary cell cultures are that there are interspecies and genomic differences and cell phenotype is sensitive to age and site of isolation. Although cells lines such as SAOS2 and MC3T3-E1-E1 cells are abundant in number and homogeneous in character, they do not reflect the entire range of OB phenotypic changes, making primary OB cultures a more preferable OB model (Wang, Christensen et al. 1999, Fernandes, Harkey et al. 2007).

Flourimetric assessment of DNA contents using PicoGreen dye is an established method of correlating DNA to cell number that is both sensitive and accurate (Rao and Otto 1992, Otto 2005). To measure changes in cell number in future OB proliferation studies the PicoGreen method was validated to ensure it did correlate to cell number, in line with the literature. The Coulter Counter analyser has previously been used to accurately and efficiently determine human OB cell numbers in the literature (Slapnicka, Fassmann et al. 2008). OB progenitor cells were used to assess the direct correlation between total DNA contents and cell number via PicoGreen and Coulter Counter analysis, respectively. The data obtained from the PicoGreen and Coulter Counter analyser show that as the number of cells increased, the total DNA contents (ng/ml) also increased. These results validate the methodology of using PicoGreen analysis of DNA contents as a surrogate for cell number.

The pre-osteoblasts are the first recognisable cell of the differentiating OB lineage. While pre-osteoblast maintain their proliferative capacity, they can simultaneously express various proteins associated with a more mature OB phenotype, including ALP enzyme (Birmingham, Niebur et al. 2012). As a result, ALP is suitable marker to be to be used in determining the optimal conditions under which the calvarial OB progenitor cells

proliferated and differentiated. Quantification of DNA contents and ALP enzymatic activity of FCS dose response experiments showed that OB progenitor cells proliferate and differentiate optimally in 10% FCS from day 8 to day 11 of differentiation. PicoGreen analysis of DNA contents and analysis of ALP activity showed that the exponential differentiation period of OB cells initiated at approximately day 8 following treatment with osteogenic media, and continued increasing up to day 15 and plateaued beyond this time-point indicating that OB progenitor cells had differentiated into mature OB cells by day 19 of differentiation. Similar results were observed by Hasegawa et al , who found that primary calvarial cells increased in cell number up to 10 days in culture and the ALP activity of these cells increased up to 15 days in culture (Hasegawa, Shimada et al. 2008). I wanted to further determine the minimum concentration of FCS which was require for the OB progenitor cells to differentiate in a similar time-frame to those cells cultured in the optimal 10% FCS dose. The rational for using a lower dose of FCS in osteogenic media relates to future planned experiments investigating the effect of OB signalling pathways/molecules, when the levels of growth factors in the FCS may mask effects of exposure to recombinant exogenous growth factors. In addition other studies have shown that the use of 10% FCS in culture media may lead to reduced ALP and type I collagen coupled with increase cell multiplication (Pradel, Mai et al. 2008). From the PicoGreen and ALP results, we can infer that OB progenitors exponentially proliferate and differentiate within roughly the same time-frame 8 to 15 days in osteogenic media containing 4% FCS. Under the light microscope, by day 15 of differentiation the adherent OB progenitors present normal morphology in 4% FCS and show no signs of physical stress.

Although there are no one set of defined markers of OB differentiation that relate to the various stages of OB maturation ranging from osteoprogenitors to mature osteoblast phenotype, Runx2 and Collagen are amongst the well characterised. Based on the literature, *Runx2* gene expression is detectable throughout OB differentiation but is suggested to be upregulated in differentiating progenitors and pre-osteoblasts compared to mature OB cells (Ducy, Zhang et al. 1997). In line with the literature, the qRT-PCR analysis of *Runx2* expression showed the high levels of *Runx2* on day 8 of OB progenitor differentiation reduced during differentiation as cells become mature.

In addition to Runx2, Wnt/β-catenin signalling is essential to OB differentiation during embryonic development. Conditional inactivation of β-catenin in skeletal progenitors in mouse embryos blocked OB differentiation (Day, Guo et al. 2005). The qRT-PCR results in this chapter showed that the gene encoding β-catenin, *CTNNB1*, was expressed at a high level in OB progenitor cultures on day 8 of differentiation compared to subsequent time points. This data suggests that although β-catenin is required throughout OB differentiation, it may have a more predominant role in osteoprogenitors. Others have reported that when β-catenin is inactivated in early skeletal progenitors, low levels of Runx2, but not OB differentiation-specific transcription factor Osterix, is detected. Reports show that at later stages of OB maturation, the inactivation of β-catenin does not inhibit Osterix expression, indicating that β-catenin is not required for Osterix expression in OB with a more mature phenotype (Rodda and McMahon 2006, Zhang, Cho et al. 2008). These results correlate with the decrease in *CTNNB1* expression observed during OB differentiation in this chapter.

COL1A2 gene expression was also detected throughout the various time points of OB progenitor differentiation. However, there were no significant differences or trends between the levels of *COL1A2* expression on differentiation stage. The level of Type I Collagen did appear to increase on day 21 compared to day 8 and this in line with the similar qRT-PCR studies by Chitteti et al investigating OB specific bone matrix markers in during OB maturation (Chitteti, Cheng et al. 2010).

To further characterise the OB model, the time-point at which differentiating OB progenitor cells started to mineralise was determined. Assessment of Alizarin red staining of mineral deposits showed that mineralisation in differentiating OB progenitor cells was significant on day 15 and 21 of differentiation, with matrix nodules visible to the eye on both these occasions. These results are similar in terms of mineralisation time-points to the studies carried out by other groups (Hasegawa, Shimada et al. 2008, Kawazoe, Katoh et al. 2008). These observations are in context with the results obtained from the ALP analysis and gene expression suggesting that the OB progenitor cells acquire a more mature phenotype following 2 weeks in osteogenic culture. Based on the optimisation studies carried out on murine calvarial OB progenitor cells, it can be concluded these cells can be classified as progenitor/pre-osteoblasts up to day 11 of differentiation.

Beyond this time point, differentiating OB progenitors presumably amplify into mature functional OB cells with the capability of forming mineralised matrix.

The analysis of ALP activity of SAOS2 cells showed that these cells in line with information in the literature had a high basal level of ALP, increasing up to day 4 of differentiation and decreasing beyond this time point (Rodan, Imai et al. 1987, Pautke, Schieker et al. 2004). The more mature OB phenotype of the SAOS2 cells makes this OB model adequate for future comparison with the calvarial primary OB progenitor cells. In summary, these studies support the hypothesis that OB differentiation is induced in murine OB progenitor cultures by treatment with osteogenic media as measured by an increase in ALP and mineralisation up to 21 days. The lowest serum concentration that reliably supported the growth and differentiation of these cells was 4% FCS. Analysis of known genes involved in OB differentiation supported that these were expressed at their maximum on day 8 of differentiation with the exception of *COL1A2* which did appear to increase at day 21.

Chapter 4 – SOSTDC1: An antagonist of Wnt and BMP signalling in Osteoblast Progenitors

4.1 Introduction

In the canonical Wnt pathway, the activation of receptors results in β-catenin stabilisation and translocation into the nucleus. Nuclear β-catenin interacts with transcription factors such as Tcf or Lef and induces the transcription of target genes (Miller, Hocking et al. 1999). Wnt-induced stabilisation of β-catenin is suggested to be the basis of the effect of Wnt ligands on proliferation and differentiation. Recently it was shown that in postnatal humans and mice, loss of function of the Wnt co-receptor LRP5 resulted in decreased bone formation (Gong, Slee et al. 2001, Kato, Patel et al. 2002). A point mutation in the LRP5 receptor also caused high bone mass (Boyden, Mao et al. 2002). Although these studies highlight the crucial role of Wnt-LRP5 signal transduction in bone development, the exact mechanisms by which Wnt signalling regulate bone formation remain unclear.

The transcription factor Runx2 plays an important role in OB differentiation (Ducy 2000) as mentioned previously. It has been reported that mice deficient in LRP5 express Runx2 normally (Kato, Patel et al. 2002) which suggests that the mechanism by which LRP5 regulates OB function is independent of Runx2. Interestingly, although several OB genes are controlled by Runx2, ALP is not one of these. On the other hand, BMP proteins are capable of inducing ALP in Mesenchymal Stem Cells (MSC) (Gong, Slee et al. 2001). These reports show that Runx2 is relevant to both the Wnt and BMP signalling pathways in OB differentiation and can be used as a mutual marker studies investigating the molecular mechanisms of Wnt and BMP signalling.

SOSTDC1 has been characterised as a BMP antagonist (Yanagita, Oka et al. 2004). There is less information on the effect of SOSTDC1 on Wnt signalling. In contrast to Itasaki *et al* identification of SOSTDC1 as a Wnt-stimulator in their genetic screen (Itasaki, Jones et al. 2003), other studies suggested SOSTDC1 can function as an inhibitor of canonical Wnt signalling, specifically in relation to Wnt1, Wnt3a and Wnt10 (Yanagita, Oka et al. 2004, Beaudoin, Sisk et al. 2005). Data implicate that SOSTDC1-Wnt signalling is regulated via interactions with Wnt co-receptor LRP5/6 and that SOSTDC1-induced BMP inhibition is regulated via direct adhesion to BMP ligands (Lintern, Guidato et al. 2009).

Previous studies have shown that BMP2, 4 and 7-induced alkaline phosphatase (ALP) activity was inhibited by Ectodin, the mouse ortholog of SOSTDC1 (Laurikkala, Kassai *et al.* 2003). Similarly recombinant SOSTDC1was found to bind directly to specific BMPs and suppress BMP2, -4 and -7 stimulated ALP activity in the mouse myoblast cell line, C2C12 (Yanagita, Oka et al. 2004). Taken together, these data provide compelling evidence that SOSTDC1 may suppress BMP-induced bone formation. BMP signals are regulated through type II and type I serine/threonine kinase receptors and are central for signal transduction. The Smad proteins which are type I BMP receptor substrates, are involved in transmitting the BMP signal from the receptor to target genes within the nucleus (Cho, Kwak et al. 2011). Although the mechanism by which SOSTDC1 inhibits BMP activity is unclear, there are suggestions that there is a direct interaction between SOSTDC1 and BMP, in which BMP (BMP2, -4 and -7 specifically) is prevented from binding to its co-receptors (Yanagita, Oka et al. 2004). There is some evidence of the inhibitory effect of SOSTDC1 on BMP action in the dental ectoderm, where SOSTDC1 expression was shown to suppress BMP2 and BMP7 activity. In a similar study by Ahn *et al*, SOSTDC1 is shown to suppress development of tooth cells via inhibition of LRP5/6–induced Wnt signalling. SOSTDC1 suppression up-regulated Wnt signalling, stimulating proliferation of tooth bud growth in toothless regions (Ahn, Sanderson et al. 2010). The evidence taken from Ahn's studies initiated the rational for a functional role of SOSTDC1 in BMP and Wnt signalling in OB cells.

In the previous chapter, I characterised the calvarial OB progenitor model and established the time points at which these cells exponentially proliferated and differentiated. In the literature, the studies investigating the effect of SOSTDC1 on Wnt/BMP signalling in bone have been carried out using cell lines. In my studies I have provided data to support the functional role of human recombinant SOSTDC1 (rhSOSTDC1) in Wnt and BMP-induced differentiation of OB progenitor cells. In this chapter, I initially assessed the dose responses of Wnt and BMP ligands on OB differentiation. Based on this, I investigated whether SOSTDC1 suppressed differentiation in OB progenitors through disruption of Wnt and BMP signalling via mechanisms similar to other known Wnt and BMP antagonists.

4.2 Hypothesis and Objectives

4.2.1 Aims

The aim of this study was to determine whether Wnt and BMP-induced OB progenitor differentiation could be suppressed in the presence of SOSTDC1.

To achieve this, the following hypothesis was tested.

4.2.1 Hypothesis

SOSTDC1 suppresses Wnt and BMP-induced cell signalling in differentiating OB progenitors.

4.2.2 Specific objectives

To test this hypothesis the following were determined:

The effects of Wnt and BMP dose response on OB progenitor proliferation and differentiation

The effects of SOSTDC1 on Wnt and BMP-induced markers of OB progenitor differentiation and mineralisation

The effect of SOSTDC1 on Wnt and BMP-induced acute intracellular signalling in differentiating OB progenitors

4.3 Chapter specific methods

Recombinant Proteins

ITEM	CATALOGUE NUMBER	SUPPLIER
Human bone morphogenic protein 2 (BMP2) 10µg/ml *10µg lyophilised stock Reconstituted in 1ml of sterile 4 mM HCL containing 0.1% BSA.*	355-BM-010	R&D Systems
Human bone morphogenic protein 7 (BMP7) 10µg/ml *10µg lyophilised stock Reconstituted in 1ml of sterile 4 mM HCL containing 0.1% BSA.*	354-BP-010	R&D Systems
Mouse Wnt3a 10µg/ml *10µg lyophilised stock Reconstituted in 1ml of sterile PBS.*	1324-WN-002	R&D Systems
Human Sclorstin Domain Containing 1 (SOSTDC1) 38µg/ml *Supplied as a 38ug/ml in50 mM Tris-HCI, 10 mM reduced Glutathione, pH=8.buffer.*	H00025928-P01	Abnova
Mouse Dikkopf 1 (Dkk1) 10µg/ml *10µg lyophilised stock Reconstituted in 1ml of sterile PBS containing 0.1% BSA.*	5439-DK-010	R&D Systems
Human noggin 25µg/ml *25µg lyophilised stock Reconstituted in 1ml of sterile PBS containing 0.1% BSA.*	6057-NG-025	R&D Systems
Human glutatione S-transferase (GST) 200µg/ml *Supplied at 200µg/ml in 25% Glycerol, 50mM Tris HCl, 150mM Sodium chloride, 0.25mM DTT, 0.1mM PMSF, pH 7.5buffer*	ab70456	Abcam

Recombinant Proteins doses required	
Recombinant protein Treatment	**Dose (ng/ml)**
PBS	n/a
Wnt3a	50
BMP2	30
BMP7	30
SOSTDC1	250
GST	250
Dkk1	100
Noggin	100

Combined Recombinant Protein treatments	
Recombinant protein	**Combination Recombinant Protein**
Wnt3a	SOSTDC1
	Dkk1
	GST
BMP2	SOSTDC1
	Noggin
	GST
BMP7	SOSTDC1
	Noggin
	GST

Table 4.1 - *Recombinant protein doses required for sole and combined treatments.*

4.3.1 Assessing Wnt3a and BMP2 and BM7 dose effect on OB progenitor differentiation using ALP analysis

ALP enzyme levels were quantified in bone cell cultures to assess the effects of Wnt3a and BMP2 and BMP7 proteins at different doses on OB progenitor differentiation. OB progenitor cells were seeded in 96 well plates at a density of 2000 cells per well. Cells were differentiated for 11 days in standard osteogenic media; exponential differentiation time point for the cells was previously determined in **section 3.4.2**. Following 72 hours in culture, cells were carefully washed once with PBS and cultured with 100µl/well of osteogenic media containing various concentrations of recombinant mouse Wnt3a (rmWnt3a) protein; 0, 10, 30, 50, 100 and 150ng/ml. In separate wells, OB progenitors were also treated with 100µl of various concentrations of recombinant human BMP2 (rhBMP2) or recombinant human BMP7 (rhBMP7); 0, 10, 30, 40, 50 60ng/ml. OB progenitor cells which were treated with osteogenic media only were used as control. Osteogenic media containing recombinant protein treatments were removed from OB progenitor cultures and replaced with 100µl of fresh media and trearment every three days. Total DNA content of OB progenitors was determined with a PicoGreen dsDNA quantitation reagent as described in **section 2.4** and total cell DNA was used to normalise ALP activity analysed on day 11 of differentiation according to **section 2.3**.

4.3.2 Assessing the effect of SOSTDC1 on the ALP activity of differentiating OB progenitors

Preliminary experiments were carried out to investigate the dose effect of Glutathione S-transferase (GST) tagged-rhSOSTDC1 on OB progenitor differentiation, OB progenitors were cultured in 96 well plates at a density of 2000 cells per well in MEM-Alpha. Following a 72 hour incubation period, OB progenitor cultures were carefully washed once with PBS and sub-cultured with 100µl/well of osteogenic media containing various doses of rhSOSTDC1: 0, 14, 8, 32, 63, 125, 250 and 500ng/ml. To determine if any effect of rhSOSTDC1 observed on OB progenitor differentiation was solely as a result of the SOSTDC1 molecules and not the GST tag protein, OB progenitors were also cultured with rhGST protein at the same concentrations as rhSOSTDC1 protein-treated cultures. OB progenitors were differentiated in osteogenic media for up to 15 days and osteogenic media containing the rhSOSDC1 or rhGST proteins were removed from the OB progenitor cultures and replaced with fresh media every 3 days. Total DNA content of

OB cultures determined using PicoGreen dsDNA quantitation reagent was used as surrogate for of cell proliferation. ALP analysis was used as a marker of OB progenitor differentiation and performed on cultures on day 8, 11 and 15 of differentiation. Calculated PicoGreen values for total cell DNA contents were used to normalise ALP activity. Based on the results of the SOSTDC1 dose responses on OB progenitor proliferation and differentiation in preliminary studies, the same experiments were repeated using a low 50ng/ml and high 250ng/ml dose of rhSOSTDC1 compared to cells cultured with PBS control. The experiments were set up in an identical manner to the experimental design outlined in the preliminary studies. The objective of these subsequent studies was to be able to select an optimal concentration of rhSOSTDC1 to be used in future studies.

4.3.3 Determining the effect of SOSTDC1 on Wnt and BMP-induced alkaline phosphatase Activity in OB progenitors and SAOS2 cells

Analysis of the ALP activity of OB progenitors was performed to investigate the effect of SOSTDC1 on Wnt and BMP-induced cell differentiation. OB progenitors were harvested from a near confluent flask following trypsinisation as outlined in the main method section. Cells were pelleted by centrifugation and counted using a haemocytometer as described in the method section. OB progenitor cells were resuspended in MEM-Alpha at 2000 cells per well in 96 well culture plates (6000cells/cm^2). Following a 72 hours period in culture, the media was removed from the adherent OB progenitor cultures and the cells were washed twice with PBS. Wnt3a protein was diluted to 50ng/ml concentration and BMP2/7 diluted to 30ng/ml concentration in a volume of osteogenic media that was sufficient for all replicates within plate/s. To test the effect of SOSTDC1 and Dkk1 on Wnt3a, osteogenic media containing 50ng/ml of rmWnt3a was combined with either 250ng/ml rhSOSTSDC1 or 100ng/ml rhDkk1. To test the effect of SOSTDC1 and noggin on BMP2/7, osteogenic media containing 30ng/ml of rhBMP2/7 was combined with either 250ng/ml rhSOSTSDC1 or 100ng/ml rhnoggin. To establish whether the GST-tag attached to the SOSTDC1 molecule had any effect on OB progenitor differentiation, rhGST protein was used as a control. In all experiments, osteogenic media containing PBS was used as a negative control and 250ng/ml of rhGST at the same dose as the corresponding rhSOSTDC1 concentration was used as the vehicle. 100 µl of osteogenic media containing the required protein/protein combination was added to each well

containing OB progenitor cells. Osteogenic media from the OB progenitors was replaced every three days with 100 µl of fresh media containing the required recombinant proteins. ALP for OB progenitors was analysed as described in the method section at day 8, 11 and 15 of differentiation. The total DNA content of OB progenitor cultures were also determined with a PicoGreen dsDNA quantitation reagent to normalise ALP activity to cell DNA content, as described in the method section.

In previous studies, I investigated the effect of SOSTDC1 on Wnt and BMP-induced differentiation in OB progenitors with differentiating potential. I wanted to compare this SOSTDC1-induced effect on differentiation in the OB progenitors to the SAOS2 cells which have a mature OB phenotype as established in Chapter 3. The same experiment design which was used to analyse ALP activity of primary OB progenitor cultures was also used to investigate the effect of rhSOSTDC1 on Wnt and BMP-induced differentiation in SAOS2 cells. The only difference between the SAOS2 and primary OB progenitor culture experiments was that ALP activity of SAOS2 cells was analysed on day 4 and 7 of differentiation. The total DNA content of SAOS2 cultures were also determined with a PicoGreen dsDNA quantitation reagent to normalise ALP activity to cell DNA content, as described in the method section.
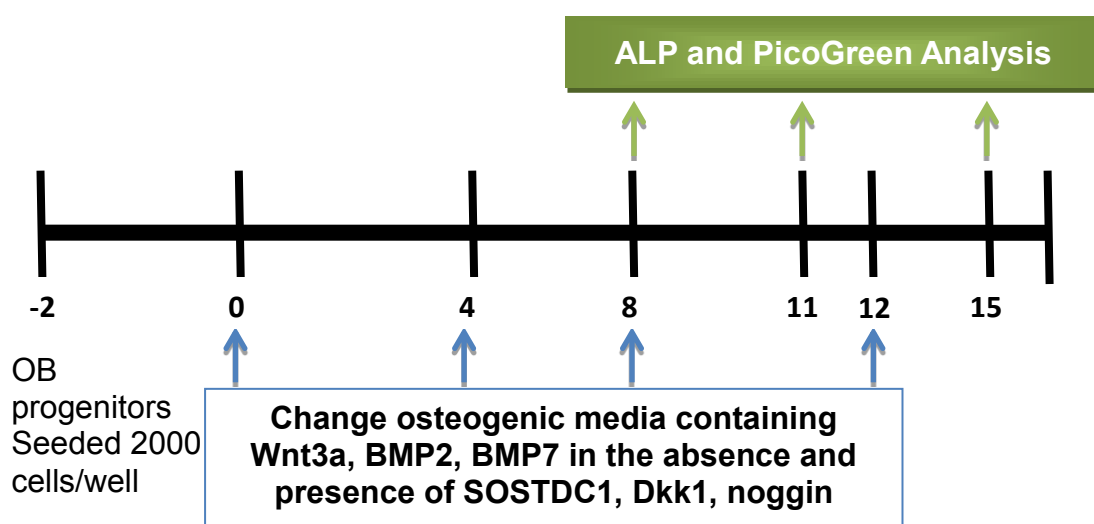
Figure 4.1 - *A time line for ALP and PicoGreen Analysis of OB progenitors*

4.3.4 Determining the effect of SOSTDC1 on Wnt and BMP-induced *Runx2* gene expression in differentiating OB progenitors

Runx2 expression was used as a second marker of OB progenitor differentiation to investigate the effect of SOSTDC1 on Wnt and BMP activity. OB progenitor cells were harvested from a near confluent flask by trypsinisation and cell pellets were counted using a haemocytometer as described in the method section. OB progenitor cells were resuspended in MEM-Alpha at 57,000 cells per well in 6 well culture plates containing 1.5ml of media within each well. Following 72 hours in culture, the media was removed from the adhered OB progenitor culture and cells were washed twice with PBS. OB progenitors were differentiated in 1500µl/well of standard osteogenic media for up to 11 days and osteogenic media was replaced with fresh osteogenic media every three days. On day 7 and 10 of differentiation, OB progenitor cultures were treated with recombinant protein for 24 hours. The rmWnt3a protein was diluted to 50ng/ml in 65µl of osteogenic media in a 0.5ml sterile eppendorfs. The rhBMP2 and rhBM7 proteins were diluted to 30ng/ml concentration in 65µl of osteogenic media in 0.5ml sterile polypropylene centrifuge tubes.

To assess the effect of SOSTDC1 and Dkk1 on Wnt3a, 50ng/ml of rmWnt3a was combined with 250ng/ml rhSOSTSDC1 and 50ng/ml of rmWnt3a was combined with 100ng/ml rmDkk1 in a 65µl volume of osteogenic media. To assess the effect of SOSTDC1 and noggin on BMP2/7, 50ng/ml of BMP2/7 was combined with 250ng/ml rhSOSTSDC1 or 100ng/ml rhnoggin in a 65µl volume of osteogenic media. All eppendorfs containing 65µl of protein/protein combinations were placed in a water bath for 1 hour at 37°C to allow interaction between combined proteins. From the 65µl of protein/protein combination, 50µl was added to each well containing OB progenitor cultures and the media containing protein treatments were mixed gently within wells by pipetting. Culture plates were placed in 37ºC culture incubators for 24 hours. RNA was isolated from the OB progenitor cultures using the RNA mini Prep kit and quantified with a Nanodrop as described in **section 2.12**. The expression of *Runx2, COL1A2* and housekeeper *B2M* gene were quantified using TaqMan® Assays for qRT-PCR analysis using the SDS2.2.1. Relative quantification of gene expression were performed by normalising to the house keeping B2M gene using the formula $\Delta CT = CT_{target} - CT_{housekeeping}$ as described in **section 2.13.3**.
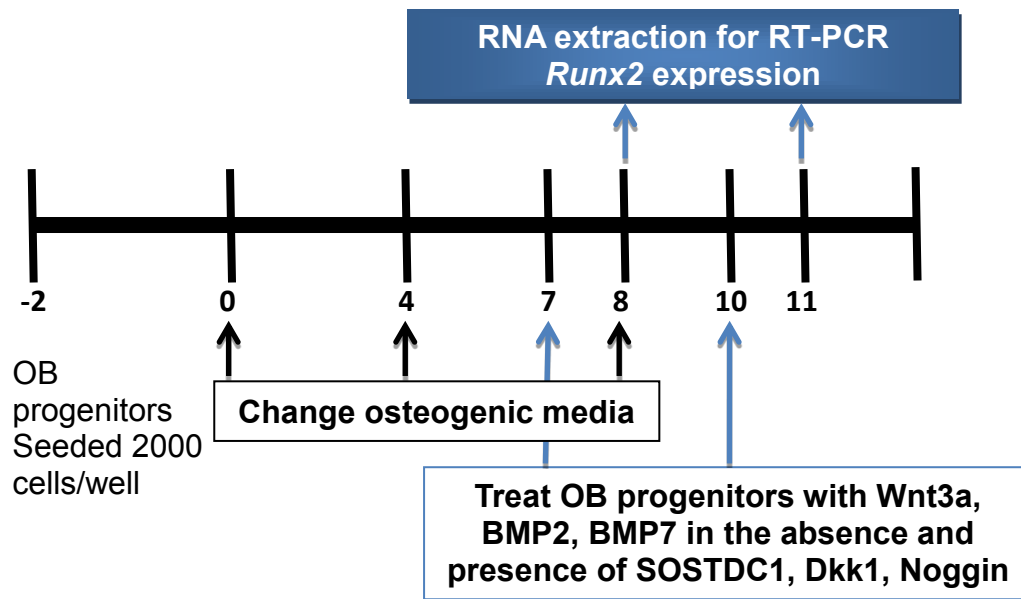
Figure 4.2 - *A time line for RNA extraction for the analysis of Runx2 gene expression of differentiating OB progenitors by RT-PCR.*

4.3.5 Determining the effect of SOSTDC1 on Wnt and BMP-induced OB progenitor mineralisation

To investigate the effect of SOSTDC1 on Wnt and BMP-induced mineralisation in OB progenitor cells, Alizarin red staining was used to detect mineral deposition. OB progenitor cultures were harvested from a near confluent flask by trypsinisation. Centrifuged cell pellets were counted using a haemocytometer, as described in **section 2.13**. OB progenitors cells were resuspended in MEM-Alpha at 5700 cells per well in 48 well culture plates. Following a 72 hours period in culture, the media was removed from the adhered OB progenitor cultures and cells were washed with PBS. Recombinant proteins were diluted to the correct concentrations from their stock solutions in a volume of osteogenic media that was sufficient for all replicates within a plate/s. The rmWnt3a protein was diluted to 50ng/ml concentration and the rhBMP2/7 diluted to 30ng/ml concentration in a volume of osteogenic media that was sufficient for all replicates within plate/s. To test the effect of SOSTDC1 and Dkk1 on Wnt3a, osteogenic media containing 50ng/ml of rmWnt3a was combined with either 250ng/ml rhSOSTSDC1 or 100ng/ml rhDkk1. To test the effect of SOSTDC1 and noggin on BMP2/7, osteogenic media containing 30ng/ml of rhBMP2/7 was combined with either 250ng/ml rhSOSTSDC1 or

100ng/ml rhnoggin. 250 µl of osteogenic media containing protein or protein combinations was added to each well. Osteogenic media from the OB progenitors were removed every three days and 250 µl of fresh media containing the required protein treatments replaced. Alizarin red staining of OB progenitor cultures was carried out and quantified on day 8, 11 and 15 of OB progenitor differentiation as described in **section 2.5**.
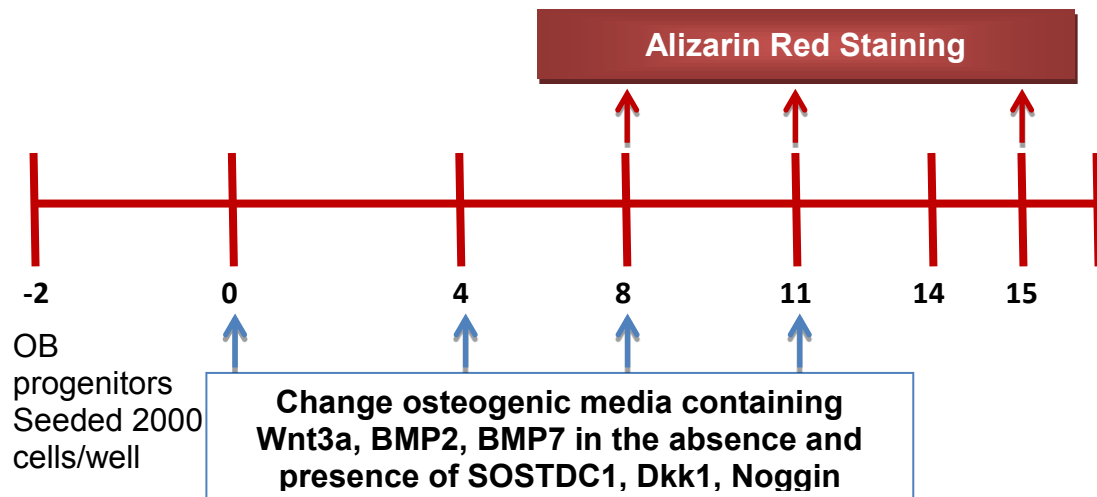
Figure 4.3 - *A time line for the analysis of differentiating OB progenitor mineralisation.*

4.3.6 Determining the effect of SOSTDC1 on acute Wnt and BMP-induced intracellular protein signalling in OB progenitors

Primary and secondary antibodies for western blot		
Antibody	**CATALOGUE NUMBER**	**SUPPLIER**
Phospho-Smad1 (Ser463/465)/ Smad5 (Ser463/465)/ Smad8 (Ser426/428) antibody *Rabbit polyclonal*	9511	Cell Signalling
Anti-β-catenin (phospho Y142) antibody *Rabbit polyclonal*	Ab-27798	Abcam
Anti-GAPDH (6C5) antibody *Mouse monoclonal*	Ab-37168	Abcam
Goat anti-Rabbit IgG –HRP antibody *Rabbit IgG*	9511	Life Technologies Novex®
Goat anti-Mouse IgG –HRP antibody *Mouse IgG*	SC-2031	SantaCruz

Table 4.2 – *Primary and secondary antibodies used in western blotting for investigating the effect of SOSTDC1 on acute Wnt and BMP-induced intracellular protein signalling in OB progenitors.*

To investigate the effect of SOSTDC1 on the acute regulation of Wnt and BMP-induced intracellular signalling in OB progenitors, phosphorylated Smads 1,5&8 and phosphorylated β-catenin protein levels were quantified using western blot analysis. OB progenitor cultures were harvested from a near confluent flask using trypsin and cells counted using a haemocytometer, as described in **section 2.1.3**. OB progenitor cells were resuspended in MEM-Alpha at 57,000 cells per well in 6 well culture plates containing 1500µl of media within each well. Following 72 hours in culture, the media was removed from the adherent OB cells and cells were washed with PBS. OB progenitors were differentiated in 1500µl/well of standard osteogenic media for up to 15 days.

On day 8, 11 and 15 of differentiation, OB progenitor cultures were treated with recombinant proteins. The rmWnt3a protein was diluted to 50ng/ml in 65µl of osteogenic media in a 0.5ml sterile eppendorf. The rhBMP2 and rhBM7 proteins were diluted to

10ng/ml concentration in 65µl of osteogenic media in a 0.5ml sterile eppendorf. To assess the effect of SOSTDC1 and Dkk1 on Wnt3a, 50ng/ml of rmWnt3a was combined with 250ng/ml rhSOSTSDC1 and 50ng/ml of rmWnt3a was combined with 100ng/ml rmDkk1 in a 65µl volume of osteogenic media. To assess the effect of SOSTDC1 and noggin on BMP2/7, 10ng/ml of BMP2/7 was combined with 250ng/ml rhSOSTSDC1 or 100ng/ml rhnoggin in a 65µl volume of osteogenic media. All eppendorfs containing 65µl of protein or protein combinations were placed in a water bath for 1 hour at 37°C to allow interaction between combined proteins. From the 65µl of protein/protein combination, 50µl was added to each well containing OB progenitor cultures and the media containing protein treatments were mixed gently within wells by pipetting. Culture plates were immediately placed in 37ºC culture incubators for 20 minutes.

The protein from OB progenitor cultures were isolated using Mammalian cell lysis kit (Sigma Aldrich) containing phosphatase and protease inhibitor cocktails as described in **section 2.6**. Protein concentration within OB progenitor cell lysates were quantified using the BCA assay as outlined in **section 2.7**. The effect of SOSTDC1 on Wnt-induced signalling in OB progenitors was determined by quantifying levels of phosphorylated β-catenin (92kD). The effect of SOSTDC1 on BMP2 and BMP7-induced signalling in OB progenitors was determined by quantification of phosphorylated Smads 1,5&8 protein complex (52kD). Phosphorylated levels of β-catenin and Smads 1,5&8 were assessed using western blotting as outlined in **section 2.8**.

In brief, 10% polyacrylamide gels were loaded with 10µg of sample protein. Each gel was also loaded with 10µl of a 10-250kD protein molecular marker at the first and last lane. Proteins were run through the stacking gel for 40 minutes at 60 Volts and then separated out for 2 hours at 100 Volts. Proteins were transferred onto PVDF membranes for 70 minutes at 70 Volts. Membranes were washed once in 0.05% PBS-Tween and cut across at just above the 75kD and just above the 35kD mark using the pre-stained molecular markers as reference points. All three pieces of membrane were blocked in 3% BSA solution for 45 minutes. The blot cut just above the 35kD mark was placed in a 1/15000 dilution of anti-GAPDH mouse antibody. The blot cut above 75kD was placed in a 1/300 dilution of anti-pβ-Catenin rabbit antibody and the blot cut between 50-75kD was probed with 1/3000 of rabbit anti-Psmad1,5&8 antibody. Antibody incubations were all carried out overnight at 4°C on a roller. Blots probed with anti-GAPDH antibody were incubated

with 1/30,000 dilution of secondary HRP-conjugated anti-mouse IgG antibody. Blots probed with anti-pβ-catenin or anti-pSmad1,5&8 antibody were incubated with 1/5,000 dilution of secondary HRP-conjugated anti-rabbit IgG antibody. The average density of SOSTDC1 protein was normalised to the average density of GAPDH using the GST-710 Calibrated Imaging Densitometer.

4.4. Results

4.4.1 Wnt3a, BMP2 and BMP7 dose dependently induced differentiation of OB progenitors

PicoGreen quantification and ALP assays were used to analyse the proliferation and differentiation of OB progenitors, respectively. In experiments in which differentiating OB progenitors were cultured with increasing concentrations of rmWnt3a protein, PicoGreen analysis showed that continuous exposure to rmWnt3a induced OB progenitor proliferation (***P=<0.0001, **Figure 4.4.1.1 A**). ALP levels increased dose-dependently in differentiating OB progenitor cells cultured with 50 to 150ng/ml rmWnt3a protein, with 100ng/ml rmWnt3a maximally increasing ALP levels (***P=<0.0001 **Figure 4.4.1.1 B**).

PicoGreen analysis showed that continuous exposure to rhBMP2 and rhBMP7 stimulated OB progenitor proliferation (*P=0.014, ***P=0.0001, **Figure 4.4.1.2 A, B**). ALP activity of OB progenitors treated with rhBMP2 increased in a concentration-dependant manner with significant increases in ALP observed from 10-60 ng/ml concentrations (**Figure 4.4.1.2 C**). Maximal BMP2-induced ALP upregulation was achieved when differentiating OB progenitors were cultured with 40ng/ml of rhBMP2 (***P= <0.0001). Although ALP levels rose at >40ng/ml rhBMP2 concentrations compared to control, ALP levels plateaued beyond the 40ng/ml treatment of rhBMP2. ALP levels of differentiating OB progenitors cultured with rhBMP7 increased in a dose-dependent manner with significant increases in ALP observed from 30-50 ng/ml of rhBMP7 (**Figure 4.4.1.2 D**). Maximal BMP7-induced ALP upregulation was observed when OB progenitors were treated with 50ng/ml of BMP7 (***P= <0.0001) and ALP levels fell beyond this concentration. The ALP levels observed as a result of rhBMP2 induction (5-15U/ml/min/ng/ml) were on a

comparatively higher scale than the rhBMP7-induced ALP levels (~0.5-1.2 U/ml/min/ng/ml).

A

B
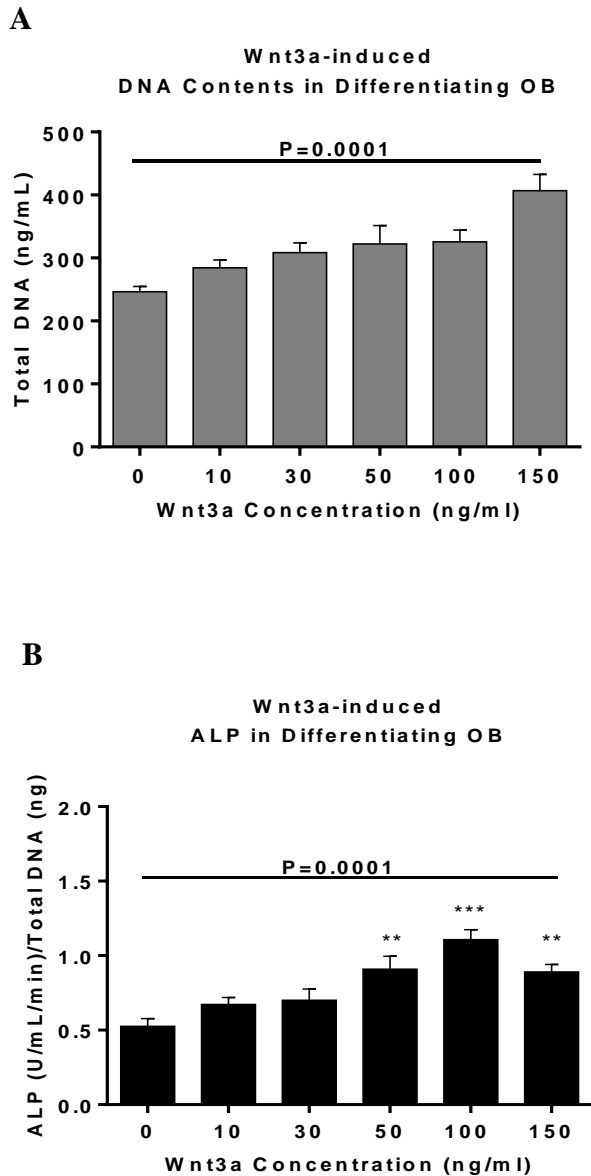
Figure 4.4.1.1 - Wnt3a increased ALP activity of differentiating OB progenitors in a dose dependent manner: *OB progenitor cells were differentiated in osteogenic media containing increasing doses of mrWnt3a. PicoGreen quantification of total DNA contents and ALP analysis were performed to determine dose effect on cell proliferation and differentiation. (A, B) Total DNA contents and ALP activity of differentiating OB progenitor cells increased following treatment with Wnt3a in comparison to control and that this effect was dose dependent. N=3 independent experiment .One way ANOVA and Holme-Sidak's post-test. Data are displayed with mean ± SEM. ***P<0.0001.*
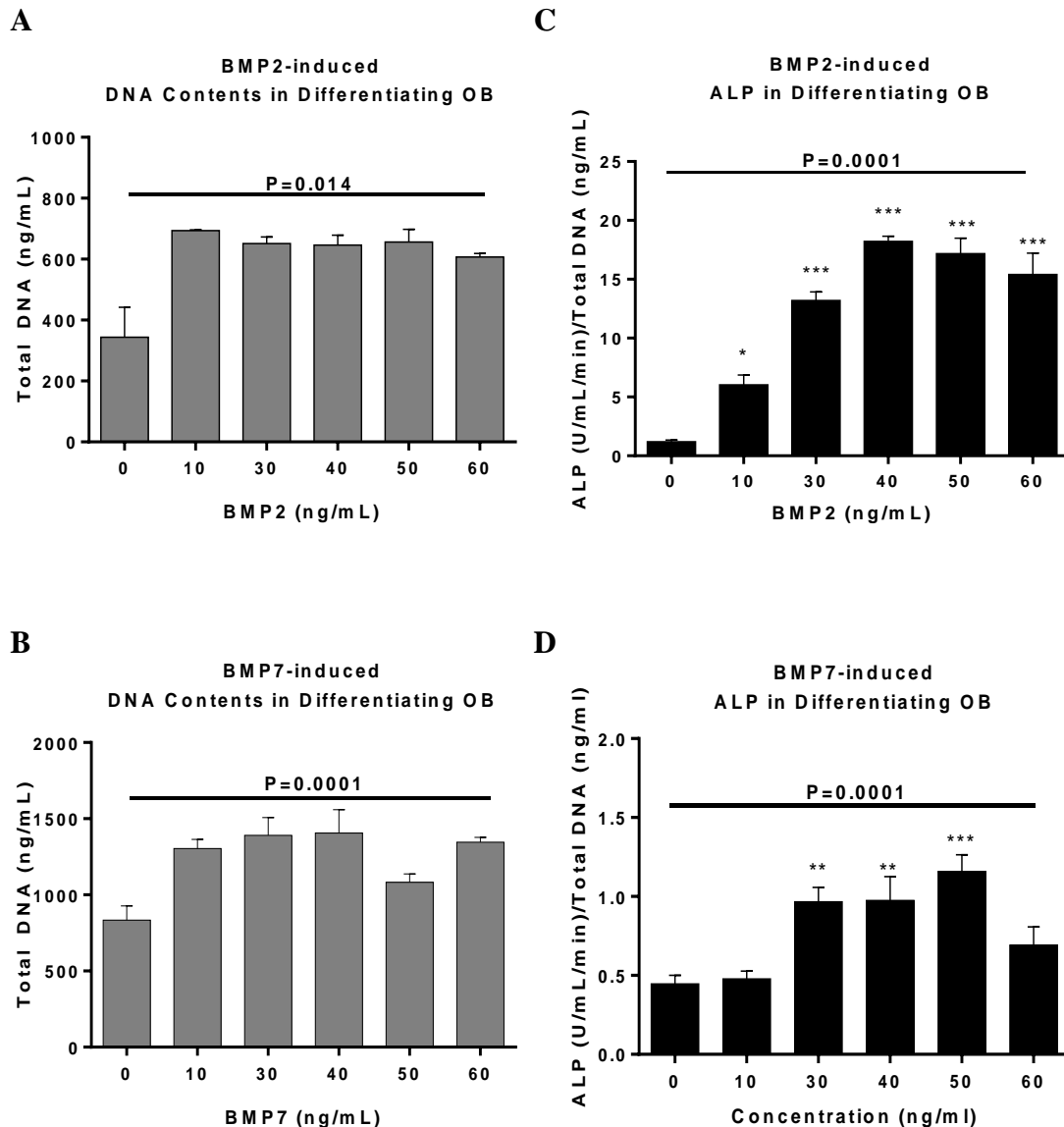
Figure 4.4.1.2 - BMP2 and BMP7 increased ALP activity of differentiating OB progenitors in a dose dependent manner – *OB progenitor cells were differentiated in osteogenic media containing increasing doses of rhBMP2 or rhBMP7. PicoGreen quantification of total DNA contents and ALP analysis were performed to determine dose effect on cell proliferation and differentiation, respectively. Graphs are representative of one of two independent experiments. (A, B) rhBMP2 and rhBMP7 induced proliferation of OB progenitors. (C, D) OB progenitor ALP levels increased following treatment with rhBMP2 or rhBMP7 in comparison to control and that this effect was dose dependent. N=3 independent experiments. One way ANOVA and Holme-Sidak's post-test. Data are displayed with mean ± SEM. *P<0.05, **P=<0.01, ***P<0.0001.*

4.4.2 SOSTDC1 had no effect on ALP levels of differentiating OB progenitors

ALP analysis was performed to analyse the effect of rhSOSTDC1 on the differentiation of OB progenitor cultures. PicoGreen analysis of total DNA contents within cells was used to normalise the ALP levels. Based on the preliminary data, I showed that ALP levels of differentiating OB progenitors were not affected when cultured with increasing concentrations of either rhSOSTDC1 or GST vehicle protein (4-500ng/ml). There was no difference in ALP levels of OB progenitors cultured in rhSOSTDC1 compared to GST vehicle on any of the day 8, 11 or 15 analysis time-points (**Figure 4.4.2 A**).

In subsequent SOSTDC1 dose response studies, direct comparisons of the effect 50ng/ml SOSTDC1 and 250 ng/ml SOSTDC1 showed that the ALP levels of differentiating OB progenitors did not differ in cells cultured with either concentration (**Figure 4.4.2 B**). In addition there was no difference between ALP levels of OB progenitors cultured with rhSOSTDC1 or PBS control. This effect was applicable throughout all differentiation time points

A
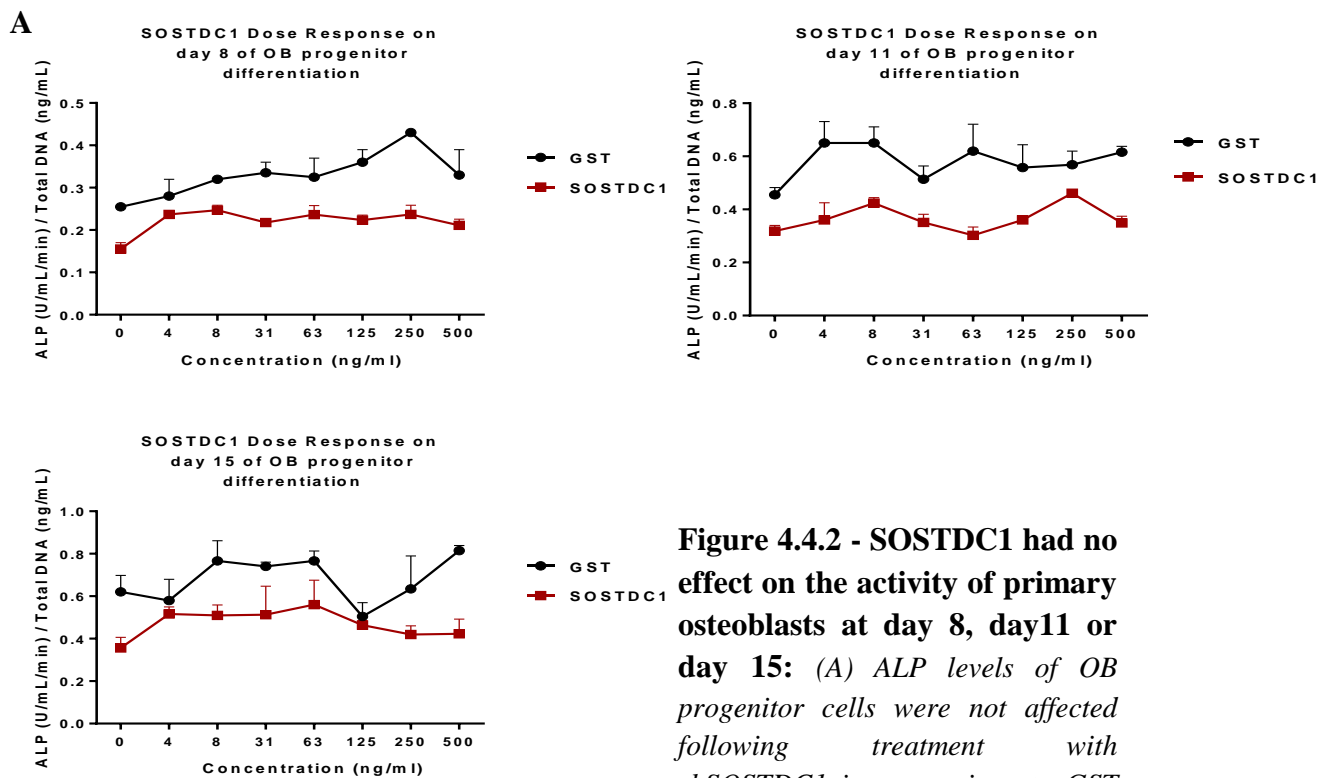
Figure 4.4.2 - SOSTDC1 had no effect on the activity of primary osteoblasts at day 8, day11 or day 15: *(A) ALP levels of OB progenitor cells were not affected following treatment with rhSOSTDC1 in comparison to GST vehicle at any dose. (B) Direct comparison of ALP levels in differentiating OB progenitors cultured in PBS, 50ng/ml rhSOSTDC1 or 250 ng/ml of rhSOSTDC1 showed that there was no difference between any of the rhSOSTDC1 doses or between the rhSOSTDC1 treated OB progenitors and PBS controls. N=3 independent experiments, Student's t-test. Data are displayed with mean ± SEM.*

B
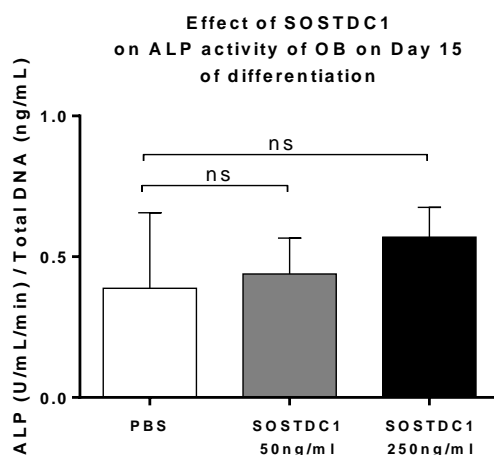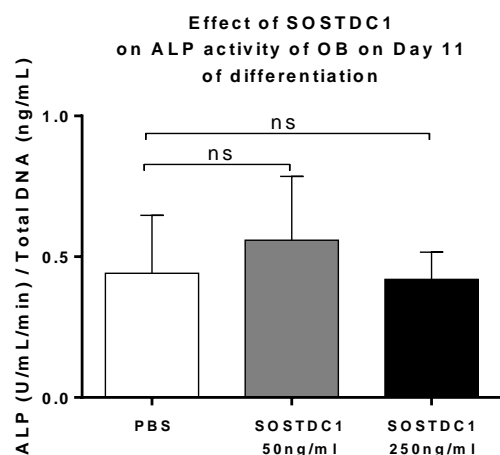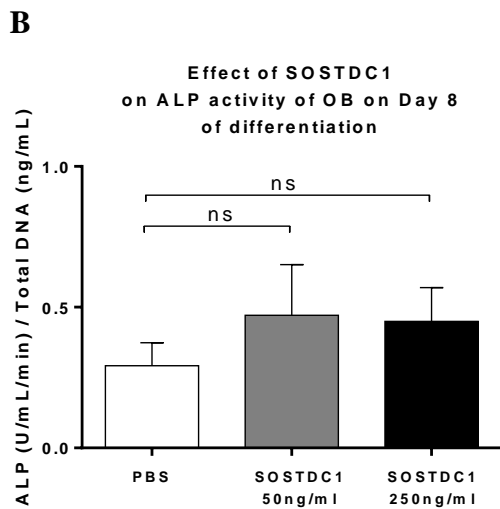
4.4.3 SOSTDC1 suppressed BMP-induced but not Wnt-induced ALP activity in differentiating OB progenitors

Differentiating OB progenitor cells were treated with rhSOSTDC1 in the presence or absence of recombinant Wnt3a, BMP2 or BMP7 proteins and differentiation was assessed via analyses of OB progenitors ALP activity. OB progenitor cultures were also treated with ligands in the presence of a well characterised antagonist specific to that ligand. The ALP activity of OB progenitors cultured with 50ng/ml rmWnt3a combined with 100ng/ml rmDkk1 and 30ng/ml rhBMP2/7 combined with 100ng/ml rhnoggin were assessed. To ensure that the GST protein tag attached to the rhSOSTDC1 protein did not affect ligand-induced OB progenitor differentiation, each experiment contained a control in which 250ng/ml rhGST protein which was added to the Wnt or BMP ligand. ALP analysis showed that there were no differences between the ALP activity of rmWnt3a, rhBMP2 and rhBMP7 treated with or without rhGST suggesting that any effect of rhSOSTDC1 observed was solely due to the rhSOSTDC1 protein, and not the rhGST (**Appendix 1**).

ALP analysis showed that 50ng/ml Wnt3a only had an inductive effect on OB progenitor differentiation on day 8 of differentiation (*P= <0.026, **Figure 4.4.3.1, A**). This Wnt3a-induced ALP activity was not significant on any other time point during OB progenitor differentiation (**Fig. 4.4.3.1 B, C**). The rhSOSTDC1 had no effect on OB progenitor ALP activity when in the presence of rmWnt3a. Canonical Wnt-antagonist Dkk1 similarly had no significant effect on Wnt3a-induced ALP activity.

Experiments assessing the effect of rhBMP on OB progenitor ALP activity showed that rhBMP2 upregulated ALP activity throughout day 8-11 of OB progenitor differentiation, although this effect lessened throughout as the OB progenitor cells matured (Day 8 ***P= <0.0001, Day11 **P=0.0051, **Figure 4.4.3.2**). The rhBMP7 also induced ALP activity of OB progenitor cells from day 8-11 of differentiation (Day 8 *P= <0.032, Day11 *P=0.021, **Figure 4.4.3.3**). The rhBMP2 and rhBMP7 and had no significant effect on OB progenitor cells on day 15 of differentiation. The rhSOSTDC1 had a modest suppressive effect on rhBMP2-induced ALP activity on day 8 of differentiation only (*P=0.038, **Figure 4.4.3.2, A**). SOSTDC1 had no effect on rhBMP7-induced ALP activity in OB at any time point during differentiation. In the presence of rhBMP2 or

rhBMP7, rhnoggin had a suppressive effect on ALP activity up to day 11 of OB progenitor differentiation (BMP2; Day 8 ***P= <0.0002, Day11 *P=0.022, **Figure 4.4.3.2,** BMP7; Day 8 **P= <0.006, Day11 *P=0.029, **Figure 4.4.3.3**).

In similar experiments assessing the effect of SOSTDC1 on Wnt and BMP-induced ALP activity in SAOS2 cells, I showed that neither Wnt3a, BMP2 nor BMP7 had any effect on ALP activity on any of the differentiation time-points. The 250ng/ml rhSOSTSDC1 did not have any effect in the absence or presence of either ligand (**Appendix 2**).

A

Effect of SOSTDC1 on Wnt3a-induced ALP in OB on Day 8 of differentiation

B

Effect of SOSTDC1 on Wnt3a-induced ALP in OB on Day 11 of differentiation

C

Effect of SOSTDC1 on Wnt3a-induced ALP in OB on Day 15 of differentiation
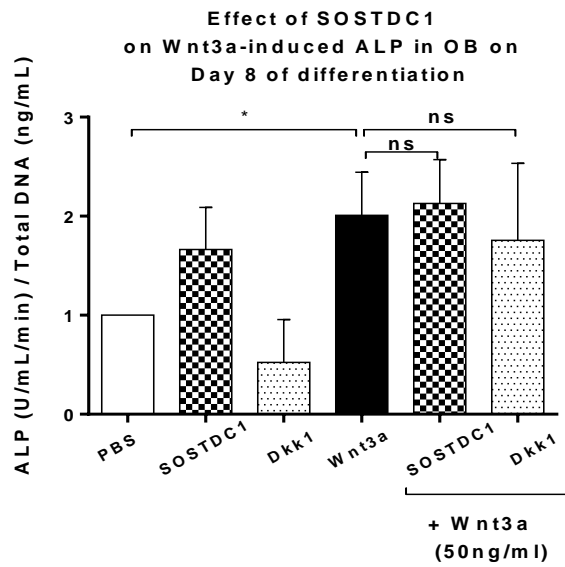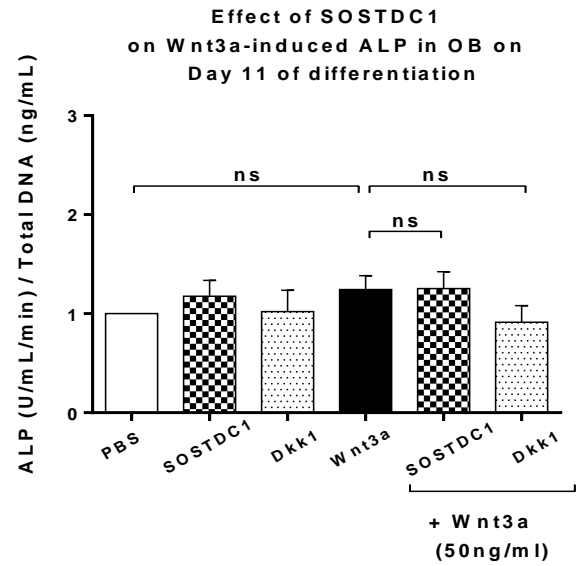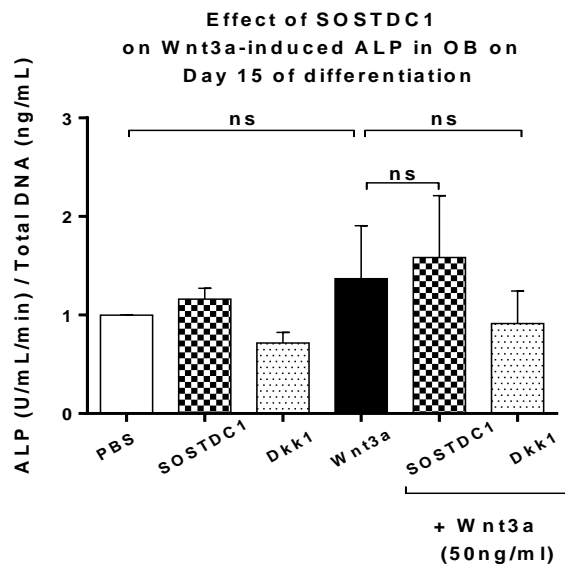
Figure 4.4.3.1 - SOSTDC1 had no effect on Wnt-induced ALP activity in differentiating OB progenitors: *Differentiating OB progenitors were treated with vehicle or 250 ng/ml rhSOSTDC1 and also separately with 50ng/ml rmWnt3a in the presence or absence of rhSOSTDC1. (A) OB progenitor cells treated with rmWnt3a had increased ALP activity in comparison to PBS control on day 8 of differentiation and neither rhSOSTDC1 or rmDkk1had an effect on Wnt3a-induced ALP activity. (B, C) Wnt3a and SOSTDC1 had no effect on day 11 or 15 of differentiation. N=4 independent experiments, One way ANOVA and Holme-Sidak's post-test. Data are displayed with mean ± SEM. *P<0.05.*

A

Effect of SOSTDC1 on BMP2-induced ALP in OB on Day 8 of differentiation

B

Effect of SOSTDC1 on BMP2-induced ALP in OB on Day 11 of differentiation

C

Effect of SOSTDC1 on BMP2-induced ALP in OB on Day 15 of differentiation
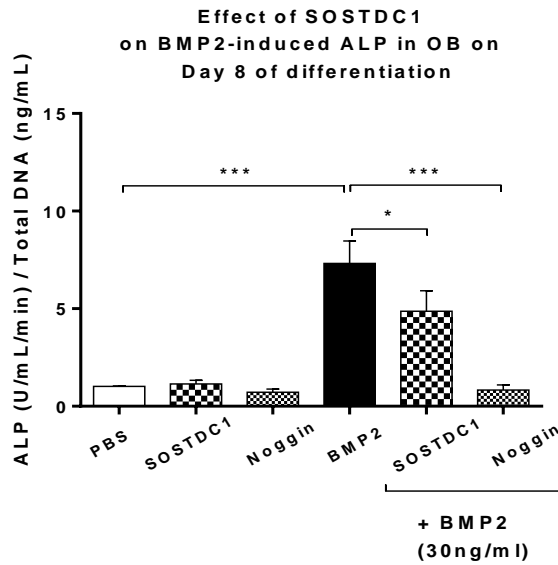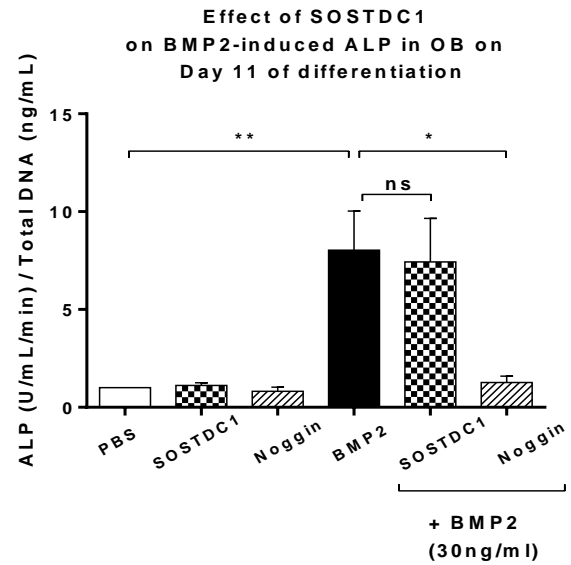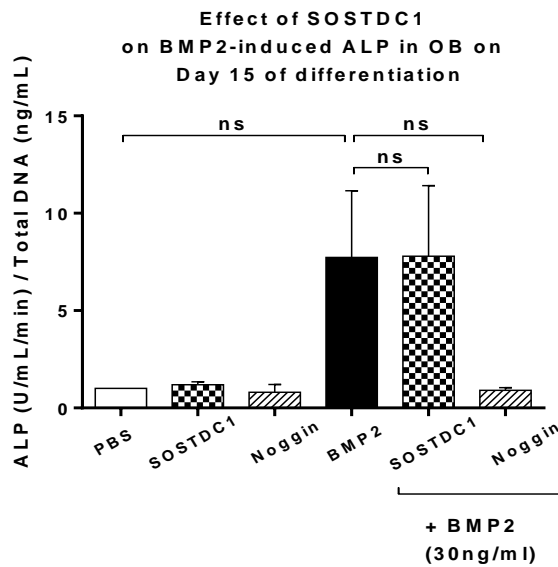
Figure 4.4.3.2 - SOSTDC1 reduced BMP2-induced ALP activity in differentiating OB progenitors: *OB progenitor cells were treated with vehicle or 250ng/ml rhSOSTDC1 and also separately with 30ng/ml rhBMP2 in the presence or absence of rhSOSTDC1. (A, B) The rhBMP2 induced OB progenitor ALP activity up to day 11 of differentiation and rhSOSTDC1 reduced rhBMP2 induction of OB progenitor ALP on day 8 of differentiation only. rhnoggin strongly suppressed BMP2-induced ALP activity up to day 11 of OB progenitor differentiation. N=4 independent experiments, One way ANOVA and Holme-Sidak's post-test. Data are displayed with mean ± SEM. *=P<0.05, **=P<0.01, ***=P<0.001*

A

Effect of SOSTDC1
on BMP7-induced ALP in OB on
Day 8 of differentiation

B

Effect of SOSTDC1
on BMP7-induced ALP in OB on
Day 11 of differentiation

C

Effect of SOSTDC1
on BMP7-induced ALP in OB on
Day 15 of differentiation
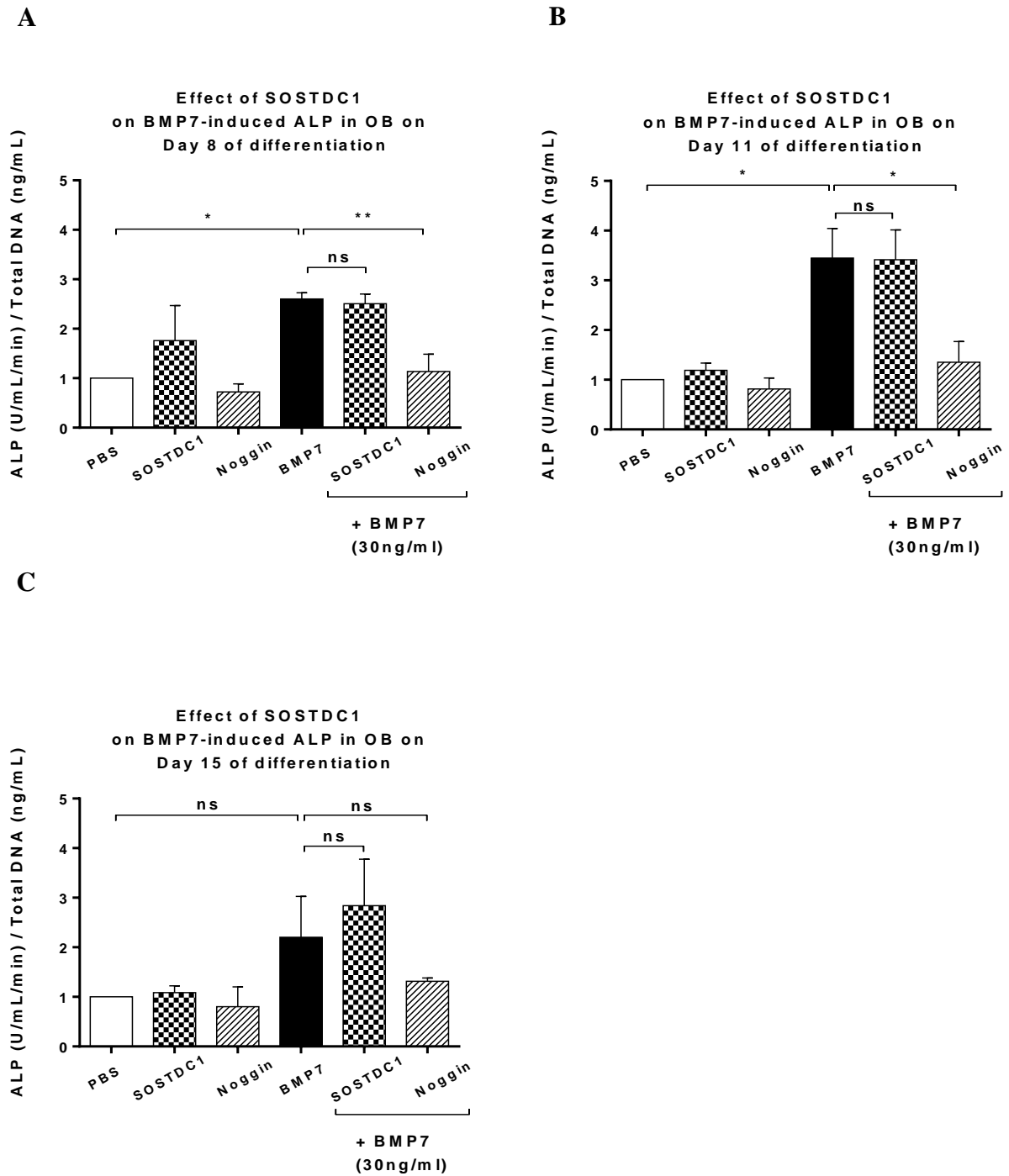
Figure 4.4.3.3 - SOSTDC1 had no effect on BMP7-induced ALP activity in differentiating OB progenitors: *OB progenitors were cultured with vehicle or 250ng/ml rhSOSTDC1 and also separately with 30ng/ml rhBMP7 in the presence or absence of rhSOSTDC1. (A, B) ALP activity of OB progenitor cultures treated with rhBMP7 increased up to day 11 of OB progenitor differentiation. The rhSOSTDC1 protein had no effect on rhBMP7-stimulated ALP on any differentiation time point analysed. rhnoggin strongly supressed BMP2-induced ALP activity up to day 11 of OB progenitor differentiation N=4 independent experiments, One way ANOVA and Holme-Sidak's post-test. Data are displayed with mean ± SEM. *=P<0.05, **=P<0.01.*

4.4.4 SOSTDC1 inhibited Wnt and BMP-induced *Runx2* gene expression in differentiating OB progenitors

Quantitative RT-PCR was performed to assess to effect of rhSOSTDC1 on Wnt and BMP-induced *Runx2* gene expression in differentiating OB progenitor cultures. RNA from OB progenitor cells was isolated on day 8 and 11 of differentiation following protein treatments in culture for 24 hours. *Runx2* and housekeeping *B2M* gene expression were quantified using qRT-PCR. Differences in *Runx2* gene expression were normalised to *B2M* expression and overall fold changes in gene expression were calculated using the ΔΔ-CT method. The effect of 100ng/ml rhDkk1 on rmWnt3a-induced *Runx2* expression was also assessed as a known Wnt-antagonist control. 100ng/ml noggin was used as a known BMP antagonist in experiments investigating *Runx2* expression. Data were normalised to PBS control. Data obtained from qRT-PCR analysis showed that 250ng/ml SOSTDC1 inhibited Wnt3a-induced *Runx2* gene expression on day 8 of OB progenitor differentiation and this relationship was not statistically significant on any other occasion with the differentiation time course (**P=0.0052, **Figure 4.4.4.1 A**). The rhDkk1 had no significant effect on rmWnt-induced *Runx2* expression during OB progenitor differentiation (**Figure 4.4.4.1 A, B**).

Analysis of qRT-PCR analysis showed that rhBMP2-induced *Runx2* gene expression on day 8 of OB progenitor differentiation and rhSOSTDC1 inhibited this inductive effect (**P=0.0047, **Figure 4.4.4.2, A**). Furthermore, rhnoggin had a similar effect to rhSOSTDC1 in that is also down-regulated rhBMP2-induced *Runx2* gene expression levels in OB progenitors on day 8 of differentiation (*P=0.049, **Figure 4.4.4.2, A**). Similarly, qRT-PCR showed that rhBMP7 stimulated *Runx2* expression in the early stages of OB progenitor differentiation and rhSOSTDC1 was able to reverse this effect significantly (*P=0.024, **Figure 4.4.4.3, A**). The rhnoggin had no effect on *Runx2* expression in OB when in presence of rhBMP7.

A
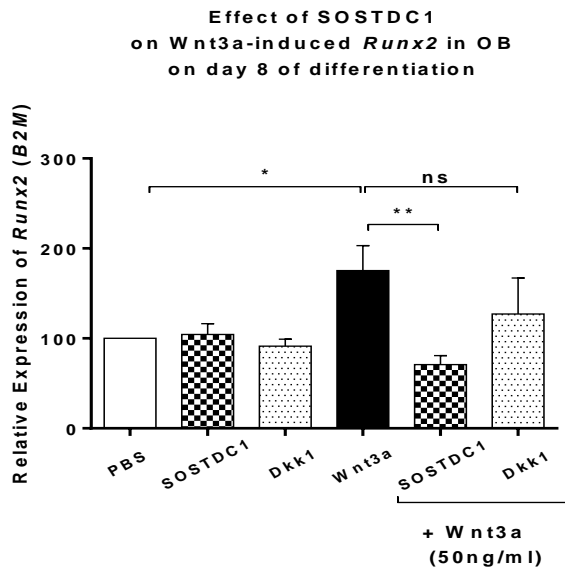
Effect of SOSTDC1 on Wnt3a-induced *Runx2* in OB on day 8 of differentiation

Wnt3a-Induced *Runx2* CT values On Day 8 of OB differentiation	
Protein Treatment	Average CT Value
Control (CT)	21.7
SOSTDC1	22.2
Dkk1	22.3
Wnt3a	20.7
Wnt3a+SOSTDC1	23.0
Wnt3a+Dkk1	22.5

B
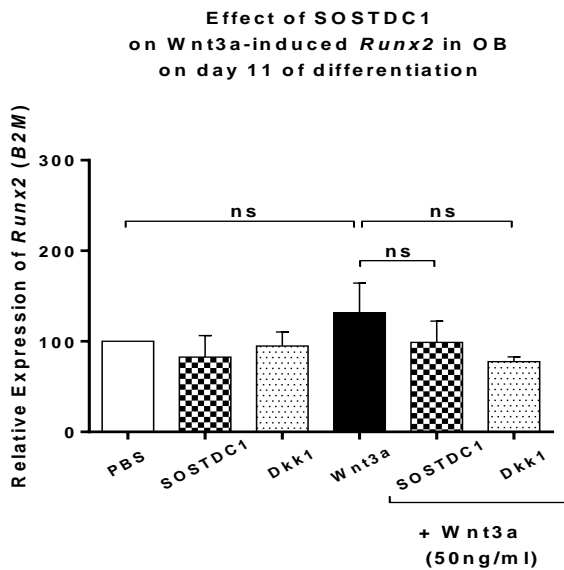
Effect of SOSTDC1 on Wnt3a-induced *Runx2* in OB on day 11 of differentiation

Wnt3a-induced *Runx2* CT values On Day 11 of OB differentiation	
Protein Treatment	Average CT Value
Control (CT)	21.4
SOSTDC1	22.3
Dkk1	21.2
Wnt3a	21.2
Wnt3a+SOSTDC1	22.4
Wnt3a+Dkk1	21.6

Figure 4.4.4.1 - SOSTDC1 suppressed Wnt3a-induced Runx2 gene expression in differentiating OB Progenitors: *Differentiating OB cells were treated with 50ng/ml rmWnt3a in the presence or absence of 250ng/ml rhSOSTDC1 or 100ng/ml rmDkk1. (A) OB progenitors stimulated with Wnt3a resulted in significant induced levels of Runx2 which were down-regulated in the presence of rhSOSTDC1 on day 8 of differentiation and (B) not day 11. N=4 independent experiments, One way ANOVA and Holme-Sidak's multiple comparisons test. Data are displayed with mean ± SEM. *P=0.05, **P=0.01.*

A

Effect of SOSTDC1 on BMP2-induced *Runx2* in OB on day 8 of differentiation
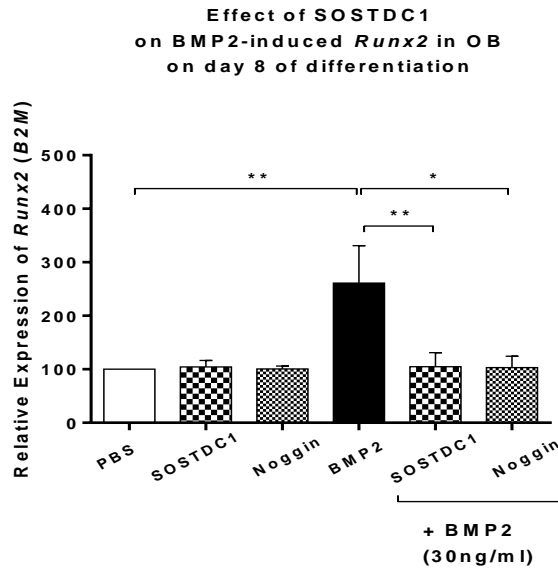
BMP2-induced *Runx2* CT values On Day 8 of OB differentiation	
Protein Treatment	**Average CT Value**
Control (CT)	21.7
SOSTDC1	22.2
Noggin	21.5
BMP2	21.1
BMP2+SOSTDC1	21.9
BMP2+noggin	21.8

B
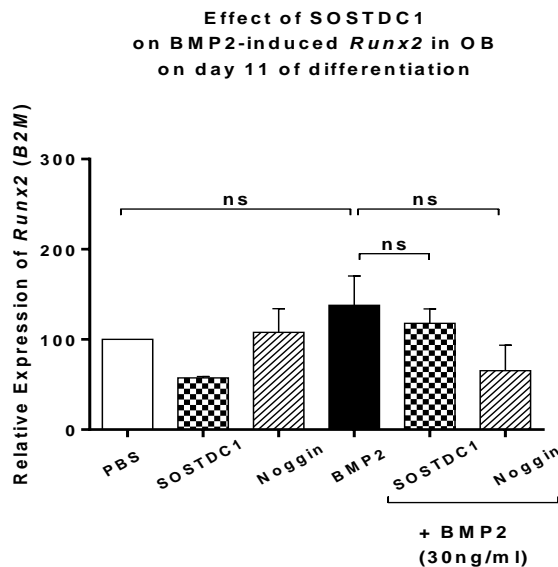
Effect of SOSTDC1 on BMP2-induced *Runx2* in OB on day 11 of differentiation

BMP2-induced *Runx2* CT values On Day 11 of OB differentiation	
Protein Treatment	**Average CT Value**
Control (CT)	21.4
SOSTDC1	22.3
Noggin	20.9
BMP2	20.8
BMP2+SOSTDC1	20.9
BMP2+noggin	22.5

Figure 4.4.4.2 - SOSTDC1 suppressed BMP2-induced Runx2 gene expression in differentiating OB progenitors: *Differentiating OB progenitor cells were treated with 30ng/ml BMP2 in the presence or absence of 250ng/ml rhSOSTDC1 or 100ng/ml rhNoggin. (A) OB progenitors stimulated with rhBMP2 resulted in significant induced levels of Runx2 which were reduced in the presence of rhSOSTDC1 on day 8 of differentiation and (B) not day 11. N=4 independent experiments, One way ANOVA and Holme-Sidak's multiple comparisons test. Data are displayed with mean ± SEM. *P=0.05, **P=0.01.*

A

Effect of SOSTDC1 on BMP7-induced *Runx2* expression on Day 8 of differentiation
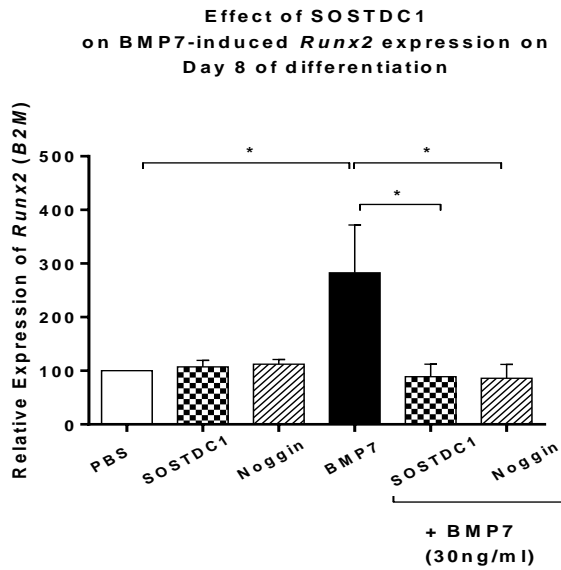
BMP7-induced *Runx2* CT values On Day 8 of OB differentiation	
Protein Treatment	**Average CT Value**
Control (CT)	21.7
SOSTDC1	22.2
Noggin	21.5
BMP7	21.2
BMP7+SOSTDC1	21.8
BMP7+noggin	21.8

B
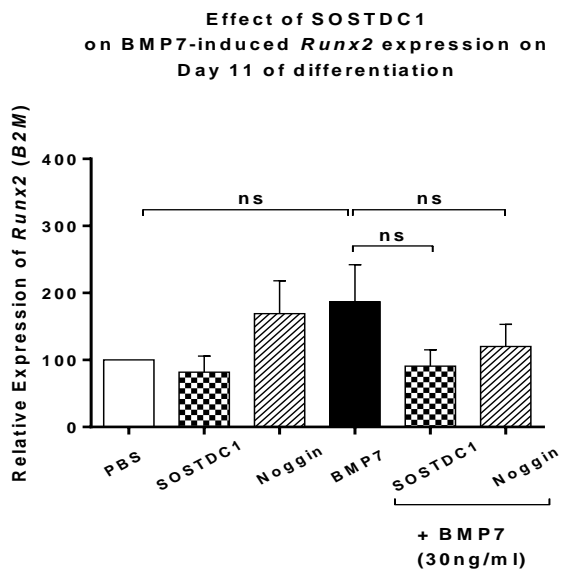
Effect of SOSTDC1 on BMP7-induced *Runx2* expression on Day 11 of differentiation

BMP7-induced *Runx2* CT values On Day 11 of OB differentiation	
Protein Treatment	**Average CT Value**
Control (CT)	21.4
SOSTDC1	22.3
Noggin	20.9
BMP7	20.8
BMP7+SOSTDC1	20.9
BMP7+noggin	22.5

Figure 4.4.4.3 - SOSTDC1 suppressed BMP7-induced Runx2 gene expression in differentiating OB progenitors: *Differentiating OB progenitor cells were treated with 30ng/ml rhBMP7 in the presence or absence of 250ng/ml rhSOSTDC1 or 100ng/ml rhnoggin. (A) OB progenitor stimulated with BMP7 resulted in significant induced levels of Runx2 which were reduced in the presence of rhSOSTDC1 on day 8 and (B) not day 11 of differentiation. N=4 independent experiments, One way ANOVA and Holme-Sidak's multiple comparisons test. Data are displayed with mean ± SEM. *P=0.05, **P=0.01.*

4.4.5 SOSTDC1 suppressed Wnt and BMP-induced OB progenitor mineralisation

Alizarin red staining was used to investigate the effect of rhSOSTDC1 on OB progenitor mineralisation in the presence of rmWnt3a, rhBMP2 or rhBMP7. Percentage (%) mineralisation relative to area was measured at day 8, day 11 and day 15 of differentiation following treatment and values were normalised to PBS control. As in the ALP experiments, the effect of 100ng/ml rmDkk1 on mineralisation when in the presence of rmWnt3a was used as an antagonist control. 100ng/ml rhnoggin was also used as a known BMP antagonist in all mineralisation experiments. When compared to PBS control, 50ng/ml rmWnt3a stimulated mineralisation of OB progenitor cells on day 8 of differentiation which was apparent visually as a result of a darker red colour in staining (***P=0.0001, **Figure 4.4.5.1 A, C**). A trend in Wnt3a-induced OB progenitor mineralisation was evident up to day 11, although this was not statistically significant using a One-Way Anova test. Addition of rhSOSTDC1 to rmWnt3a treated OB progenitors, resulted in a moderate reduction of OB progenitor mineralisation on day 8 of differentiation (*P=0.016, **Figure 4.4.5.1, A**). The rhSOSTDC1 protein did not inhibit Wnt3a-induced OB progenitor mineralisation at any further differentiation time-point. The rhDkk1 had no suppressive effects on Wnt3a-induced mineralisation on any differentiation time-points. Analysis of Alizarin red staining showed that rhBMP2 significantly induced OB mineralisation up to day 11 of differentiation (Day 8 **P= <0.0026, Day11 **P=0.0023, **Figure 4.4.5.2**). The rhBMP7 also stimulated mineralisation in differentiating OB progenitor cells (Day 8 *P= <0.049, Day11 ***P=0.0004, **Figure 4.4.5.3**). Although not significant, rhSOSTDC1 appeared to have some suppressive effect on rhBMP2 and BMP7-induced OB progenitor mineralisation on day 8 of differentiation. On day 11 of OB progenitor differentiation, rhSOSTDC1 significantly inhibited BMP2-stimulated OB progenitor mineralisation (*P=0.044, **Figure 4.4.5.2, B**) and also suppressed BMP7-induced OB progenitor mineralisation (*P=0.018 **Figure 4.4.5.3, B**). When OB progenitor cultures were treated with rhnoggin in the presence of rhBMP2 or rhBMP7, the Alizarin red staining of OB progenitors did appear to be reduced visually. However this suppressive effect was not statistically significant at any time-point during OB progenitor differentiation.

A

Effect of SOSTDC1
on Wnt-induced OB mineralisation on
Day 8 of differentiation

B

Effect of SOSTDC1
on Wnt-induced OB mineralisation on
Day 11 of differentiation

C

Effect of SOSTDC1
on Wnt-induced OB mineralisation on
Day 15 of differentiation
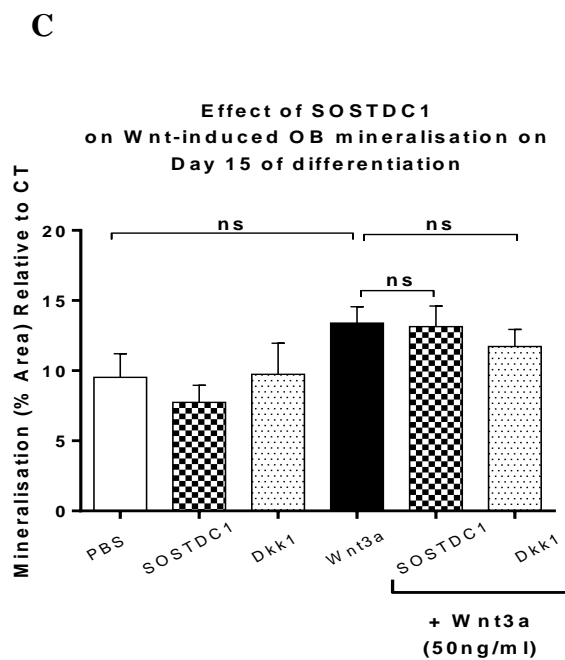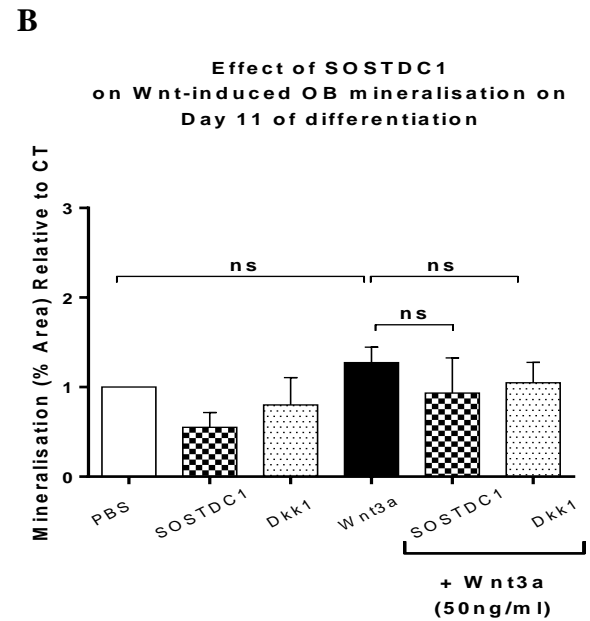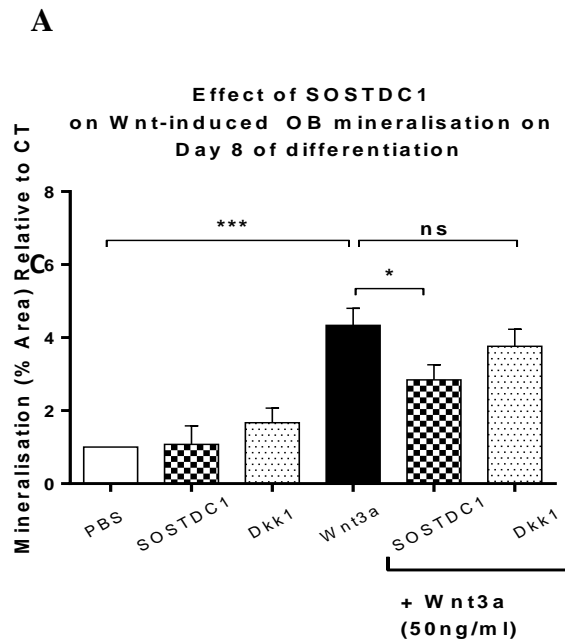
Figure 4.4.5.1 - Wnt3a induced mineralisation in OB progenitor cultures and SOSTDC1 reduced this effect on day 8 of differentiation: *OB progenitor cells were treated with 250 ng/ml rhSOSTDC1 or 100ng/ml rmDkk1 and also separately with 50ng/ml rmWnt3a in the presence or absence of SOSTDC1/Dkk1. The image is representative of mineralisation on day 11 of differentiation. (A) On day 8 of OB progenitor differentiation, rmWnt3a induced mineralisation and rhSOSTDC1 reduced this effect. The rmDkk1 had no significant effect on Wnt3a-stimulated mineralisation. (B, C) SOSTDC1 had no effect on mineralisation on day 11 or 15 of differentiation. N=4 independent experiments, One way ANOVA and Holme-Sidak's multiple comparisons test. Data are displayed with mean ± SEM. *P=0.05, ***P=0.001.*

PBS	Wnt3a 50ng/ml	Wnt3a 50ng/ml + SOSTDC1

A

Effect of SOSTDC1 on BMP2-induced OB mineralisation on Day 8 of differentiation

B

Effect of SOSTDC1 on BMP2-induced OB mineralisation on Day 11 of differentiation

C

Effect of SOSTDC1 on BMP2-induced OB mineralisation on Day 15 of differentiation
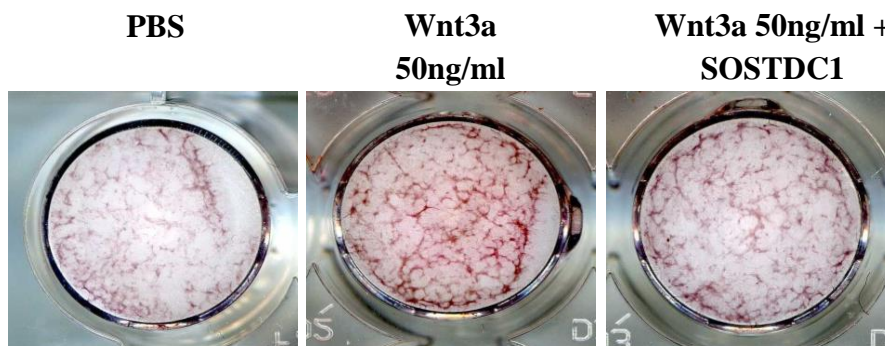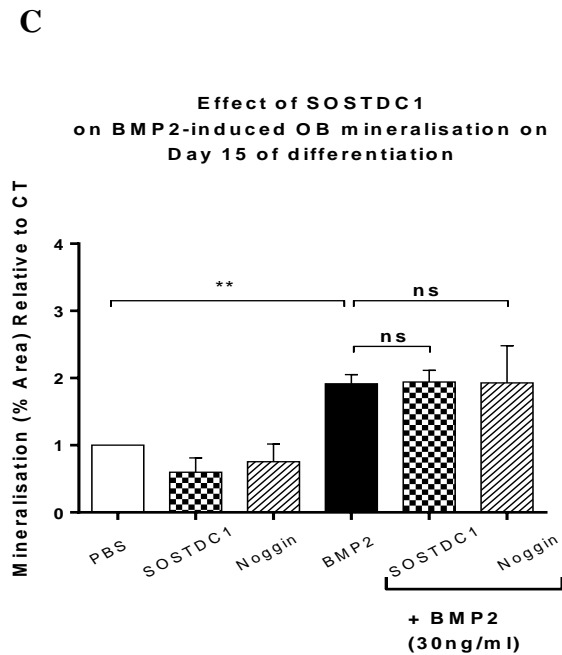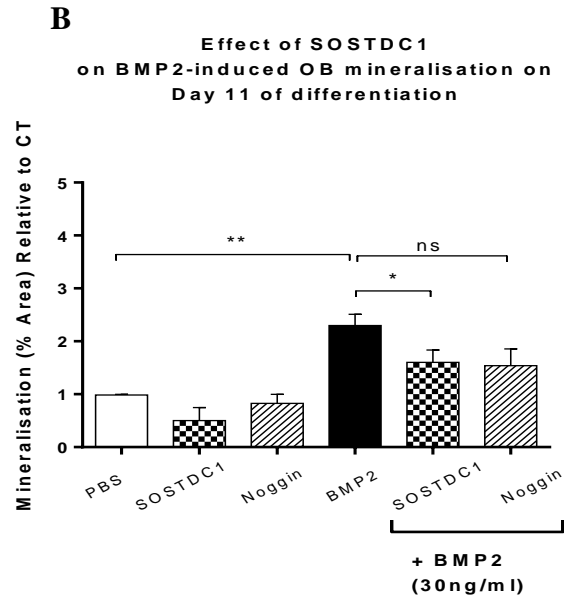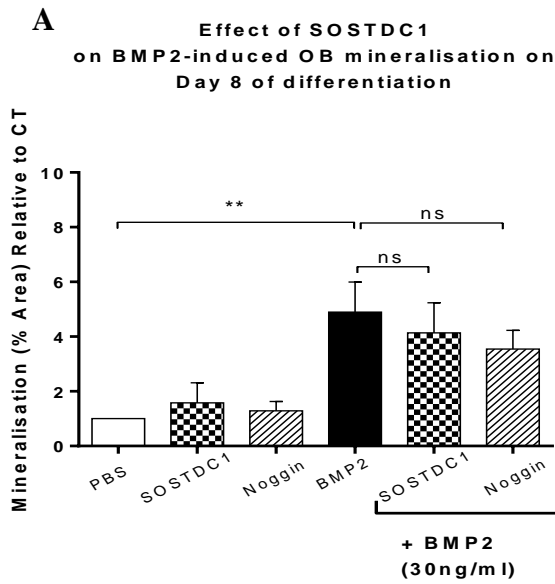
Figure 4.4.5.2 - BMP2 induced mineralisation in OB progenitors and SOSTDC1 reduced this effect on day 11 of differentiation: *OB progenitor cultures were treated with 250 ng/ml rhSOSTDC1 or 100ng/ml rhNoggin and also separately with 30ng/ml rhBMP2 in the presence or absence of SOSTDC1/Noggin. The image is representative of mineralisation on day 11 of differentiation. (A, B, C) The rhBMP2 induced OB progenitor mineralisation up to day 15 of differentiation and SOSTDC1 reduced this effect significantly on day 11 of differentiation only. The rhNoggin had no significant effect on BMP2-stimulated mineralisation. N=4 independent experiments, One way ANOVA and Holme-Sidak's multiple comparisons test. Data are displayed with mean ± SEM. *P=0.05, **P=0.01.*

PBS **BMP2** **BMP2 50ng/ml + SOSTDC1**

A

Effect of SOSTDC1 on BMP7-induced OB mineralisation on Day 8 of differentiation

B

Effect of SOSTDC1 on BMP7-induced OB mineralisation on Day 11 of differentiation

C

Effect of SOSTDC1 on BMP7-induced OB mineralisation on Day 15 of differentiation
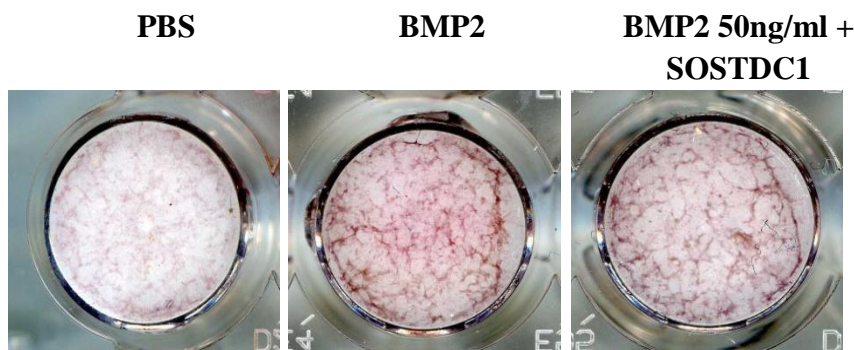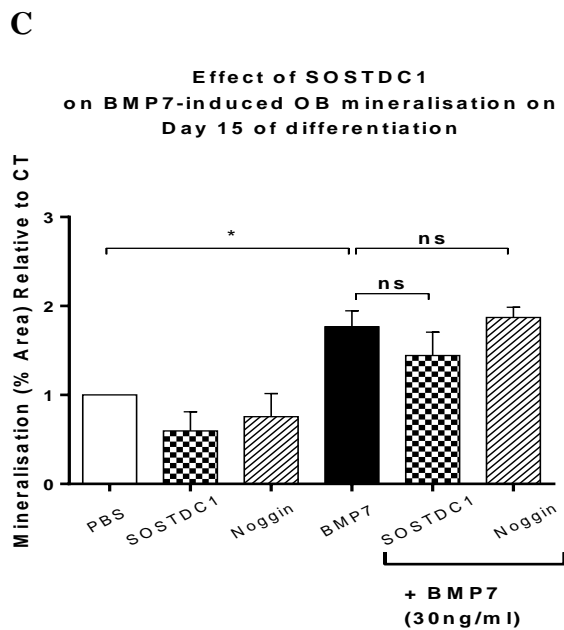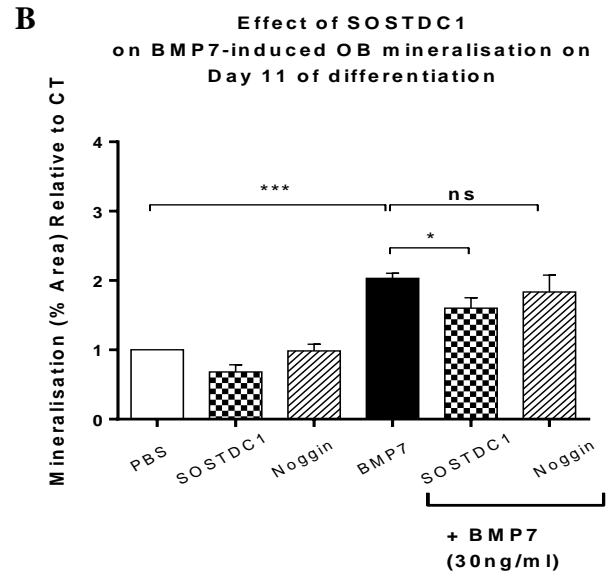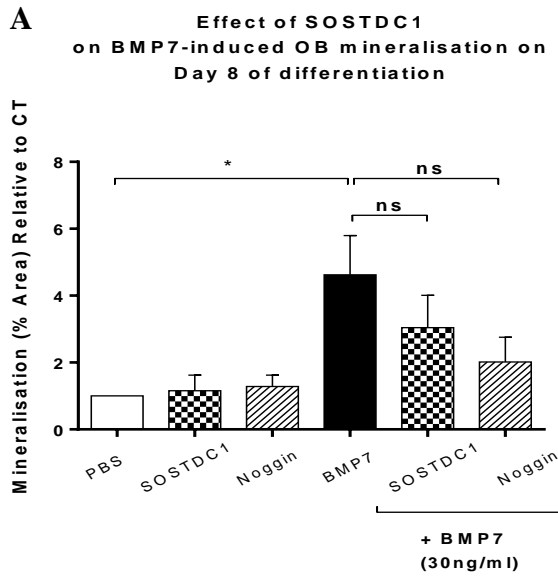
Figure 4.4.5.3 - BMP7 induced mineralisation in OB progenitors and SOSTDC1 reduced this effect on day 11 of OB differentiation: *OB progenitor cultures were treated with 250ng/ml rhSOSTDC1 or 100ng/ml rhnoggin and also separately with 30ng/ml rhBMP7 in the presence or absence of SOSTDC1/Noggin. The image is representative of mineralisation on day 11 of differentiation. (A, B, C) The rhBMP7 induced OB progenitor mineralisation up to day 15 of differentiation and SOSTDC1reduced this effect significantly on day 11 of differentiation. The rhnoggin had no significant effect on BMP7-stimulated mineralisation. N=4 independent experiments, One way ANOVA and Holme-Sidak's multiple comparisons test. Data are displayed with mean ± SEM. *P=0.05, ***P=0.001.*

| PBS | BMP2 | BMP2 50ng/ml + SOSTDC1 |
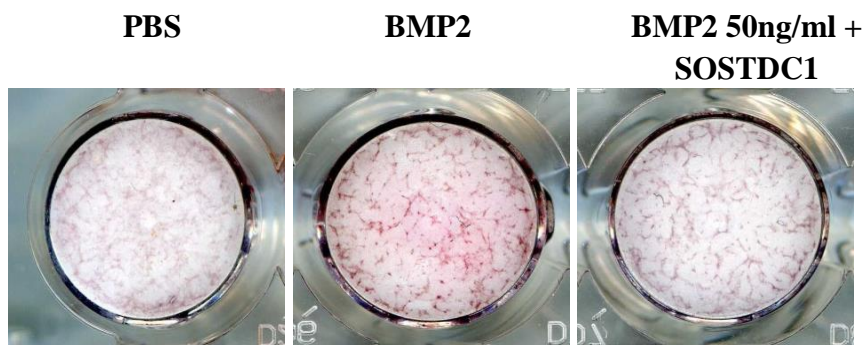
4.4.6 SOSTDC1 inhibited acute Wnt and BMP-induced intracellular signalling

To investigate the effect of SOSTDC1 on Wnt and BMP-induced intracellular signalling, downstream signalling molecules of the Wnt and BMP pathways were separately assessed following addition of rhSOSTDC1 protein treatment to OB cultures. OB progenitor cultures were differentiated for up to 15 days and on days 8, 11 and 15, cells were stimulated with single or combination protein treatments for 20 minutes, after which OB progenitor cultures were lysed. To assess the effect of rhSOSTDC1 on Wnt-induced intracellular signalling, phosphorylated levels of β-catenin (pβ-Catenin) protein were measured using western blot analysis. The effect of SOSTDC1 on BMP2 and BMP7-induced downstream signalling was further determined via quantification of phosphorylated levels of Smads 1,5&8 protein using the same western blotting technique. 100ng/ml rmDkk1 and 100ng/ml rhnoggin were used in all experiments as known Wnt and BMP antagonists, respectively. The average density of the bands on the X-ray images representing each OB progenitor sample were quantified and normalised to the corresponding GAPDH relative density and the calculated values normalised to PBS control.

Western blot analysis showed that rhSOSTDC1 in the presence of rmWnt3a, suppressed pβ-Catenin protein levels in OB progenitor cultures on day 8 of differentiation (**P=0.0059, **Figure 4.4.6.1, A, C**). Although the post hoc test between the average density values of PBS control and rmWnt3a was not statistically significant, the overall trend in pβ-Catenin levels between CT, rmWnt3a and rmWnt3a+rhSOSTDC1 were statistically significant on day 8 (**P=0.0092, **Figure 4.4.6.1, A**). No further inhibitory effects of rhSOSTDC1 on Wnt3a-induced pβ-Catenin levels were evident at other time points in differentiation. The rmDkk1 protein had no significant effect on Wnt-induced pβ-Catenin protein levels. Densitometry showed that rhBMP2 and rhBMP7 both induced pSmad 1,5&8 levels on day 8 of differentiation and rhSOSTDC1 reversed this effect (BMP2; *P=0.032, **Figure 4.4.6.2,** BMP7; ***P=0.0002 **Figure 4.4.6.3**). Similarly, rhnoggin also down-regulated BMP-induced pSmad 1,5&8 protein levels in the early stages of OB progenitor differentiation (BMP2; *P=0.033, **Figure 4.4.6.2,** BMP7; ***P<0.0001 **Figure 4.4.6.3**).
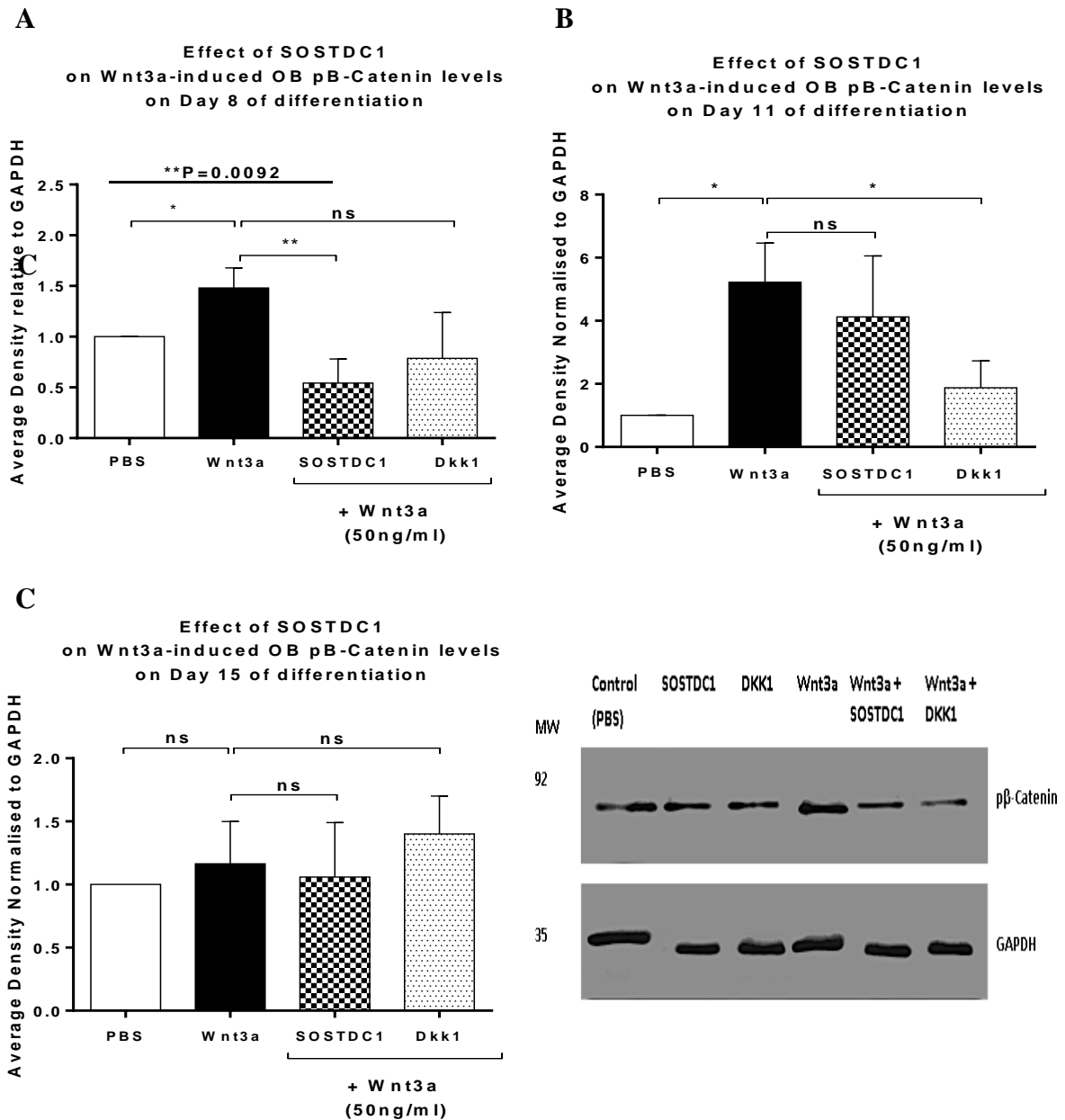
Figure 4.4.6.1 - SOSTDC1 suppressed acute Wnt3a-induced β-catenin phosphorylation protein levels in differentiating OB progenitors: *Phosphorylated levels of pβ-Catenin protein were measured using western blotting. The western blot image is representative of one out of three experiments. (A) The rmWnt3a acutely induced pβ-Catenin protein levels in OB progenitors on day 8 of differentiation and (B, C) not on day 11 or 15 .N=4 independent experiments, One way ANOVA and Holme-Sidak's multiple comparisons test. Data are displayed with mean ± SEM.*P=0.05, **P=0.01.*
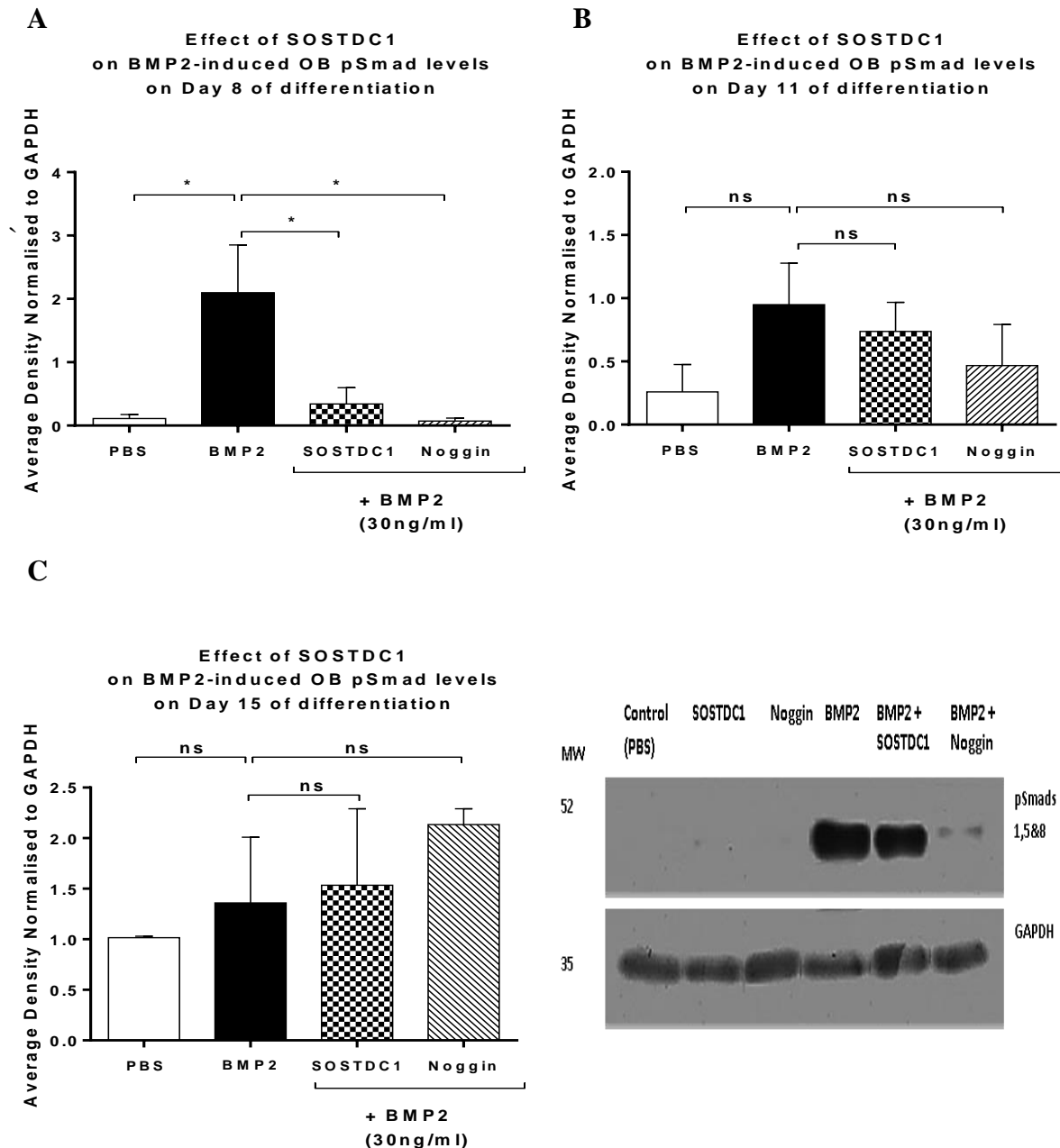
Figure 4.4.6.2 - SOSTDC1 suppressed acute BMP2-induced phosphorylation of Smad 1,5&8 complex levels in differentiating OB progenitors: *Phosphorylated levels of Smads 1,5&8 (pSmads 1,5&8) protein were measured using western blotting. Data represents the average density normalised to GAPDH. The western blot image is representative of one of three experiments on day 8 of differentiation. (A) The rhBMP2 acutely induced pSmad protein levels in OB progenitors on day 8 of early differentiation only. The rhSOSTDC1 and rhNoggin inhibited pSmad levels on day 8 of differentiation. (B, C) SOSTDC1 had no effect on BMP-2 induced Smad phosphorylation on day 11 or 15 of differentiation. N=4 independent experiments, One way ANOVA and Holme-Sidak's multiple comparisons test. Data are displayed with mean ± SEM.*P=0.05.*
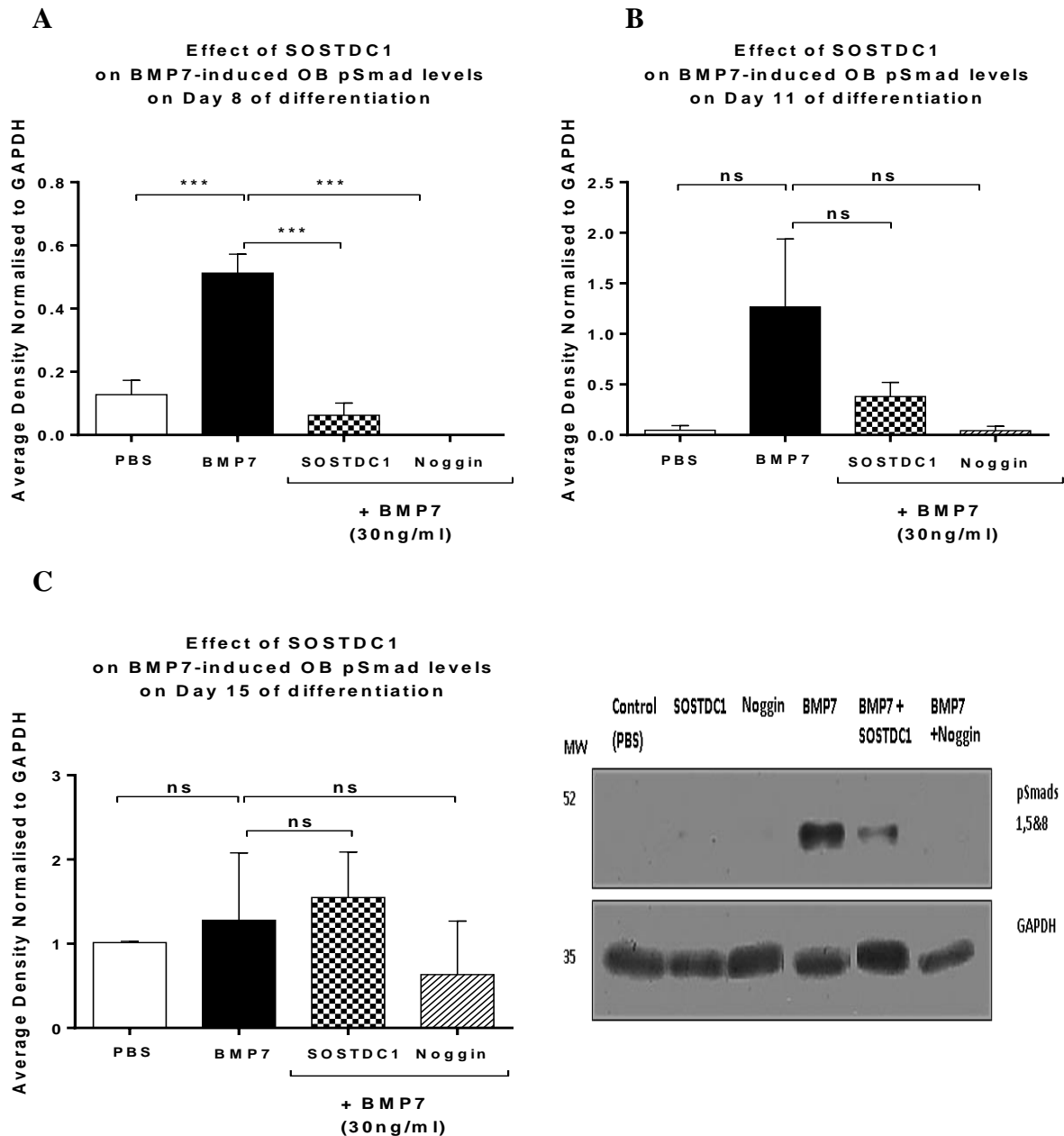
Figure 4.4.6.3 - SOSTDC1 suppressed acute BMP7-induced phosphorylation of Smad 1,5&8 complex levels in differentiating OB progenitors: *Phosphorylated levels of Smads 1,5&8 (pSmads 1,5&8) protein were measured using western blot analysis. The western blot image is representative of one of three experiments on day 8 of differentiation. (A) The rhBMP7 acutely induced pSmad protein levels in OB progenitors on day 8 of early differentiation only and both rhSOSTDC1 and rhnoggin strongly inhibited pSmad levels on day 8 of differentiation. (B, C) SOSTDC1 had no effect on BMP-7 induced Smad phosphorylation on day 11 or 15 of differentiation. N=4 independent experiments, One way ANOVA and Holme-Sidak's multiple comparisons test. Data are displayed with mean ± SEM. ***P=0.0001.*

4.5 Discussion

In this chapter, I investigated the effect of rhSOSTDC1 on the Wnt and BMP pathways in OB progenitors during various maturation stages of differentiation. The aim of this part of the study was to firstly determine whether SOSTDC1 antagonised Wnt and BMP signalling in OB progenitors on a similar level to well characterised Wnt and BMP antagonists. The second aim was to determine whether any antagonistic SOSTDC1 effect observed was dependent on OB maturity. My data support the hypothesis of this particular part of the study in that SOSTDC1 suppresses Wnt and BMP-induced cell signalling in differentiating OB progenitors.

ALP and Runx2 were selected as well characterised markers of OB differentiation. ALP is an early marker of OB differentiation and is secreted by differentiating OB cells. Runx2 is an early to mid-marker of OB differentiation and is detected in pre-osteoblasts, with the expression increasing in immature OB and decreasing in mature OB (Komori 2010). OB matrix mineralisation was assessed by detection of mineral deposition by quantification of Alizarin red staining as described by Hesegawa et al (Hasegawa, Shimada et al. 2008).

Firstly to observe the effects of SOSTDC1 on Wnt/BMP-induced OB progenitor differentiation, each experiment contained a control in which GST protein at the same concentration as the –GST component of the GST-SOSTDC1 fusion protein was added to the ligand. ALP analysis showed that there were no difference between Wnt3a, BMP2 and BMP7-induced differentiation of OB progenitor cultures treated with or without GST. This data confirmed that the GST protein component of the SOSTDC1 molecule had no regulatory effect on Wnt3a/BMP-induced OB differentiation. Secondly, as can be seen from the presented data demonstrating the effects of potential regulators of OB differentiation, systematic and exhaustive experimentation was required over time courses in low doses of FCS and specific concentrations of Wnt and BMP molecules and antagonists. At least three independent experiments with a minimum of four replicates were used in each of analysis.

In preliminary experiments investigating the effect of SOSTDC1 on ALP activity of OB progenitors, my findings show that SOSTSDC1 has variable effect on OB progenitor differentiation depending on cell maturity. In agreement with the literature my findings showed that continuous exposure to recombinant Wnt3a, BMP2 and BMP7 induced ALP in cultured OB cells (Rawadi, Vayssiere et al. 2003). In the later stages of the OB progenitor cell differentiation (day 11 onwards), the same dosage of 50ng/ml Wnt3a and 30ng/ml BMP2/7 no longer significantly induced differentiation. Presumably as towards the end of the exponential phase of OB progenitor differentiation when differentiation potential of cells reaches their peak, OB progenitor cultures require a higher concentration of ligand to induce ALP activity. Interestingly in similar experiments assessing the effect of SOSTDC1 on Wnt and BMP-induced ALP activity in SAOS2 cells, I showed that SOSTSDC1 did not have any effect in the absence or presence of either Wnt or BMP ligand, even in the very stages of differentiation (**Appendix 2**) This data is not surprising as the SAOS2 cells have a more mature/differentiated OB phenotype compared to primary OB progenitor cells and the all the effects of SOSTDC1 observed in my studies have been in early differentiation time-points.

Similar to the effect Laurikkala, Kassai *et al* found using MC3T3-E1 cells (Laurikkala, Kassai *et al.* 2003), I showed that SOSTDC1 inhibited BMP2-induced ALP activity. This antagonistic effect of SOSTDC1 was only observed in BMP2 and not BMP7-induced ALP activity. I further showed that SOSTDC1 had no significant effect on Wnt3a-induced ALP activity. This differed from the data in the literature, where an inhibitory effect of SOSTDC1 was seen in MC3T3-E1 cells over expressing Wnt3a (Rawadi, Vayssiere et al. 2003). The contradictory results may be due to the phenotypic differences observed between cell-lines and primary OB cells and also the differences in methodology.

To compare results obtained from ALP analysis, the more sensitive approach of investigating *Runx2* gene expression by qRT-PCR was utilised. From the the qRT-PCR data I showed that on the early day 8 time point when *Runx2* expression is known to be high in immature differentiating OB progenitor cells (Prince, Banerjee et al. 2001), SOSTDC1 had a clear inhibitory effect on *Runx2* when in the presence of recombinant Wnt3a, BMP2 or BMP7 proteins.Next the effect of SOSTDC1 on Wnt and BMP-induced mineralisation in OB using Alizarin red staining was investigated. Again, the antagonistic

effect of SOSTDC1 when in the presence of Wnt and BMP ligands was evident when OB progenitor cells were in immature stages of differentiation. Although results indicated towards the inhibitory role of SOSTDC1 in OB progenitor differentiation and mineralisation, which was in line with the data in the literature, we wanted a clearer insight into the molecular mechanisms by which SOSTDC1 interfered with Wnt and BMP signalling. To determine whether SOSTDC1 antagonised acute Wnt/BMP signalling in OB progenitors, western blotting was used to quantify protein levels downstream of either Wnt or BMP signalling pathways. Western blot analysis showed that when differentiating OB progenitors were treated with SOSTDC1 in the presence of Wnt3a, the protein level of molecular mediator pβ-catenin reduced significantly. Similarly, western blotting was used for the quantification of pSmad 1,5&8 protein complex levels following treatment with rhSOSTDC1 in the presence of BMP2 or BMP7. In line with the literature, addition of recombinant BMP2 and BMP7 for just 20 minutes was able to induce pSmad levels in differentiating OB progenitor cells. Addition of rhSOSTDC1 to OB progenitor cells was able to effectively reverse BMP-induced Smad phosphorylation

Wnt-antagonists such as Dkk1 function by interacting physically with Wnt-receptor LRP5/6 and as a result intracellular pβ-catenin protein levels are reduced. In the experiments investigating ALP, *Runx2* and mineralisation, only a trend in Dkk1-induced Wnt3a suppression was observed. Interestingly, where SOSTDC1 inhibitory effects on Wnt3a-induced differentiation and mineralisation were significant, Dkk1 appeared less effective (no significant effect) in the same experiments. This could mean that LRP5/6 may have higher affinity for SOSTDC1 in comparison to Dkk1. BMP antagonist noggin had variable suppressive effect on OB progenitors throughout differentiation and mineralisation. Noggin inhibited BMP-induced ALP activity and *Runx2* expression on day 8 and 11 of OB progenitor differentiation. Interestingly, the negative effect of noggin on OB progenitor mineralisation was not significant at any time point throughout differentiation compared to SOSTDC1 in the same experiments.

In this chapter I showed that SOSTDC1 suppressed Wnt-induced differentiation and mineralisation in immature OB progenitor cells by blocking the Wnt-signalling pathway. I also showed that SOSTDC1 suppressed BMP-induced differentiation and mineralisation via interference with the regulation of Smad phosphorylation. Thus, my data support the

hypothesis of this particular part of the study in that SOSTDC1 suppresses Wnt and BMP-induced cell signalling in differentiating OB progenitors.

It is interesting to note that the suppressive SOSTDC1 effects within this study were only observed when OB progenitors were in the presence of Wnt or BMP ligand. Immunohistochemical and *in situ* hybridization analyses carried out as early as the 1970's demonstrated that OB express BMPs and their receptors during bone formation, skeletal development and fracture repair (Helder, Ozkaynak et al. 1995, Lyons, Hogan et al. 1995, Yamaguchi, Komori et al. 2000). The canonical Wnt proteins have been shown to induce OB differentiation (Westendorf, Kahler et al. 2004, Kubota, Michigami et al. 2009). These studies correlate with data that indicate towards SOSTDC1's regulatory role on OB is evident when BMP and Wnt protein levels in OB are very high.

Chapter 5 – SOSTDC1 is a Dual Regulator of Wnt-BMP Crosstalk

5.1 Introduction

In the regulation of differentiation and haemostasis, it is highly likely that the actions of one signalling pathway can influence that of others, resulting in cellular responses that differ from the one achieved by just one single signalling cascade. The availability of intrinsic factors including cofactors and target genes, and the link between signalling pathways amplifies both the level and complexity of cell responses. The dependency between two signalling pathways is often referred to as the "crosstalk" of multiple signalling pathways. The Wnt and BMP signalling pathways are function independently of each other according to their own unique ligands, receptors and cytoplasmic/nuclear signal transducers, without requiring components of the other pathway. However recent studies have shown that in some biological contexts there is evidence of Wnt-BMP crosstalk. Depending on the cellular context, this Wnt-BMP crosstalk is found to be either synergistic or antagonistic (Azpiazu et al.,1996; Carmena et al.,1998). For example, in early Xenopus embryos, Wnt8 and BMP4 are co-expressed in overlapping domains and are both reliant on each other to regulate normal vertebrate development (Hoppler and Moon,1998). On the other hand, Wnt signalling is required for melanocyte development, whereas BMP signalling represses melanogenesis (Jin et al.,2001).

In bone formation, Wnt and BMP pathways function cooperatively. The activation of Wnt signalling stimulates the differentiation of pluripotent MSC into OB progenitors and maintains the precursor lineage of these osteoprogenitors. BMP signalling then stimulates these cells to further differentiate into OB cells. Once the OB progenitors have become mature functional OB cells, both the Wnt and BMP pathways induce differentiation, evidenced by increased ALP activity and mineralization (Bain, Muller et al. 2003, Hill, Spater et al. 2005). Studies have shown the interaction between BMP and Wnt signalling results in synergistic effects on OB differentiation and bone development (Fukuda, Kokabu et al. 2010). Zhou et al showed BMP2 increased the nuclear β-catenin levels and the expression of Wnt15, 3a, 5b in pre-osteoblastic cell (Zhou 2011). The same group also showed that β-catenin directs osteogenic lineage allocation by enhancing MSC responsiveness to BMP-2 via Tcf/Lef response elements (TREs). This synergism is known to increase new bone formation *in-vivo* (Mbalaviele and Sheikh et al, 2009).

Various molecular studies have shown that the functional communication which exists between Wnt and BMP signalling pathways involves several mechanisms. On an intracellular level, Smads have been shown to form complexes with molecules downstream of the Wnt signalling pathway including β-catenin, Dishevelled-1, Axin and GSK3. The formation of these complexes consequently regulates the phosphorylation and activity of Smads and β-catenin (Edlund, Lee et al. 2005, Liu, Tang et al. 2006, Fuentealba, Eivers et al. 2007). Interestingly, the transcriptional regulation of Wnt and BMP common target genes can involve both Smad and TREs. In response to BMP-Wnt dependent signalling the Smads can form transcriptional complexes with β-catenin/Tcf/Lef and co-activate transcription of various target genes including Msx2 and Myc via these binding elements (Hussein, Duff et al. 2003, Hu and Rosenblum 2005).

Some extracellular proteins, such as sclerostin, cerberus and sFRPs, are known to bind ligands and/or receptors of both the BMP and Wnt pathways (Piccolo, Agius et al. 1999, Kusu, Laurikkala et al. 2003, Misra and Matise 2010). Data suggests that SOSTDC1-Wnt signalling is regulated via interactions with Wnt co-receptor LRP5/6 and that SOSTDC1-induced BMP inhibition is regulated via direct adhesion to BMP ligands (Lintern, Guidato et al. 2009). X-raycrystallography has revealed that the SOSTDC1 protein consists of 3 cystine loops, 2 of which provide stability whilst the third has a functional role in receptor/ligand binding, specifically binding to LRP5/6 (Avsian-Kretchmer and Hsueh 2004). Lintern's study showed SOSTDC1 deletion construct lacking the LRP-specific loop domain still bound BMP4 and consequently inhibited BMP signalling (Lintern, Guidato et al. 2009). This data suggests that SOSTDC1 may function simultaneously as a dual Wnt and BMP antagonist. However, to my knowledge no studies have investigated the regulatory role of SOSTDC1 in Wnt-BMP cooperative signalling in OB progenitors. In light of my previous data suggesting SOSTDC1 down-regulated both Wnt and BMP signalling in OB progenitor cultures at early stages of differentiation, the objective of this study were to investigate the potential regulatory role of SOSTDC1 in the cooperative mechanisms between Wnt and BMP signalling in differentiating OB progenitors. In this study I also assessed the strength of the molecular interactions of SOSTDC1-LRP receptor and SOSTDC1-BMP ligands to provide clearer insight into the regulatory role of SOSTDC1 on Wnt-BMP dependent signalling.

5.2 Hypothesis and Objectives

5.2.1 Aims

The aim of this study was to determine whether SOSTDC1 had an antagonistic effect on Wnt-BMP dependent signalling within OB progenitor cells

To achieve this, the following hypothesis was tested.

5.2.2 Hypothesis

SOSTDC1 suppresses Wnt-BMP crosstalk in signalling OB progenitor cells.

5.2.3 Specific objectives

To test this hypothesis the following were determined:

Whether intracellular downstream signalling molecules of Wnt and BMP pathways in OB progenitor cells are dependent on each other

The effect of SOSTDC1 on Wnt and BMP-induced acute intracellular signalling in OB progenitors

5.3 Chapter specific methods

Recombinant Proteins		
ITEM	**CATALOGUE NUMBER**	**SUPPLIER**
Human bone morphogenic protein 2 (BMP2) 10µg/ml *10µg lyophilised stock Reconstituted in 1ml of sterile 4 mM HCL containing 0.1% BSA.*	355-BM-010	R&D Systems
Human bone morphogenic protein 7 (BMP7) 10µg/ml *10µg lyophilised stock Reconstituted in 1ml of sterile 4 mM HCL containing 0.1% BSA.*	354-BP-010	R&D Systems
Mouse Wnt3a 10µg/ml *10µg lyophilised stock Reconstituted in 1ml of sterile PBS.*	1324-WN-002	R&D Systems
Human Sclorstin Domain Containing 1 (SOSTDC1) 38µg/ml *Supplied as a 38ug/ml in50 mM Tris-HCl, 10 mM reduced Glutathione, pH=8.buffer.*	H00025928-P01	Abnova
Human glutatione S-transferase (GST) 200µg/ml *Supplied at 200µg/ml in 25% Glycerol, 50mM Tris HCl, 150mM Sodium chloride, 0.25mM DTT, 0.1mM PMSF, pH 7.5buffer.*	ab70456	Abcam
Mouse Dikkopf 1 (Dkk1) 10µg/ml *10µg lyophilised stock Reconstituted in 1ml of sterile PBS containing 0.1% BSA.*	5439-DK-010	R&D Systems
Human noggin 25µg/ml *25µg lyophilised stock Reconstituted in 1ml of sterile PBS containing 0.1% BSA.*	6057-NG-025	R&D Systems

Table 5.1 - *Recombinant proteins required for investigating the effect of SOSTDC1 on Wnt-BMP dependent signalling in OB progenitors.*

Recombinant Protein doses	
Recombinant protein Treatment	**Dose (ng/ml)**
PBS	n/a
Wnt3a	50
BMP2	30
BMP7	30
SOSTDC1	250
Dkk1	100
Noggin	100

Combined Recombinant Protein treatments	
Recombinant protein	**Combination Recombinant Protein**
Wnt3a	SOSTDC1
	Dkk1
BMP2	SOSTDC1
	Noggin
BMP7	SOSTDC1
	Noggin

Table 5.2 - *Recombinant protein doses required for sole and combined treatments to investigate the effect of SOSTDC1 on Wnt-BMP dependent signalling in OB progenitors.*

5.3.1 Determining the effect of SOSTDC1 on Wnt-BMP dependent intracellular protein signalling in differentiating OB progenitors

Primary and Secondary antibodies for western blot		
ITEM	**CATALOGUE NUMBER**	**SUPPLIER**
Phospho-Smad1 (Ser463/465)/ Smad5 (Ser463/465)/ Smad8 (Ser426/428) antibody *Rabbit polyclonal*	9511	Cell Signalling
Anti-β-catenin (phospho Y142) antibody *Rabbit polyclonal*	Ab-27798	Abcam
Anti-GAPDH (6C5) antibody *Mouse monoclonal*	Ab-37168	Abcam
Goat anti-Rabbit IgG –HRP antibody *Rabbit IgG*	9511	Life Technologies Novex®
Goat anti-Mouse IgG –HRP antibody *Mouse IgG*	SC-2031	SantaCruz

Table 5.3 - *Recombinant protein doses required for sole and combined treatments to investigate the effect of SOSTDC1 h on Wnt-BMP dependent signalling in OB progenitors.*

The objective of the first part of this chapter was to establish whether intracellular Wnt signalling was dependent on BMP signalling. At the same time I also wanted to determine whether SOSTDC1 had a regulatory role on potential Wnt-BMP dependency. OB progenitor cultures were harvested from a near confluent flask using trypsin and cells counted using a haemocytometer, as described in **section 2.1.3**. OB progenitors were resuspended in MEM-Alpha at 57,000 cells per well in 6 well culture plates containing 1500µl of media within each well. Following 72 hours in culture, the media was removed from the adherent OB progenitors and cells were washed with PBS. OB progenitors were differentiated in 1500µl/well of standard osteogenic media for up to 15 days and osteogenic media was replaced with fresh media every three days. On day 8, 11 and 15 of differentiation, OB progenitor cultures were treated with recombinant proteins on day 8, 11 and 15 of differentiation. The rmWnt3a protein was diluted to 50ng/ml in 65µl of osteogenic media in a 0.5ml sterile eppendorf. The rhBMP2 and rhBM7 proteins were diluted to 10ng/ml concentration in 65µl of osteogenic media in 0.5ml sterile eppendorfs.

50ng/ml of rmWnt3a was combined with 250ng/ml rhSOSTSDC1 and 50ng/ml of rmWnt3a was combined with 100ng/ml rmDkk1 in a 65µl volume of osteogenic media. In separate tubes, 10ng/ml of rhBMP2 or rhBMP7 was combined with 250ng/ml rhSOSTSDC1 or 100ng/ml rhnoggin in a 65µl volume of osteogenic media. All eppendorfs containing 65µl of protein/protein combinations were placed in a water bath for 1 hour at 37°C to allow interaction between combined proteins. From the 65µl of protein/protein combination, 50µl was added to each well containing OB progenitor cultures and the media containing protein treatments were mixed gently within wells by pipetting. 6 well culture plates were immediately placed in 37ºC culture incubators for 20 minutes. The protein from OB progenitor cultures were isolated using Mammalian cell lysis kit containing phosphatase and protease inhibitor cocktails as described **section 2.6**. Protein concentrations within OB progenitor cell lysates were quantified using the BCA assay as outlined in the method **section 2.7**.

The effect of Wnt3a ligand on downstream intracellular BMP signalling was tested via quantification of Wnt3a-induced phosphorylated levels of Smad 1,5&8 protein complex (52kD). The effect of BMP2 and BMP7 ligand on downstream intracellular Wnt signalling was determined by quantifying the level of BMP-induced phosphorylated β-catenin protein (92kD). The influence of SOSTDC1 on Wnt-induced Smad phosphorylation and BMP-induced β-catenin phosphorylation in differentiating OB progenitors was determined by western blotting as outlined in **section 2.8**.

In brief, 10% polyacrylamide gels were loaded with 10µg of sample protein. Each gel was also loaded with 10µl of a 10-250kD protein molecular marker at the first and last lane and the proteins were run through the stacking gel for 40 minutes at 60 Volts. Proteins were separated with the separating gel according to their molecular weight for 2 hours at 100 Volts. Proteins were transferred onto PVDF membranes for 70 minutes at 70 Volts. Membranes were washed once in 0.05% PBS-Tween. Membranes were blocked in 3% BSA solution for 45 minutes. Transferred proteins from Wnt-induced OB progenitor cell lysates were cut just below the 50kD mark using the pre-stained molecular markers as reference points and then incubated with 1/3000 of rabbit anti-Psmad1,5&8 antibody. Transferred proteins from BMP-induced OB progenitor cell lysates were cut just above the 75kD mark and incubated with a 1/300 dilution of anti-pβ-Catenin rabbit antibody. The remainder of the blot containing proteins <50kD was placed in a 1/15000 dilution of

anti-GAPDH mouse antibody. Antibody incubations were all carried out overnight at 4°C on a roller. Blots incubated with anti-pβ-catenin or anti-pSmad1,5&8 antibody were probed with 1/5,000 dilution of secondary HRP-conjugated anti-rabbit IgG antibody. Blots incubated with anti-GAPDH antibody were incubated with 1/30,000 dilution of secondary HRP-conjugated anti-mouse IgG antibody. Protein bands were visualised and the average density quantified using GelDoc software. The average density of SOSTDC1 protein was normalised to the average density of GAPDH to account for any loading variability.

5.3.2 Determining the effect of SOSTDC1 on Wnt-BMP dependent *CTNNB1* gene levels in differentiating OB progenitors

To investigate the effect of SOSTDC1 on BMP-induced Wnt signalling in differentiating OB progenitors on a gene expression level, *CTNNB1* (the gene encoding β-catenin protein) was determined using qRT-PCR as described in **section 2.14.3**. Wnt3a-induced *CTNNB1* expression was also assessed as a positive control for *CTNNB1* expression. OB progenitor cells were harvested from a near confluent flask by trypsinisation and cell pellets were counted using a haemocytometer as described in **section 2.1.3**. OB progenitor cells were resuspended in MEM-Alpha at 57,000 cells per well in 6 well culture plates containing 1.5ml of media within each well. Following 72 hours in culture, the media was removed from the adhered OB progenitor culture and cells were washed with PBS. OB progenitors were differentiated in 1500µl/well of standard osteogenic media for up to 11 days and osteogenic media was replaced with fresh media every three days. On day 7 and 10 of differentiation, OB progenitors were cultured with recombinant protein for 24 hours. To determine the effect of Wnt and BMP on *CTNNB1* expression in differentiating OB progenitors, rmWnt3a protein was diluted to 50ng/ml in 65µl of osteogenic media in a 0.5ml sterile eppendorf. The rhBMP2 or rhBM7 proteins were diluted to 30ng/ml concentration in 65µl of osteogenic media in 0.5ml sterile eppendorfs. To assess the effect of SOSTDC1 and Dkk1 on Wnt3a-induced *CTNNB1* expression, 50ng/ml of rmWnt3a was combined with 250ng/ml rhSOSTSDC1 and 50ng/ml of rmWnt3a was combined with 100ng/ml rmDkk1 in 65µl volumes of osteogenic media. The effect of SOSTDC1 and noggin on BMP2/7-induced *CTNNB1* levels were assessed by combining 50ng/ml of rhBMP2/7 with 250ng/ml rhSOSTSDC1 or 100ng/ml rhnoggin in a 65µl volume of osteogenic media. All eppendorfs containing 65µl of protein

sample/protein combinations were placed in a water bath for 1 hour at 37°C to allow interaction between combined proteins. From the 65µl of protein sample/protein combination, 50µl was added to each well containing OB progenitor cultures and mixed gently within wells by pipetting. Culture plates were placed back in 37ºC culture incubators for 24 hours.

RNA was isolated and quantified from the OB progenitor culture as described in **section 2.13**. The *CTNNB1* and *B2M* gene expression were quantified using TaqMan® Assays for qRT-PCR analysis using the SDS2.2.1. Relative quantification of *CTNNB1* expression was performed by normalising to the house keeping *B2M* gene using the formula **ΔCT = CT $_{target}$ − CT $_{housekeeping}$** as described in **section 2.13.3.**

5.3.3 Determining the affinity (KD) of recombinant SOSTDC1 for LRP-6, BMP2 and BMP7 by Bio-layer interferometry

Recombinant Proteins		
ITEM	**CATALOGUE NUMBER**	**SUPPLIER**
CF Human bone morphogenic protein 2 (BMP2) 10µg - *lyophilised*	355-BM-010-CF	R&D Systems
CF Human bone morphogenic protein 7 (BMP7) 10µg - *lyophilised*	354-BP-010-CF	R&D Systems
CF Mouse Wnt3a 10µg/ml *Lyophilised*	1324-WN-002-CF	R&D Systems
Human Sclorstin Domain Containing 1 (SOSTDC1) 38µg/ml	H00025928-P01	Abnova
Human glutatione S-transferase (GST) 200µg/ml .	ab70456	Abcam

Table 5.4 - *Recombinant proteins required for determining the affinity of SOSTDC1 for LRP-6, BMP2 and BMP7 by Bio-layer interferometry*

The affinity of Wise, the mouse orthologue to SOSTDC1 for LRP-6 receptor, BMP2 and BMP7 ligands has been previously been tested using BIAcore technology and Immunoprecipitation analysis (Laurikkala, Kassai et al. 2003). However to my knowledge, there are currently no reported KD values associated with the binding affinity of rhSOSTDC1 for LRP-6, BMP2 or BMP7. In this study the affinity of rhSOSTDC1 protein for LRP-6, BMP2 and BMP7 was determined using the Bio-layer Interferometry technology of the Blitz Analysis system according to **section 2.15.**

Briefly, all recombinant proteins were purchased in the carrier-free state in a lyophilised form. The rmLRP-6 protein was reconstituted to 100µg/ml concentration in the recommended buffer. The rhBMP2 and rhBMP7 proteins were reconstituted to 100µg/ml concentration in the recommended buffer. Recombinant protein samples were prepared in their corresponding buffers to 1, 10, 25, 50 and 100 µg/ml (neat) concentrations within sterile 0.5ml eppendorfs. 100 µg/ml of rhSOSTDC1 was immobilized on a pre-hydrated disposable ARG2 biosensor. For each SOSTDC1-analyte binding assay, a blank (buffer only) negative control was also performed to establish any non-specific binding.

Eppendorf tubes containing LRP-6, BMP2 or BMP7 recombinant proteins in their various concentrations were placed on the Blitz Analyser one at a time starting with the highest 100 µg/ml concentration. The rhSOSTDC1-coated ARG2 biosensor was placed into an eppendorf containing the analyte (LRP-6, BMP2 or BMP7 recombinant proteins). The molecular interaction between rhSOSTDC1 and decreasing concentrations of the protein analyte were assessed one at a time using the BLItz Pro™ software. The ARG2 Biosensors were replaced following the assessment of the association of rhSOSTDC1 with each concentration of analyte. Due to the fact that the rhSOSTDC1 had a GST-tag, the binding interaction between rhGST protein and rmLRP-6, rhBMP2 and rhBMP7 was also assessed as a control. The 100µg/ml rhGST protein was immobilised on an ARG2 disposable biosensor and the binding affinity of rhGST for 100µg/ml of rmLRP-6, rhBMP2 or rhBMP7 assessed. The sensogram data was collected in real time and presented as binding (nm) affinity at the start of rhSOSTDC1-analyte association and the start of complex dissociation. The measured affinity of the interaction KD (M) between the two proteins was reported by the BLItz Pro™ software as outlined in **section 2.15.1**

5.4 Results

5.4.1 SOSTDC1 down regulated Wnt-BMP dependent intracellular in differentiating OB progenitors

Western blotting was performed to determine whether Wnt3a upregulated Smad phosphorylation downstream of the BMP signalling pathway in differentiating OB progenitors. Wnt-induced levels of phosphorylated Smads1,5&8 protein were quantified as the average density of the bands on x-ray images and normalised to the corresponding GAPDH relative density. Western blot analysis showed that 50ng/ml Wnt3a acutely induced pSmad1,5&8 protein levels in differentiating OB progenitors and this effect was significant on day 8 of differentiation (**Figure 5.4.1.1 A**, *P<0.05). In the same experiments, the effect of SOSTDC1 and Dkk1 on Wnt3a-induced Smad phosphorylation was assessed. I showed rhSOSTDC1 and rhDkk1 both suppressed Wnt3a-induced pSmad 1,5&8 protein levels on day 8 of OB progenitor differentiation (**Figure 5.4.1.2 A**, *P<0.05). The pSmad protein levels within OB progenitors were not affected in the presence of rhSOSTDC1 or rmDkk1 (**Figure 5.4.1.2 D).**

The effect of BMP ligands on downstream canonical Wnt signalling was assessed by western blotting. The level of β-Catenin phosphorylation within differentiating OB progenitors was assessed following stimulation with rhBMP2 or rhBMP7 protein. I showed that both rhBMP2 and rhBMP7 were able to induce pβ-Catenin protein levels downstream of the Wnt signalling pathway (**Figure 5.4.1.3 A and B 5.4.1.5 B,** *P<0.05). The BMP2-induced phosphorylation of β-Catenin protein levels was significant on day 8 and day 11 of differentiation whereas BMP7-induced pβ-Catenin levels significantly on day 11 only (*P<0.05). Within the same experiments, the effect of SOSTDC1 and noggin on BMP-induced phosphorylation of β-Catenin protein was assessed using western blotting. I showed rhSOSTDC1 and rhnoggin both suppressed BMP2-induced pβ-Catenin levels on day 8 and 11 of OB progenitor differentiation (**Figure 5.4.1.4 A**, *P<0.05). The rhSOSTDC1 and rhnoggin recombinant proteins also suppressed BMP7-induced pβ-Catenin levels on day 11 of OB progenitor differentiation (**Figure 5.4.1.6 B**, *P<0.05). The phosphorylated levels of β-Catenin protein within OB progenitors were not affected in the presence of rhSOSTDC1 or rhnoggin alone (**Figure 5.4.1.6 D).**

A

Effect of Wnt3a on
pSmad1,5&8 levels
on Day 8 of OB differentiation

B

Effect of Wnt3a on
pSmad1,5&8 levels
on Day 11 of OB differentiation

C

Effect of Wnt3a on
pSmad1,5&8 levels
on Day 15 of OB differentiation
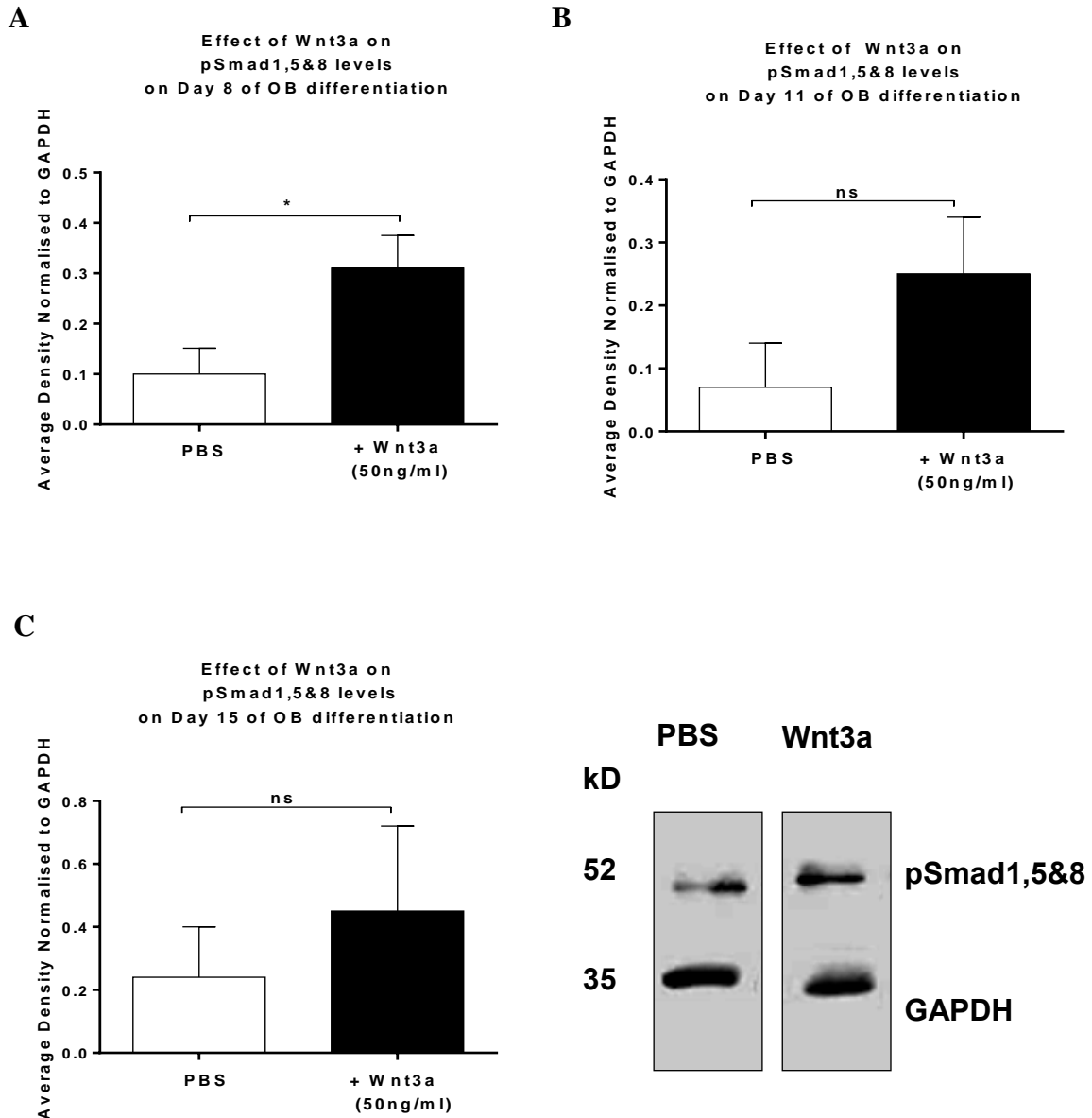
Figure 5.4.1.1 - Wnt3a induced phosphorylated Smad protein levels downstream of the BMP pathway in differentiating OB progenitors: *Western blot analysis was used to determine whether Wnt3a upregulated pSmad 1,5&8 protein levels in differentiating OB progenitors. Data represent the Average Density of pSmad 1,5&8 levels normalised to GAPDH. The western blot image is representative of one out of three experiments. Recombinant rmWnt3a acutely induced pSmad1,5&8 protein levels in OB progenitors on day 8 of differentiation (A) and not on any other occasion (B, C). N=3 independent experiments, Students unpaired t-test. Data are displayed with mean ± SEM.*P=0.05.*

A

Effect of SOSTDC1
on Wnt3a-induced pSmad1,5&8 levels
on Day 8 of OB differentiation

B

Effect of SOSTDC1
on Wnt3a-induced pSmad1,5&8 levels
on Day 11 of OB differentiation

C

Effect of SOSTDC1
on Wnt3a-induced pSmad1,5&8 levels
on Day 15 of OB differentiation
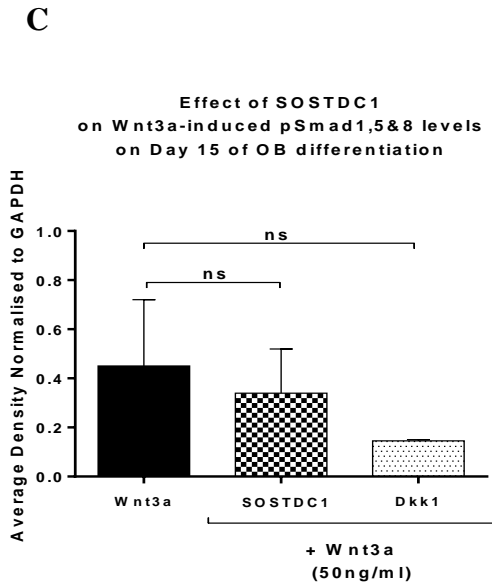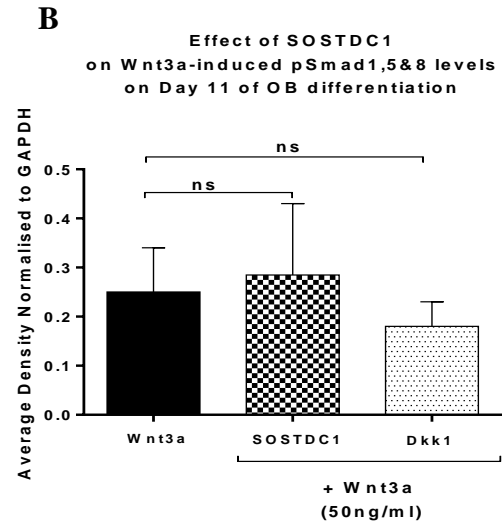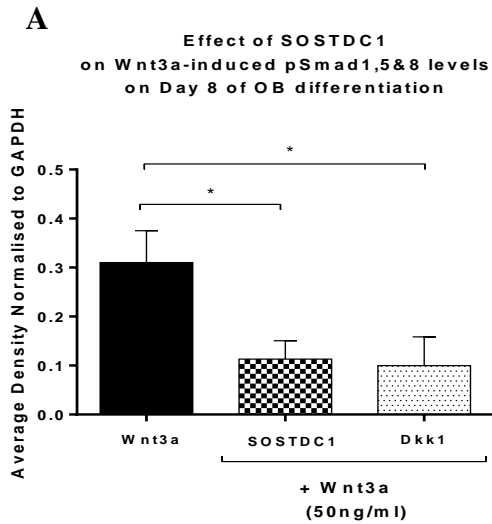
Figure 5.4.1.2 - SOSTDC1 reduced Wnt3a-induced Smad phosphorylation in differentiating OB progenitors: *Western blot analysis was used to determine whether SOSTDC1 down-regulated Wnt3a-induced pSmad 1,5&8 protein levels downstream of the BMP signalling pathway in differentiating OB progenitors. Data represent the Average Density of pSmad 1,5&8 levels normalised to GAPDH. The western blot image is representative of one out of three experiments. 250ng/ml rhSOSTDC1 and 100ng/ml rmDkk1 reduced Wnt3a- induced pSmad1,5&8 protein levels in OB progenitors on day 8 of differentiation (A). N=3 independent experiments, Students unpaired t-test. Data are displayed with mean ± SEM.*P=0.05.*

D
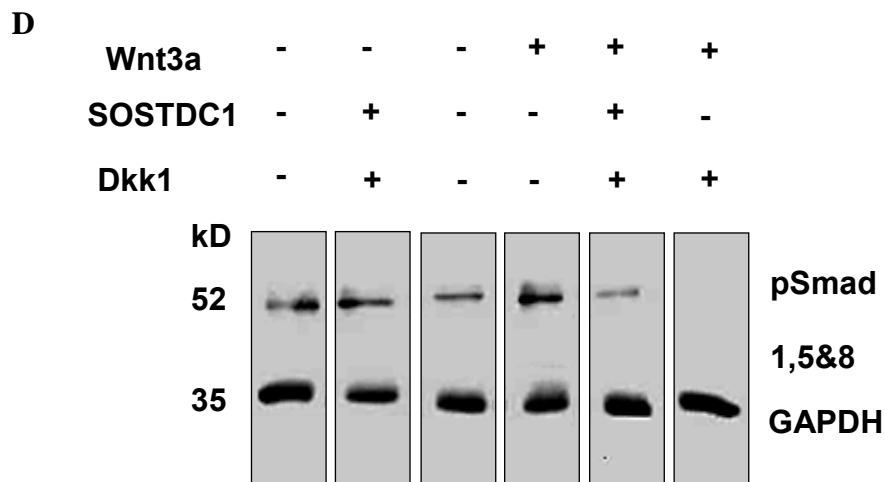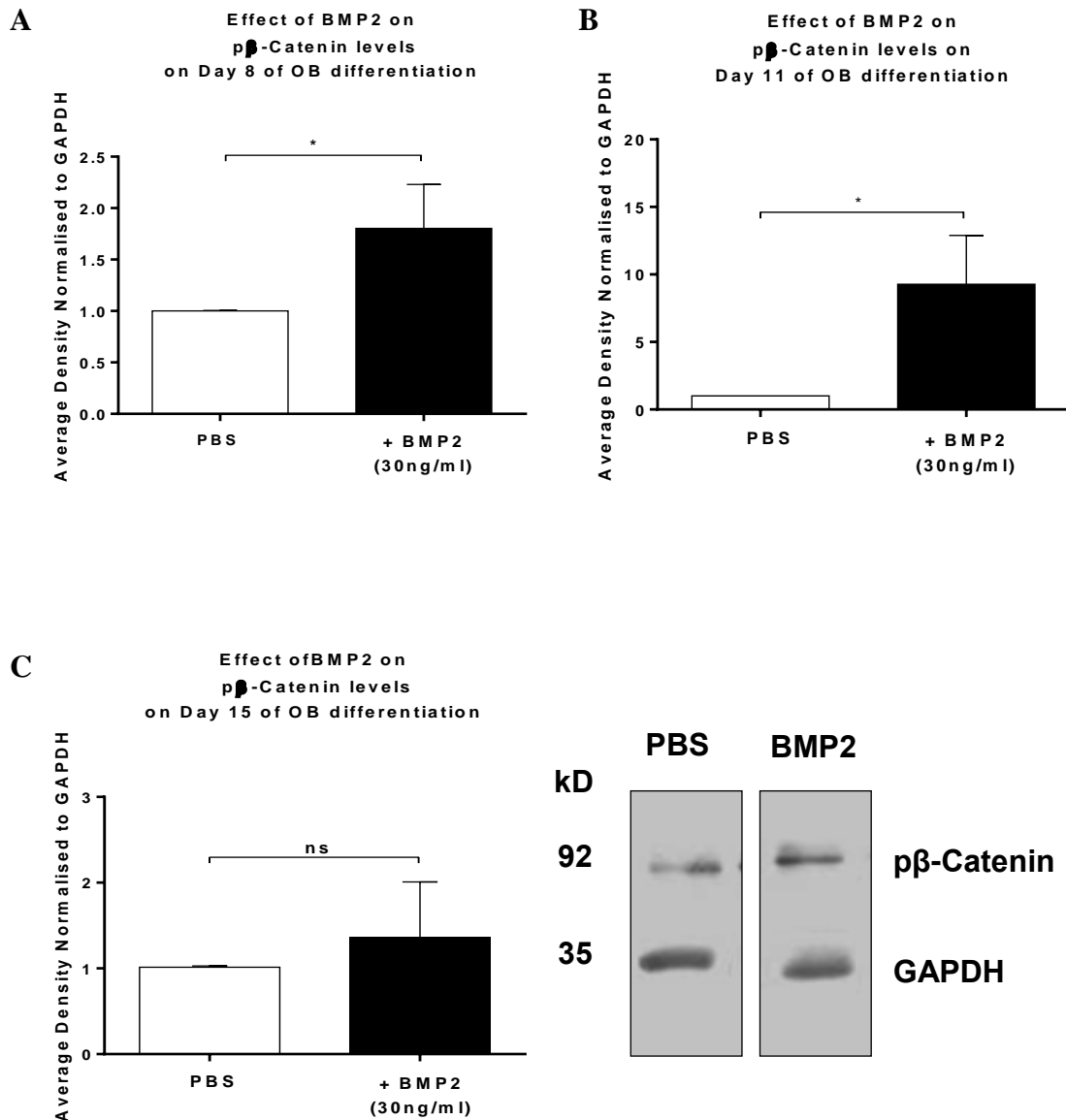
Figure 5.4.1.3 - BMP2 induced phosphorylated β-Catenin protein levels downstream of the Wnt pathway in differentiating OB progenitors: *Western blot analysis was used to determine whether 30ng/ml rhBMP2 upregulated pβ-Catenin levels in differentiating OB progenitors. Data represent the Average Density of pβ-Catenin levels normalised to GAPDH. The western blot image is representative of one out of three experiment. Recombinant hBMP2 acutely induced pβ-Catenin protein levels in OB progenitors on day 8 and 11 of differentiation (A, B). N=3 independent experiments, Students unpaired t-test. Data are displayed with mean ± SEM.*P=0.05.*

A

Effect of BMP2 on
pβ-Catenin levels on
Day 8 of OB differentiation

B

Effect of SOSTDC1
on BMP2- induced pβ-Catenin levels on
Day 11 of OB differentiation

C
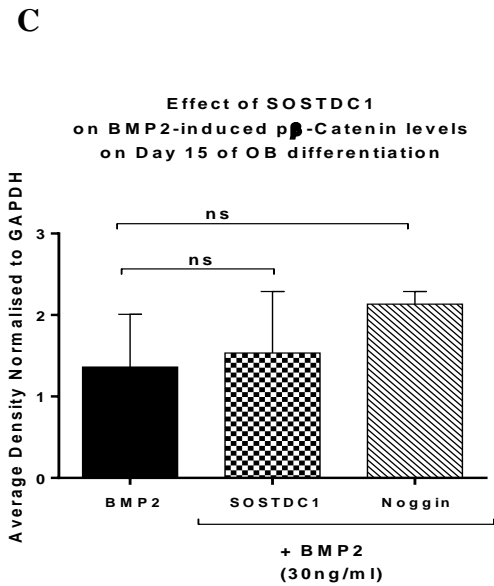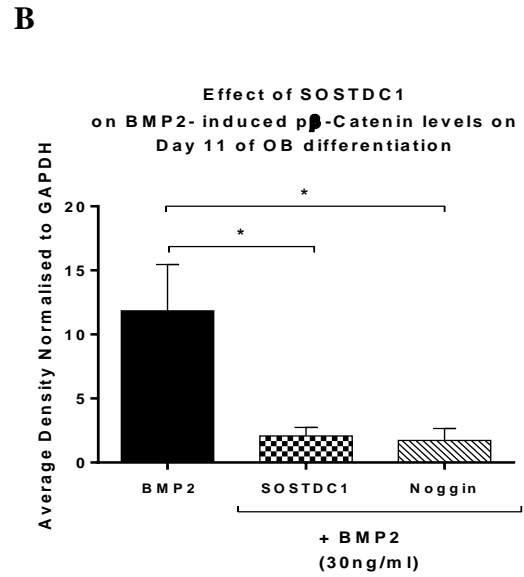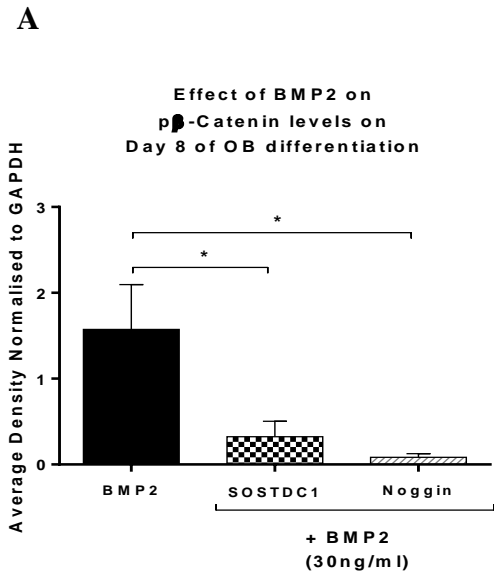
Effect of SOSTDC1
on BMP2-induced pβ-Catenin levels
on Day 15 of OB differentiation
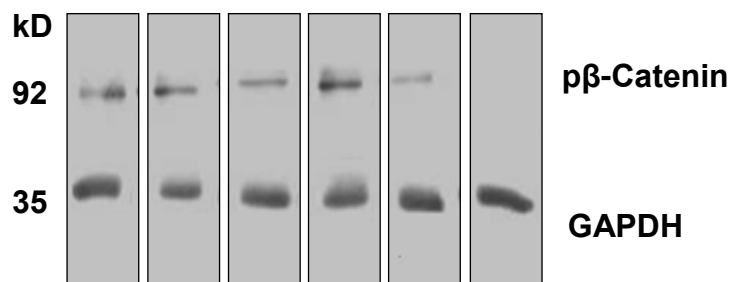
Figure 5.4.1.4 - SOSTDC1 reduced BMP2-induced phosphorylated β-Catenin protein levels in differentiating OB progenitors: *Western blot analysis was used to determine whether SOSTDC1 down-regulated BMP2-induced pβ-Catenin protein levels downstream of the canonical Wnt signalling pathway in differentiating OB progenitors. Data represent the Average Density of pβ-Catenin levels normalised to GAPDH. The western blot image is representative of one out of three experiments. 250ng/ml rhSOSTDC1 reduced BMP2- induced pβ-Catenin protein levels in OB progenitors on day 8 and 11 of differentiation (A, B). N=3 independent experiments, Students unpaired t-test. Data are displayed with mean ± SEM.*P=0.05.*

D
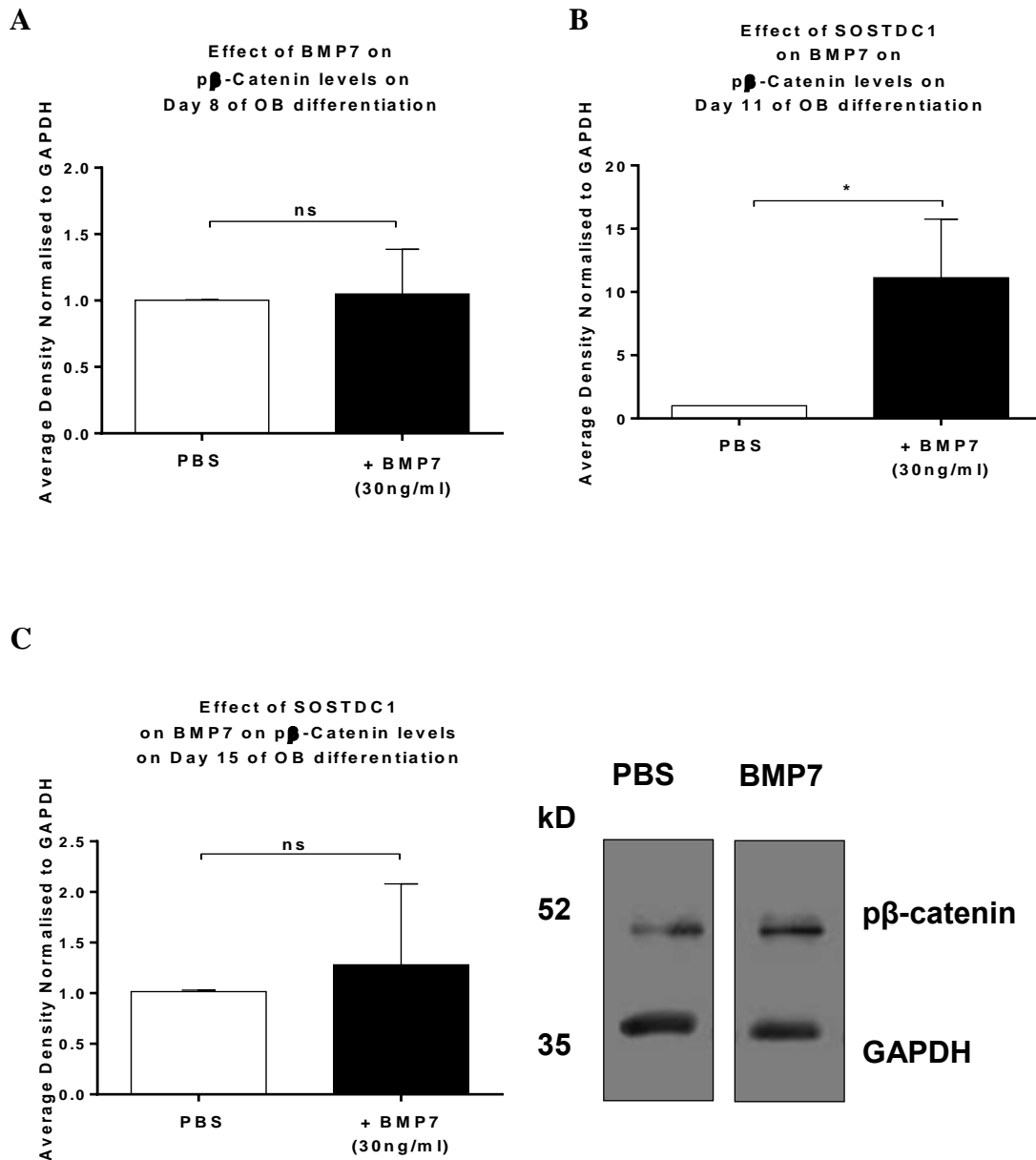
Figure 5.4.1.5 - BMP7 induced phosphorylated β-Catenin protein levels downstream of the Wnt pathway in differentiating OB progenitors: *Western blot analysis was used to determine whether 30ng/ml rhBMP7 upregulated pβ-Catenin levels in differentiating OB progenitors. Data represent the Average Density of pβ-Catenin levels normalised to GAPDH. The western blot image is representative of one out of three experiments. Recombinant h BMP7 acutely induced pβ-Catenin protein levels in OB progenitors on day 11 of differentiation only (B). N=3 independent experiments, Students unpaired t-test. Data are displayed with mean ± SEM.*P=0.05.*

A

Effect of SOSTDC1 on BMP7- induced pβ-Catenin levels on Day 8 of OB differentiation

B

Effect of SOSTDC1 on BMP7- induced pβ-Catenin levels on Day 11 of OB differentiation

C

Effect of SOSTDC1 on BMP7- induced pβ-Catenin levels on Day 15 of OB differentiation
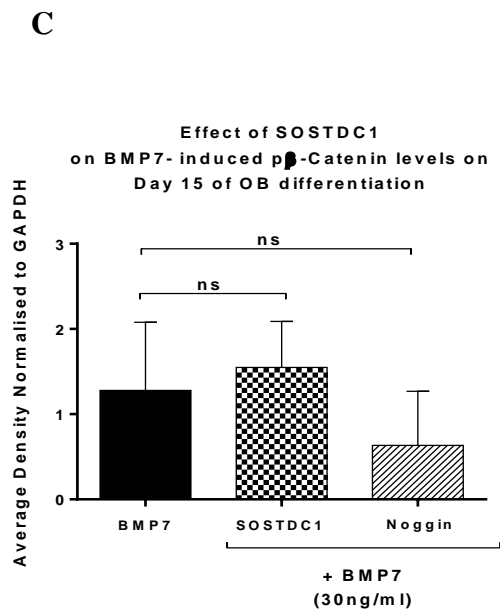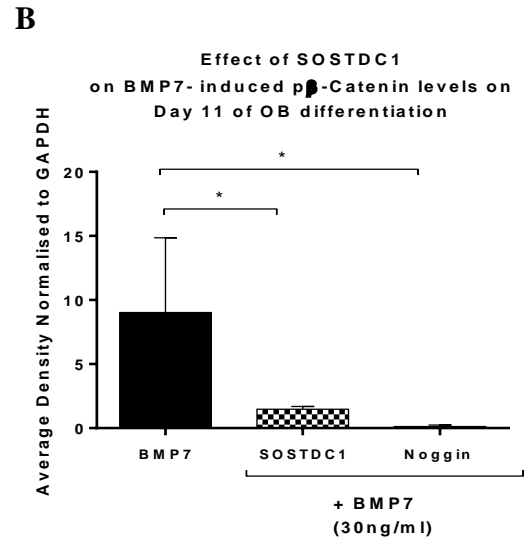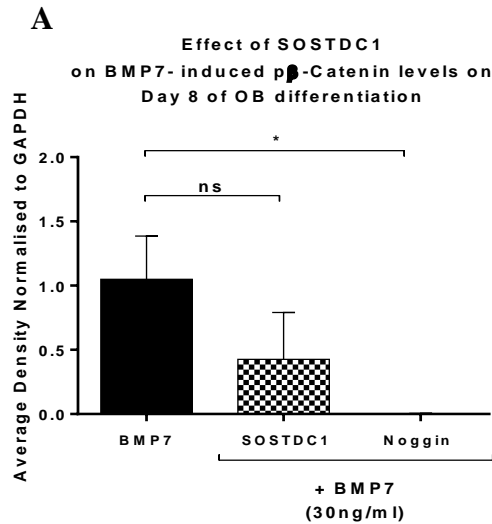
Figure 5.4.1.6 - SOSTDC1 reduced BMP7-induced phosphorylated β-Catenin protein levels in differentiating OB progenitors: *Western blot analysis was used to determine whether SOSTDC1 down-regulated BMP7-induced pβ-Catenin protein levels downstream of the canonical Wnt signalling pathway in differentiating OB progenitors. Data represent the Average Density of pβ-Catenin levels normalised to GAPDH. The western blot image is representative of one out of three experiments. 250ng/ml rhSOSTDC1 reduced BMP2-induced pβ-Catenin protein levels in OB progenitors on day 8 and 11 of differentiation (A, B). N=3 independent experiments, Students unpaired t-test. Data are displayed with mean ± SEM. *P=0.05.*

D

5.4.2 SOSTDC1 inhibited BMP-induced *CTNNB1* gene expression in differentiating OB progenitors

To determine whether BMP could upregulate the expression of *CTNNB1* downstream of the Wnt signalling pathway, the effect of Wnt ligand on *CTNNB1* expression was initially assessed. The levels of *CTNNB1* and *B2M* expression were quantified by qRT-PCR in OB progenitor cells obtained on day 8 and 11 of differentiation. The effects of Dkk1 on Wnt3a-induced and the effect of noggin on BMP-induced *CTNNB1* expression were also assessed. Differences in *CTNNB1* gene expression were normalised to *B2M* expression and overall fold changes in gene expression were calculated using the ΔΔ-CT method. Data were normalised to the PBS control. The data obtained from qRT-PCR analysis showed 50ng/ml rmWnt3a upregulated *CTNNB1* expression in differentiating OB progenitors on day 8 of differentiation (**Figure 5.4.2.1, A,** *P=0.022).

In the same experiments, 250ng/ml rhSOSTDC1 and 100ng/ml rmDkk1 reduced Wnt3a-induced *CTNNB1* levels (*P<0.05). The *CTNNB1* expression of OB progenitors was not affected in the presence of rhSOSTDC1 or rmDkk1 alone. Further qRT-PCR analysis of CTNNB1 expression in BMP-stimulated OB progenitors showed that 30ng/ml rhBMP2 and rhBMP7 induced *CTNNB1* gene expression on day 8 of OB progenitor differentiation on a similar level observed in Wnt3a-induced *CTNNB1* expression (**Figure 5.4.2.2 A,** **P=0.0057 and **Figure 5.4.2.3 A** *P=0.025). In the presence of rhBMP2, 250ng/ml rhSOSTDC1 reduced *CTNNB1* levels in OB progenitors on day 8 of differentiation (**Figure 5.4.2.2 A,** ***P=0.0001). The 100ng/ml rhnoggin also had a suppressive effect on rhBMP2-induced *CTNNB1* levels in OB progenitors on the same occasion (**Figure 5.4.2.2 A,** **P=0.0057). The qRT-PCR analysis further showed that rhBMP7-induced *CTNNB1* expression was reduced in the presence of 250ng/ml rhSOSTDC1 on day 8 of OB progenitor differentiation (**Figure 5.4.2.2 A,** *P=0.01). 100ng/ml rhnoggin also reduced rhBMP7-induced *CTNNB1* levels in OB progenitors on day 8 of differentiation (**Figure 5.4.2.3 A,** **P=0.0081).

A

Effect of SOSTDC1 on Wnt3a-induced *CTNNB1* on Day 8 of OB differentiation

B
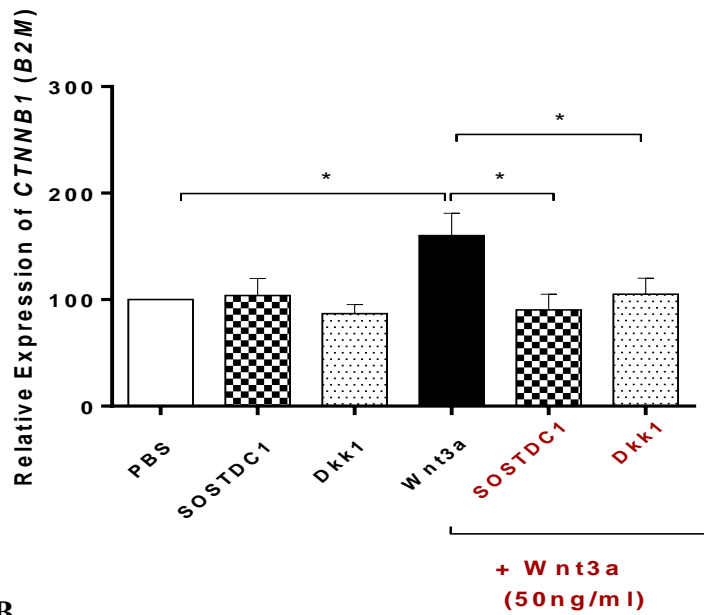
Effect of SOSTDC1 on Wnt3a-induced *CTNNB1* on Day 11 of OB differentiation
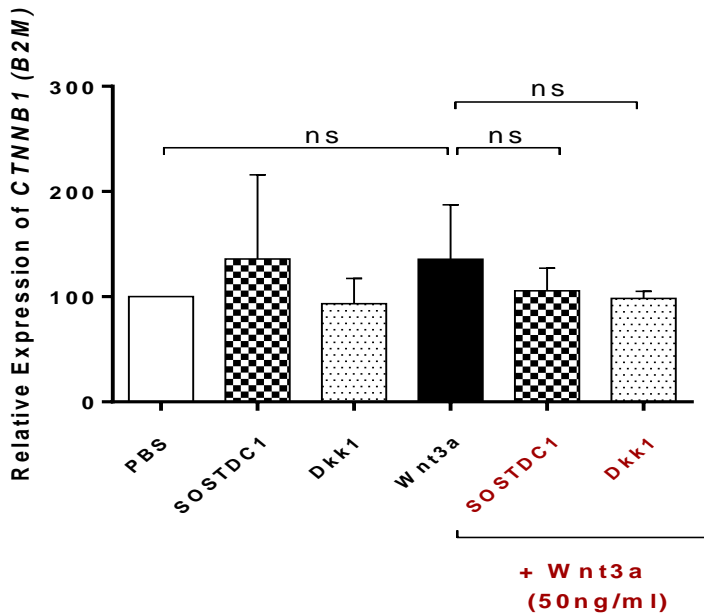
Figure 5.4.2.1 - SOSTDC1 inhibited Wnt-induced *CTNNB1* expression in differentiating OB progenitors: *OB progenitor cells were cultured with 50ng/ml rmWnt3a in the presence or absence of 250ng/ml rhSOSTDC1 or 100ng/ml rmDkk1 and the CTNNB1 expression quantified using qRT-PCR. Data represent the relative expression of CTNNB1 normalised to B2M. (A) The rmWnt3a upregulated CTNNB1 expression in OB progenitors on day 8 of differentiation. On this occasion rhSOSTDC1 and rmDkk1 reduced the Wnt3a-induced CTNNB1 levels. N=4 independent experiments, One way ANOVA and Holm-Sidak multiple comparisons test. Data are displayed with mean ± SEM.*P=0.05.*

A

Effect of SOSTDC1 on BMP2-induced *CTNNB1* on Day 8 of OB differentiation

B
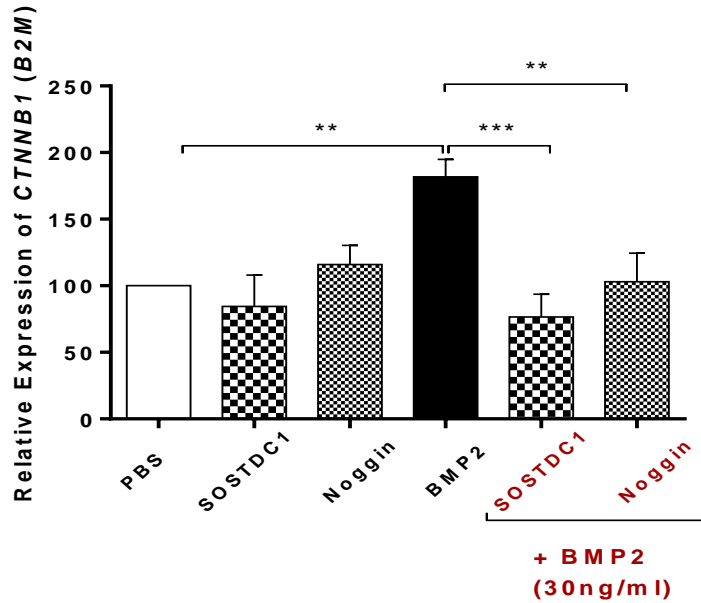
Effect of SOSTDC1 on BMP2-induced *CTNNB1* on Day 11 of OB differentiation
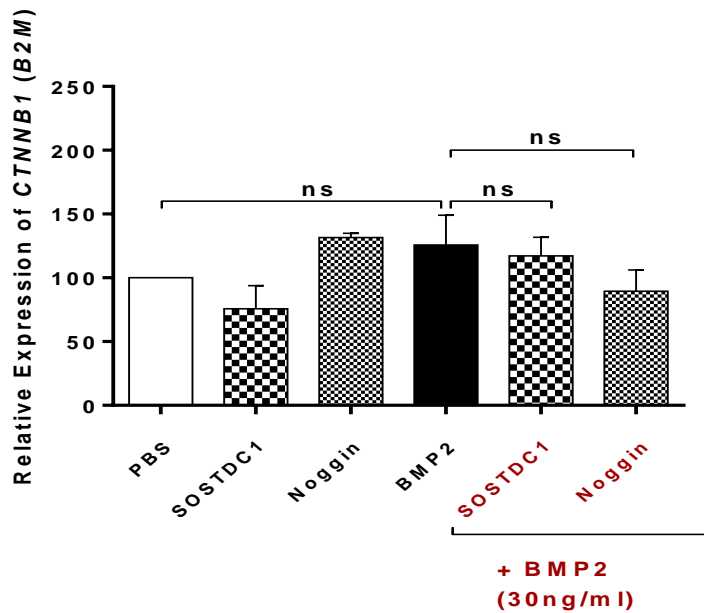
Figure 5.4.2.2 - SOSTDC1 inhibited BMP2-induced *CTNNB1* expression in differentiating OB progenitors: *OB progenitor cells were cultured with 30ng/ml rhBMP2 in the presence or absence of 250ng/ml rhSOSTDC1 or 100ng/ml rhnoggin and the CTNNB1 expression quantified using qRT-PCR. Data represent the relative expression of CTNNB1 normalised to B2M. (A) The rhBMP2 upregulated CTNNB1 expression in OB progenitors on day 8 of differentiation. On this occasion rhSOSTDC1 and rhnoggin reduced the rhBMP2-induced CTNNB1 levels. N=4 independent experiments, Holm-Sidak multiple comparisons test. Data are displayed with mean ± SEM. **P=0.01, ***P=0.001.*

A

Effect of SOSTDC1 on BMP7-induced *CTNNB1* on Day 8 of OB differentiation

B

Effect of SOSTDC1 on BMP7-induced *CTNNB1* on Day 11 of OB differentiation
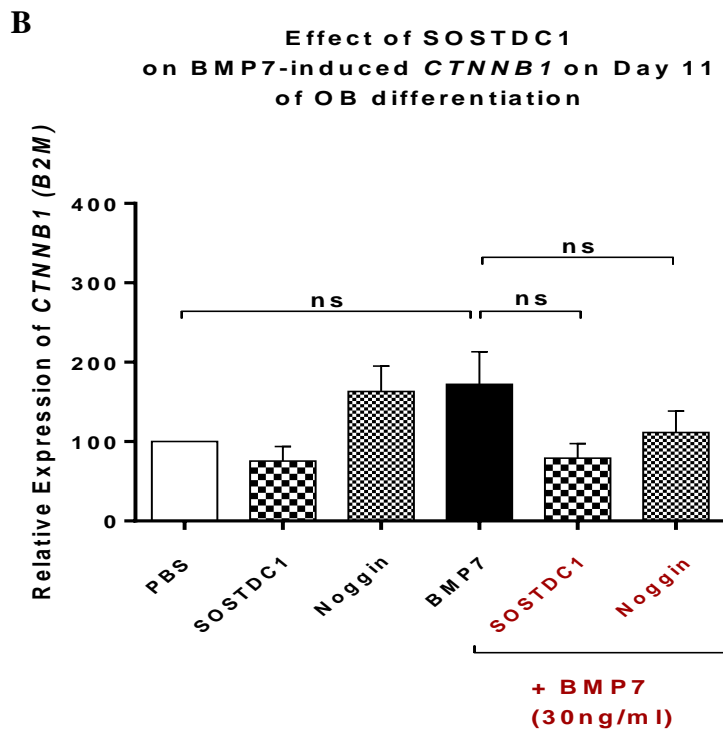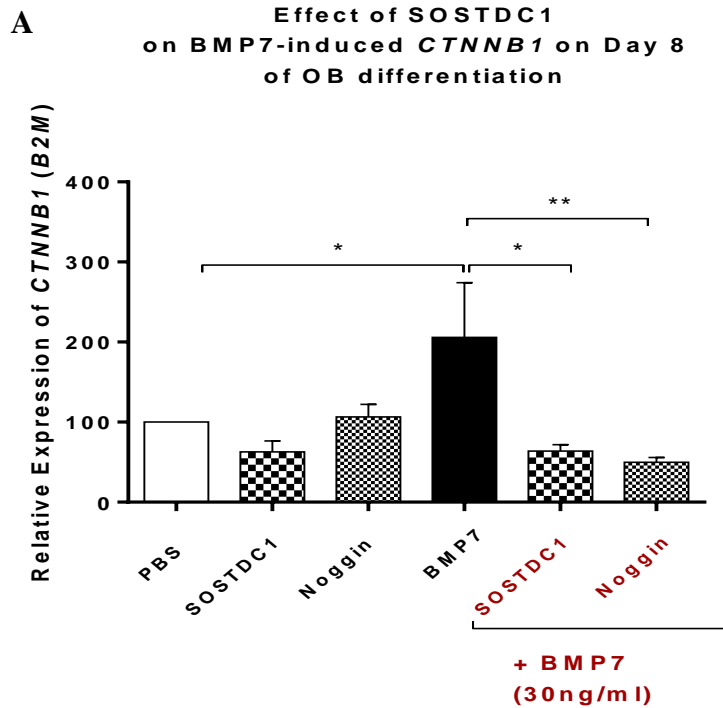
Figure 5.4.2.3 - SOSTDC1 inhibited BMP7-induced *CTNNB1* expression in differentiating OB progenitors: *OB progenitor cells were cultured with 30ng/ml rhBMP7 in the presence or absence of 250ng/ml rhSOSTDC1 or 250ng/ml rhnoggin and the CTNNB1 expression quantified using qRT-PCR. Data represent the relative expression of CTNNB1 to B2M. (A) The rhBMP7 upregulated CTNNB1 expression in OB progenitors on day 8 of differentiation. On this occasion rhSOSTDC1 and rhnoggin reduced the rhBMP7-induced CTNNB1 levels. N=4 independent experiments, Holm-Sidak multiple comparisons test. Data are displayed with mean ± SEM. *P=0.05. **P=0.01.*

5.4.3 Recombinant SOSTDC1 protein bound with high affinity to recombinant LRP-6, BMP2 and BMP7 determined by Bio-layer interferometry

The affinity of 100µg/ml rhSOSTDC1 protein for purified carrier-free rmLRP-6, rhBMP2 and rhBMP7 were determined using the Blitz Analysis system as outlined in **section 2.15.1**. The measured affinity of the interaction KD (M) between the rhSOSTDC1 protein and rmLRP-6, rhBMP2 or rhBMP7 was reported by the BLItz Pro™ software. Interferometry data were globally fit to a 1:1 Langmuir model calculating the affinities and rate constants. The interaction of rhSOSTDC1 for multiple concentrations (µg/ml) of rmLRP-6, rhBMP2 or rhBMP7 was used for the Langmuir model fitting. The association and dissociation responses were baseline corrected and processed using the Octet Software to rise to the affinity constant KD.

In addition, the interactions between 100µg/ml rhGST protein and 100µg/ml rmLRP-6, rhBMP2 and rhBMP7 were also assessed. The rhGST-analyte binding assays were carried out to ensure that the KD values obtained for interaction between rhSOSTDC1 and rmLRP-6, rhBMP2 and rhBMP7 were not affected by the presence of the GST-tag. The sensogram data collected in real time showed that rhSOSTDC1 bound with high affinity to rmLRP-6, rhBMP2 and rhBMP7 (**Figure 5.4.3).**

The binding affinity of rhSOSTDC1 for the Wnt receptor rmLRP-6 was determined as 8.502e-10M KD (**Figure 5.4.3 A**). The affinity of rhSOSTDC1 for rhBMP2 was determined as 9.569e-9M KD (**Figure 5.4.3 B**) and the affinity of rhSOSTDC1 for rhBMP7 was calculated at <1.0e-12M KD (**Figure 5.4.3 C**). The affinity of rhSOSTDC1 for the rmLPR-6 receptor protein was one-fold higher compared to the affinity of rhSOSTDC1 rhBMP2 ligand protein. Subsequently, I showed that rhSOSTDC1 had the highest binding affinity for the ligand BMP7 protein out of all three rhSOSTDC1-protein interactions. The rhSOSTDC1 protein had a three-fold higher binding affinity for rhBMP7 compared to rmLRP-6. The 100µg/ml of rhGST did not bind at detectable levels to rmLRP-6 or rhBMP7 protein and the KD value of 1.096e-4M calculated for rhGST-rhBMP2 interaction was negligible, indicating little or no binding (**Appendix 3**).

A

100µg/ml SOSTDC1 interaction with LRP-6		
Sample	Concentration (µg/ml)	kD (M)
LRP-6	100	8.502e-10
LRP-6	50	
LRP-6	25	
LRP-6	10	
LRP-6	1	
LRP-6	0 (buffer only)	-

B

100µg/ml SOSTDC1 interaction with BMP2		
Sample	Concentration (µg/ml)	kD (M)
BMP2	100	9.569e-9
BMP2	50	
BMP2	25	
BMP2	10	
BMP2	1	
BMP2	0 (buffer only)	-

C

100µg/ml SOSTDC1 interaction with BMP7		
Sample	Concentration (µg/ml)	kD (M)
BMP7	100	<1e-12
BMP7	50	
BMP7	25	
BMP7	10	
BMP7	1	
BMP7	0 (buffer only)	-

Figure 5.4.3 - Recombinant SOSTDC1 protein bound with high affinity to recombinant LRP, BMP2 and BMP7 proteins: *The affinity KD (M) of rhSOSTDC1 for purified carrier-free rmLRP-6, rhBMP2 and rhBMP7 proteins were determined using the Blitz Analysis system. (A) Binding (nm) association showed 100ug/ml of rhSOSTDC1bound to; rmLRP-6 with a kD of 8.502e-10M (B) rhBMP2 with a kD of 9.569e-9M and (C) rhBMP7 with a kD of <1.0e-12M.*

5.5 Discussion

This chapter focused on the role of SOSTSDC1 in Wnt-BMP crosstalk in OB progenitor differentiation, in which the main aim of the study was to determine whether SOSTDC1 had an antagonistic effect on Wnt-BMP dependent signalling within OB progenitor cells. The hypothesis of SOSTDC1 suppresses Wnt-BMP crosstalk in signalling OB progenitor cells was supported by my finding. Previously my data provided evidence for the antagonistic actions of SOSTDC1 on Wnt and BMP signalling in differentiating OB progenitors. Evidence of regulation between canonical Wnt signalling and BMP signalling has previously been demonstrated in embryonic development and tumourgenesis (Zhang, Yan et al. 2009). In studies by Bill et al, Wnt signalling was found to induce expression of BMP2, BMP4, BMP7 and BMP target genes including Msx2 and gremlin in the mesenchyme (Bill et al, 2006). In gastrointestinal cancer cells, β-catenin induced BMP2 expression (Kim, Crooks et al. 2002). The downstream target genes of BMP signalling and cross-interaction between BMP ligands and Wnt signalling in OB are poorly understood. Recent studies demonstrate that BMP2 has a synergic effect with β-catenin on OB differentiation *in-vitro* (Rawadi, Vayssiere et al. 2003, Mbalaviele, Sheikh et al. 2005). However, the effects of Wnt signalling on BMP expression in OB and the associated molecular mechanisms remain unclear.

Specific secreted molecules have an effect on Wnt and BMP signalling by binding to the extracellular components of both pathways. For example, Cerberus which is known to induce head formation in *Xenopus* inhibits Wnt and BMP signalling by binding directly to Wnt and BMP ligands, regulating head formation (Silva, Filipe et al. 2003). Another secreted molecule includes connective tissue growth factor (CTGF) which can bind BMP4, TGFβ1 and LRP6 (Silva, Filipe et al. 2003). As mentioned previously Sclerostin is another molecule that can inhibit bone formation by binding to BMP ligands (Kusu, Laurikkala et al. 2003) and the LRP5/6 receptors (Ellies, Viviano et al. 2006). Interestingly the interaction of Sclerostin, which has a very similar homology to SOSTDC1, with BMP ligands and LRP5/6 has been shown to interfere with Wnt signalling (ten Dijke, Krause et al. 2008). It would therefore seem that extracellular mechanisms modulating both Wnt and BMP signalling regulate simultaneous suppression of both signalling pathways providing a rational for investigating the role of SOSTDC1 in Wnt-BMP crosstalk.

A limited number of studies have investigated the role of SOSTDC1 in Wnt-BMP crosstalk and these studies have been specific to tooth development and kidney disease. In a study by Liu et al SOSTDC1 mouse mutants exhibited supernumerary teeth, which were thought to be a result of increased BMP and Wnt/β-catenin activity (Liu, Chu et al. 2008). I investigated the effect of Wnt3a ligand on phosphorylated levels of Regulatory Smad protein complex downstream of the BMP pathway and subsequently assessed this effect in the presence of recombinant SOSTDC1 in differentiating OB progenitors. In my study, Wnt3a induced phosphorylation of Smad1,5&8 protein in OB progenitors and SOSTDC1 reversed this effect during the early stage of differentiation. In similar studies by Rawadi et al investigating the crosstalk between Wnt-BMP signalling, blocking Wnt/LRP5 signalling resulted in the inhibition of BMP2-induced ALP activity in MSC. Moreover, MC3T3-E1 cells overexpression of Dkk1 reduced BMP2-induced extracellular matrix mineralization (Rawadi et al, 2003).

In the same experiments, I showed that SOSTDC1 suppressed Wnt3-induced phosphorylated Smad 1,5&8 levels in in differentiating OB progenitor cells on a similar level to Dkk1. Based on the literature it can be deduced that SOSTSDC1 antagonises Wnt signalling in a similar mechanism to that of antagonist Dkk1. SOSTDC1 and Dkk1 both bind to the LRP/Frz Wnt receptor and in doing so block Wnt ligand interaction with the LRP/Fz receptor. In the same study by Liu et al, overexpression of Dkk1 blocked tooth formation and this was accompanied by down-regulation of BMP and Msx1/2 expression domains. The BMP4 induction of *Msx1/2* expression was not affected in Dkk1-overexpression suggesting that Wnt/β-catenin signals are required upstream of BMP4 function (Liu, Chu et al. 2008). Based on the similarities between the antagonistic role of SOSTSDC1 and Dkk1 in Wnt-BMP crosstalk in differentiating OB progenitors, it may be assumed that both molecules have a similar detrimental effect in osteolytic bone disease. One possibility for this similarity may be that in osteolytic bone disease, if one molecule is not in abundance, then the other is produced at high levels to compensate.

In my studies investigating BMP stimulation of downstream intracellular Wnt signalling, I found that both BMP2 and BMP7 increased phosphorylated levels of β-catenin protein and active *CTNNB1* gene expression. SOSTSDC1 reduced BMP-induced β-catenin levels in the early stages of OB progenitor differentiation. This data is similar to that found by Papathanasiou et al showing treatment of chondrocyte cultures with BMP2 resulted in an

up-regulation of β-catenin nuclear translocation and LRP-5 expression. Papathanasiou showed that BMP2-induced LRP-5 expression was mediated through Smad1/5/8 binding on the *LRP-5* promoter. In these studies, LRP-5 silencing resulted in reduction of nuclear β-catenin protein, MMPs and collagen X expression, whereas phosphorylated β-catenin protein levels in BMP-2-treated chondrocyte increased (Papathanasiou, Malizos et al. 2012).

Fukuda et al showed that in the presence of BMP-4, canonical Wnt1 and Wnt3a but not non-canonical Wnt5a and Wnt11 stimulated ALP activity of OB-like C2C12 cells. This group also showed that Type I collagen and osteonectin expression increased in response to Wnt3a and BMP4 stimulation and both noggin and Dkk1 suppressed the synergistic effect of BMP-4 and Wnt3a (Fukuda, Kokabu et al. 2010). Stimulation of GSK3β activity in the presence of BMP-4 caused induction of ALP activity. The Fukuda et al showed that Wnt3a did not stimulate BMP receptor/Smad1-induced ALP level and overexpression of β-catenin did not affect BMP4-induced ALP levels in C2C12 cells. Fukuda et al concluded that Wnt-BMP regulation of OB differentiation, especially at the early stages, through a GSK3β-dependent but β-catenin-independent mechanism (Fukuda, Kokabu et al. 2010). In comparison the Zhang et al data was contradictory as in these studies BMP2 stimulated *Lrp5* expression and enhanced protein levels of the active form of β-catenin in OB. The *in-vitro* deletion of the *CTNNB1* gene supressed OB proliferation and differentiation and reduced BMP2-induced OB differentiation. BMP2 also increased nuclear β-catenin protein levels suggesting the interaction between Wnt and BMP2 signalling during OB differentiation is (Zhang et al, 2009). Recently Zhang et al also showed that similar to BMP2, Wnt3a increased transcriptional activity of BMP/Smad reporter and noggin blocked this Wnt3a-induced effect, concluding that Wnt signalling acts as an upstream regulator of BMP signalling (Zhang, Oyajobi et al. 2013). There data is complimentary to mine in that in my studies, noggin significantly suppressed BMP-induced nuclear β-catenin levels.

It is of particular interest that the Wnt-BMP crosstalk relationship that Fukada et al demonstrated was especially specific to the early stages of OB differentiation (Fukuda, Kokabu et al. 2010). The increase in BMP-induced β-catenin levels was also observed in preosteblastic cells in Zhang et al study (Zhang et al, 2009). The data from these studies

are in line with my results in showing that the Wnt-BMP crosstalk may be occur on when OB cells have a more immature phenotype.

Having established that SOSTDC1 may potentially have an important role Wnt-BMP crosstalk in osteoprogenitors cells, I wanted to determine the relative binding characteristics of this molecule for BMPs and Wnt receptors. To produce informative results, the binding affinity of SOSTDC1 for each potential partner ligand/receptor was determined using the same recombinant proteins used for all functional and signalling assays. I showed that recombinant SOSTDC1 had a higher binding affinity for the LRP6 (8.502e-10M) receptor protein compared to the recombinant BMP2 protein (9.569e-9M). Interestingly, SOSTDC1 had the highest affinity for BMP7 (<1.0e-12M) out of the three SOSTDC1-protein partner interactions assessed. To my knowledge there are no studies that have investigated the binding affinity of rhSOSTDC1 for LPR6, BMP2 and BMP7. However Laurikkala et al did examine the binding of Ectodin (recombinant mouse SOSTDC1) to BMP2, BMP4, BMP6, and BMP7 ligands using the BIAcore system with a recombinant Ectodin protein-fixed sensor tip. This group found that Ectodin bound to BMP2, BMP4, BMP6, and BMP7 with high affinity (Laurikkala, Kassai et al. 2003) similar to my data. Lintern et al did attempt to quantify binding affinity of Wise to LRP6 and to compare it with that to BMPs, however they were unsuccessful in express pure Wise protein in bacteria (Lintern et al, 2009). Krause et al also investigated the binding of the SOSTDC1 homolog Sclerostin for LRP5 using the Biacore system. They revealed a relatively low binding affinity with KD values ranging from 2 to 8.6 μm for full-length murine and human sclerostin, respectively (Krause, Korchynskyi et al. 2010). This data is interesting in the sense that if SOSTDC1 has a higher binding affinity for LRP5/6 receptor compared to sclerostin, SOSTDC1 may potentially have a more important role in OB dysfunction in osteolytic bone disease.

In summary, my findings provide compelling evidence for the molecular mechanisms by which SOSTDC1 antagonises both the canonical Wnt pathway and BMP signalling pathways in OB differentiation through Wnt-BMP dependency. The data in my studies suggests that the functional communication between Wnt-BMP involves β-catenin and SOSTDC1 may play an important role in integrating the anabolic functions of both pathways in bone.

Chapter 6 – The Role of SOSTDC1 in Myeloma Bone Disease

6.1 Introduction

The formation of lytic lesions in the skeleton is an established hallmark of MM growth in bone. However, our understanding of the processes involved in MM bone disease is limited. Recently, animal models have been used to identify the pathways and molecules involved in the mechanisms responsible for the suppression of bone formation and although a number of molecules have been implicated, there is a lack of functional data defining the roles of the latter in MM bone disease.

Preliminary gene array data (unpublished) produced by the Myeloma group in Sheffield has identified SOSTDC1 as a molecule upregulated in the bone of syngeneic mice bearing the 5T2MM mouse myeloma model compared to naive non-tumour bearing animals. Initially described by Radl *et al*, the 5TMM series of MM were aging immune-competent C57BL/KalwRij mice that displayed numerous clinical characteristics of human MM disease. These characteristics included spontaneous age-related origin, plasma cell proliferation within the BM, elevated paraprotein levels, reduced levels of normal immunoglobulin, and development of osteolytic bone lesions (Radl, Croese et al. 1988). The 5TMM models have since been maintained via the injection of tumour cells isolated from tumour-infiltrated C57BL/KaLwRij mice into 6-8 week old mice of the same strain. The 5TGM1MM model similar to 5T33MM is an aggressive form of the disease that develops over a 4 week period. The two models do vary in that the 5TGM1MM cells appear to be independent of their environment and growth of myeloma tumours develop in numerous locations including the bone, spleen and liver. Another important variable between the two models is that osteolytic bone disease occurs in the 5TGM1MM model and not in the 5T33MM model (Croese, Vas Nunes et al. 1987, Vanderkerken, De Raeve et al. 1997).

In previous chapters, my functional and signalling data identified SOSTDC1 as a Wnt and BMP signalling antagonist in OB cells. It is not clear which cells in the BM express SOSTDC1 and whether the interaction between OB and myeloma cells, induce production of SOSTDC1. Although data is limited, there is evidence that SOSTDC1 can regulate cell activity through BMP and Wnt signalling pathways within other cancers. Studies by Clausen *et al* into SOSTDC1 secretion and BMP/Wnt signalling in breast cancer cells, link decreased SOSTDC1 expression to increased tumour size, highlighting

the role of SOSTDC1 as a potential clinical target (Clausen, Blish et al. 2010). However, the function of SOSTDC1 in relation to bone disease secondary to cancer growth in bone has not been studied to date within any type of cancer.

In myeloma patients, abnormalities in osteoprogenitor cells and the production of OB inhibitors by both myeloma cells and myelomatous bone microenvironment cells result in a reduction in osteoblastogenesis (Yaccoby 2010). In MM the osteolytic lesions arise in close proximity to the tumour indicating that in addition to the soluble factors that regulate osteoblastogenesis suppression, the close or direct contact between myeloma cells and MSC may also influence bone remodelling. As an example myeloma cells partially suppress osteocalcin levels in osteogenic cells through direct cell contact (Roodman 2004). This data supports the rational that direct myeloma and OB interaction may induce SOSTDC1 production in either myeloma, OB or indeed both cell types. Determining the conditions under which SOSTDC1 is expressed in myeloma is key in understanding the role of this protein in MM osteolytic bone disease.

6.2 Hypothesis and Objectives

6.2.1 Aims

The aim of this study was to determine the conditions under which myeloma and OB progenitor cells produce SOSTDC1.

To achieve this, the following hypothesis was tested.

6.2.1 Hypothesis

The 5T Series of MM produce SOSTDC1

OB progenitors produce SOSTDC1

Direct myeloma and OB progenitor interaction upregulates the production of SOSTDC1 in myeloma and OB progenitor cells

6.2.2 Specific Objectives

To test this hypothesis the following were determined:

Whether SOSTDC1 is produced by 5T33MM/5TGM1MM myeloma cells or OB progenitors

Whether co-culture of myeloma and OB cells upregulates SOSTDC1 levels

The distribution of SOSTDC1 in 5T33MM and 5TGM1MM tibia

Whether SOSTDC1 is expressed at higher levels in myeloma cells that produce lytic versus non-lytic lesions *in-vivo*

6.3 Chapter specific methods

Primary and Secondary Antibodies			
Antibody	**Concentration of stock**	**CATALOGUE NUMBER**	**SUPPLIER**
Anti-SOSTDC1 antibody *Rabbit polyclonal*	0.5mg/ml	Ab56079	Abcam
Normal Rabbit IgG (Isotype Control) *Rabbit polyclonal*	1.0mg/ml	AB-105-C	R&D
PE Rat IgG2a Isotype Control	0.2 mg/ml	400508	BioLegend
Anti-GAPDH (6C5) antibody *Mouse monoclonal*	1.0mg/ml	Ab-37168	Abcam
PE Rat Anti-Mouse CD138 *Mouse monoclonal*	0.2mg/ml	581070	BD Pharmingen™
Donkey Anti-Rabbit IgG NL637 NorthernLights 637 *Rabbit polyclonal*	1.0mg/ml	NL005	R&D
HRP-Rabbit Anti-Mouse IgG *Mouse polyclonal*	2.0mg/ml	613420	Cell Signalling
HRP-Goat Anti-Rabbit IgG *Rabbit polyclonal*	2.0mg/ml	HAF008	R&D
Biotinylated Goat Anti Rabbit IgG (H+L)	1.0mg/ml	ab64256	Abcam

Table 6.1 - *Recombinant proteins required for the detection of SOSTDC1 in OB progenitors and myeloma cells cultures and co-cultures.*

6.3.1 Detection of SOSTDC1 in OB progenitors and myeloma cells cultured on their own and co-cultured together by immunofluorescent microscopy

There are currently no publications that show SOSTDC1 is expressed in OB or myeloma cells. The aim of the first part of this study was to qualitatively establish whether OB or myeloma cells produced SOSTDC1. Human kidney cells were used as a positive control in this study as they are known to secrete SOSTDC1 (Blish, Clausen et al. 2010). To

validate immunological methods of SOSTDC1 detection, protocols were optimised with Human Kidney-2 (HK-2) cells derived from the cortex/proximal tubules of the human kidney. Immunofluorescent microscopy was initially used to determine whether there was any production of SOSTDC1 protein in OB progenitors, 5T33MM and 5TGM1MM cells cultured on their own. HK-2, OB progenitors, 5T33MM and 5TGM1MM were plated in 48 well culture plates at a cell density of 5700 cells per well (6000 cell/cm^2) and allowed to adhere to the plate surface for 48 hours. OB progenitors were differentiated in standard osteogenic media for up to 8 days. HK-2 cells were maintained in standard keratinocyte media and 5T33MM and 5TGM1MM were maintained in standard RPMI for the duration of the 8 days. Media was removed and 500µl of fresh media replaced every three days. To determine whether SOSTDC1 production was affected by contact between myeloma and OB, 5T33MM or 5TGM1MM myeloma cells were counted and co-cultured on the differentiating OB progenitors on day 8 of differentiation. Myeloma cells were co-cultured at a cell density of approximately 12000 cell/cm^2 or 11400 cells per well in a 48-well plate that was similar to the estimated OB progenitor cell number on day of 8 of differentiation. This cell density was based on the OB progenitor growth curves performed in Chapter 3, suggesting that OB cultures approximately doubled in DNA contents/cell number by day 8 of differentiation. Myeloma cells were co-cultured with the OB progenitors for 24 hours in 1ml of RPMI. The immunostaining method for microscopy was carried out according to **section 2.11**.

Cells were stained with 1µg/ml (1:500 dilution) anti-SOSTDC1 antibody or isotype control at the same concentration overnight at 4ºC and then stained with a secondary 3.3µg/ml (1:300) dilution of Donkey anti-Rabbit IgG NL637 antibody for 1 hour at room temperature. Cells were co-stained with 6.6 µg/ml (1:300 dilution) PE Rat Anti-Mouse CD138 for 1 hour. Images of phase contrast, DAPI, CD138 and SOSTDC1 staining were visualised simultaneously and represented as a single stain on their own or merged as one image. Blue staining represented positive nuclear staining for DAPI and the green staining represented positive nuclear staining for CD138. Any SOSTDC1 staining, both intra and extra-cellular, were represented by the red colour within images (**Figure 6.3.1**).

OB progenitors differentiated in osteogenic media

Myeloma-OB progenitors co-cultured

Immunofluorescent Microscopy Detection of DAPI, CD138 and SOSTDC1
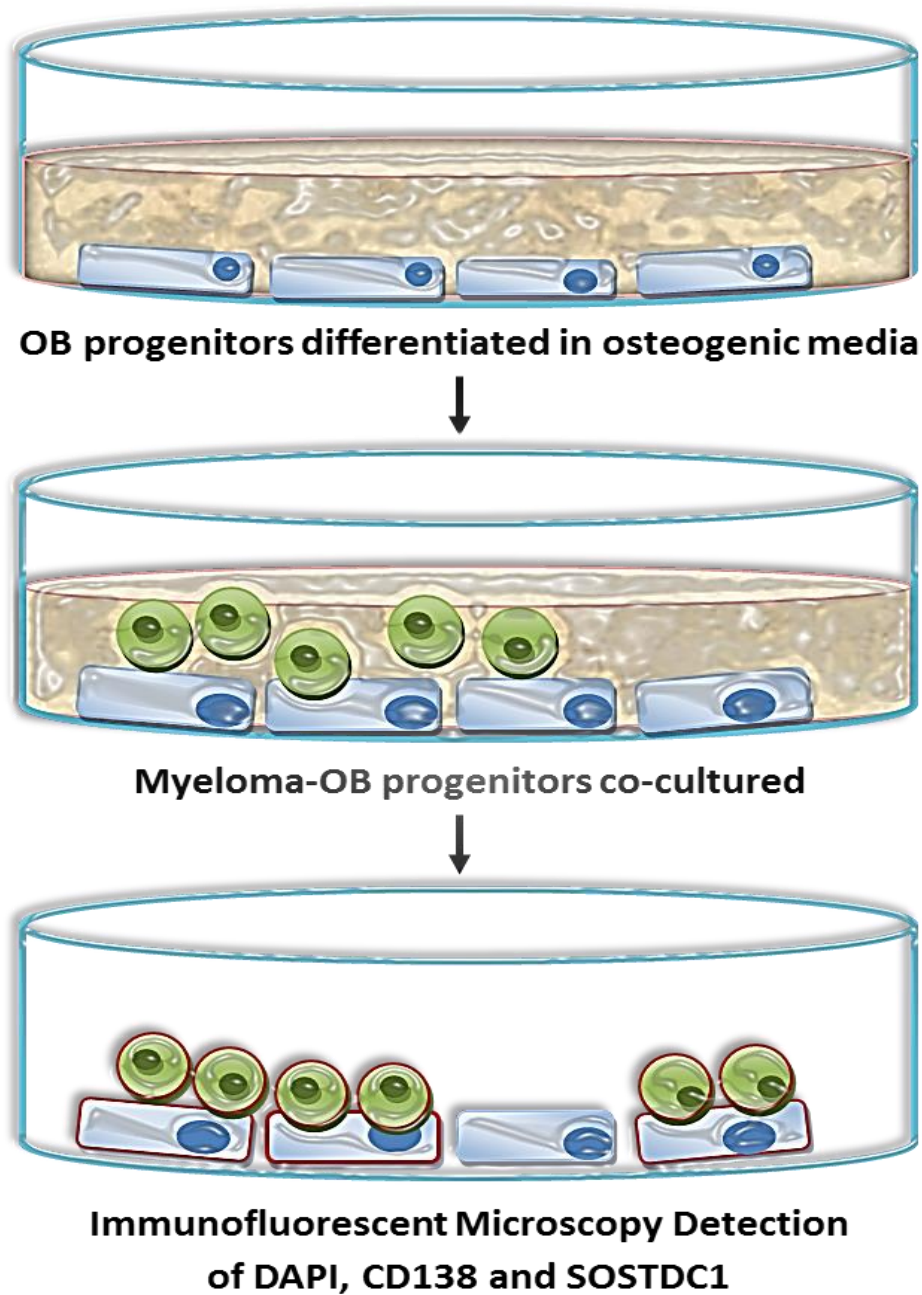
Figure 6.3.1 – Diagrammatic representation of 5T33MM/ 5TGM1MM and osteoblast co-culture: *OB progenitors were seeded at 5700 cells per well in 48 well plates and then differentiated in osteogenic media for 8 days. Differentiating OB progenitor cells were co-cultured with myeloma cells at a cell density of 11400 cell per well for 24 hours. Co-cultures were stained with anti-CD138 and anti-SOSTDC1 antibodies.*

6.3.2 Flow Cytometric analysis of SOSTDC1 production in myeloma-OB progenitor co-cultures

Flow cytometry was used as a quantitative method for SOSTDC1 detection in myeloma-OB progenitor co-cultures. Using HK-2 cells as a positive control, HK-2, OB progenitors, 5T33MM-GFP and 5TGM1MM-GFP were seeded in $25cm^2$ culture flasks at a density of 150,000 per flask (6000 cell/cm^2). Cells were allowed to adhere to the plate surface for 48 hours in 7ml of media. OB progenitors were differentiated in standard osteogenic media for up to 8 days. On day 8 of OB progenitor cell differentiation, 5T33MM-GFP or 5TGM1MM-GFP myeloma cells were counted and seeded onto the differentiating OB progenitors at a cell density of 300,000 cells per flask (12000 cell/cm^2). Myeloma cells were co-cultured with the OB progenitor cells for 24 hours in 14ml of RPMI. After 24 hours HK-2 cells, OB progenitor and myeloma-OB progenitor co-cultures were detached by trypsinisation as outlined in **section 2.1.3**. Media containing 300,000 5T33MM/5TGM1MM cells cultured on their own were transferred to 15ml Falcon™ tubes and myeloma cells centrifuged at 1000 RPM for 5 minutes.

1ml of ice cold PBS was added to the cell pellets and cell/PBS solution transferred to 1.5ml eppendorfs in preparation for flow cytometric analysis. The method for flow cytometry analysis was carried out according to the protocol outlined in **section 2.9**. Cells were stained with 1µg/ml (1:500 dilution) anti-SOSTDC1 antibody for 30 minutes and then stained with a secondary 2µg/ml (1:500 dilution) of Donkey anti-Rabbit IgG NL637 antibody for 30 minutes at room temperature in the dark. The percentage of SOSTDC1 positive (%SOSTDC1+) cells within separate OB progenitors, 5T33MM-GFP and 5TGM1MM-GFP cell population were determined first and following this the co-cultures samples containing both myeloma and OB progenitor populations were analysed. Gating was set so that separate GFP-positive and negative cell populations could be distinguished. The GFP-positive myeloma cells appeared at the top half of the scatter plot gate and GFP-negative OB progenitor at the bottom half of the scatter plot. A right shift in the population of either myeloma or OB progenitor cells indicated positive for SOSTDC1 staining.

6.3.3 Detecting SOSTDC1 levels in sorted myeloma and OB progenitor populations *in-vitro* by western blotting and end-point PCR

FACS Aria flow cytometry technology was used to sort myeloma and OB progenitor cells from myeloma-OB progenitor co-cultures to determine the level of SOSTDC1 in individual cell populations. OB progenitor cells were seeded into T175 culture flasks at cell density of 1,050,000 cells (6000 cells/cm2) containing 24ml of standard Alpha-MEM media. Following 48 hours in culture, the Alpha-MEM was removed from the OB progenitor cells and replaced with standard osteogenic media and OB progenitors were differentiated for 8 days. At the same time HK-2 cells, 5T33MM-GFP and 5TGM1MM-GFP were cultured separately in 175ml culture flasks at a cell density of 1,050,000 cells (6000 cell/cm^2).

On day 8 of OB progenitor differentiation, 5T33MM-GFP or 5TGM1MM-GFP myeloma cells were counted and co-cultured with the OB progenitors at a cell density of approximately 2,000,000 cells (12000 cell/cm^2). Myeloma cells were co-cultured with the differentiating OB progenitor cells for 24 hours in 50ml of RPMI. Following the 24 hour culture period, the OB progenitor cultures and co-cultures were detached from culture surfaces by trypsinisation as outlined in **section 2.1.3**. The 5T33MM/5TGM1MM cells cultured on their own were transferred to 50ml Falcon™ tubes and myeloma cells pelleted by centrifugation at 1000 RPM for 5 minutes. 1ml of PBS was added to the cell pellets and cell/PBS solution transferred to flow 1.5ml BD flow cytometry tubes.

Whole 5T33MM/5TGM1MM and OB progenitor co-cultures were sorted into separate OB and myeloma cell populations using the FACS Aria flow cytometer according to **section 2.10**. Myeloma-GFP and OB progenitor cells cultured alone were sorted first so that the correct gating could be applied for each individual population (**Figure 6.3.2**). Cells from OB-myeloma co-cultures were sorted into 1ml of RPMI for approximately 30 minutes. 1ml sorted cell populations were then split into two tubes containing 500µl each; from which protein or RNA was extracted according to section 2.6 and section 2.12, respectively (**Figure 6.3.3**).
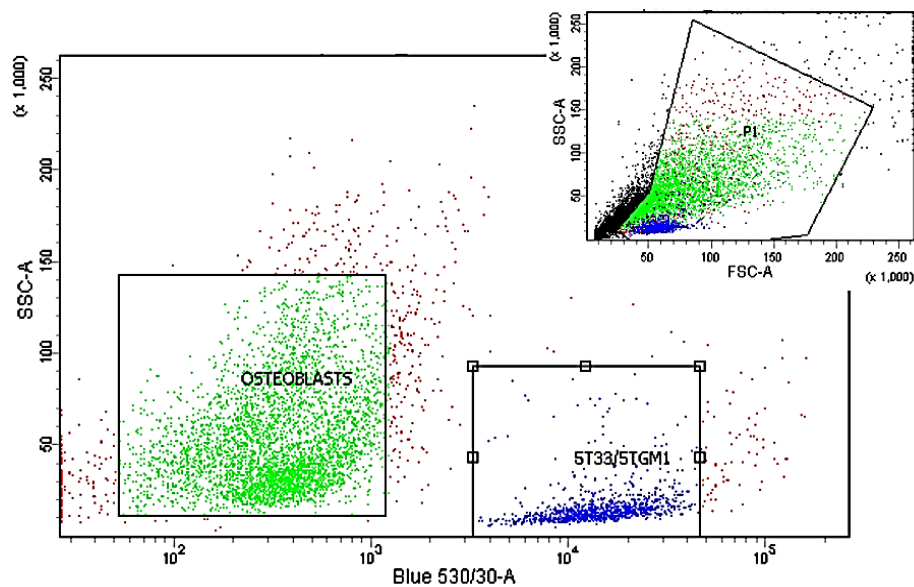
Figure 6.3.2 - Sort gating for OB progenitor-5TMM-GFP co-cultures using the FACS Aria flow cytometer: *Cells were sorted on the basis of fluorescence and scatter characteristics i.e. GFP fluorescence vs non-GF cells. Nonviable cells that fell outside of the gates were excluded from the counts. OB progenitor cultures and 5T33MM-GFP and 5TGM1MM-GFP were sorted separately and the appropriate gating applied. This gating was used as a sorting template for separating the OB progenitor and myeloma-GFP population.*

Western blotting was used to detect SOSTDC1 protein levels in 5T33MM-GFP and 5TGM1MM-GFP myeloma cells co-cultured with differentiating OB as outlined in **section 2.8**. Briefly, 12% polyacrylamide gels were loaded with 10μg of protein and 10μl of a 10-250kD protein molecular marker at the first lane. Proteins lysates were run through the stacking gel for 40 minutes at 60 Volts and then separated out for 1 hour at 100 Volts. Proteins were transferred onto PVDF membranes for 70 minutes at 70 Volts in 4°C. Membranes were washed once in 0.05% PBS-Tween and probed with 1μg/ml (1:500 dilution) primary anti-SOSTDC1 antibody overnight at 4°C. Blots were incubated for 1 hour at RT with 0.2μg/ml (1:10,000 dilution) of secondary HRP-conjugated anti-rabbit IgG antibody to detect SOSTDC1 protein. HK-2 cell lysates were used as a positive control for SOSTDC1 protein production. SOSTDC1 protein bands were visualised at ~47kD using the molecular marker as a reference point and the average density quantified using the GS-710 Calibrated Imaging Densitometer.

The same membranes were 'stripped' using Mild Stripping Buffer as described in **section 2.8.5**. The newly exposed proteins on the blots were re-probed with 0.07μg/ml (1:15,000 dilution) of anti-GAPDH mouse antibody overnight at 4°C. Blots were incubated with 0.1μg/ml (1:20,000 dilution) of secondary HRP-conjugated anti-mouse IgG antibody. GAPDH bands were visualised at ~35kD and the average density of SOSTDC1 protein was normalised to the average density of GAPDH to account for any loading variability.

End-point PCR was used to qualitatively determine *SOSTDC1* expression in OB progenitors, myeloma cells and sorted myeloma-OB progenitor co-culture cell populations. Following cDNA synthesis end-point PCR reaction was performed to detect *SOSTDC1* expression using the forward and reverse primers set for *SOSTDC1* sequences as described in **section 2.14.3.1.** PCR products were run on a 1.5% agarose gels stained with ethidium bromide and bands detected using the Gel Doc XR System and Quantity One Software as described in **section 2.14.3.2**. *SOSTDC1* expression was indicated by a product size of 198bp. PCR products were sequenced verify *SOSTDC1* expression by the DNA sequencing Core Facility housed within the University of Sheffield, Medical School as described in **section 2.14.3.3.**
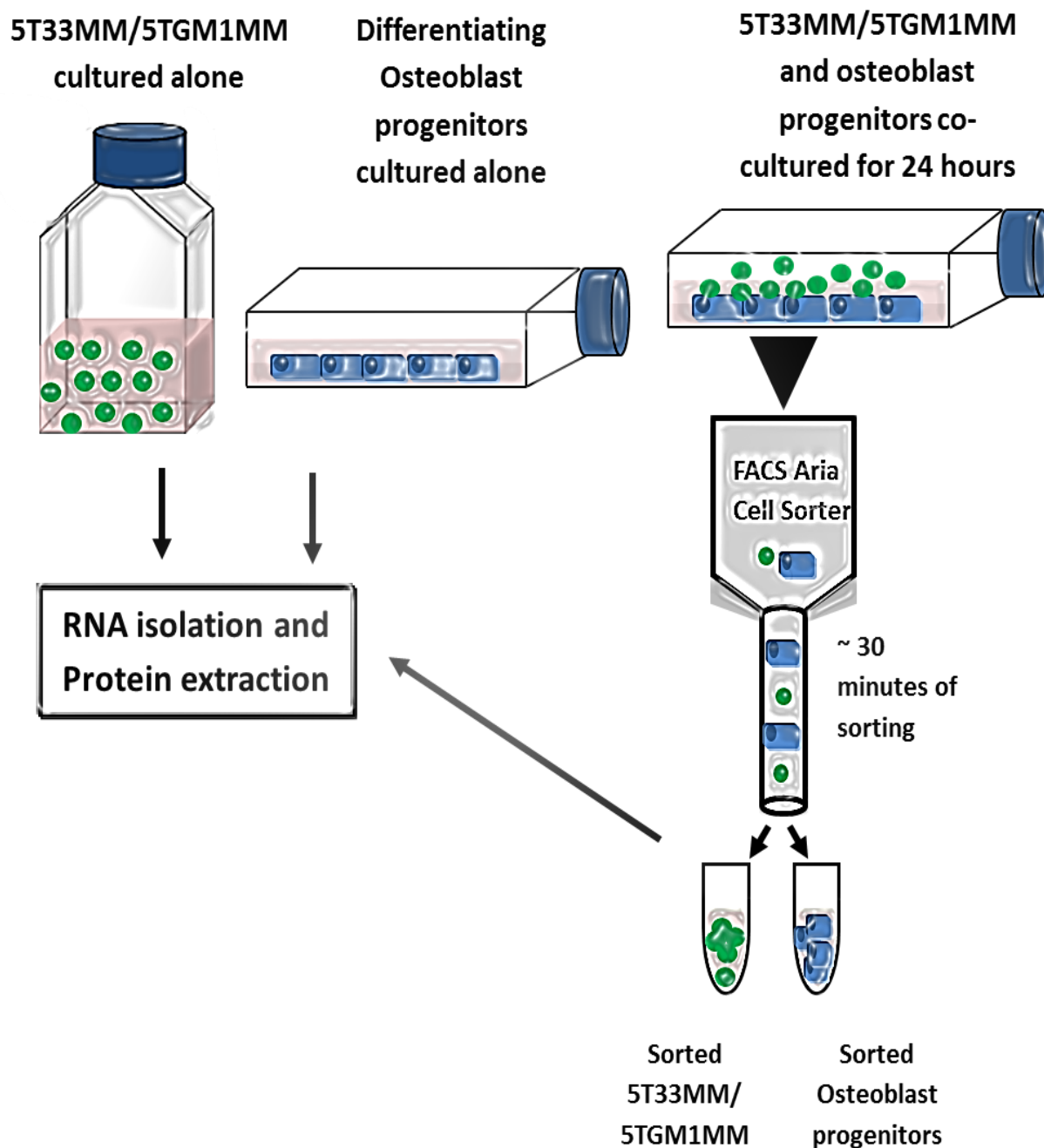
Figure 6.3.3 - Myeloma-OB progenitor co-cultures sorted into separate populations by FACS Aria and SOSTDC1 level detection using end-point PCR and western blotting: *5T33MM/5TGM1MM and differentiating OB progenitors were cultured in T175 culture flasks on their own for 8 days after which the RNA and protein was extracted. In separate flasks, differentiating day 7 OB progenitors were co-cultured with 5T33MM/5TGM1MM cells for 24 hours. Co-cultures were then sorted for approximately 30 minutes by FACS Aria into separate myeloma and OB progenitor populations. RNA and protein were extracted from sorted cells. SOSTDC1 levels were determined by western blot and end-point RT-PCR.*

6.3.4 Assessing the dependency of SOSTDC1 production on direct myeloma-OB progenitor interaction

To test the concept that SOSTDC1 is upregulated in myeloma cells as a result of direct interaction between OB progenitors and myeloma cells, co-culture experiments were set up as previously described in **section 6.2**. In these experiments, co-culture of 5T33MM-GFP or 5TGM1MM-GFP with differentiating OB progenitor cells for 24 hours resulted in some myeloma cells adhering to the OB progenitor cells. From these co-cultures, the media that contained the non-adhering myeloma population was removed and transferred to 50ml Falcon™ tubes and cells pelleted by centrifugation. 1ml of PBS was added to the cell non adherent myeloma cell pellets and cell/PBS solution was transferred to 1.5ml eppendorfs tubes. Flow cytometry was used to determine the percentage of SOSTDC1+ myeloma cells that had physically attached to the OB progenitors compared to the percentage of SOSTDC1+ myeloma cells that had not adhered to the OB progenitors but were present in co-culture.

In separate experiments, myeloma-OB progenitor co-cultures were set up and sorted by FACS Aria into separate populations as previously described in **section 6.3.3**. Again the media from the myeloma-OB progenitor co-culture that contained the non-adhering myeloma cells was transferred to 50ml Falcon™ tubes and cells pelleted by centrifugation. 1ml of PBS was added to the non-adherent myeloma cell pellets and cell/PBS solutions were transferred to 1.5ml eppendorfs tubes in preparation for the protein lysing, BCA and western blotting procedure outlined in **sections 2.6, -2.7 and -2.8**, respectively. Western blotting was used to compare SOSTDC1 protein levels in non-adherent 5T33MM-GFP/5TGM1MM-GFP myeloma cells taken from the media of myeloma-OB progenitor co-cultures and compared to adherent 5T33MM-GFP/5TGM1MM-GFP cells sorted from co-cultures. Briefly, 12% polyacrylamide gels were loaded with 10μg of protein and blots were probed with 5μg/ml (1:100 dilution) primary anti-SOSTDC1 antibody overnight at 4°C. Blots were incubated with 0.13μg/ml (1:15,000 dilution) of secondary HRP-conjugated anti-rabbit IgG antibody to detect SOSTDC1 protein. Membranes were stripped using mild stripping buffer as described in **section 2.8.5** and proteins re-probed with 0.1μg/ml (1:20,000 dilution) dilution of mouse anti-GAPDH overnight at 4°C. The average density of SOSTDC1 protein was normalised to the average density of GAPDH using the GS-710 Calibrated Imaging Densitometer.

6.3.5 Detection of SOSTDC1 in tibiae bearing myeloma tumour *in-vivo*

Leading groups have characterised the 5TMM series myeloma cell lines which include the 5T33MM and 5TGM1MM and have reported protocols for the production and maintenance of the 5T model in C57BL/KaLwRijHsd mice (Asosingh, Radl et al. 2000, Oyajobi, Munoz et al. 2007). Our Myeloma group in Sheffield has used these protocols to reproduce the 5T33MM-GFP and 5TGM1MM-GFP myeloma model in our laboratory. In brief, bone marrow isolated from the long bones of 5TMM bearing mice were injected into the lateral tail of young naïve syngeneic mice. The growth of myeloma tumour was monitored by ELISA quantification of serum paraprotein. The long bones were then dissected from the terminally diseased mice and the bone marrow contents flushed out of the bones. Isolated bone marrow contents were purified by Lymphocyte M gradient centrifugation and the mononuclear layer of cells retained. 1,000,000 mononuclear cells were re-injected back into other naïve syngeneic mice. At the same time naïve mice were injected with PBS and used as tumour-negative controls. 5T33 and 5TGM1MM mice developed myeloma within 6-12 weeks of inoculation. The 5TGM1MM animals developed osteolytic bone disease associated with myeloma tumour burden and the 5T33 animals did not. Naïve animals were sacrificed at the same time as terminally ill 5T33MM and 5TGM1MM animals.

Tibiae from all animals were dissected and fixed in 4% paraformaldehyde ready for tissue processing and sectioning. Immunohistochemical analysis of mouse tibiae sections infiltrated with 5T33MM and 5TGM1MM myeloma *in-vivo* were used to detect SOSTDC1 staining in tumour bearing mice compared to naïve animals. Details of immunohistochemical staining are outlined in **section 2.12.** 5T33MM and 5TGM1MM tibiae sections were de-waxed and antigen removal was performed using 1/4 dilution of trypsin reagent. Non-specific binding was blocked using 10% normal goats serum and sections were stained with the manufactured 1μg/ml (1:500 dilution) primary anti-SOSTDC1 rabbit antibody or rabbit IgG isotype control overnight at 4ºC. Sections were further stained with a 2.5μg/ml (1:400 dilution) dilution of goat anti-rabbit biotinylated secondary antibody. SOSTDC1 staining was developed using DAB and counter-stained with Gills haematoxylin.

6.3.6 Comparing SOSTDC1 expression in lytic 5TGM1MM versus non-lytic 5T33MM myeloma cells *in-vitro*

As mentioned previously, mice injected with 5TGM1MM cells developed lytic bone disease similar to that observed in MM patients. However, 5T33MM mice did not develop bone disease associated with tumour burden. To test the hypothesis that SOSTDC1 expression was upregulated in lytic 5TGM1MM myeloma cells compared to non-lytic 5T33MM cells, the data obtained from the SOSTDC1 western blot and cDNA samples obtained from the experiment outlined in **section 6.3.3** and **6.3.4** were re-analysed.

6.3.7 Blocking SOSTDC1 production in myeloma-OB progenitor co-cultures

In previous chapters I had shown that recombinant SOSTDC1 suppressed *Runx2* and *CTNNB1* expression via Wnt and BMP signalling in differentiation OB progenitor cells. To relate this mechanism to MM bone disease, I investigated the effect of the SOSTDC1 produced by lytic 5TGM1 cells on *Runx2* and *CTNNB1* gene expression. If the 5TGM1MM cells were indeed producing SOSTDC1 and this SOSTDC1 was suppressing markers of OB differentiation, then blocking the effect of SOSTDC1 would reverse this suppressive effect.

Quantitative RT-PCR was used to determine whether blocking SOSTDC1 in 5TGM1MM-OB progenitor co-cultures had an effect on *Runx2* and *CTNNB1* gene expression. OB progenitor cells were harvested from a near confluent flask by trypsinisation and cell pellets were counted using a haemocytometer as described in **section 2.1.3**. OB progenitor cells were resuspended in MEM-Alpha medium at 57,000 cells per well in 6 well culture plates containing 1.5ml of media within each well. Following 72 hours in culture, the media was removed from the adhered OB progenitor culture and cells were washed with PBS. Cells were differentiated in 1500μl/well of standard osteogenic media for up to 8 days. On day 8 of differentiation, 5TGM1MM myeloma cells were counted and co-cultured on the differentiating OB progenitors at a cell density of approximately 100,000 cells per well. Myeloma cells were co-cultured with the OB progenitors for 24 hours in 1ml of RPMI. In the same experiments, OB progenitors cultured alone, 5TGM1MM cultured alone and 5TGM1MM-OB progenitor

co-cultures were also incubated with 1.5µg/ml anti-SOSTDC1 polyclonal antibody from Abcam for the 24 hour duration.

RNA was isolated from the OB progenitor cultures using the RNA mini Prep kit and quantified with a Nanodrop as described in **section 2.13**. The expression of *Runx2, CNTTB1* and housekeeper *B2M* gene were quantified using TaqMan® Assays for qRT-PCR analysis. Relative quantification of gene expression were performed by normalising to the house keeping *B2M* gene using the formula $\Delta\text{CT} = \text{CT}_{\text{target}} - \text{CT}_{\text{housekeeping}}$ as described in **section 2.13.3**.

6.4 Results

6.4.1 The level of immunofluorescent SOSTDC1 staining in myeloma and OB progenitor co-cultures increased in both cell types

Using HK-2 cells as a SOSTDC1-producing positive control, immunofluorescent microscopy was used to determine the presence of SOSTDC1 protein in OB progenitor cells, 5T33MM and 5TGM1MM cells cultured on their own. Images obtained from immunofluorescent microscopy of permeabilised HK-2 stained with anti-SOSTDC1 antibody showed that HK-2 cells were positive for SOSTDC1 throughout the culture period (**Figure 6.4.1.1 A**). The red staining representing SOSTDC1 protein was apparent in both the nucleus and membrane of cells. HK-2 cells stained with isotype control antibody were negative for SOSTDC1 staining (**Figure 6.4.1.1 B**).

In the same experiments, immunofluorescent microscopy of permeabilised OB progenitors stained with either anti-SOSTDC1 antibody or isotype control showed that OB progenitor cells were negative for SOSTDC1, indicated by the lack of red staining (**Figure 6.4.1.2 A and B**). Permeabilised 5T33MM and 5TGM1MM cells stained with anti-SOSTDC1 antibody showed variable SOSTDC1 staining (**Figure 6.4.1.3** and **6.4.1.4**) in that in some experiments, some of the cells were positive for SOSTDC1 and in others no staining was visible. In summary, immunofluorescent microscopy data indicated that 5T33MM and 5TGM1MM cells produced low levels of SOSTDC1.

Co-culture of 5T33MM or 5TGM1MM myeloma cells with OB progenitor cells for the duration of 24 hours resulted in some myeloma cells adhering to the OB progenitors, whilst other myeloma cells that were not bound were washed off during the immunocytochemistry procedure. In contrast to the variable staining associated with the 5T33MM and 5TGM1MM cells cultured on their own, the immunofluorescent images taken from the co-culture cells showed clear and strong SOSTDC1 staining compared to the isotype controls (**Figure 6.4.1.5** and **Figure 6.4.1.6**). The SOSTDC1 staining appeared to be both intracellular and membrane bound. Furthermore, the red staining representing the SOSTDC1 protein was highly distinct and intense where there was direct contact between a myeloma cell and a OB within both 5T33MM and 5TGM1MM experiments. Both the OB progenitors and myeloma cells appeared to be positive for SOSTDC1 red fluorescence when in contact.
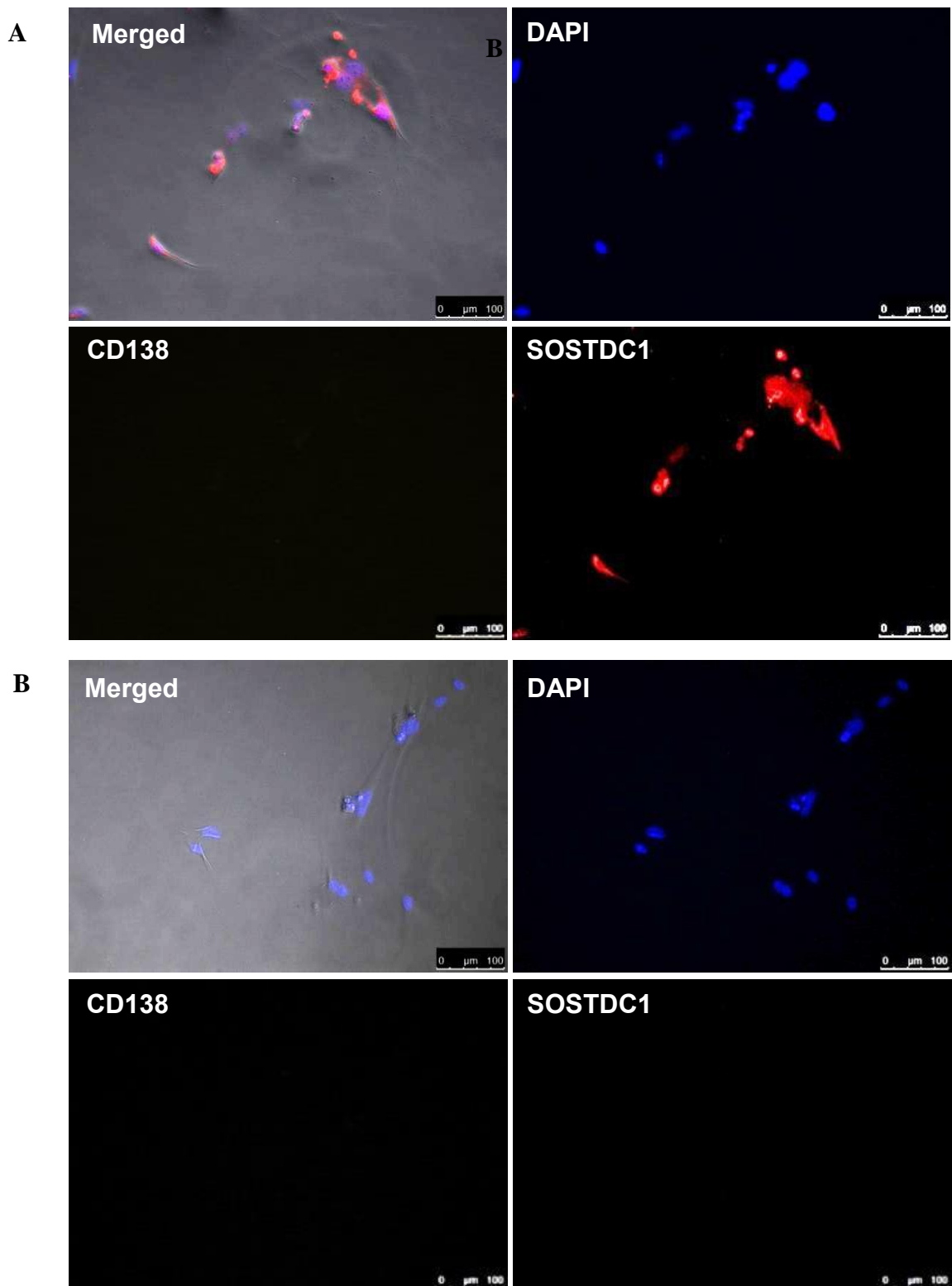
Figure 6.4.1.1 - SOSTDC1 was detected in HK-2 cells by immunofluorescent microscopy: *(A) The red colour in the images indicated SOSTDC1 could be detected throughout permeabilised HK-2 cells using 1ug/ml of anti-SOSTDC1 antibody. (B) No staining was detected in HK-2 cells incubated with 1ug/ml isotype control antibody. Images of phase contrast, DAPI, CD138 and SOSTDC1 staining were visualised simultaneously. Images are representative of at least two replicates across three independent experiments (N=3).*
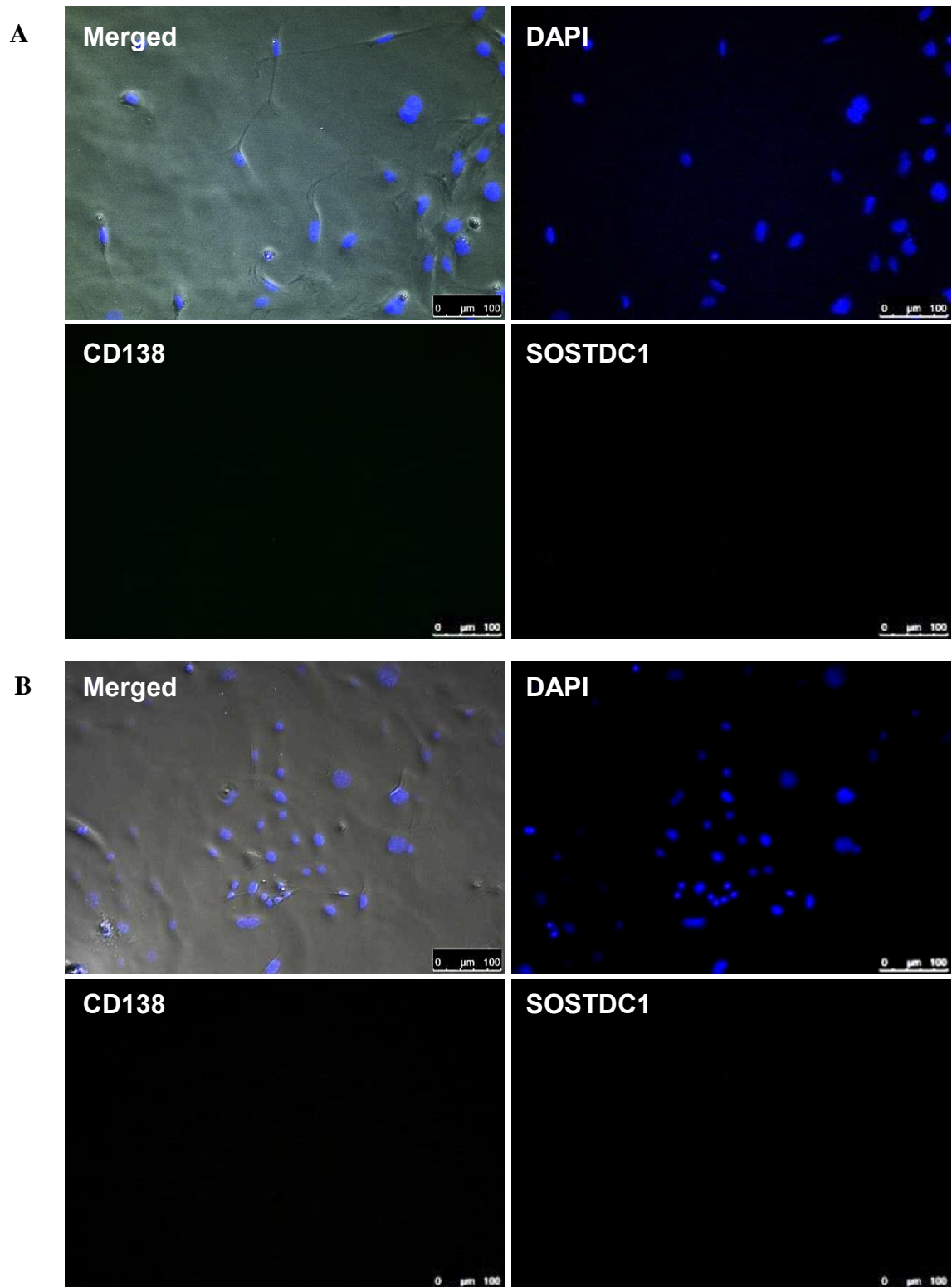
Figure 6.4.1.2 - SOSTDC1 could not be detected in OB progenitors cultured on their own using immunofluorescent microscopy: *(A) Red staining for SOSTDC1 could not be detected in permeabilised OB progenitors stained with anti-SOSTDC1. (B) No staining was detected in OB progenitor cells incubated with isotype control antibody. Images of phase contrast, DAPI, CD138 and SOSTDC1 staining were visualised simultaneously. Images are representative of at least at least two replicates across three independent experiments (N=3)*
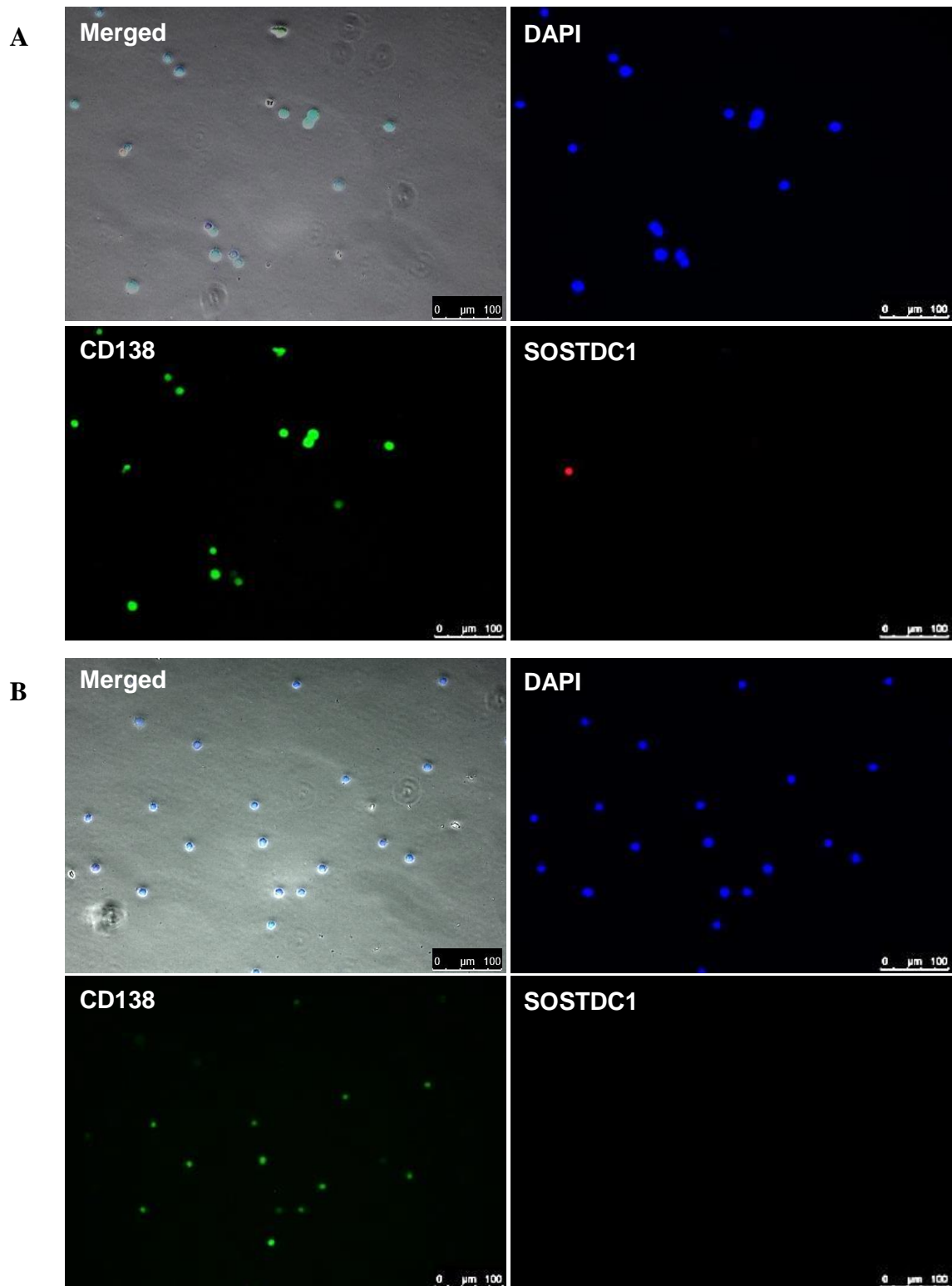
Figure 6.4.1.3 - SOSTDC1 could be detected in low levels in 5T33MM cells cultured on their own using immunofluorescent microscopy: *(A) 5T33MM cells were CD138+ and red staining representing SOSTDC1 was detected in some permeabilised 5T33MM cells. (B) No SOSTDC1 staining was detected in 5T33MM cells incubated with isotype control antibody. Images of phase contrast, DAPI, CD138 and SOSTDC1 staining were visualised simultaneously. Images are representative of at least two replicates within three independent experiments (N=3).*
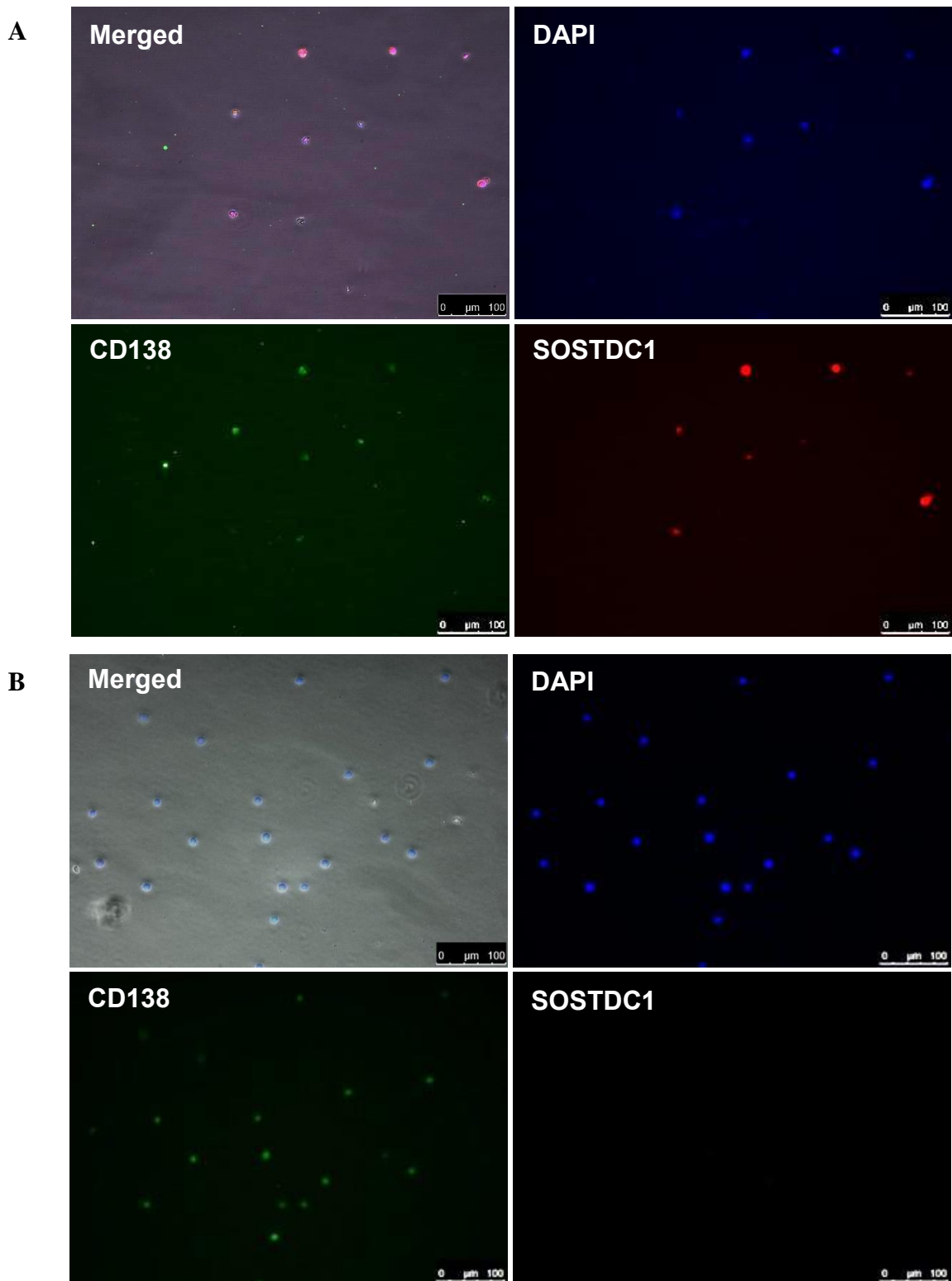
Figure 6.4.1.4 – SOSTDC1 could be detected in 5TGM1MM cells cultured on their own using immunofluorescent microscopy:.*(A) 5TGM1MM cells were CD138+ and red staining representing SOSTDC1 was detected in permeabilised 5TGM1MM cells. (B) No SOSTDC1 staining was detected in 5TGM1MM cells incubated with isotype control antibody. Images of phase contrast, DAPI, CD138 and SOSTDC1 staining were visualised simultaneously. Images are representative of at least two replicates within three independent experiments (N=3).*
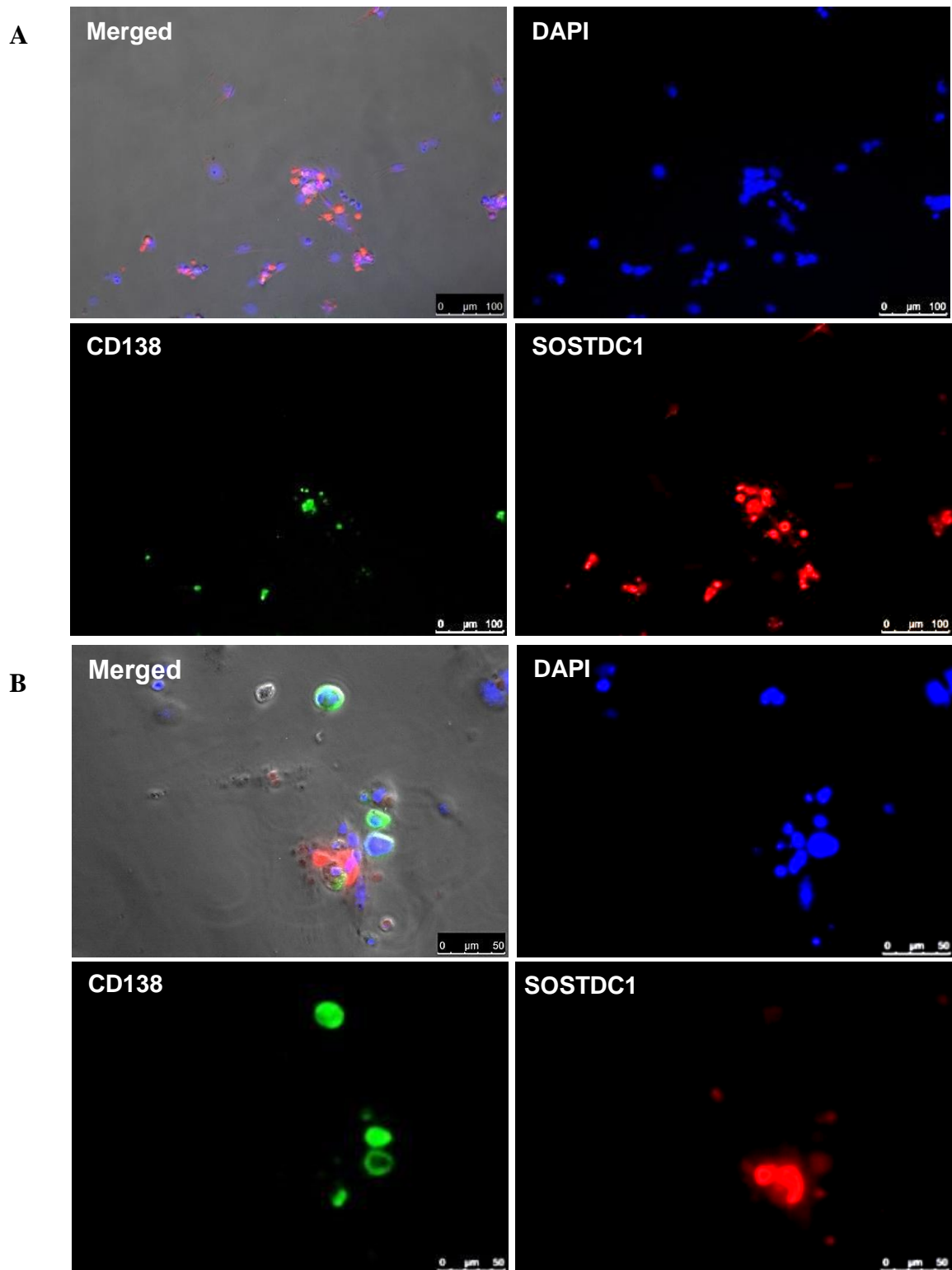
Figure 6.4.1.5 – The levels of SOSTDC1 immunofluorescent staining in 5T33MM and OB co-cultures increased in both cell types: *(A) SOSTDC1 staining was detected in permeabilised 5T33MM and OB progenitor co-cultures (B) The SOSTDC1 staining detected in 5T33MM-OB progenitor co-cultures appeared intense where there was direct contact between 5T33MM and the OB progenitor. Images of phase contrast, DAPI, CD138 and SOSTDC1 staining were visualised simultaneously. Images are representative of at least two replicates within three independent experiments (N=3).*
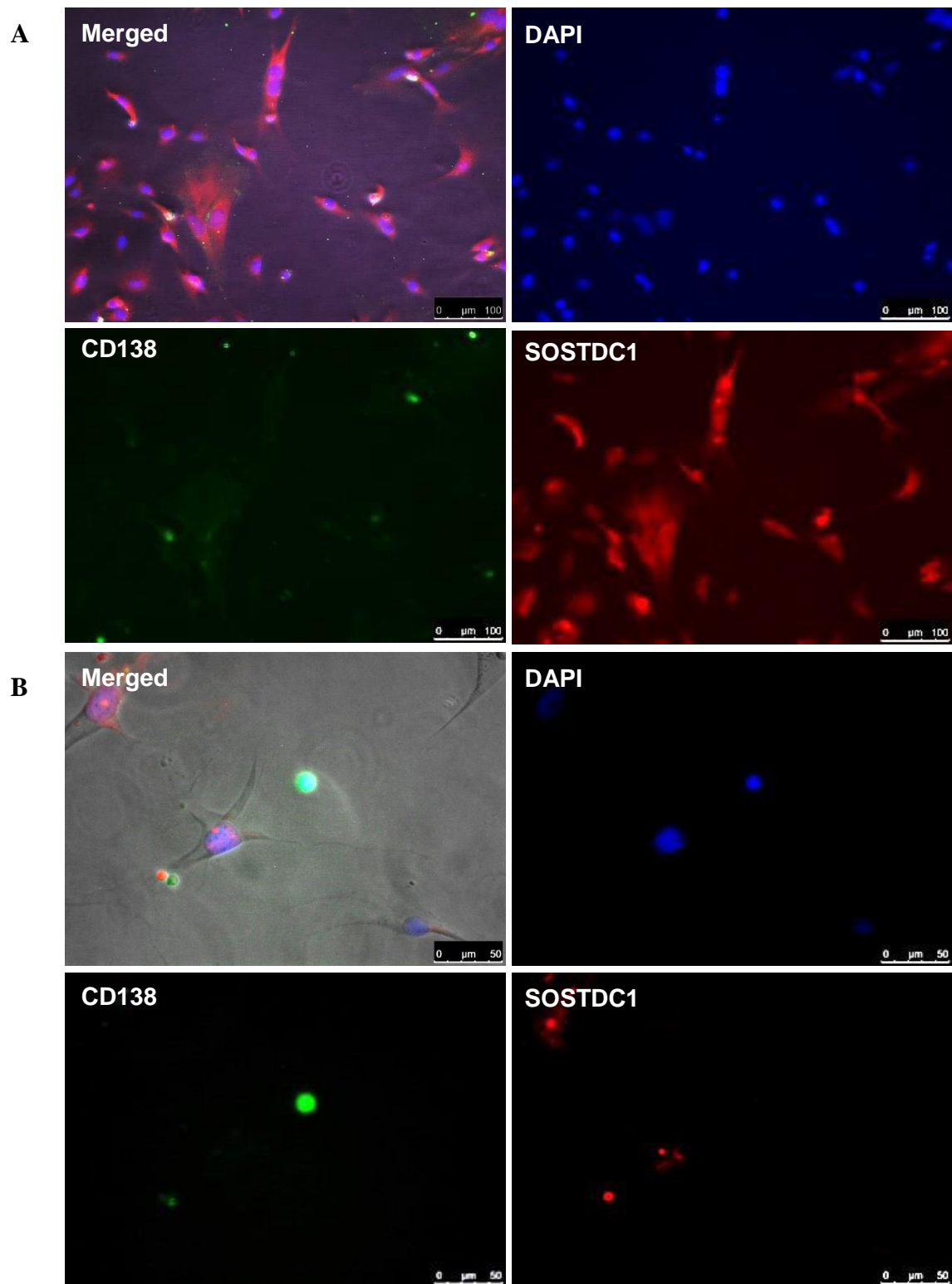
Figure 6.4.1.6 - The levels of SOSTDC1 immunofluorescent staining in 5TGM1MM and OB progenitor co-cultures increased in both cell types: *(A) SOSTDC1 staining was detected in permeabilised 5TGM1MM and OB progenitor co-cultures. (B) The SOSTDC1 staining detected in 5TGM1MM-OB progenitor co-cultures appeared to be more intense within both OB progenitor and 5TGM1MM cells that were in direct contact compared to cells that were not in contact. Images are representative of at least two replicates within three independent experiments (N=3).*

6.4.2 The population of SOSTDC1-positive cells detected by Flow cytomtery increased in co-cultured myeloma and OB cell populations compared to either population cultured alone

Data obtained from immunofluorescent microscopy showed that SOSTDC1 was not produced by OB progenitors but was produced at low levels in 5T33MM and 5TGM1MM myeloma cells when cultured on their own. There was evidence that co-culture of OB progenitors and myeloma cells stimulated SOSTDC1 production. The immunocytochemistry results were qualitative and therefore flow cytometric analysis was used to quantify SOSTDC1 production in individual OB progenitors and myeloma cells cultured on their own compared to cells co-cultured together.

Scatter plots obtained from flow cytometric analysis of permeabilised HK-2 stained with anti-SOSTDC1 antibody showed that on average approximately 40% of HK-2 cells were positive for SOSTDC1. Less than 1% of the HK-2 cell population were positive for SOSTDC1 when stained with isotype control antibody (**Figure 6.4.2.1 C**). A population of the permeabilised 5T33MM-GFP and 5TGM1MM-GFP cells that were cultured on their own and stained with anti-SOSTDC1 antibody were SOSTDC1+ (**Figure 6.4.2.1**). This data confirms that myeloma cells do produce SOSTDC1 and this production can be seen using a more sensitive assay such as flow cytometry. Data also showed that in the population of OB progenitor cultured alone and stained with either anti-SOSTDC1 antibody or isotype control, there was no significant right shift (<1%) on the scatter plots suggesting no specific staining. This flow cytometry data was confirmatory of the immunofluorescent microscopy data, suggesting that OB progenitor cells cultured on their own do not produce SOSTDC1 (**Figure 6.4.2.2**).

Flow cytometry scatter plots obtained from myeloma-OB progenitor co-cultures showed that some cells within the 5T33MM/5TGM1MM myeloma population as well as within the OB progenitor population were SOSTDC1+ compared to their respective isotype controls (**Figure 6.4.2.3 and Figure 6.4.2.4**). Findings showed that 5T33MM-OB progenitor co-culture resulted in the 'switch on' of SOTSDC1 in the OB progenitor population. However, the percentage of SOSTDC1+ 5T33MM cells from the co-culture did not increase compared to percentage of SOSTDC1+ 5T33MM cells cultured on their own (**Figure 6.4.2.2**). Flow cytometry data from the 5TGM1MM co-culture experiments also showed that that 5TGM1MM-OB progenitor co-culture resulted in the 'switch' on of

SOTSDC1 in the OB progenitor population (**Figure 6.4.2.3 A, B**). Interestingly, the proportion of SOSTDC1+ 5TGM1MM cells from the co-culture increased in comparison to the proportion SOSTDC1+ 5TGM1MM cells cultured on their own. This data provides evidence for the rational that if SOSTDC1 has a key role in OB progenitor suppression, then its upregulation by myeloma cells is dependent on contact between tumour and the bone microenvironment. This data suggested that interaction between myeloma-OB progenitors stimulated the OB progenitor cells to produce SOSTDC1, illustrated by the right shift in the OB progenitor population in the scatter plots.

A

5T33MM-GFP SOSTDC1+ Population

B

5TGM1MM-GFP SOSTDC1+ Population

C
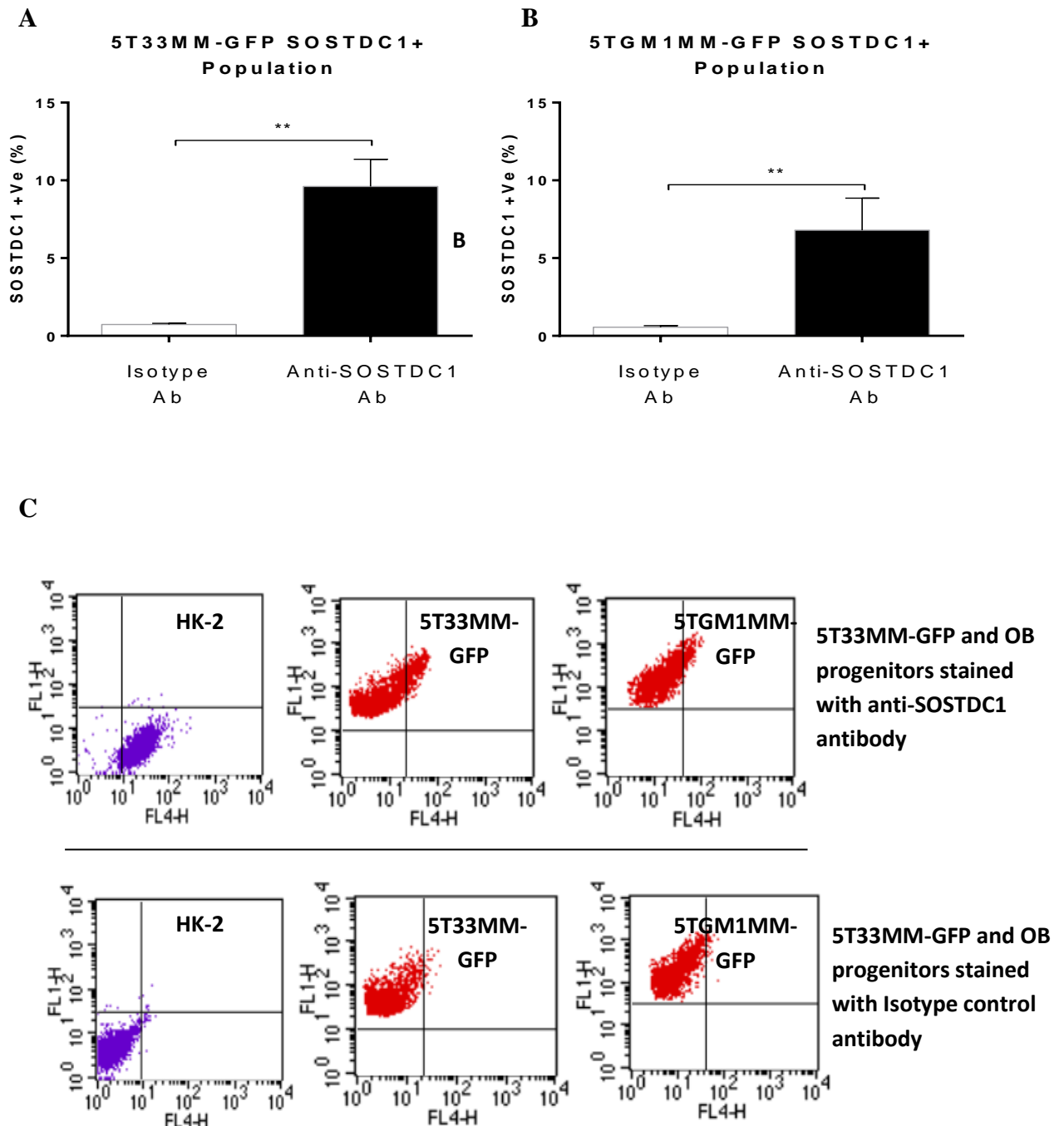
Figure 6.4.2.1 – SOSTDC1 was detected in 5T33MM and 5TGM1MM myeloma cells by Flow cytometry: *HK-2 cells were used as a positive control. The percentage of SOSTDC1 positive cells was determined by setting gating threshold at <1% for the isotype control. (A) A population of 5T33MM-GFP cells were positive for SOSTDC1 protein in comparison to the isotype control (B) A comparably sized population of 5TGM1MM-GFP cells were also positive for SOSTDC1 protein in comparison to the isotype control. (C) SOSTDC1+ cells are represented by a right shift in Hk-2 and myeloma cell populations. N=8, Man-Whitney, ***P<0.001, ****P<0.0001)*
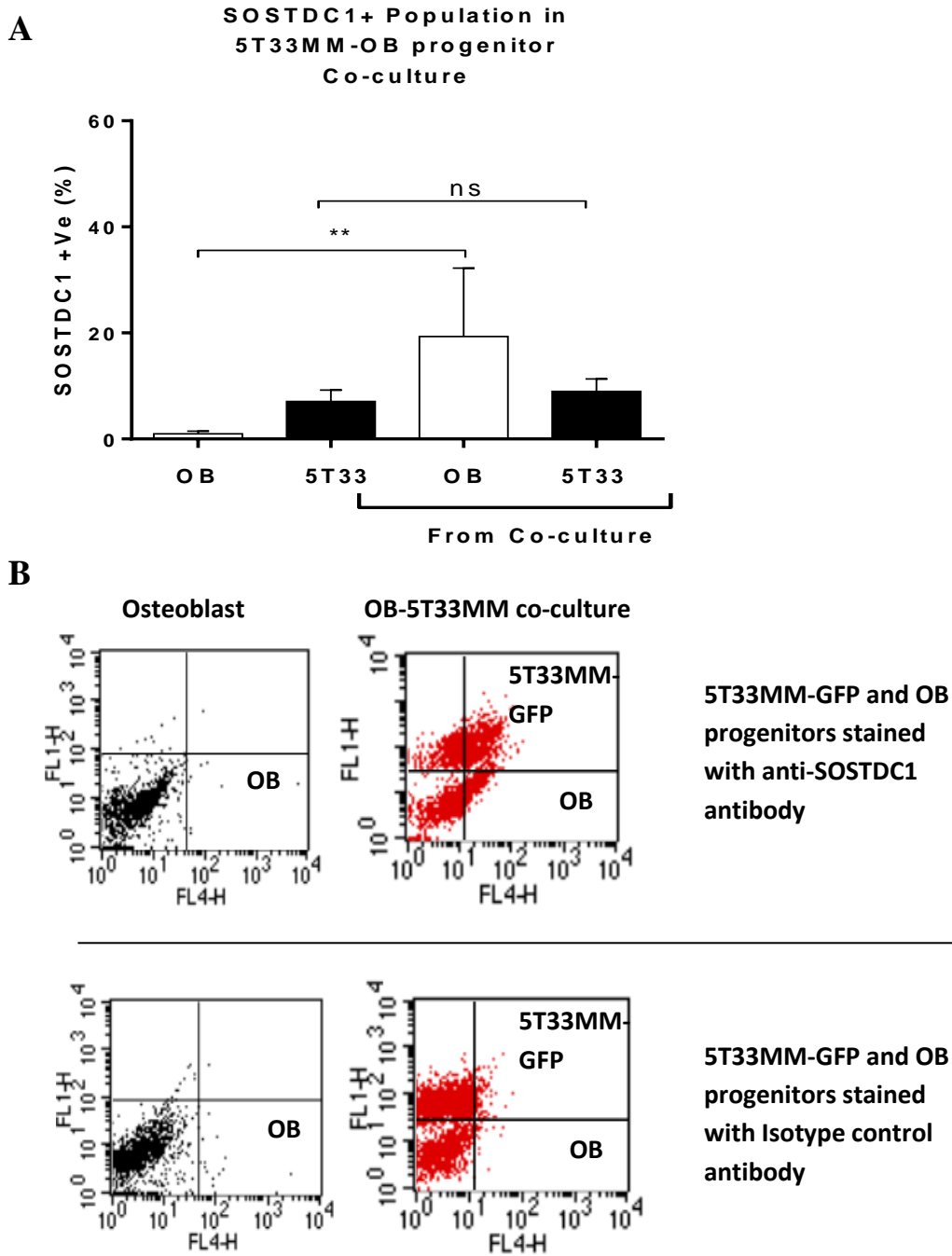
Figure 6.4.2.2 - SOSTDC1 was upregulated in OB progenitor cells that were co-cultured with 5T33MM cells as detected by flow cytometry: *(A) OB progenitors cultured on their own were not SOSTDC1+ (<1%). OB progenitors co-cultured with 5T33MM-GFP cells were positive for SOSTDC1 protein. Some 5T33MM-GFP cells cultured alone produced SOSTDC1. (B) SOSTDC1+ cells are represented by a right shift in OB progenitors and 5T33MM -GFP populations in the scatter plots. N=4 independent experiments, Man-Whitney, **P<0.01.*

A

SOSTDC1+ Population in 5TGM1MM-OB progenitor Co-culture

B

Osteoblast   OB-5TGM1MM co-culture

5GM1MM-GFP and OB progenitors stained with anti-SOSTDC1 antibody

5GM1MM-GFP and OB progenitors stained with Isotype control antibody
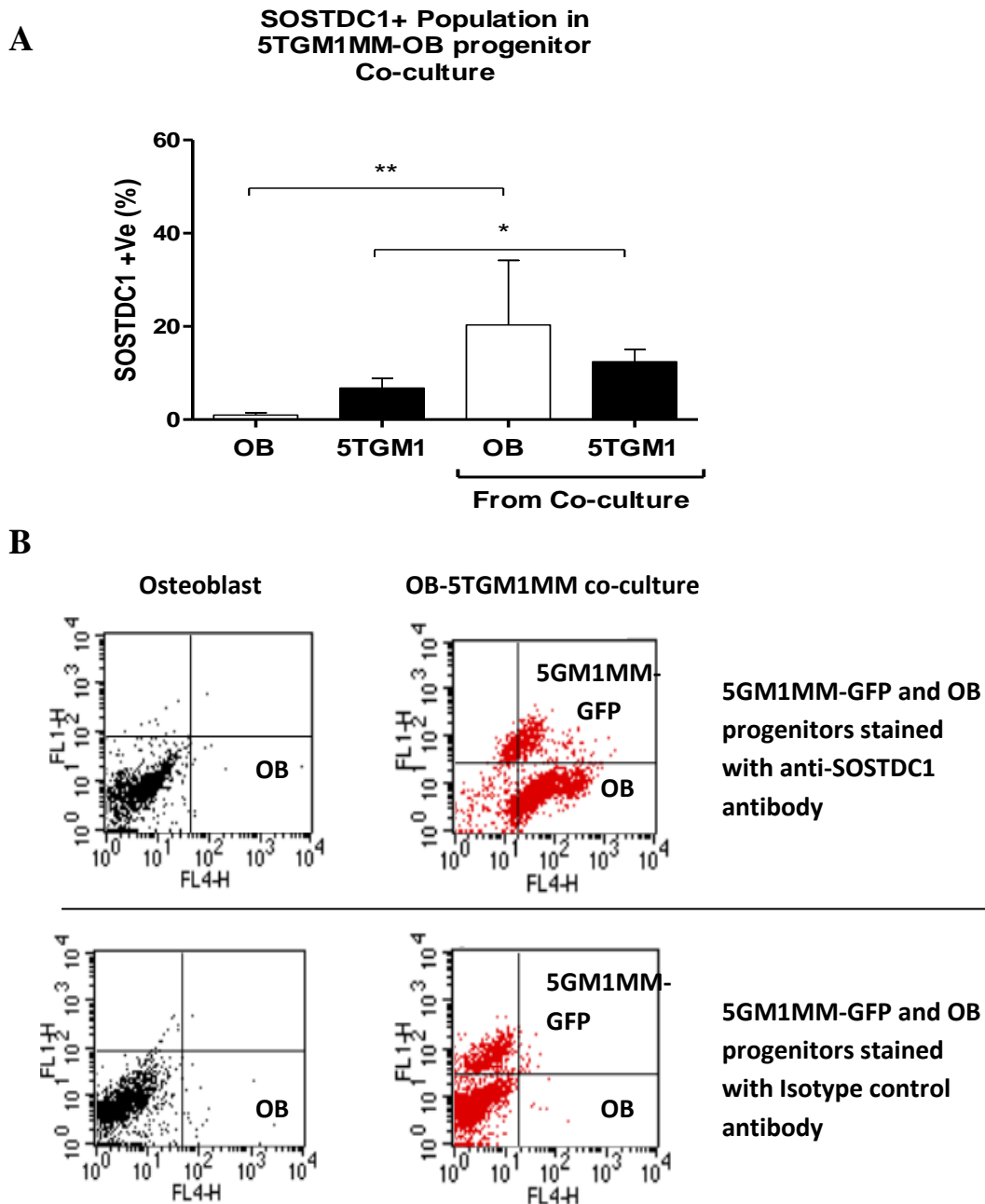
Figure 6.4.2.3 - SOSTDC1 was upregulated in both OB progenitor and 5TGM1 populations co-cultured together as detected by flow cytometry: *(A) OB progenitors cultured on their own were not SOSTDC1 positive (<1%). SOSTDC1 was switched on in OB progenitors that were co-cultured with 5TGM1-GFP cells. Some 5TGM1MM-GFP cells cultured alone were positive for SOSTDC1. Compared to 5TGM1MM-GFP cells cultured alone, a larger proportion of 5TGM1MM-GFP cells that were co-cultured with OB progenitors produced SOSTDC1. (B) SOSTDC1+ cells are represented by a right shift in OB progenitor and 5TGM1MM populations on the scatter plots. N=3 independent experiments, Man-Whitney, *P=<0.05, **P<0.001.*

6.4.3 SOSTDC1 protein and RNA levels increased in myeloma/OB progenitor cells sorted from co-cultures

To confirm that SOSTDC1 levels were upregulated in both individual myeloma and OB progenitor cell populations from co-cultures, whole co-cultures were sorted into separate OB and myeloma cell populations using FACS Aria technology. Western blotting was used to detect SOSTDC1 protein levels in sorted 5T33MM-GFP and 5TGM1MM-GFP myeloma cells co-cultured with differentiating OB progenitors. Similar to results obtained from flow cytometric analysis, western blot analysis confirmed SOSTDC1 detection in the OB progenitor population sorted from both 5T33MM-OB progenitor and 5TGM1MM-OB progenitor co-cultures in comparison to an absence of SOSTDC1 in OB progenitors cultured alone. Furthermore, there was no difference between the SOSTDC1 levels in 5T33MM cells co-cultured with OB progenitors compared to 5T33MM cultured on their own (**Figure 6.4.3.1 A**). However, there was an increase in SOSTDC1 protein in the 5TGM1MM cells sorted from the co-cultures compared to 5TGM1MM cultured on their own (**Figure 6.4.3.1 B**).

End-point RT-PCR was performed to assess the expression of SOSTDC1 as an RNA gene transcript. End-point PCR confirmed *SOSTDC1* expression in the OB progenitor population sorted from both 5T33MM-OB progenitors and 5TGM1MM-OB progenitors co-cultures (band was visible) in comparison no *SOSTDC1* expression in OB progenitors cultured alone (no band detected). In addition, the PCR product band representative of *SOSTDC1* expression in myeloma cells sorted from myeloma-OB progenitor co-cultures appeared stronger suggesting a higher level of *SOSTDC1* expression compared to myeloma cells cultured on their own (**Figure 6.4.3.2 A, B**). Sequencing of the end-point RT-PCR products were used to verify that the myeloma and co-cultured cells did express SOSTDC1. The sequence of bases obtained from the sequencing analysis of OB progenitors cultured alone showed that these cells did not have a similar homology to any form of SOSTDC-specific nucleotide collection using the BLAST software (**Appendix 4**). However, data did show that the 5T33MM, 5TGM1MM, OB and 5T33MM/5TGM1sorted from myeloma-OB progenitor co-cultures did have between 98-100% homology to the Mus musculus Sostdc1, mRNA (NM_025312.3) sequence (**Figure 6.4.3.3**).

A

5T33-OB Co-Culture

B

5TGMM-OB Co-Culture
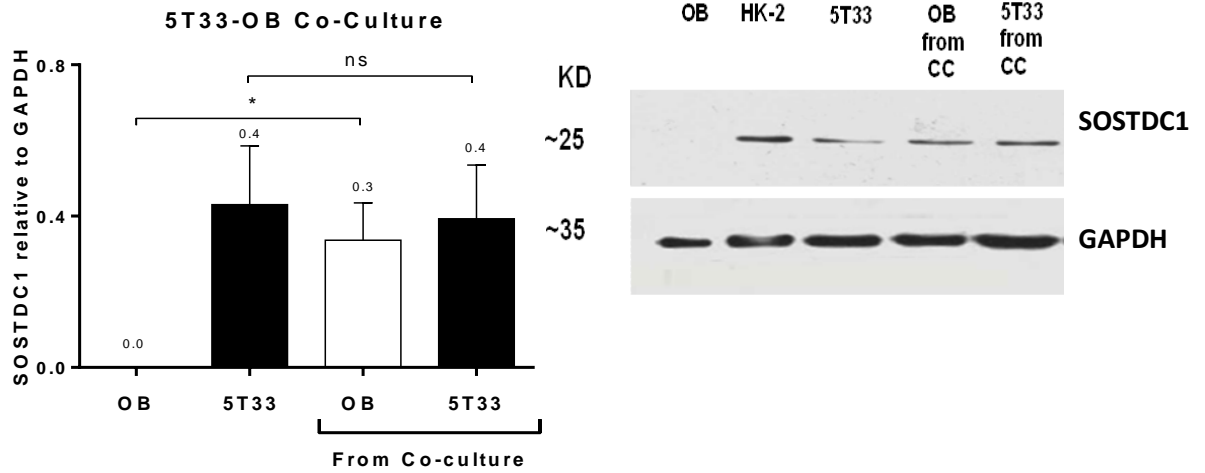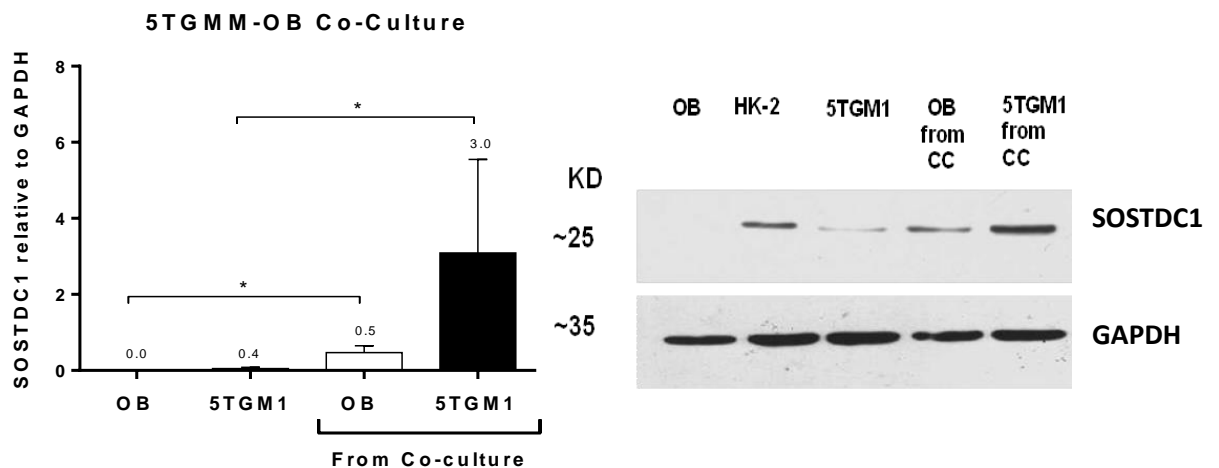
Figure 6.4.3.1 – SOSTDC1 protein levels detected by western blotting were upregulated in osteoblast and myeloma cell populations sorted from osteoblast-myeloma co-cultures: *Protein was extracted from sorted samples and non-adherent 5T33MM cells obtained from co-culture media. HK-2 cell lysates were used as a positive control for SOSTDC1 protein production. The western blot image is representative of three independent experimental repeats. (A and B) SOSTDC1 was detected in the OB population sorted from OB-5T33MM and OB-5TGM1MM co-culture in comparison to an absence of SOSTDC1 in OB cultured alone (*P<0.05). (B) SOSTDC1 protein levels obtained from adherent 5TGM1MM cells increased compared with no-adherent 5TGM1MM. N=3 independent experiments, Man-Whitney, *P<0.05.*

A

B
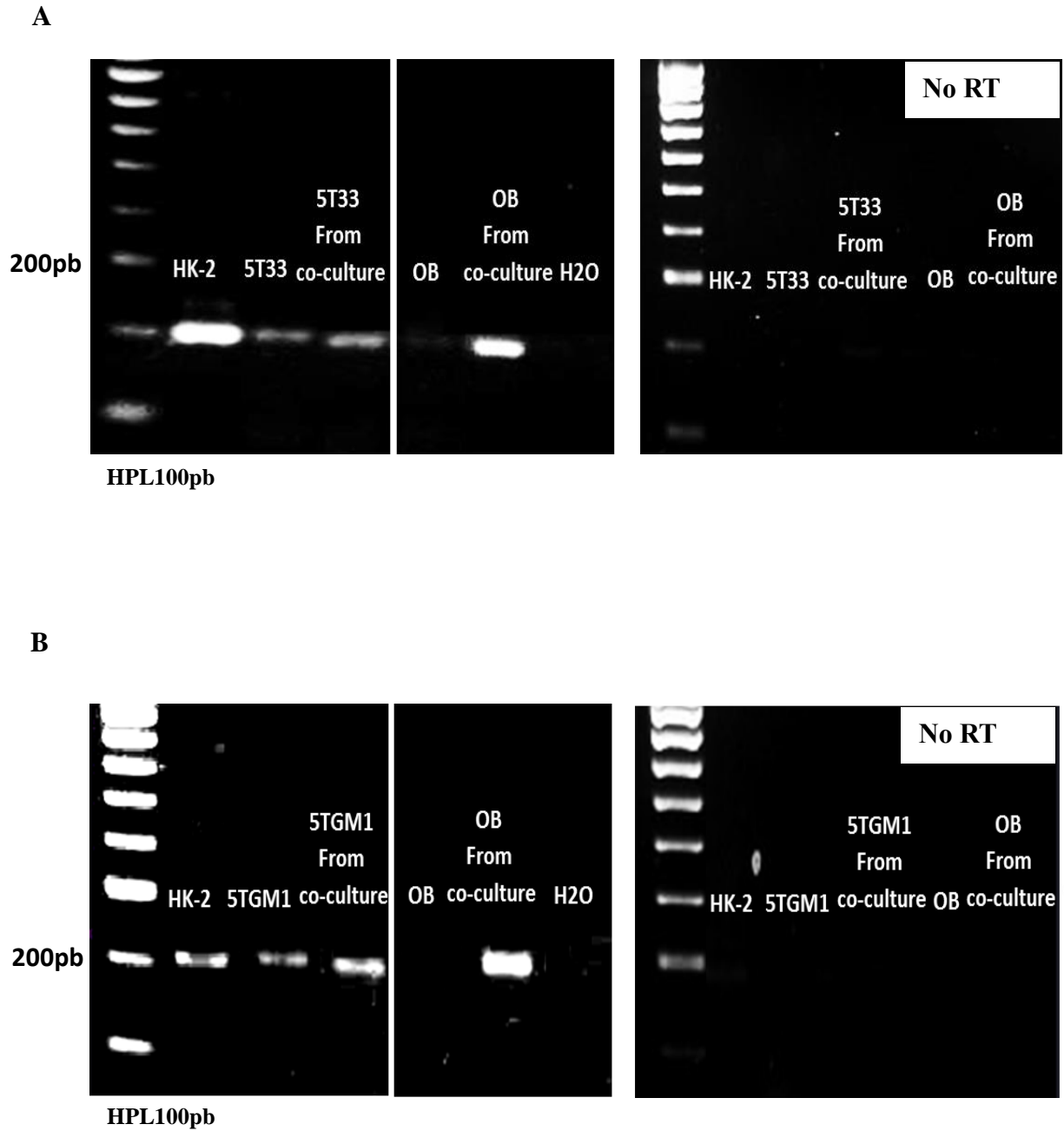
Figure 6.4.3.2 - SOSTDC1 expression was detected by end-point RT-PCR in sorted OB progenitor and 5T33MM/5TGM1MM cells that had been co-cultured together: *(A, B) SOSTDC1 was expressed in the OB progenitor population sorted from 5T33MM/5TGM1MM-OB progenitor co-cultures in comparison to no SOSTDC1 expression in OB progenitors cultured alone. SOSTDC1 expression was detectable in 5T33MM and 5TGM1MM cells cultured on their own. N=3 independent experiments. The HK-2 was used as a positive control for SOSTDC1 expression at 200pb. The gel image is representative of three independent experimental repeats.*
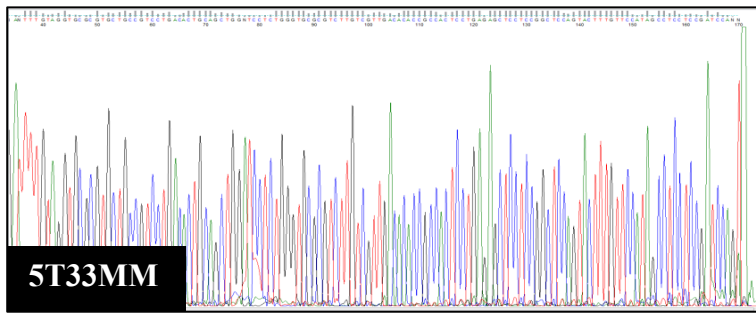
A

Score	Expect	Identities	Gaps	Strand

241 bits(130) 1e-60   131/132(99%) 0/132(0%) Plus/Minus

```
Query 1    TTTGTAGGTGCGCGTGCTGCCGTCCTGACACTGCAGCTGGNTCCTCTGGGTGCGCGTCTT   60
           |||||||||||||||||||||||||||||||||||||||| |||||||||||||||||||
Sbjct 593  TTTGTAGGTGCGCGTGCTGCCGTCCTGACACTGCAGCTGGATCCTCTGGGTGCGCGTCTT   53

Query 61   GTCGTTGACACACCGCCACTCCTGAGAGCTCCTCCGGCTCCAGTACTTTGTTCCATAGCC   120
           ||||||||||||||||||||||||||||||||||||||||||||||||||||||||||||
Sbjct 533  GTCGTTGACACACCGCCACTCCTGAGAGCTCCTCCGGCTCCAGTACTTTGTTCCATAGCC   474

Query 121  TCCTCCGATCCA   132
           ||||||||||||
Sbjct 473  TCCTCCGATCCA   462
```

B
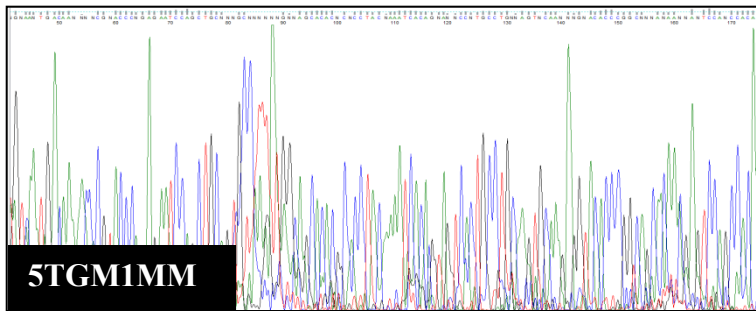
Score	Expect	Identities	Gaps	Strand

165 bits(89) 7e-38   106/118(90%) 0/118(0%) Plus/Plus

```
Query 1    CGTACCCAGAGAATCCAGCTGCAGTGCCNTTANGGCAGCACACGCACCTACAAAATCACA   60
           ||||||||||||||||||||||||||||     | ||||||||||||||||||||||||||
Sbjct 606  CGTACCCAGAGAATCCAGCTGCAGTGCCAAGATGGCAGCACACGCACCTACAAAATCACA   665

Query 61   GTANTCCCTGCCTGCCAGTGCAAGANGTACACCCGGCAGCanaannaGTCCAGCCACA   118
           ||| || |||||||| ||||||||| |||||||||||||| ||  ||||||| ||||
Sbjct 666  GTAGTCACTGCCTGCAAGTGCAAGAGGTACACCCGGCAGCACAACGAGTCCAGTCACA   723
```

Figure 6.4.3.3 - SOSTDC1 cDNA sequencing of 5T33MM and 5TGM1MM cells: *End-point RT-PCR products obtained from 5T33MM/5TGM1MM myeloma cells were sequenced for SOSTDC1 using SOSTDC1-specific primers. The (A)5T33MM and (B) 5TGM1MM had >98% homology with the SOSTDC1-specific sequence identified in BLAST (NCBI Reference Sequence: NM_025312.3). Images are representative of one sequencing assay with the reverse primer for SOSTDC1 (5'-TGTGGCTGGACTCGTTGTGC-3'). N=3 independent experiments.*

A

5T33MM from Co-culture

Score	Expect	Identities	Gaps	Strand

113 bits(61) 1e-22 66/70(94%) 0/70(0%) Plus/Minus

```
Query  1    GTCATTGACACACCGCCACTCCTGGNANCTCCTCCTGCTCCAGTACTTTGTTCCATANCC  60
            |||||||||||||||||||||||||| | |||||||||||||||||||||||||||| ||
Sbjct  599  GTCATTGACACACCGCCACTCCTGGGAGCTCCTCCTGCTCCAGTACTTTGTTCCATAGCC  540

Query  61   TCCTCCGATC  70
            ||||||| |||
Sbjct  539  TCCTCCAATC  530
```

B

OB from 5TGM1MM Co-culture

Score	Expect	Identities	Gaps	Strand

130 bits(70) 2e-27 74/77(96%) 0/77(0%) Plus/Minus

```
Query  2    TTTTGTCATTGACACACCGCCACTCCTGGNANCTCCTCCTGCTCCAGTACTTTGTTCCAT  61
            ||||||||||||||||||||||||||||| | ||||||||||||||||||||||||||||
Sbjct  603  TTTTGTCATTGACACACCGCCACTCCTGGGAGCTCCTCCTGCTCCAGTACTTTGTTCCAT  544

Query  62   AGCCTCCTCCGATCCAG  78
            |||||||||| ||||||
Sbjct  543  AGCCTCCTCCAATCCAG  527
```

Figure 6.4.3.4 - SOSTDC1 cDNA sequencing of 5T33MM/5TGM1MM sorted from myeloma-OB progenitor co-cultures: *End-point RT-PCR products obtained from myeloma cells sorted from OB progenitor co-cultures were sequenced for SOSTDC1 using SOSTDC1-specific primers. The co-cultured (A) 5T33MM and (B) 5TGM1MM cells had 100% homology with the SOSTDC1-specific sequence identified in BLAST (NM_025312.3).Images are representative of one sequencing assay with the reverse primer for SOSTDC1 (5'-TGTGGCTGGACTCGTTGTGC-3'). N=3 independent experiments.*

A

5TGM1MM from Co-culture

Score	Expect	Identities	Gaps	Strand
148 bits(80)	4e-33	80/80(100%)	0/80(0%)	Plus/Minus

```
Query  1    GCGCGTCTTGTCGTTGACACACCGCCACTCCTGAGAGCTCCTCCGGCTCCAGTACTTTGT  60
            ||||||||||||||||||||||||||||||||||||||||||||||||||||||||||||
Sbjct  542  GCGCGTCTTGTCGTTGACACACCGCCACTCCTGAGAGCTCCTCCGGCTCCAGTACTTTGT  483

Query  61   TCCATAGCCTCCTCCGATCC  80
            ||||||||||||||||||||
Sbjct  482  TCCATAGCCTCCTCCGATCC  463
```

B

OB from 5T33MM Co-culture

Score	Expect	Identities	Gaps	Strand
241 bits(130)	1e-60	131/132(99%)	0/132(0%)	Plus/Minus

```
Query  1    TTTGTAGGTGCGCGTGCTGCCGTCCTGACACTGCAGCTGGATCCTCTGGGTGCGCGTCTT  60
            ||||||||||||||||||||||||||||||||||||||||||||||||||||||||||||
Sbjct  593  TTTGTAGGTGCGCGTGCTGCCGTCCTGACACTGCAGCTGGATCCTCTGGGTGCGCGTCTT  534

Query  61   GTCGTTGACACACCGCCACTCCTGANAGCTCCTCCGGCTCCAGTACTTTGTTCCATAGCC  120
            |||||||||||||||||||||||| |||||||||||||||||||||||||||||||||||
Sbjct  533  GTCGTTGACACACCGCCACTCCTGAGAGCTCCTCCGGCTCCAGTACTTTGTTCCATAGCC  474

Query  121  TCCTCCGATCCA  132
            ||||||||||||
Sbjct  473  TCCTCCGATCCA  462
```

Figure 6.4.3.5 - SOSTDC1 cDNA sequencing of OB progenitors sorted from myeloma-OB progenitor co-cultures: *End-point RT-PCR products obtained from OB progenitors sorted from 5T33MM/5TGM1MM myeloma co-cultures were sequenced for SOSTDC1 using SOSTDC1-specific primers. The OB progenitor cells collected from (a) 5T33MM and (B) 5TGM1MM co-cultures had 100% homology with the SOSTDC1-specific sequence identified in BLAST (NM_025312.3). Images are representative of one sequencing assay with the reverse primer for SOSTDC1 (5'-TGTGGCTGGACTCGTTGTGC-3'). N=3 independent experiments.*

6.4.4 Assessing the dependency of SOSTDC1 production on direct OB-myeloma interaction

In section 6.4.3 I observed an increase in the proportion of SOSTDC1+ 5TGM1MM cells that were co-cultured with OB progenitors. To test the concept that SOSTDC1 is upregulated in myeloma cells as a result of direct interaction between the myeloma and OB progenitor cell, co-culture experiments were set up as previously described in section 6.2. In these experiments, co-culture of 5T33MM-GFP/5TGM1MM-GFP with OB progenitor resulted in some myeloma cells adhering to the OB progenitors. From these co-cultures, the media that contained the non-adhering myeloma population was removed and maintained as a separate sample ready for flow cytomtery analysis. Flow cytomteric analysis was used to compare the proportion of SOSTDC1+ myeloma cells from adherent and non-adherent populations, I showed that there was no difference between the proportions of SOSTDC1+ non-adherent 5T33MM cells compared to adherent 5T33MM cells sorted from 5T33MM-OB progenitor co-cultures. Flow cytometric analysis of adherent and no-adherent 5TGM1MM showed a significantly higher number of adherent 5TGM1MM cells sorted from the myeloma-OB progenitor co-cultures were SOSTDC1+ compared to the non-adherent 5TGM1MM population (**Figure 6.4.4.1 A, B**).

In other experiments, co-cultures were set up and sorted by FACS Aria into separate populations prior to protein extraction as previously described in section 6.3. Western blot analysis was performed to assess SOSTDC1 protein level in adherent and non-adherent myeloma cells. Densitometry, normalised to GAPDH protein levels showed that the average density of bands representing SOSTDC1 protein did not differ between the non-adherent population and adherent 5T33MM cells sorted from 5T33MM-OB progenitor co-cultures (**Figure 6.4.4.2 A**). Similar to the flow cytomtery data, western blotting showed adherent 5TGM1MM cells sorted from the myeloma-OB progenitor co-cultures had higher SOSTDC1 protein levels compared to the non-adherent 5TGM1MM cells that were floating the media of co-cultures (**Figure 6.4.4.2 B**).

A SOSTDC1+ 5T33MM cells from non-adherent and adherent 5T33MM-OB progenitor Co-culture

B SOSTDC1+ 5TGM1MM cells from non-adherent and adherent 5TGM1MM-OB progenitor Co-culture
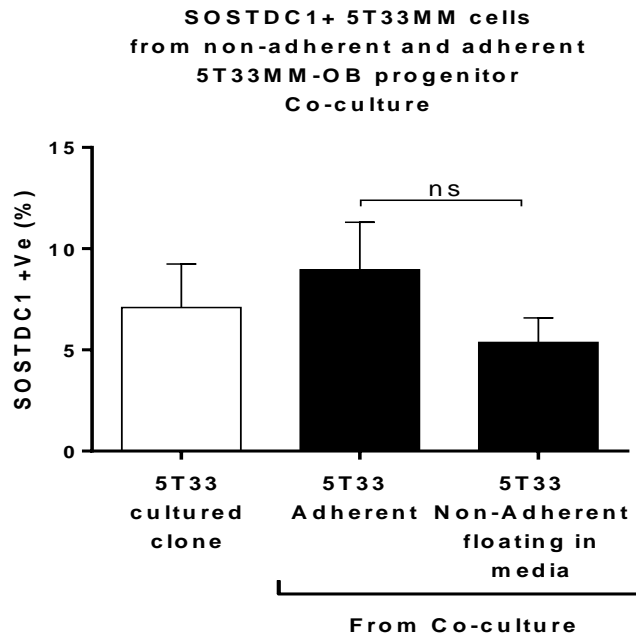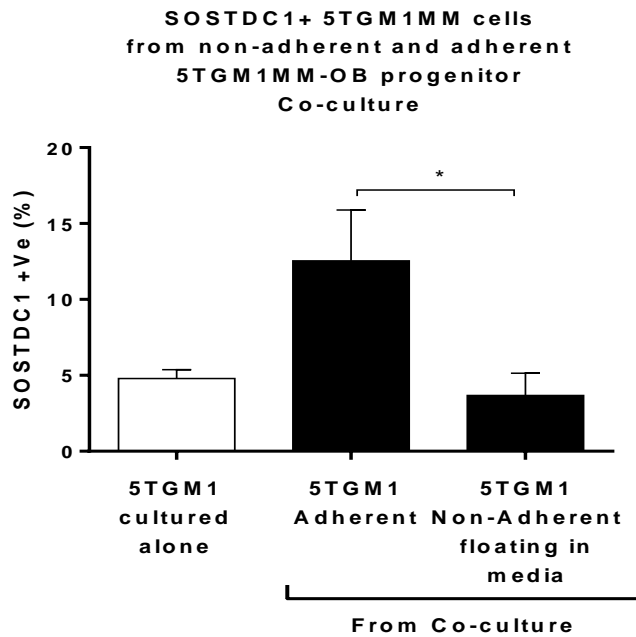
Figure 6.4.4.1 – The proportion of SOSTDC1+ 5TGM1MM cells increased as a result of direct myeloma-OB progenitor interaction: *(A) There was no difference in the proportion of SOSTDC1+ cells from non-adherent 5T33MM-GFP cells compared to the 5T33MM-GFP adherent population. (B) The proportion of SOSTDC1+ 5TGM1MM-GFP cells was higher in adherent myeloma cells compared to non-adherent cells floating in the co-culture media. N=3 independent experiments, Man-Whitney, *P<0.05.*

A

SOSTDC1 protein in 5T33MM cells from non-adherent and adherent 5T33MM-OB progenitor Co-culture

B

SOSTDC1 protein in 5TGM1MM cells from non-adherent and adherent 5TGM1MM-OB progenitor Co-culture
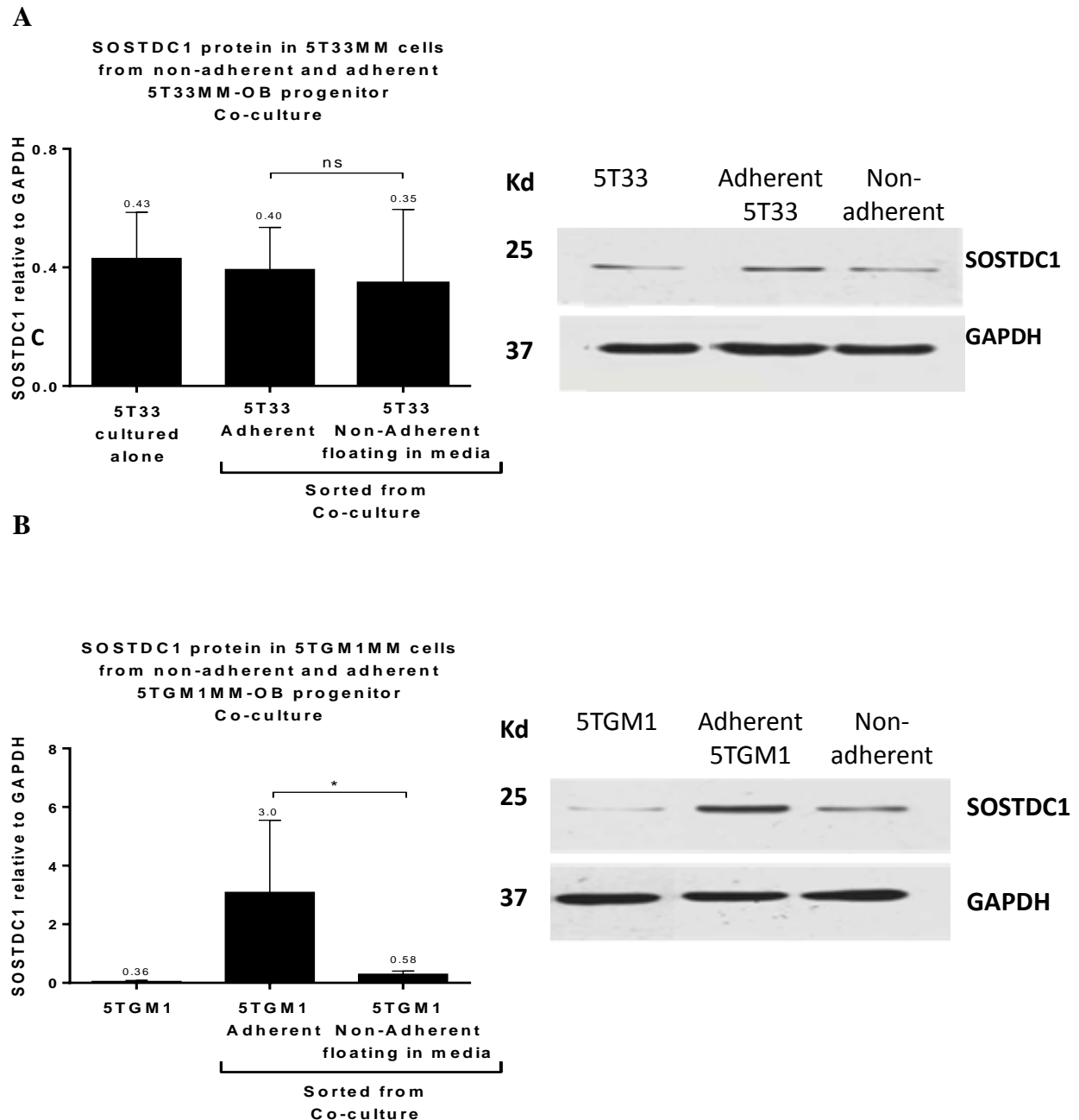
Figure 6.4.4.2 - Direct 5TGM1MM-OB progenitor interaction upregulated SOSTDC1 protein levels: *Following co-culture, 5T33MM-GFP/5TGM1MM-GFP cells that had adhered to the OB progenitors were sorted by FACS Aria into separate populations. Western blot images are representative of three independent experimental repeats. (A) There was no difference in SOSTDC1 levels in 5T33MM cells co-cultured compared to 5T3MM cells cultured alone (B) SOSTDC1 protein levels obtained from 5TGM1MM cells adherent to OB progenitors increased compared to non-adherent 5TGM1MM cells. N=3 independent experiments, Man-Whitney, *P<0.05.*

6.4.5 SOSTDC1 was present in tibea bearing myeloma tumour and not naïve animals determined by immunohistochemical analysis

Immunohistochemical analysis of mouse tibiae sections infiltrated with 5T33MM and 5TGM1MM myeloma *in-vivo* was used to detect SOSTDC1 staining in diseased mice compared to naïve animals. 5T33MM and 5TGM1MM tibiae sections were stained with anti-SOSTDC1 rabbit or isotype control antibody to detect the presence of SOSTDC1 protein. Immunohistochemical staining showed that SOSTDC1 protein was present in both 5T33MM and 5TGM1MM sections compared to their respective isotype controls. This staining appeared mainly focused in the myeloma cells/colony vicinity, strongest within the myeloma cells themselves. The staining appeared around the myeloma cells as well as within the cells themselves; correlating with the fact that SOSTDC1 is a secreted protein (**Figure 6.4.5.1 A, B**). Naïve tibiae sections that were did not have myeloma did not appear to have SOSTDC1 present. Some light brown staining did appear around the megakaryocytes but this staining was also present in some of the isotype controls (**Figure 6.4.5.1 C**).

In immunohistochemical analysis of mouse tibiae sections infiltrated with myeloma, it was difficult to identify many OB cells in close proximity of myeloma colonies. The OB cells that were identified appeared to be more morphologically similar to bone lining cells. Immunohistochemical analysis showed a lack of OB cells in close proximity to 5TGM1MM myeloma cells which were stained positive for SOSTDC1 (**Figure 6.4.5.2 A**). In the same 5TGM1MM section where no myeloma colony was present OB/bone lining cells were present (**Figure 6.4.5.2 B**).

A

5T33MM+ SOSTDC1 Ab

5T33MM+ Isotype CT

B

5TGM1MM+ SOSTDC1 Ab

5TGM1MM + Isotype CT

C

Naive+ SOSTDC1 Ab

Naive+ Isotype CT
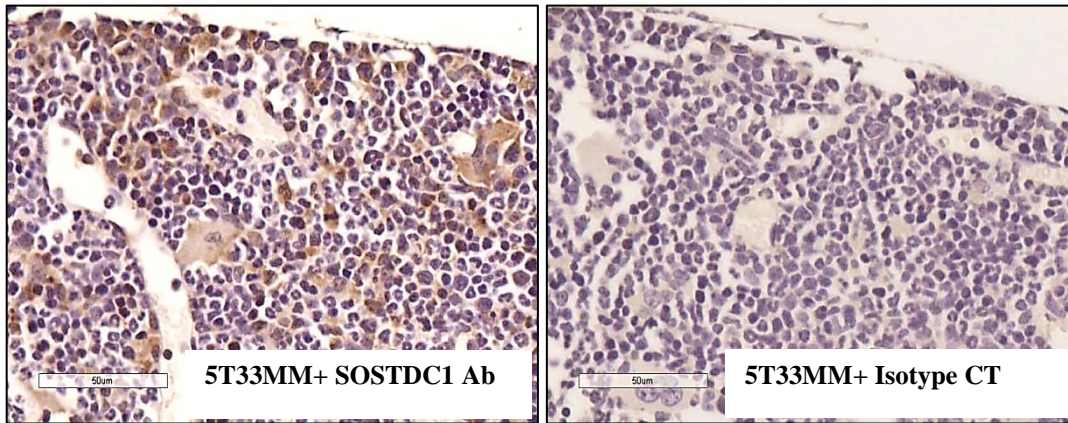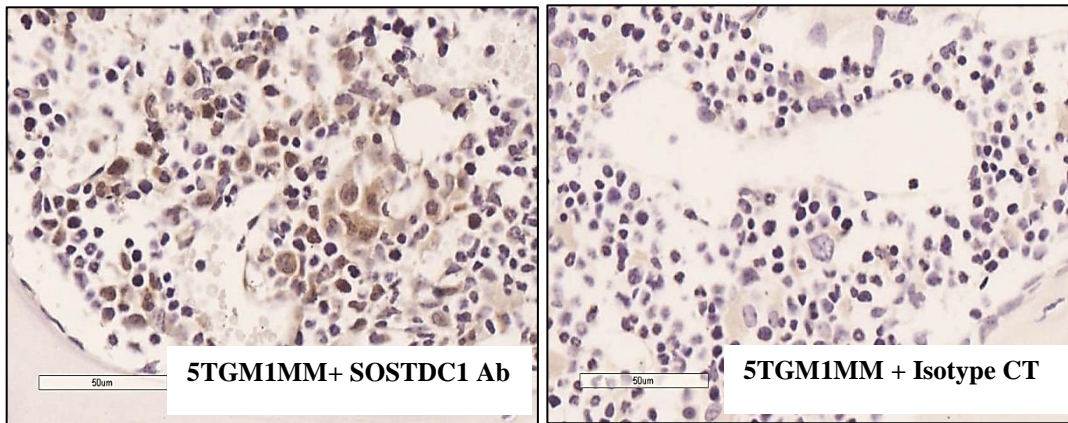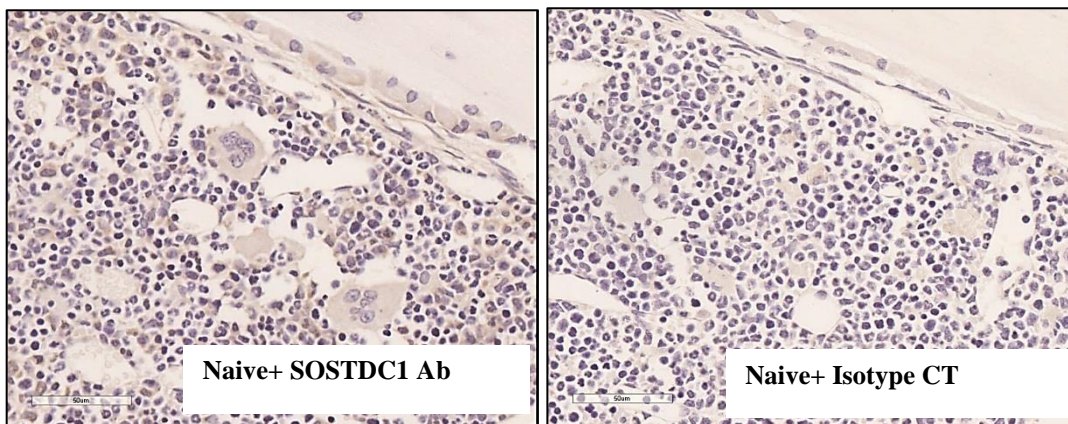
Figure 6.4.5.1 - SOSTDC1 was detected using immunohistochemistry in 5T33MM and 5TGM1MM tibia *in vivo*: *(A) SOSTDC1 staining was present in 5T33MM sections compared to the isotype antibody and this staining was mainly confined to the myeloma cells/colony area. (B) SOSTDC1 staining was present in 5TGM1MM sections compared to the isotype CT and this staining was specific in regions the myeloma cells/colonies were present. (C) Naïve tibia sections did not appear to produce SOSTDC1. Images are representative of at 3 slides from N=6.*

A

Myeloma
Cells

50um

5TGM1MM
colony

B

OB/Bone-lining Cells

50um

No 5TGM1MM
colony
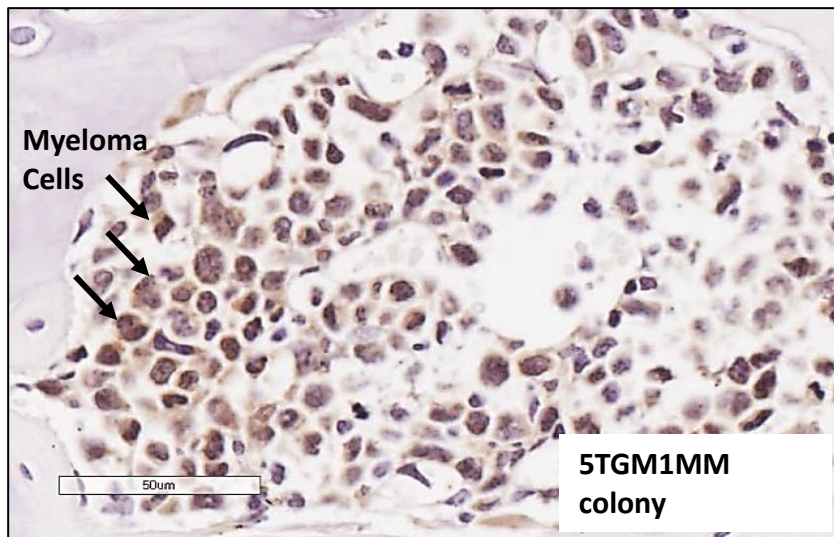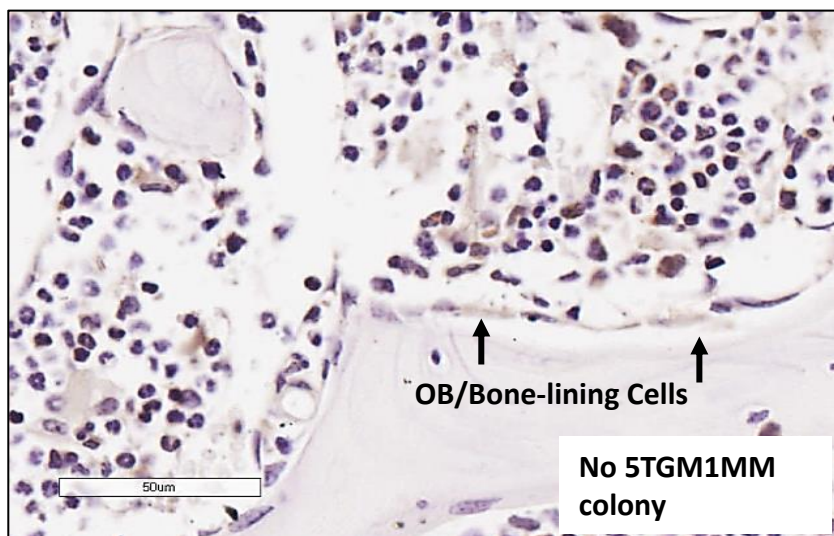
Figure 6.4.5.2 - There were few OB/bone-lining cells in proximity of SOSTDC1-positive myeloma colonies: *Images are representative of different areas within the same slide. (A) There were few OB cells or bone- lining in close proximity of myeloma colonies that were positive for SOSTDC1 staining. (B) In the same 5TGM1MM section , where no myeloma colony was present, more OB cells were present.*

6.4.6 Lytic 5TGM1MM myeloma cells express more SOSTDC1 compared to non-lytic 5T33MM myeloma cells

As mentioned previously, mice injected with 5TGM1MM cells developed lytic bone disease similar to that observed in MM patients. However 5T33MM mice did not develop bone disease associated with tumour burden. To test the hypothesis that SOSTDC1 expression was upregulated in lytic 5TGM1MM myeloma cells compared to non-lytic 5T33MM cells, the data obtained from the SOSTDC1 western blot and end-point RT-PCR experiment outlined in section 6.4 were re-analysed.

Western blotting analysis of the average density calculated for SOSTDC1 protein levels (normalised to GAPDH), was upregulated in lytic 5TGM1MM cells produced compared to non-lytic 5T33MM myeloma cells (*P<0.05, **Figure 6.4.6.1 A**). End-point RT-PCR analysis was used to determine whether lytic 5TGM1MM myeloma cells had higher *SOSTDC1* expression in comparison to non-lytic 5T33MM myeloma cells. The average density of *SOSTDC1* PCR product bands were normalised to GAPDH. Lytic 5TGM1MM cells expressed more *SOSTDC1* compared to non-lytic 5T33MM myeloma cells (*P<0.05, **Figure 6.4.6.1 B**).

A
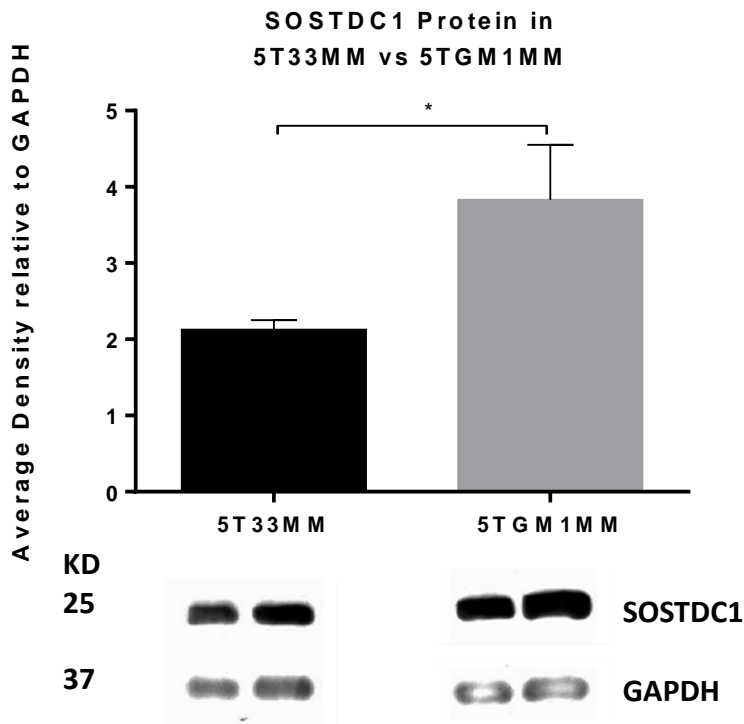
B
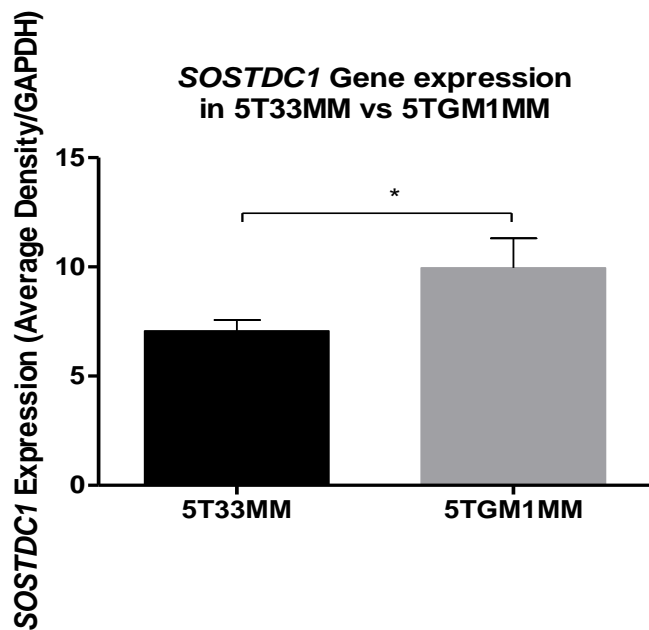
Figure 6.4.6.1 - 5TGM1MM cells produced more SOSTDC1 than 5T33MM cells: *(A) Western blot analysis showed that lytic 5TGM1MM cells produce more SOSTDC1 protein compared to non-lytic 5T33MM myeloma cells (B) End-point RT-PCR analysis showed that lytic 5TGM1MM cells express higher level of SOSTDC1 compared to non-lytic 5T33MM myeloma cells. N=3 independent experiments, Man-Whitney, *P<0.05.*

A

Anti-SOSTDC1 Antibody had no effect on 5TGM1 or OB Progenitor *Runx2* expression
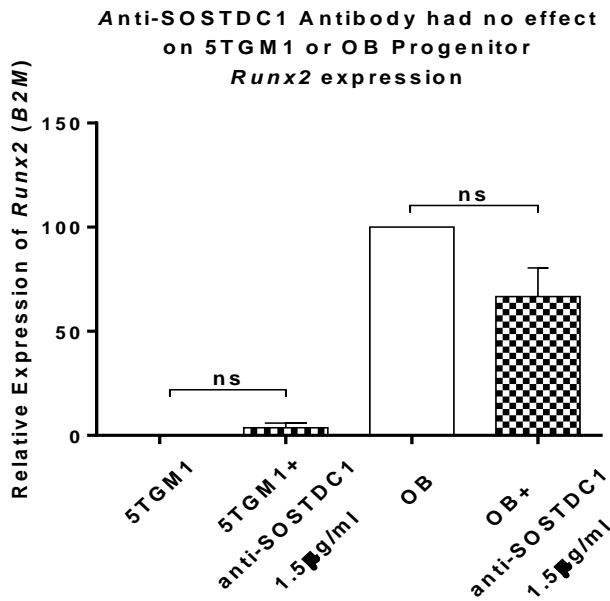
Average CT values

Sample	CT Value
5TGM1	37.0
5TGM1 + anti-SOSTDC1 antibody	31.2
OB	25.8
OB + anti-SOSTDC1 antibody	26.3

B

Anti-SOSTDC1 antibody reversed 5TGM1-induced suppression of *Runx2* expression in OB progenitors
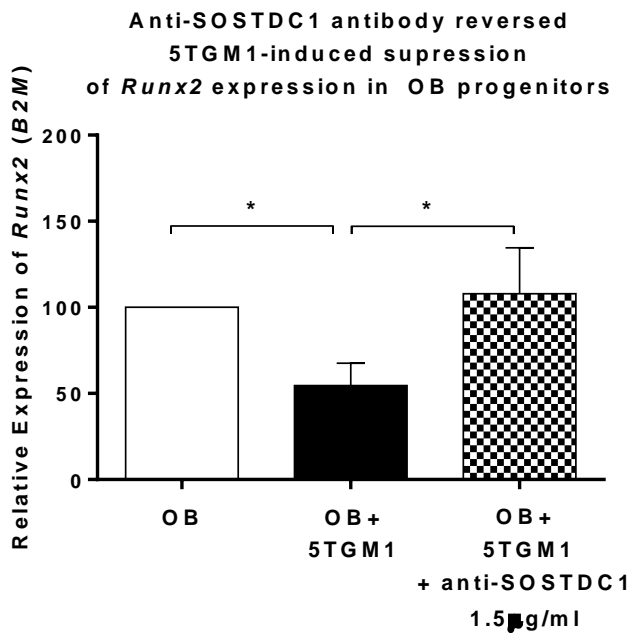
Average CT values

Sample	CT Value
OB	25.8
OB+5TGM1	26.4
OB + 5TGM1 + anti-SOSTDC1 antibody	26.7

Figure 6.4.6.2 – Anti-SOSTDC1 antibody reversed 5TGM1-induced suppression of Runx2 expression in OB progenitors: *(A) 5TGM1MM cells cultured alone did not produce detectable levels of Runx2. Runx2 was detected in differentiating OB progenitors cultured alone. (B) Runx2 gene expression in OB progenitors was reduced in the presence of 5TGM1MM myeloma cells and treatment of 5TGM1MM-OB progenitor co-cultures with anti-SOSTDC1 antibody reversed this effect restoring Runx2 levels. N=3 independent experiments, Students t-tes (A). One-Way Anova, with Holme-Sidak's adhoc test (B) *P<0.05.*

6.5 Discussion

MM is associated with the suppression of OB activity leading to osteolytic bone disease. In recent years it has been suggested that myeloma and OB interaction may be involved in the regulation and promotion of osteolytic bone disease via suppression of osteoblastogensis. The molecular mechanisms by which myeloma cells inhibit OB activity and the consequences of myeloma-OB interaction on myeloma cell growth and OB suppression are unclear. In previous chapters I showed that SOSTDC1 had more of suppressive effect on OB progenitors when they were in the stages of differentiation (day 8-11 in culture). This provided the rational for assessing SOSTDC1 expression during the early phase of OB progenitor differentiation. The aim of this study was to determine whether myeloma cells and OB progenitors express SOSTDC1 and to also establish the conditions under which SOSTDC1 is expressed with reference to the question; is SOSTDC1 expression dependent on myeloma-OB progenitor interaction? Thus the main aim of this study was to determine the conditions under which myeloma and OB progenitor cells produced SOSTDC1, testing the hypotheses that the 5TMM and OB progenitors produce SOSTDC1 and that the direct interaction between myeloma and OB progenitors upregulates the production of SOSTDC1 in both myeloma and OB progenitor cells. Interestingly my data support the hypothesis that myeloma cells produce SOSTDC1 and refute the hypothesis that OB progenitors produce SOSTDC1. Additionally, my findings from this study also support the hypothesis that myeloma-OB progenitor interaction upregulates SOSTDC1 expression in both cell types.

Due to the heterogeneity associated with myeloma disease, cell cultures originating from both 5T33MM and 5TGM1MM C57BL/KaLwRij mice were tested separately in this study. In preliminary experiments, the presence of SOSTDC1 was tested qualitatively by immunofluorescent microscopy. Originally, 5T33MM-GFP and 5TGM1MM-GFP myeloma cells were used to verify the presence of myeloma cells in immunocytochemistry experiments, particularly so that the myeloma cells could be distinguished from the OB progenitor cells when in co-culture. However, the GFP in myeloma cells was difficult to detect following fixation (live cells were tested to compare). One possible reason for this may have been the cell fixation process in 4% formalin (pH 6.8) in PBS resulted in some degradation of the GFP on the myeloma cells. Studies have shown that GFP is more stable in a hypotonic solution with a pH range of

7.5 - 8.5 and shifts in structure/stability outside this pH range (Tavare, Fletcher et al. 2001). An alternative would have been to use Paraformaldyhye (PFA). However all aspects of the immunostaining protocol had been optimised using the anti-SOSTDC1 antibody which only stained using 4% formalin as a fixative. As an alternative, CD138 plasma cell protein was used to verify the presence of myeloma cells.

In my studies, a known density of myeloma and differentiated OB progenitor cells cultured on their own were fixed with 4% formalin and stained with the commercial anti-SOSTDC1 rabbit polyclonal antibody overnight. To further determine that the myeloma cells were positive for the plasma cell marker CD138, the cells were co-stained with an anti- CD138 rabbit antibody. These immunofluorescent experiments were consistent in showing that differentiating OB progenitor cells did not stain positive for SOSTDC1 compared to the HK-2 cell positive controls, which were strongly positively stained for SOSTDC1.

On the other hand, the immunofluorescent staining for SOSTDC1 in the 5T33MM-GFP and 5TGM1MM-GFP myeloma cells showed myeloma cells produced SOSTDC1 in low levels. The problem with using immunofluorescent microscopy as a method of SOSTDC1 detection in myeloma cells was that non-adherent myeloma cells has to be artificially attached to the culture plate surface. The main issue was that although Poly-L-Lysine was used to facilitate the adherence of the myeloma cells to the culture plate wells, the washing steps throughout the immunoassay resulted in many of the myeloma cells detaching. In some experiments SOSTDC1 was detected in a few of remaining attached myeloma cells, whilst in others no SOSTDC1 was detected. Flow cytometry was used to verify the data obtained from the immunofluorescent microscopy analysis using the same experimental setup. This time when myeloma cells were screened for the presence of SOSTDC1 using flow cytometry, GFP could be detected using the same method as immunofluorescent microscopy. Although the reason for this is unclear, a possible explanation is that various studies looking at protein detection in cells using both flow cytometry and immunofluorescent microscopy have shown that flow cytometry is more sensitive of the two methods (Jenson, Grant et al. 1998, Muratori, Forti et al. 2008).

Flow cytometric analysis showed that between 5-10% of the 5T33MM and 5TGM1MM myeloma cells were positive for SOSTDC1, suggesting that variability seen in the

immunofluorescent microscopy may have been due to technical issues. The low number of myeloma cells that were adherent to the plate surface by the end stage of the immunofluorescent assay and the small percentage of myeloma cells that were positive for SOSTDC1 as detected by flow cytometry, could mean that many SOSTDC1 positive cells were detached and washed off during the immunofluorescent assay. This may explain why in immunofluorescent microscopy experiments, some myeloma cells produced SOSTDC1 whilst in others SOSTDC1 could not be detected.

Initially, co-culture conditions were tested to determine the minimum time required for SOSTDC1 to be produced and the optimal media conditions that both the OB progenitor and myeloma cells required for growth. This pilot data determined that in order to produce SOSTDC1, OB progenitors and 5T33MM cells required co-culturing overnight and SOSTDC1 was still present at 48 hours following co-culture. To maintain minimum variability between experiments, all co-cultures were carried out for 24 hours. In addition, it was determined that although OB progenitors could be maintained for up to 48 hours in RPMI myeloma media, the 5T33MM cells started to die and would not adhere to the OB progenitors at 24 hours in co-culture when in OGM. Therefore, differentiated OB progenitor cells were co-cultured with 5T33MM or 5TGM1MM cells for 24 hours in RPMI.

Flow cytometry and immunofluorescent microscopy data were clear in showing that compared to cells cultured on their own, OB progenitors and myeloma co-cultured together produced SOSTDC1. The immunofluorescent analysis of co-cultures showed that SOSTDC1 appeared to be present within both the myeloma cells and also the OB progenitors. This staining was focused where the OB progenitor and myeloma cells were physically interacting. Flow cytometric data was able to confirm this quantitatively where the myeloma-GFP-population could actually be distinguished from the OB progenitor population. The proportion of SOSTDC1 positive myeloma cells were compared to the proportion of SOSTC1 positive OB progenitor cells. I showed that where OB progenitors did not produce detectable levels of SOSTDC1 when cultured on their own, SOSTDC1 production was induced in the OB progenitor as a result of interaction with the myeloma cells. Interestingly, although SOSTDC1 levels did not vary in 5T33MM that were co-cultured with OB progenitors compared to 5T33MM cells that

cultured on their own, a significant difference could be seen in the same experiments using 5TGM1MM cells.

Although flow cytometry data indicated that SOSTDC1 production was induced as a result of OB progenitors and myeloma cell co-culture, there was a need for a more sophisticated method of separating the two cell populations for analysis of SOSTDC1 expression. Myeloma-GFP-OB progenitor co-cultures were sorted by FACS Aria in a similar method to the one outlined by C. Edwards et al (Edwards, Lwin et al. 2009). Western blot analysis and End-point PCR showed that the sorted GFP positive myeloma cells and GFP-negative OB progenitor, as individual populations, were positive for SOSTDC1 expression. Both western blot and End-point RT-PCR data correlated with the flow cytometry analysis, in that SOSTDC1 production was switched on in OB progenitor cells following co-culture with myeloma cells. Western blotting further determined that SOSTDC1 protein levels increased in 5TGM1MM cells that had been co-cultured with OB progenitor cells compared to 5TGM1MM cells cultured on their own.

The hypothesis that SOSTDC1 expression is dependent on myeloma-OB physical interaction is important in understanding role of SOSTDC1 in osteolytic bone disease in MM. To test this hypothesis, I determined the levels of SOSTDC1 protein present in the myeloma cells that were co-cultured with OB progenitors but had not adhered to the OB progenitor cells. Western blot and flow cytometry analysis showed that co-cultured 5TGM1MM cells that had adhered to OB progenitors contained higher SOSTDC1 protein levels compared to those myeloma cells that had not adhered to the OB progenitors. Identical experiments with 5T33MM showed that there was no difference between adherent and non-adherent 5T33MM cells co-cultured with OB progenitors.

Immunohistochemical analysis of 5T33MM and 5TGM1MM tibiae sections stained with anti-SOSTDC1 antibody confirmed that SOSTDC1 was present in bone that was infiltrated with myeloma disease. There was a lack of SOSTDC1 staining in naïve bone sections, indicating that SOSTDC1 was only expressed in sites associated with myeloma bone disease. The presence of SOSTDC1 appeared most focused where the myeloma cell colonies were located. As the myeloma sections were obtained 10 days post-injection, some OB/bone-lining cells were still present within the myeloma-infiltrated bone. In parts of these 5T33MM/5TGM1MM sections, where myeloma colonies were stained for

SOSTDC1, no OB/bon-lining cells could be identified. However in parts of the same 5T33MM/5TGM1MM sections where no myeloma colonies were present, there was a lack of SOSTDC1 staining and some OB/bone-lining cells were present.

Western blotting and end-point RT-PCR data indicated that 5TGM1MM cells expressed a higher level of SOSTDC1 compared to 5T33MM cells. The 5T33MM myeloma model is an aggressive form of myeloma with evident signs of morbidity at 4 weeks. Reports vary on the development of osteolytic bone disease in 5T33MM models. Although some laboratories have reported diffuse osteolytic bone lesions in their 5T33MM mice, in our laboratory the C57BL/KaLwRij mice injected with 5T33MM cells did not develop bone disease. This variability could be explained as mice are injected with *in-vitro* growing variants rather than parental cells. In the literature the 5T33MM model is now used more for investigating myeloma cell homing and proliferation the more recently developed 5TGM1MM model is preferred for the study of bone disease related to tumour burden (Croese, Vas Nunes et al. 1987, Vanderkerken, De Raeve et al. 1997). These data support the rational that SOSTDC1 is a molecule that may be involved in the induction of osteolytic bone disease in myeloma. Therefore would be predicted that SOSTDC1 would be more of a regulator role in the lytic 5TGM1MM model in comparison to the non-lytic 5T33MM model. Furthermore, the Taqman gene expression assays showed that *Runx2* expression levels decreased in OB progenitors co-cultured with 5TGM1MM myeloma cells and treatment with anti-SOSTDC1 antibody reversed this effect. This data is compelling in that is suggests that SOSTDC1 in fact does module the suppression of OB differentiation induced by myeloma cells.

Although the 5TMM series are reproducible and an excellent model for MM studies, there is a constant need for the development of these animal models to further enhance our understanding of MM as well as the limitations associated with them. In humans, MM is heterogeneous as a disease and this poses a problem in that no single animal model can constitute of all MM features. This study would benefit from looking into SOSTDC1 expression in human myeloma cell lines and human BM samples so as to move into translational research for potential therapeutic purposes.

Chapter 7 – General Discussion

7.1 Discussion

To better understand the molecular mechanism involved in osteolytic bone destruction associated with MM, the biochemical pathways and soluble factors involved need to be identified. Until recently, research has focused on identifying the mechanisms resulting in increased osteoclastogenesis and OC activation, with particular interest in the role of the RANK/OPG signalling axis (Pearse, Sordillo et al. 2001). The current therapies that are administered to MM patients suffering from bone disease target increased osteolysis mainly caused by osteoclasts-induced bone resorption . Bisphosphonates such as pamidronate, zoledronic acid and clodronate form the foundations of the management of myeloma-related bone disease on an international scale (Terpos, Roodman et al. 2013). However, in the past few years, it has become apparent that the impairment of bone formation is key to the uncoupling of bone remodelling in MM. As a result there is an essential need for therapeutic agents that also target the OB suppression observed in MM bone disease.

Myeloma cells themselves have been implicated in the inhibition of bone formation by preventing OB differentiation (Oshima, Abe et al. 2005, Giuliani, Rizzoli et al. 2006). However, functional data is limited and little is known about the causal roles of the suppression of bone formation in MM bone disease. A number of extracellular molecules have been implicated in the reduced osteoblastogensis observed in patients with MM, including the Dkk and SFRP family of proteins (Tian, Zhan et al. 2003, Giuliani, Morandi et al. 2007). In the last decade studies have linked increased Dkk1 protein levels in MM with decreased OB activity in bone remodelling (Tian, Zhan et al. 2003). Further to this, our group has shown that blocking Dkk1 impedes suppression of bone formation and prevents osteolytic bone disease from developing in MM. Nevertheless, data also show that Dkk1 levels are not up-regulated in the serum of all MM patients (Heath, Chantry et al. 2009). Consequently, MM patients with normal Dkk1 levels cannot be treated with the current

Based on these findings, we can assume that other molecules, either produced by the myeloma cells, or produced by other cells within the bone microenvironment, are involved in suppression of bone formation. In our search to identify other molecules that that could have a potential causal role in the suppression of osteoblastogenesis in MM, we

identified *SOSTDC1* (data unpublished), as a gene that was highly upregulated in the murine 5T2MM myeloma model compared to naïve animals using Affymetrix GeneChip™, TaqMan™ gene expression assays and immunohistochemistry (Buckle et al, 2014). The identification of SOSTDC1 in the 5T2MM model was particularly interesting due the fact that mice which are injected with 5T2MM cells develop osteolytic bone disease that is similar to that observed in human MM patients. With the exception of the present study, SOSTDC1 has previously not been associated with myeloma-related bone disease.

Within the literature there is evidence for the expression of SOSTDC1 and its orthologues in various tissues including embryos, teeth, hair follicles, breast and kidney, with particular focus on a modulatory role for SOSTDC1 in Wnt and BMP signalling (Laurikkala, Kassai et al. 2003, Yanagita, Oka et al. 2004, Beaudoin, Sisk et al. 2005, Clausen, Blish et al. 2010). There is less known in regards to the effect of SOSTDC1 on osteoblastogenesis with the exception of a few key studies that have shown the mouse orthologue (Wise) of SOSTDC1 to be an inhibitor of BMP2, -4, or -7 induced bone differentiation in MC3T3-E1. Similarly recombinant SOSTDC1 was found to bind directly to specific BMPs and suppress BMP2, -4 and -7 stimulated ALP activity in the mouse myoblast cell line, C2C12 (Yanagita, Oka et al. 2004). The antagonistic effect on BMP signalling is apparently through its ability to bind directly to the BMP ligands themselves (Laurikkala et al., 2003 and Yanagita et al., 2004). Other studies have also shown that SOSTDC1-Wnt signalling is regulated via interactions with Wnt co-receptors LRP5/6, with data suggesting SOSTDC1 consists of separating binding domains for the BMP ligands and Wnt receptors (Lintern, Guidato et al. 2009). This information provided some insight into the interactions of SOSTDC1 with its BMP ligands and LRP receptors on a molecular level.

The compelling data from our group showing that SOSTDC1 was upregulated in the lytic 5T2MM myeloma model compared to naïve mice, combined with other reports indicating SOSTDC1 may modulate BMP signalling in OB-like cells, encouraged the rational that SOSTDC1 could have a fundamental role in the suppression of OB differentiation in MM. In a clinical setting, SOSTDC1 could potentially be targeted as a therapeutic agent reversing the suppression in osteoblastogenesis, which ultimately leads to osteolytic bone

disease in MM. In particular, in cases where MM patients do not exhibit elevated levels of Dkk1, targeting SOSTDC1 could be the ideal Dkk1-substitute therapy in MM.

In the first part of the present study I characterised an *in-vitro* culture system using OB progenitor cultures derived from the calvaria of naïve neonatal C57BLkawRij mice. This system reflected the different stages of osteogenic maturation during cell differentiation. These primary cells exhibit a wide range of OB phenotypic changes, making them the preferable murine OB model which is used widely in the literature (Wang, Christensen et al. 1999, Fernandes, Harkey et al. 2007). Characterisation of the OB progenitor model was fundamental to understanding experimental data obtained from studying the molecular mechanisms involved in OB differentiation. The primary OB progenitor cultures had a clear OB phenotype, including ALP enzymatic activity, extracellular matrix mineralisation, Runx2, Collagen and β-catenin expression, which were in line with the literature (Ecarot-Charrier, Glorieux et al. 1983, Prince, Banerjee et al. 2001, Komori 2006).

In this model, the exponential differentiation period of OB progenitor cultures started at approximately day 8 and cells become mature at around day 15. This data agreed with existing reports with the literature demonstrating that ALP of MC3T3-E1 and murine primary calvarial cells increased up to 14 and 15 days in culture, respectively (Yazid, Ariffin et al. 2010, Birmingham, Niebur et al. 2012). Furthermore, the mineralisation assays showed by day 15 of culture, OB progenitors had produced matrix nodules visible to the eye and these results were similar to the studies carried out by other groups (Hasegawa, Shimada et al. 2008, Kawazoe, Katoh et al. 2008). From the data in chapter 1, I established that the primary OB progenitors had differentiation profiles that were specific to progenitor/pre-osteoblasts up to day 11 of differentiation and beyond this time point amplified into mature functional OB cells.

Using the OB progenitor characterisation data from Chapter 1 as an experimental platform, I investigated the effect of rhSOSTDC1 on Wnt/BMP-induced differentiation and intracellular signalling in OB progenitor cells *in-vitro*. The hypothesis was; SOSTDC1 antagonises Wnt and BMP-induced differentiation and acute signalling in OB progenitors. Any regulatory effect of SOSTDC1 was assessed throughout the various stages of OB progenitor maturation established during the earlier characterisation of the

OB progenitor model. In these studies, the effect of SOSTDC1 on Wnt and BMP signalling in OB progenitors was compared simultaneously to that of well characterised Wnt antagonist Dkk1 and BMP antagonist noggin.

The data from these studies showed that SOSTDC1 alone did not have any effect on OB progenitor differentiation markers ALP and Runx2 or OB mineralisation. It is unclear whether the levels of BMP and Wnt proteins which are known to be present within the FCS (Sasse, Lengwinat et al. 2000) or produced by the OB progenitor cells (Zhang, Oyajobi et al. 2013), were impeding the physiological effect of SOSTDC1. Although in this study it was not possible to use serum-free media, it may be that elimination of the Wnt/BMP proteins from culture serum or from within the cells themselves could magnify the suppressive effect of SOSTDC1. Continuous exposure of OB progenitor cultures to recombinant Wnt3a, BMP2 and BMP7, induced ALP enzyme activity and an antagonistic effect of SOSTDC1 was evident in BMP2 and not BMP7 or Wnt-induced ALP activity. The inhibitory effect of SOSTDC1 was only significant on the first analysed day 8 time-point of OB progenitor differentiation. These findings were partially similar to Laurikkala, Kassai *et al* study which found the mouse orthologue of SOSTDC1 inhibited both Wnt and BMP-induced ALP activity of MC3T3-E1 cells (Laurikkala, Kassai et al. 2003; Rawadi et al. 2004). Although unclear, the differences between the present study and those of Laurikkala may be due to the phenotypic differences observed between cell-lines and primary OB progenitor cultures as well as differences in methodology.

Based on the literature, Runx2 seems to be a transcription factor that is mutually important in both the Wnt and BMP signalling in OB cells. In fact, studies showing that mice deficient in LRP5 express Runx2 normally, suggest that Runx2–regulated OB differentiation also occurs through the BMP pathway (Kato, Patel et al. 2002; Ducy 2000; Gong, Slee et al. 2001). As a result, Runx2 expression was used as the second marker of OB progenitor differentiation to assess any modulatory effect of SOSTDC1 on both Wnt and BMP signalling. Interestingly, in these experiments SOSTDC1 did exert a suppressive effect on OB progenitor differentiation when in the presence of Wnt3a, BMP2 or BMP7. The *Runx2* Taqman gene expression assays suggest that SOSTDC1 inhibits *Runx2* expression when in the presence of recombinant Wnt3a, BMP2 or BMP7 proteins. Similar to the ALP data, the suppressive effect of SOSTDC1 was again

observed on the earliest day 8 time point, when *Runx2* expression is known to be high in immature differentiating OB progenitor cells (Prince, Banerjee et al. 2001).

Measurement of mRNA is thought to be a more sensitive approach of detection compared to protein assays such as ALP analysis (Sperisen, Wang et al. 1992), however, any effects of SOSTDC1 on Wnt and BMP-induced mineral deposition would establish a clearer insight. Alizarin red staining showed that OB progenitors cultured continuously with recombinant SOSTDC1 protein suppressed Wnt3a, BMP2 and BMP7-induced OB progenitor mineralisation. The detrimental effect of SOSTDC1 when in the presence of Wnt and BMP ligands was again only evident during early OB progenitor differentiation. In all the latter experiments performed in which SOSTDC1 exerted inhibitory effects on Wnt3a-induced differentiation and mineralisation significantly, Dkk1 appeared less effective in general. This is interesting as Dkk1, similar to SOSTDC1, is known to block β-catenin/Wnt-signalling by forming a complex with Wnt- LRP receptors (Brott and Sokol 2002). One possibility that has not been tested is comparing the affinity of LRP5/6 for SOSTDC1 in comparison to Dkk1. BMP antagonist noggin also had variable suppressive effect on the differentiation and mineralisation activity of OB progenitor cultures. Noggin inhibited BMP-induced ALP activity and Runx2 expression throughout early OB progenitor differentiation. This is consistent with other reports which have shown noggin to inhibit differentiation in BMC and pre-osteoblastic UAMS-33 cell cultures (Lecka-Czernik, Gubrij et al. 1999, Abe, Yamamoto et al. 2000). The negative effect of noggin on OB progenitor mineralisation was not significant at any time point throughout differentiation compared to SOSTDC1 in the same experiments. This may have been due to the dosage of noggin used in these studies; i.e. higher dosage of noggin may have suppressed BMP-induced OB progenitor mineralisation.

To establish a clearer understanding of the molecular mechanisms by which SOSTDC1 interfered with Wnt and BMP signalling, protein levels downstream of activated Wnt and BMP signalling pathways were quantified following acute treatments with recombinant SOSTDC1 protein. In Wnt signalling, the activation of the LRP5/6 receptors results in β-catenin stabilisation, phosphorylation and its translocation into the nucleus inducing the transcription of target genes (Miller, Hocking et al. 1999). Wnt-induced stabilisation of β-catenin is central to the effect of Wnt ligands on proliferation and differentiation in OB cells. Studies have shown that loss of function in LRP5 causes reduced bone formation in

245

postnatal humans and mice (Gong, Slee et al. 2001, Kato, Patel et al. 2002) and point mutations in the LRP5 receptor increase bone mass (Boyden, Mao et al. 2002), highlighting the crucial role of Wnt-LRP signal transduction in bone development. It is not known whether SOSTDC1 has any influence on β-catenin/Wnt signalling in differentiating OB cells. The western blot data in the present study showed that SOSTDC1 in the presence of Wnt3a, reduced protein level of β-catenin phosphorylation. Similarly, western blotting was also used to quantify phosphorylated levels of regulatory Smad complexes downstream of the BMP signalling pathway following treatment with recombinant SOSTDC1 protein in the presence of BMP2 or BMP7. The Addition of SOSTDC1 in the presence of BMP ligands reversed BMP-induced Smad phosphorylation in OB progenitor cells of an early lineage. Consistently throughout the present studies it was apparent that SOSTDC1 antagonised Wnt/BMP signalling in OB progenitors that were still in the early phase of differentiation. This is interesting as data from *in-vitro* studies have suggested that Dkk1 mainly affects the function of mature OB cells and drives pluripotent cells to an OB linage (Morvan, Boulukos et al. 2006). It may be that Dkk1 targets mature OB cells and SOSTDC1 targets immature osteoprogenitors in an MM setting.

It is interesting to note that the suppressive SOSTDC1 effects within the present study were only observed when OB progenitors were in the presence of excess Wnt or BMP ligand. Immunohistochemical and *in situ* hybridization analyses carried out as early as the 1970's demonstrated that OB express BMPs and their receptors at high fracture repair (Helder, Ozkaynak et al. 1995, Lyons, Hogan et al. 1995, Yamaguchi, Komori et al. 2000). The canonical Wnt proteins are also known to be upregulated at the sites of bone fractures, inducing osteoblastogensis. Hadjiargyrou et al reported increased mRNAs for Wnt ligands, LRP5 receptors and β-catenin at bone fracture sites. There data suggests that Wnts have an essential role in the early stages of bone healing which involve the upregulation of OB activity (Hadjiargyrou, Lombardo et al. 2002). On the basis of the above data, it could be hypothesised that SOSTDC1 antagonises Wnt and BMP-induced signalling when the OB is under stress and producing high levels of Wnt and BMP molecules. In osteolytic bone disease in MM, where fractures are common, there may be high levels of Wnt and BMP ligands providing the optimal molecular environment for SOSTDC1 activity. This hypothesis can be supported by reports that Dkk1 also prevents

the activation of the Wnt/β-catenin/Tcf reporter during early fracture healing and supresses bone regeneration (Kim, Leucht et al. 2007).

Studies by Lintern and Guidato et al addressed the notion that SOSTDC1 may have separate domains for Wnt and BMP interaction. Immunoprecipitation analysis revealed the independent binding capabilities of SOSTDC1 to LRP6 and BMP4, as SOSTDC1-LRP6 binding was not disrupted by the addition of BMP4. Conversely, addition of LRP6 impeded the effect of BMP4 suppression by SOSTDC1, implicating that SOSTDC1 bound to LRP6 loses its full potential as a BMP antagonist (Lintern, Guidato et al. 2009). It is not known whether BMP2 and Wnt3a interactions occur independently, synergistically or competitively. Crosstalk between the β-Catenin/Wnt signalling and BMP signalling is poorly understood. There is a lack of functional for identifying downstream target genes of Wnt-BMP signalling intracellular molecules involved in Wnt-BMP dependency. A few recent *in-vitro* studies have demonstrated a synergic relationship between BMP2 and β-catenin during OB differentiation (Rawadi, Vayssiere et al. 2003, Mbalaviele, Sheikh et al. 2005). Although BMP and WNT signalling have been shown to have opposing effects in osteoprogenitors, it seems that they primarily function cooperatively in OB cells (Baron and Kneissel 2013). As an example, Bain and colleagues showed that BMP2 may regulate OB function via modulation of β-catenin/Wnt signalling (Bain, Muller et al. 2003).

The crosstalk between Wnt and BMP is thought to be context dependent, where exogenous BMP ligands have been shown to induce bone regeneration and ectopic bone formation, suggesting differences in the effects of BMP signalling. Exogenous BMPs are thought to be inducers in bone induction and repressors of β-catenin/Wnt signalling in bone homeostasis (Baron and Kneissel 2013). This could provide an explanation for why Baud'huin et al found that in a preclinical rodent model, inhibition of BMPRIA-dependent BMP signalling by the soluble BMPRIA receptor–Fc fusion protein was bone anabolic (Baud'huin, Solban et al. 2012). In the same study, deletion of noggin resulted in a reduction in BMD and bone formation in mice (Baud'huin, Solban et al. 2012). Therefore, BMP activation in the mature skeleton reduces bone formation/mass and this could be regulated through inhibition of Wnt signalling.

Extracellular secreted molecules such as Cerberus and Sclerostin that have a OB-inhibiting function as SOSTDC1, can bind to both BMP/Wnt ligands (Silva, Filipe et al. 2003) and receptors (Ellies, Viviano et al. 2006). There are currently no studies that have investigated the regulatory role of SOSTDC1 on Wnt-BMP crosstalk on differentiating OB progenitors. In the present study I investigated the effect of Wnt3a ligand on Smad phosphorylation downstream of the BMP pathway. This effect was assessed in the presence and absence of SOSTDC1. Western blotting analysis showed Wnt3a induced phosphorylation of Smad1,5&8 protein in OB progenitors and SOSTDC1 reversed this effect during the early stage of differentiation. Furthermore, I found that both BMP2 and BMP7 upregulated phosphorylation β-catenin protein and gene (*CTNNB1*) expression and again SOSTSDC1 supressed this effect in the early stages of OB progenitor differentiation.

Rawadi et al previously studied the crosstalk between Wnt-BMP signalling. This group demonstrated that blocking Wnt/LRP5 signalling with Dkk1 in MSC inhibited of BMP2-induced ALP activity (Rawadi et al, 2003). In the present crosstalk studies, I also demonstrated that SOSTDC1 reduced Wnt3-induced Smad phosphorylation differentiating OB progenitor cells on a similar level to Dkk1. Dkk1 has been shown to targets the BMPRIA BMP receptor in OB and mediate suppression of BMP signalling in mature bone (Kamiya 2012). Furthermore, the data by Liu et al suggested that overexpression of Dkk1 in tooth blocked tissue development and this was associated with the down-regulation of BMP and Msx1/2 expression domains. The BMP-induced *Msx1/2* expression was unaffected in Dkk1-overexpression suggesting that Wnt/β-catenin signals are required upstream of BMP to function (Liu, Chu et al. 2008). SOSTDC1 and Dkk1 both target the LRP/Frz Wnt receptors, blocking Wnt ligand interaction with the receptor complex. Based on these similarities between the antagonistic role of SOSTSDC1 and Dkk1 in Wnt-BMP crosstalk in differentiating OB progenitors, it may be assumed that both molecules have a similar detrimental effect in osteolytic bone disease. One possibility for this similarity may be that in osteolytic bone disease, if one molecule is not in abundance, then the other is produced at high levels to compensate.

Papathanasiou et al in showed that BMP2-induced LRP-5 expression was mediated through Smad1/5/8 binding on the *LRP-5* promoter (Papathanasiou, Malizos et al. 2012). Fukuda et al study a elaborated on the Wnt-BMP regulation of OB differentiation at the

early stages of differentiation in preosteblastic cells, suggesting that crosstalk occurred through a GSK3β-dependent but β-catenin-independent mechanism (Fukuda, Kokabu et al. 2010). This data contradicted Zhang et al, who showed *Lrp5* expression was BMP-induced and BMP2 also upregulated nuclear β-catenin protein levels (Zhang *et al*, 2009). This data suggested that the interaction between Wnt and BMP signalling during OB differentiation is β-catenin-dependent. Similar to the data that I have presented, Zhang e t al also reported that Wnt3a increased transcriptional activity of BMP/Smad reporter and noggin inhibited this effect (Zhang, Oyajobi et al. 2013). In light of the data in the present study and reports within the literature, it can be deduced that the corporative action between Wnt-BMP is mediated by β-catenin-and the regulatory Smad complex within OB progenitors and SOSTDC1 antagonises this interaction. This data also supports findings within the literature showing SOSTDC1 having the molecular ability to bind to both BMP ligands and Wnt LRP receptors. However, it is unknown whether SOSTDC1 binds to LRP6 with a higher affinity than with to BMP2, -4 or -7.

Determining the potency of this molecule for its ligands and receptors allows for a better understanding of the mechanisms involved between SOSTDC1 and Wnt-BMP signalling in OB progenitors. Although no studies have investigated the binding affinity of human recombinant SOSTDC1 protein for LPR6, BMP2 and BMP7, Laurikkala et al did examine the binding of recombinant mouse SOSTDC1 (Ectodin) to BMP2, BMP4, BMP6, and BMP7 ligands using the BIAcore system. Although they showed Ectodin bound to BMP2, BMP4, BMP6, and BMP7 with high affinity (Laurikkala, Kassai et al. 2003), they have not quantified the binding affinity to LRP6. In my study, the affinity of rhSOSTDC1 for BMP2, BMP7 and LRP6 were determined using BLItz technology, which works on a similar principle to Biacore technology. The recombinant SOSTDC1 had a highest binding affinity for BMP7, followed by LRP6 and lastly BMP2. These findings are compelling in that in osteolytic bone disease, SOSTDC1 has a preference for BMP signalling and yet antagonises both the canonical Wnt pathway and BMP signalling pathways in OB differentiation through the Wnt-BMP dependency.

With the exception of breast and renal cancers, the role of SOSTDC1 as a BMP and Wnt antagonist in cancer is not well established. In breast cancer, SOSTDC1 is under-expressed, yet increases Wnt3a and decreases BMP7 signalling (Clausen, Blish et al. 2010). Similarly, in kidney tumours, SOTSDC1 is down-regulated and restoration of

SOSTDC1 expression impairs carcinoma cell proliferation. Both Wnt3a signalling and BMP7 induced phosphorylation of Smads are found to be suppressed by SOSTDC1 (Blish, Wang et al. 2008). There is very little data on the effect of either BMP or Wnt signalling, in myeloma. Nevertheless, Yamaguchi et al did show that BMP2 and -4 induce apoptosis and suppress proliferation of human myeloma cells Yamaguchi, Komori *et al.* 2000). This data is of interest in the context of the present study findigs: perhaps SOSTDC1 binds to BMP7 competitevely and therefore prevents the BMP from exerting its supressive effects on the myeloma cell. The effect of Wnt3a on MM associated bone disease is variable. Qiang *et al* investigated *in-vitro* and *in-vivo* effects of Wnt3a on bone disease and MM cell growth. Their data show that Wnt3a had no effect on MM cell growth *in-vitro*. However, bones engrafted with Wnt3a-expressing NCIH-929 MM cells and mice carrying primary disease, treated with recombinant Wnt3a, exhibited increased OB number and reduced tumour burden (Qiang *et al,* 2008). Along with the findings from this report, these data suggest that both the Wnt and BMP are necessary for bone formation, and that they can potentially interact with each other to induce OB differentiation, in line with the findings from my study.

With this concept in mind, I wanted to further explore the role of SOSTDC1 in the well-characterised mouse 5TMM myeloma models and determine whether this molecule had the potential to contribute to the suppression in osteoblastic activity observed in myeloma. The aim of the final part of the study was to determine whether myeloma and OB progenitor cells expressed SOSTDC1 and to then reveal the conditions under which SOSTDC1 was expressed. Previously, the 'seed and soil' theory has been the predominant concept in myeloma bone disease, in that the myeloma cells use the bone's fertile microenvironment to flourish and exert their detrimental effect on the bone (Guise and Mundy 1998). In this study I considered a new dimension to the 'seed and soil' theory in respect to SOSTDC1 in that myeloma cells may require a direct interaction with the OB cells in order to supress OB differentiation optimally.

Unpublished gene array data from our group had previously shown that SOSTDC1 was upregulated in the 5T2MM myeloma model. This model was no longer available, and as a substitute the 5TGM1MM and 5T33MM models were used. The C57BL/KaLwRij mice injected with 5T33MM myeloma cells did not develop bone disease, so were used to compare any variance in SOSTDC1 with the osteolytic 5TGM1MM model. The data

obtained from immunofluorescent microscopy, flow cytometry, western blotting, end-point PCR and sequencing all showed that 5T33MM and 5TGM1MM cells produced SOSTDC1, in line with the gene array analysis previously performed on 5T2MM cells. However, SOSTDC1 was not detectable in OB progenitor cells under the same experimental conditions used for SOSTDC1 detection in myeloma cells and HK-2 cell positive control.

To determine whether interaction between the myeloma cells and OB progenitors had any effect on SOSTDC1 expression, the myeloma cells were co-cultured with the differentiating OB progenitors. Using cells cultured on their own, the level of SOSTDC1 was also determined. The data from this study showed that SOSTDC1 was upregulated in the co-cultured 5TGM1MM cells but not 5T33MM cells. Interestingly, OB progenitors that had been co-cultured with myeloma cells and then sorted now expressed SOSTDC1 detectable on a protein and gene level. This 'switch on' in SOSTDC1 expression was further confirmed by sequencing the end-point PCR reaction products obtained from sorted OB progenitor cells. The SOSTDC1 levels in myeloma cells that were co-cultured with OB progenitors but had not adhered to the OB progenitor cells were semi-quantitatively measured to compare with SOSTDC1 levels in adherent myeloma cells. This experiment addressed the question of whether SOSTDC1 production in myeloma cells was dependent on the cells physically adhering to OB progenitors. The 5TGM1MM cells that had adhered to OB progenitors expressed a higher level of SOSTDC1 compared to cells that had not adhered to the OB progenitors. Interestingly, in experiments with 5T33MM cells there were no differences SOSTDC1 levels of adherent and non-adherent 5T33MM cells. The fact that SOSTDC1 seemed to have more of a role in the lytic 5TGM1MM-OB progenitor interactions compared to the non-lytic 5T33MM model in general was important. Direct comparison of the SOSTDC1 levels in 5T33MM versus 5TGM1MM showed that 5TGM1MM cells expressed a higher level of SOSTDC1. This is perhaps not surprising as in the literature the 5T33MM model is commonly used for investigating myeloma cell homing and proliferation whereas the 5TGM1MM model is preferred for the study of bone disease (Croese, Vas Nunes et al. 1987, Vanderkerken, De Raeve et al. 1997). If SOSTDC1 is indeed upregulated in myeloma-OB interaction and exerts its antagonistic effects on osteoblastogensis, then it would be expected that SOSTDC1 would have more of a regulatory role in the lytic 5TGM1MM cells.

Immunohistochemical analysis of 10 days post-injection 5T33MM and 5TGM1MM tibiae sections stained confirmed that SOSTDC1 was present in bone that was infiltrated with myeloma disease compared to an absence of SOSTDC1 in naïve bone sections. This data complemented the *in-vitro* results in that SOSTDC1 staining was mainly observed in sites were myeloma cells formed colonies. In areas of the 5T33MM/5TGM1MM sections were myeloma colonies were stained for SOSTDC1, OB/bon-lining cells could be identified. However, in the same 5T33MM/5TGM1MM sections, in areas were no myeloma colonies were present, there was little SOSTDC1 staining and some OB/bone-lining cells could be identified.

Finally, my studies have linked concept that SOSTDC1 is upregulated as a result of myeloma-OB progenitor interaction to the proposed hypothesis that excess SOSTDC1 available in the bone microenvironment then has a detrimental effect on the OB-progenitor differentiation. The myeloma-OB progenitor co-cultures were treated with 1.5µg/ml of commercial anti-SOSTDC1 antibody, previously determined to be specific for SOSTDC1 by western blotting.

Detection of Runx2 gene expression, known to have a pivotal role in OB differentiation (Philip, Bulbule et al. 2001), was detected in OB progenitor cultures and 5TGM1MM cells cultures alone and together in the presence and absence of the anti-SOSTDC1 antibody. Runx2 was detectable in OB progenitor cultures but not in 5TGM1MM cells in context with the literature, with the exception of a study by Colla et al, demonstrating for the first time the expression and of Runx2/Cbfa1 in human myeloma cells (Colla, Morandi et al. 2005). The co-culture of 5TGM1MM and OB progenitors resulted in reduced levels of Runx2. Furthermore, treatment of myeloma-OB progenitor co-cultures with the anti-SOSTDC1 antibody resulted in reversal of this myeloma-induced Runx2 suppression. Taken together this compelling data provides a clearer insight into the role of SOSTDC1 in myeloma-bone disease, which is best summarised diagrammatically as illustrated in **Figure 7.**
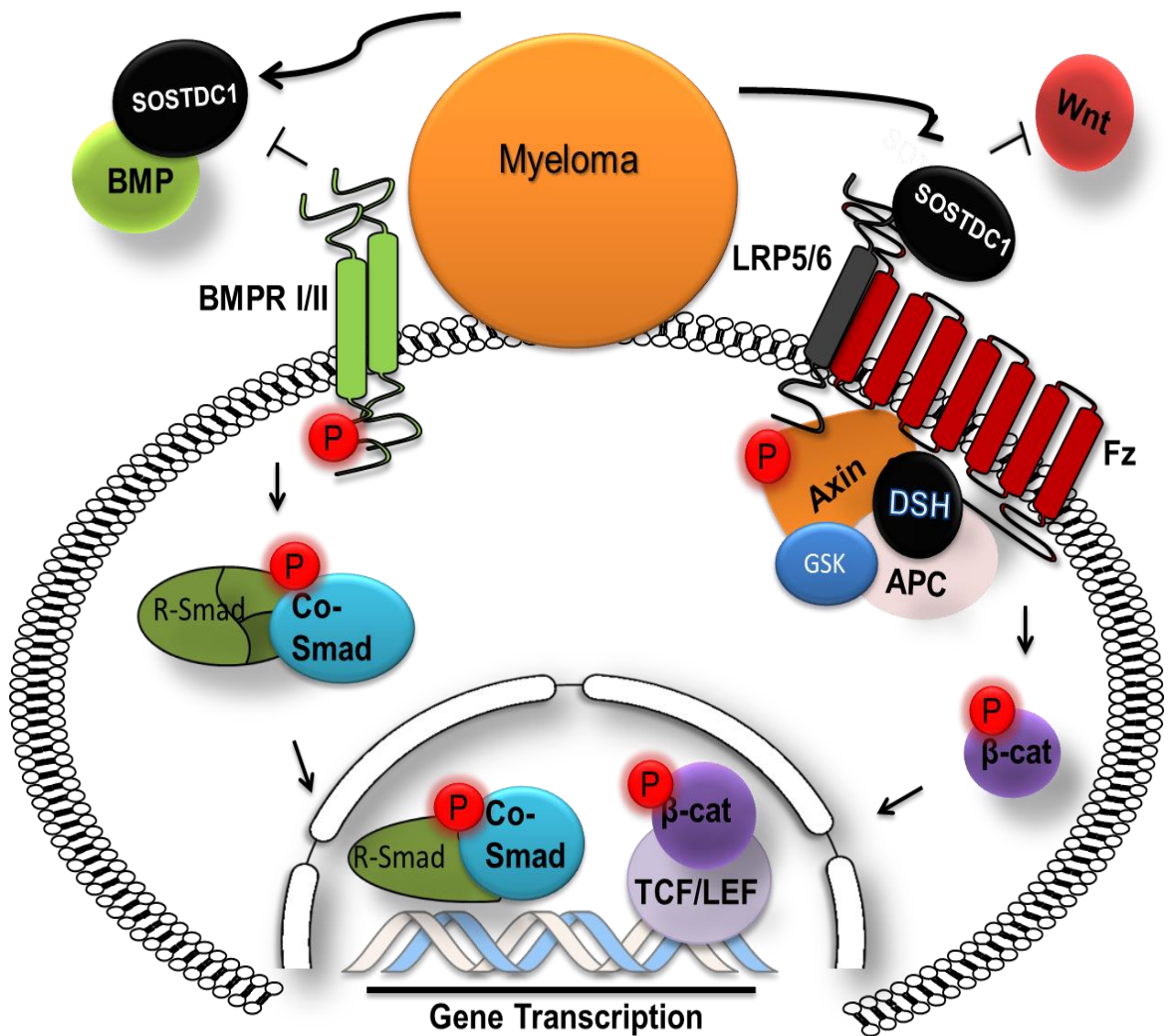
Figure 7 - *Schematic diagram of the potential antagonistic effect of myeloma induced SOSTDC1 expression on Wnt and BMP signalling pathways.*

7.2 Future Studies

Despite the high incidence of bone related complications secondary to MM, there is an obvious need for improved preventative regimes and drug treatments (Roodman 2011). Although we now have a relatively clear insight into the mechanism by which myeloma-induced bone resorption is up-regulated, our understanding of the mechanism responsible for OB suppression is not so clear. SOSTDC1 expression and its role within both Wnt and BMP signalling, has been implicated as a mechanism in various tissues (Lintern, Guidato et al. 2009). However, to date no data has been published on the role of SOSTDC1 in the suppression of bone formation in MM. Determination of SOSTDC1 effect if any, on OB differentiation and proliferation *in-vitro* is key to understanding the role of this novel protein in myeloma-induced suppression of bone formation and perhaps bone resorption.

We have raised monoclonal antibodies against SOSTDC1 in rats. Western blot analysis will be used to characterise the specificity of these anti-SOSTDC1 antibodies. The monoclonal anti-SOSTDC1 antibody will be a more useful tool due to its specificity, particularly when used in *in-vivo* investigations. Currently there are no available manufactured monoclonal antibodies against SOSTDC1. Therefore, characterisation of in-house antibodies is potentially a very important tool in both the detection and blockade of SOSTDC1 expression MM experimental models. The next step is to determine the effect of administrating rhSOSTDC1 as well as blocking SOSTDC1 on of bone formation in experimental models of myeloma *in-vivo*. We have already carried out a pilot study in investigation the ability of SOSTDC1 to inhibit bone formation *in-vivo*. C57BLkawRij mice were injected locally with rhSOSTDC1 on one side of the calvaria and vehicle (rh-GST) on the condralateral side. MicroCT analysis revealed significantly reduced OB number. The next pilot study will involve administration of systemic injection to mouse tibia and vertebrae and then in the presence or absence of the BMP and Wnt ligands. The effect on bone structure will be determined by microCT analysis as well as static and dynamic bone histomorphometry. To look at blocking SOSTDC1 in MM models, C57BLkawRij mice will be injected with 5T2MM murine myeloma cells and treated with antibodies to SOSTDC1. The effect of treatment on the development of myeloma bone disease will be determined by microCT analysis, as well as static and dynamic bone histomorphometry. Although the 5TMM series are reproducible and an excellent model for MM studies, there is a constant need for the development of these animal models to

further enhance our understanding of MM as well as the limitations associated with them. In humans, MM is heterogeneous as a disease and this poses a problem in that no single animal model can constitute of all MM features. This study would benefit from looking into SOSTDC1 expression in human myeloma cell lines and human BM samples so as to move into translational research for potential therapeutic purposes.

From the data in this study, it has become apparent that interaction between myeloma and the OB cell is a requirement in stimulating the production of SOSTDC1 in both myeloma and OB cells. Previously, the 'seed and soil' theory has been the predominant concept in myeloma bone disease, in that the myeloma cells use the bone's fertile microenvironment to flourish and exert their detrimental effect on the bone (Guise and Mundy 1998). The data presented in this study could add a dimension to this concept, in that not only do the myeloma cells select the environment that best suits their requirements to thrive, but they may also switch on OB-signalling antagonists by interacting with the OB cells directly. It would be interesting to determine whether myeloma interact with any other cells within the bone marrow as there no data within the literature. The role of SOSTDC1 has not been investigated in myeloma-OC interaction. It would be valuable to determine whether SOSTDC1 role is specific to OB-mediated osteolytic bone disease or also regulates the increased OC activity observed in MM. This theory is based on Pederson et al data showing that stimulation of human MSC nodule formation by OC conditioned media was diminished by Dkk1 and a BMP6-neutralizing antibody (Pederson, Ruan et al. 2008).

Therapeutic neutralising antibodies against Sclerostin and Dkk1 are currently in late preclinical/early clinical development for the treatment of osteolytic lesions in MM. Although these therapeutic antibodies are a good starting point for the modulation of Wnt signalling pharmacologically, the ultimate objective would be to develop orally active compounds that target both OC and OB activity (Ke, Richards et al. 2012). Future projects could focus on combining Dkk1 and SOSTDC1 as one treatment to determine whether the two together could be a more effective form of therapy.

Bibliography

Abe, E., Yamamoto, M., Taguchi, Y., Lecka-Czernik, B., O'Brien, C. A., Economides, A. N., Stahl, N., Jilka, R. L. and Manolagas, S. C. (2000). "Essential requirement of BMPs-2/4 for both osteoblast and osteoclast formation in murine bone marrow cultures from adult mice: antagonism by noggin." Journal of Bone and Mineral Research 15(4): 663-673.

Aeschlimann, D. and Evans, B. A. (2004). "The vital osteoclast: how is it regulated?" Cell Death and Differentiation 11 Suppl 1: S5-7.

Ahn, Y., Sanderson, B. W., Klein, O. D. and Krumlauf, R. (2010). "Inhibition of Wnt signaling by Wise (Sostdc1) and negative feedback from Shh controls tooth number and patterning." Development 137(19): 3221-3231.

Alarmo, E. L., Kuukasjarvi, T., Karhu, R. and Kallioniemi, A. (2007). "A comprehensive expression survey of bone morphogenetic proteins in breast cancer highlights the importance of BMP4 and BMP7." Breast Cancer Research and Treatment 103(2): 239-246.

Alarmo, E. L., Rauta, J., Kauraniemi, P., Karhu, R., Kuukasjarvi, T. and Kallioniemi, A. (2006). "Bone morphogenetic protein 7 is widely overexpressed in primary breast cancer." Genes Chromosomes Cancer 45(4): 411-419.

Arnett, T. (2003). "Regulation of bone cell function by acid-base balance." The Proceedings of the Nutrition Society 62(2): 511-520.

Asosingh, K., Radl, J., Van Riet, I., Van Camp, B. and Vanderkerken, K. (2000). "The 5TMM series: a useful in-vivo mouse model of human multiple myeloma." The Hematology Journal 1(5): 351-356.

Attal, M., Harousseau, J. L., Stoppa, A. M., Sotto, J. J., Fuzibet, J. G., Rossi, J. F., Casassus, P., Maisonneuve, H., Facon, T., Ifrah, N., Payen, C. and Bataille, R. (1996). "A prospective, randomized trial of autologous bone marrow transplantation and chemotherapy in multiple myeloma. Intergroupe Francais du Myelome." New England Journal of Medicine 335(2): 91-97.

Avcu, F., Ural, A. U., Yilmaz, M. I., Ozcan, A., Ide, T., Kurt, B. and Yalcin, A. (2005). "The bisphosphonate zoledronic acid inhibits the development of plasmacytoma induced in BALB/c mice by intraperitoneal injection of pristane." European Journal of Hematology 74(6): 496-500.

Avsian-Kretchmer, O. and Hsueh, A. J. (2004). "Comparative genomic analysis of the eight-membered ring cystine knot-containing bone morphogenetic protein antagonists." Molecular Endocrinology 18(1): 1-12.

Bain, G., Muller, T., Wang, X. and Papkoff, J. (2003). "Activated beta-catenin induces osteoblast differentiation of C3H10T1/2 cells and participates in BMP2 mediated signal transduction." Biochemical and Biophysical Research Communications 301(1): 84-91.

Barille, S., Collette, M., Bataille, R. and Amiot, M. (1995). "Myeloma cells upregulate interleukin-6 secretion in osteoblastic cells through cell-to-cell contact but downregulate osteocalcin." Blood **86**(8): 3151-3159.

Baron, R. and Kneissel, M. (2013). "WNT signaling in bone homeostasis and disease: from human mutations to treatments." Nature Medicine **19**(2): 179-192.

Bataille, R., Chappard, D., Marcelli, C., Dessauw, P., Baldet, P., Sany, J. and Alexandre, C. (1991). "Recruitment of new osteoblasts and osteoclasts is the earliest critical event in the pathogenesis of human multiple myeloma." Journal of Clinical Investigation **88**(1): 62-66.

Baud'huin, M., Solban, N., Cornwall-Brady, M., Sako, D., Kawamoto, Y., Liharska, K., Lath, D., Bouxsein, M. L., Underwood, K. W., Ucran, J., Kumar, R., Pobre, E., Grinberg, A., Seehra, J., Canalis, E., Pearsall, R. S. and Croucher, P. I. (2012). "A soluble bone morphogenetic protein type IA receptor increases bone mass and bone strength." Proceedings of the National Academy of Sciences of the United States of America **109**(30): 12207-12212.

Beaudoin, G. M., 3rd, Sisk, J. M., Coulombe, P. A. and Thompson, C. C. (2005). "Hairless triggers reactivation of hair growth by promoting Wnt signaling." Proceedings of the National Academy of Sciences of the United States of America **102**(41): 14653-14658.

Beck, G. R., Jr., Zerler, B. and Moran, E. (2001). "Gene array analysis of osteoblast differentiation." Cell Growth & Differentiation **12**(2): 61-83.

Bennett, C. N., Longo, K. A., Wright, W. S., Suva, L. J., Lane, T. F., Hankenson, K. D. and MacDougald, O. A. (2005). "Regulation of osteoblastogenesis and bone mass by Wnt10b." Proceedings of the National Academy of Sciences of the United States of America **102**(9): 3324-3329.

Birmingham, E., Niebur, G. L., McHugh, P. E., Shaw, G., Barry, F. P. and McNamara, L. M. (2012). "Osteogenic differentiation of mesenchymal stem cells is regulated by osteocyte and osteoblast cells in a simplified bone niche." European Cells & Materials **23**: 13-27.

Blish, K. R., Clausen, K. A., Hawkins, G. A., Garvin, A. J., Willingham, M. C., Turner, J. C., Torti, F. M. and Torti, S. V. (2010). "Loss of heterozygosity and SOSTDC1 in adult and pediatric renal tumors." Journal of Experimental & Clinical Cancer Research **29**: 147.

Blish, K. R., Wang, W., Willingham, M. C., Du, W., Birse, C. E., Krishnan, S. R., Brown, J. C., Hawkins, G. A., Garvin, A. J., D'Agostino, R. B., Jr., Torti, F. M. and Torti, S. V. (2008). "A human bone morphogenetic protein antagonist is down-regulated in renal cancer." Molecular Biology of the Cell **19**(2): 457-464.

Boise, L. H., Kaufman, J. L., Bahlis, N. J., Lonial, S. and Lee, K. P. (2014). "The Tao of myeloma." Blood **124**(12): 1873-1879.

Bonewald, L. F. (2011). "The amazing osteocyte." Journal of Bone Mineral Research **26**(2): 229-238.

Boyden, L. M., Mao, J., Belsky, J., Mitzner, L., Farhi, A., Mitnick, M. A., Wu, D., Insogna, K. and Lifton, R. P. (2002). "High bone density due to a mutation in LDL-receptor-related protein 5." New England Journal of Medicine **346**(20): 1513-1521.

Brott, B. K. and Sokol, S. Y. (2002). "Regulation of Wnt/LRP signaling by distinct domains of Dickkopf proteins." Journal of Molecular Cell Biology **22**(17): 6100-6110.

Brounais, B., Ruiz, C., Rousseau, J., Lamoureux, F., Blanchard, F., Heymann, D. and Redini, F. (2008). "Novel anti-cancer strategy in bone tumors by targeting molecular and cellular modulators of bone resorption." Recent Patents on Anti-Cancer Drug Discovery **3**(3): 178-186.

Brunetti, G., Oranger, A., Mori, G., Specchia, G., Rinaldi, E., Curci, P., Zallone, A., Rizzi, R., Grano, M. and Colucci, S. (2011). "Sclerostin is overexpressed by plasma cells from multiple myeloma patients." Annals of the New York Academy of Sciences **1237**: 19-23.

Brunkow, M. E., Gardner, J. C., Van Ness, J., Paeper, B. W., Kovacevich, B. R., Proll, S., Skonier, J. E., Zhao, L., Sabo, P. J., Fu, Y., Alisch, R. S., Gillett, L., Colbert, T., Tacconi, P., Galas, D., Hamersma, H., Beighton, P. and Mulligan, J. (2001). "Bone dysplasia sclerosteosis results from loss of the SOST gene product, a novel cystine knot-containing protein." American Journal of Human Genetics **68**(3): 577-589.

Buckle, C. H., Neville-Webbe, H. L., Croucher, P. I. and Lawson, M. A. (2010). "Targeting RANK/RANKL in the treatment of solid tumours and myeloma." Current Pharmaceutical Design **16**(11): 1272-1283.

Cancer Research UK. (2014). "Myeloma statistics." Retrieved 28/11/2014, from http://www.cancerresearchuk.org/cancer-info/cancerstats/types/myeloma/uk-multiple-myeloma-statistics.

Chen, G., Deng, C. and Li, Y. P. (2012). "TGF-beta and BMP signaling in osteoblast differentiation and bone formation." International Journal of Biological Sciences **8**(2): 272-288.

Chen, Y., Whetstone, H. C., Lin, A. C., Nadesan, P., Wei, Q., Poon, R. and Alman, B. A. (2007). "Beta-catenin signaling plays a disparate role in different phases of fracture repair: implications for therapy to improve bone healing." PLoS medicine **4**(7): e249.

Chen, Z., Orlowski, R. Z., Wang, M., Kwak, L. and McCarty, N. (2014). "Osteoblastic niche supports the growth of quiescent multiple myeloma cells." Blood **123**(14): 2204-2208.

Chiang, A. C. and Massague, J. (2008). "Molecular basis of metastasis." New England Journal of Medicine **359**(26): 2814-2823.

Chitteti, B. R., Cheng, Y. H., Streicher, D. A., Rodriguez-Rodriguez, S., Carlesso, N., Srour, E. F. and Kacena, M. A. (2010). "Osteoblast lineage cells expressing high levels of Runx2 enhance hematopoietic progenitor cell proliferation and function." Journal of Cellular Biochemistry **111**(2): 284-294.

Cho, S. W., Kwak, S., Woolley, T. E., Lee, M. J., Kim, E. J., Baker, R. E., Kim, H. J., Shin, J. S., Tickle, C., Maini, P. K. and Jung, H. S. (2011). "Interactions between Shh, Sostdc1 and Wnt signaling and a new feedback loop for spatial patterning of the teeth." Development **138**(9): 1807-1816.

Clausen, K. A., Blish, K. R., Birse, C. E., Triplette, M. A., Kute, T. E., Russell, G. B., D'Agostino, R. B., Jr., Miller, L. D., Torti, F. M. and Torti, S. V. (2011). "SOSTDC1 differentially modulates Smad and beta-catenin activation and is down-regulated in breast cancer." Breast Cancer Research and Treatment **129**(3): 737-746.

Coelho, M. J. and Fernandes, M. H. (2000). "Human bone cell cultures in biocompatibility testing. Part II: effect of ascorbic acid, beta-glycerophosphate and dexamethasone on osteoblastic differentiation." Biomaterials **21**(11): 1095-1102.

Colla, S., Morandi, F., Lazzaretti, M., Rizzato, R., Lunghi, P., Bonomini, S., Mancini, C., Pedrazzoni, M., Crugnola, M., Rizzoli, V. and Giuliani, N. (2005). "Human myeloma cells express the bone regulating gene Runx2/Cbfa1 and produce osteopontin that is involved in angiogenesis in multiple myeloma patients." Leukemia **19**(12): 2166-2176.

Crockett, J. C., Rogers, M. J., Coxon, F. P., Hocking, L. J. and Helfrich, M. H. (2011). "Bone remodelling at a glance." Journal of Cell Science **124**(Pt 7): 991-998.

Croese, J. W., Vas Nunes, C. M., Radl, J., van den Enden-Vieveen, M. H., Brondijk, R. J. and Boersma, W. J. (1987). "The 5T2 mouse multiple myeloma model: characterization of 5T2 cells within the bone marrow." British Journal of Cancer **56**(5): 555-560.

Czekanska, E. M., Stoddart, M. J., Richards, R. G. and Hayes, J. S. (2012). "In search of an osteoblast cell model for in-vitro research." European Cells & Materials **24**: 1-17.

Dankbar, B., Padro, T., Leo, R., Feldmann, B., Kropff, M., Mesters, R. M., Serve, H., Berdel, W. E. and Kienast, J. (2000). "Vascular endothelial growth factor and interleukin-6 in paracrine tumor-stromal cell interactions in multiple myeloma." Blood **95**(8): 2630-2636.

Day, T. F., Guo, X., Garrett-Beal, L. and Yang, Y. (2005). "Wnt/beta-catenin signaling in mesenchymal progenitors controls osteoblast and chondrocyte differentiation during vertebrate skeletogenesis." Developmental Cell **8**(5): 739-750.

Del Fattore, A., Teti, A. and Rucci, N. (2012). "Bone cells and the mechanisms of bone remodelling." Frontiers in Bioscience **4**: 2302-2321.

Delgado-Calle, J., Bellido, T. and Roodman, G. D. (2014). "Role of osteocytes in multiple myeloma bone disease." Current Opinion in Supportive and Palliative Care **8**(4):407-13.

Dougall, W. C., Glaccum, M., Charrier, K., Rohrbach, K., Brasel, K., De Smedt, T., Daro, E., Smith, J., Tometsko, M. E., Maliszewski, C. R., Armstrong, A., Shen, V., Bain, S., Cosman, D., Anderson, D., Morrissey, P. J., Peschon, J. J. and Schuh, J. (1999). "RANK is essential for osteoclast and lymph node development." Genes and Development 13(18): 2412-2424.

Ducy, P. (2000). "Cbfa1: a molecular switch in osteoblast biology." Developmental Dynamics 219(4): 461-471.

Ducy, P., Schinke, T. and Karsenty, G. (2000). "The osteoblast: a sophisticated fibroblast under central surveillance." Science 289(5484): 1501-1504.

Ducy, P., Zhang, R., Geoffroy, V., Ridall, A. L. and Karsenty, G. (1997). "Osf2/Cbfa1: a transcriptional activator of osteoblast differentiation." Cell 89(5): 747-754.

Ecarot-Charrier, B., Glorieux, F. H., van der Rest, M. and Pereira, G. (1983). "Osteoblasts isolated from mouse calvaria initiate matrix mineralization in culture." Journal of Cell Biology 96(3): 639-643.

Edlund, S., Lee, S. Y., Grimsby, S., Zhang, S., Aspenstrom, P., Heldin, C. H. and Landstrom, M. (2005). "Interaction between Smad7 and beta-catenin: importance for transforming growth factor beta-induced apoptosis." Journal of Molecular Cell Biology 25(4): 1475-1488.

Edwards, C. M., Lwin, S. T., Fowler, J. A., Oyajobi, B. O., Zhuang, J., Bates, A. L. and Mundy, G. R. (2009). "Myeloma cells exhibit an increase in proteasome activity and an enhanced response to proteasome inhibition in the bone marrow microenvironment in-vivo." American Journal of Hematology 84(5): 268-272.

Egan, J. B., Shi, C. X., Tembe, W., Christoforides, A., Kurdoglu, A., Sinari, S., Middha, S., Asmann, Y., Schmidt, J., Braggio, E., Keats, J. J., Fonseca, R., Bergsagel, P. L., Craig, D. W., Carpten, J. D. and Stewart, A. K. (2012). "Whole-genome sequencing of multiple myeloma from diagnosis to plasma cell leukemia reveals genomic initiating events, evolution, and clonal tides." Blood 120(5): 1060-1066.

Ehrlich, L. A., Chung, H. Y., Ghobrial, I., Choi, S. J., Morandi, F., Colla, S., Rizzoli, V., Roodman, G. D. and Giuliani, N. (2005). "IL-3 is a potential inhibitor of osteoblast differentiation in multiple myeloma." Blood 106(4): 1407-1414.

Ellies, D. L., Viviano, B., McCarthy, J., Rey, J. P., Itasaki, N., Saunders, S. and Krumlauf, R. (2006). "Bone density ligand, Sclerostin, directly interacts with LRP5 but not LRP5G171V to modulate Wnt activity." Journal of Bone and Mineral Research 21(11): 1738-1749.

Feng, X. and McDonald, J. M. (2010). "Disorders of Bone Remodeling." Annual Review of Pathology 6(1): 121-45.

Fernandes, R. J., Harkey, M. A., Weis, M., Askew, J. W. and Eyre, D. R. (2007). "The post-translational phenotype of collagen synthesized by SAOS-2 osteosarcoma cells." Bone 40(5): 1343-1351.

Fogh, J., Fogh, J. M. and Orfeo, T. (1977). "One hundred and twenty-seven cultured human tumor cell lines producing tumors in nude mice." Journal of the National Cancer Institute **59**(1): 221-226.

Forsman, C. L., Ng, B. C., Heinze, R. K., Kuo, C., Sergi, C., Gopalakrishnan, R., Yee, D., Graf, D., Schwertfeger, K. L. and Petryk, A. (2013). "BMP-binding protein twisted gastrulation is required in mammary gland epithelium for normal ductal elongation and myoepithelial compartmentalization." Developmental Biology **373**(1): 95-106.

Fowler, J. A., Edwards, C. M. and Croucher, P. I. (2011). "Tumor-host cell interactions in the bone disease of myeloma." Bone **48**(1): 121-128.

Fowler, J. A., Mundy, G. R., Lwin, S. T., Lynch, C. C. and Edwards, C. M. (2009). "A murine model of myeloma that allows genetic manipulation of the host microenvironment." Disease Models & Mechanisms **2**(11-12): 604-611.

Fuentealba, L. C., Eivers, E., Ikeda, A., Hurtado, C., Kuroda, H., Pera, E. M. and De Robertis, E. M. (2007). "Integrating patterning signals: Wnt/GSK3 regulates the duration of the BMP/Smad1 signal." Cell **131**(5): 980-993.

Fukuda, T., Kokabu, S., Ohte, S., Sasanuma, H., Kanomata, K., Yoneyama, K., Kato, H., Akita, M., Oda, H. and Katagiri, T. (2010). "Canonical Wnts and BMPs cooperatively induce osteoblastic differentiation through a GSK3beta-dependent and beta-catenin-independent mechanism." Differentiation **80**(1): 46-52.

Gartland, A., Rumney, R. M., Dillon, J. P. and Gallagher, J. A. (2012). "Isolation and culture of human osteoblasts." Methods in Molecular Biology **806**: 337-355.

Girasole, G., Passeri, G., Jilka, R. L. and Manolagas, S. C. (1994). "Interleukin-11: a new cytokine critical for osteoclast development." Journal of Clinical Investigation **93**(4): 1516-1524.

Giuliani, N., Colla, S., Morandi, F., Lazzaretti, M., Sala, R., Bonomini, S., Grano, M., Colucci, S., Svaldi, M. and Rizzoli, V. (2005). "Myeloma cells block RUNX2/CBFA1 activity in human bone marrow osteoblast progenitors and inhibit osteoblast formation and differentiation." Blood **106**(7): 2472-2483.

Giuliani, N., Ferretti, M., Bolzoni, M., Storti, P., Lazzaretti, M., Dalla Palma, B., Bonomini, S., Martella, E., Agnelli, L., Neri, A., Ceccarelli, F. and Palumbo, C. (2012). "Increased osteocyte death in multiple myeloma patients: role in myeloma-induced osteoclast formation." Leukemia **26**(6): 1391-1401.

Giuliani, N., Morandi, F., Tagliaferri, S., Lazzaretti, M., Donofrio, G., Bonomini, S., Sala, R., Mangoni, M. and Rizzoli, V. (2007). "Production of Wnt inhibitors by myeloma cells: potential effects on canonical Wnt pathway in the bone microenvironment." Cancer Research **67**(16): 7665-7674.

Giuliani, N., Rizzoli, V. and Roodman, G. D. (2006). "Multiple myeloma bone disease: Pathophysiology of osteoblast inhibition." Blood **108**(13): 3992-3996.

Glass, D. A., 2nd, Bialek, P., Ahn, J. D., Starbuck, M., Patel, M. S., Clevers, H., Taketo, M. M., Long, F., McMahon, A. P., Lang, R. A. and Karsenty, G. (2005). "Canonical Wnt signaling in differentiated osteoblasts controls osteoclast differentiation." Developmental Cell **8**(5): 751-764.

Gong, Y., Slee, R. B., Fukai, N., Rawadi, G., Roman-Roman, S., Reginato, A. M., Wang, H., Cundy, T., Glorieux, F. H., Lev, D., Zacharin, M., Oexle, K., Marcelino, J., Suwairi, W., Heeger, S., Sabatakos, G., Apte, S., Adkins, W. N., Allgrove, J., Arslan-Kirchner, M., Batch, J. A., Beighton, P., Black, G. C., Boles, R. G., Boon, L. M., Borrone, C., Brunner, H. G., Carle, G. F., Dallapiccola, B., De Paepe, A., Floege, B., Halfhide, M. L., Hall, B., Hennekam, R. C., Hirose, T., Jans, A., Juppner, H., Kim, C. A., Keppler-Noreuil, K., Kohlschuetter, A., LaCombe, D., Lambert, M., Lemyre, E., Letteboer, T., Peltonen, L., Ramesar, R. S., Romanengo, M., Somer, H., Steichen-Gersdorf, E., Steinmann, B., Sullivan, B., Superti-Furga, A., Swoboda, W., van den Boogaard, M. J., Van Hul, W., Vikkula, M., Votruba, M., Zabel, B., Garcia, T., Baron, R., Olsen, B. R. and Warman, M. L. (2001). "LDL receptor-related protein 5 (LRP5) affects bone accrual and eye development." Cell **107**(4): 513-523.

Griffiths, T. D. and Ling, S. Y. (1991). "Effect of UV light on DNA chain growth and replicon initiation in xeroderma pigmentosum variant cells." Mutagenesis **6**(4): 247-251.

Guise, T. A. and Mundy, G. R. (1998). "Cancer and bone." Endocrine Reviews **19**(1): 18-54.

Gundle, R. and Beresford, J. N. (1995). "The isolation and culture of cells from explants of human trabecular bone." Calcified Tissue International **56 Suppl 1**: S8-10.

Hadjiargyrou, M., Lombardo, F., Zhao, S., Ahrens, W., Joo, J., Ahn, H., Jurman, M., White, D. W. and Rubin, C. T. (2002). "Transcriptional profiling of bone regeneration. Insight into the molecular complexity of wound repair." The Journal of Biological Chemistry **277**(33): 30177-30182.

Hameed, A., Brady, J. J., Dowling, P., Clynes, M. and O'Gorman, P. (2014). "Bone disease in multiple myeloma: pathophysiology and management." Cancer Growth Metastasis **7**: 33-42.

Hasegawa, Y., Shimada, K., Suzuki, N., Takayama, T., Kato, T., Iizuka, T., Sato, S. and Ito, K. (2008). "The in-vitro osteogenetic characteristics of primary osteoblastic cells from a rabbit calvarium." Journal of Oral Science **50**(4): 427-434.

He, J. W., Yue, H., Hu, W. W., Hu, Y. Q. and Zhang, Z. L. (2011). "Contribution of the sclerostin domain-containing protein 1 (SOSTDC1) gene to normal variation of peak bone mineral density in Chinese women and men." Journal of Bone and Mineral Metabolism **29**(5): 571-581.

Heath, D. J., Chantry, A. D., Buckle, C. H., Coulton, L., Shaughnessy, J. D., Jr., Evans, H. R., Snowden, J. A., Stover, D. R., Vanderkerken, K. and Croucher, P. I. (2009). "Inhibiting Dickkopf-1 (Dkk1) removes suppression of bone formation and prevents the

development of osteolytic bone disease in multiple myeloma." Journal of Bone and Mineral Research **24**(3): 425-436.

Helder, M. N., Ozkaynak, E., Sampath, K. T., Luyten, F. P., Latin, V., Oppermann, H. and Vukicevic, S. (1995). "Expression pattern of osteogenic protein-1 (bone morphogenetic protein-7) in human and mouse development." The Journal of Histochemistry and Cytochemistry **43**(10): 1035-1044.

Henriksen, K., Karsdal, M. A. and Martin, T. J. (2014). "Osteoclast-derived coupling factors in bone remodeling." Calcified Tissue International **94**(1): 88-97.

Hill, T. P., Spater, D., Taketo, M. M., Birchmeier, W. and Hartmann, C. (2005). "Canonical Wnt/beta-catenin signaling prevents osteoblasts from differentiating into chondrocytes." Developmental Cell **8**(5): 727-738.

Hofbauer, L. C., Khosla, S., Dunstan, C. R., Lacey, D. L., Boyle, W. J. and Riggs, B. L. (2000). "The roles of osteoprotegerin and osteoprotegerin ligand in the paracrine regulation of bone resorption." Journal of Bone and Mineral Research **15**(1): 2-12.

Holmen, S. L., Zylstra, C. R., Mukherjee, A., Sigler, R. E., Faugere, M. C., Bouxsein, M. L., Deng, L., Clemens, T. L. and Williams, B. O. (2005). "Essential role of beta-catenin in postnatal bone acquisition." The Journal of Biological Chemistry **280**(22): 21162-21168.

Hu, M. C. and Rosenblum, N. D. (2005). "Smad1, beta-catenin and Tcf4 associate in a molecular complex with the Myc promoter in dysplastic renal tissue and cooperate to control Myc transcription." Development **132**(1): 215-225.

Hussein, S. M., Duff, E. K. and Sirard, C. (2003). "Smad4 and beta-catenin co-activators functionally interact with lymphoid-enhancing factor to regulate graded expression of Msx2." The Journal of Biological Chemistry **278**(49): 48805-48814.

International Myeloma Working, G. (2003). "Criteria for the classification of monoclonal gammopathies, multiple myeloma and related disorders: a report of the International Myeloma Working Group." British Journal of Haematology **121**(5): 749-757.

Itasaki, N. and Hoppler, S. (2010). "Crosstalk between Wnt and bone morphogenic protein signaling: a turbulent relationship." Developmental Dynamics **239**(1): 16-33.

Itasaki, N., Jones, C. M., Mercurio, S., Rowe, A., Domingos, P. M., Smith, J. C. and Krumlauf, R. (2003). "Wise, a context-dependent activator and inhibitor of Wnt signalling." Development **130**(18): 4295-4305.

Jenson, H. B., Grant, G. M., Ench, Y., Heard, P., Thomas, C. A., Hilsenbeck, S. G. and Moyer, M. P. (1998). "Immunofluorescence microscopy and flow cytometry characterization of chemical induction of latent Epstein-Barr virus." Clinical and Diagnostic Laboratory Immunology **5**(1): 91-97.

Jorgensen, N. R., Henriksen, Z., Sorensen, O. H. and Civitelli, R. (2004). "Dexamethasone, BMP-2, and 1,25-dihydroxyvitamin D enhance a more differentiated osteoblast phenotype: validation of an in-vitro model for human bone marrow-derived primary osteoblasts." Steroids **69**(4): 219-226.

Kamiya, N. (2012). "The role of BMPs in bone anabolism and their potential targets SOST and DKK1." Current Molecular Pharmacology **5**(2): 153-163.

Kamiya, N., Ye, L., Kobayashi, T., Lucas, D. J., Mochida, Y., Yamauchi, M., Kronenberg, H. M., Feng, J. Q. and Mishina, Y. (2008). "Disruption of BMP signaling in osteoblasts through type IA receptor (BMPRIA) increases bone mass." Journal of Bone and Mineral Research **23**(12): 2007-2017.

Karsenty, G., Kronenberg, H. M. and Settembre, C. (2009). "Genetic control of bone formation." Annual Review of Cell and Developmental Biology **25**: 629-648.

Kato, M., Patel, M. S., Levasseur, R., Lobov, I., Chang, B. H., Glass, D. A., 2nd, Hartmann, C., Li, L., Hwang, T. H., Brayton, C. F., Lang, R. A., Karsenty, G. and Chan, L. (2002). "Cbfa1-independent decrease in osteoblast proliferation, osteopenia, and persistent embryonic eye vascularization in mice deficient in Lrp5, a Wnt coreceptor." Journal of Cell Biology **157**(2): 303-314.

Katsamba, P. S., Navratilova, I., Calderon-Cacia, M., Fan, L., Thornton, K., Zhu, M., Bos, T. V., Forte, C., Friend, D., Laird-Offringa, I., Tavares, G., Whatley, J., Shi, E., Widom, A., Lindquist, K. C., Klakamp, S., Drake, A., Bohmann, D., Roell, M., Rose, L., Dorocke, J., Roth, B., Luginbuhl, B. and Myszka, D. G. (2006). "Kinetic analysis of a high-affinity antibody/antigen interaction performed by multiple Biacore users." Analytical Biochemistry **352**(2): 208-221.

Kawazoe, Y., Katoh, S., Onodera, Y., Kohgo, T., Shindoh, M. and Shiba, T. (2008). "Activation of the FGF signaling pathway and subsequent induction of mesenchymal stem cell differentiation by inorganic polyphosphate." International Journal of Biological Sciences **4**(1): 37-47.

Ke, H. Z., Richards, W. G., Li, X. and Ominsky, M. S. (2012). "Sclerostin and Dickkopf-1 as therapeutic targets in bone diseases." Endocrine Reviews **33**(5): 747-783.

Kikuchi, A. (2003). "Tumor formation by genetic mutations in the components of the Wnt signaling pathway." Cancer Science **94**(3): 225-229.

Kim, J. B., Leucht, P., Lam, K., Luppen, C., Ten Berge, D., Nusse, R. and Helms, J. A. (2007). "Bone regeneration is regulated by wnt signaling." Journal of Bone and Mineral Research **22**(12): 1913-1923.

Kim, J. H., Liu, X., Wang, J., Chen, X., Zhang, H., Kim, S. H., Cui, J., Li, R., Zhang, W., Kong, Y., Zhang, J., Shui, W., Lamplot, J., Rogers, M. R., Zhao, C., Wang, N., Rajan, P., Tomal, J., Statz, J., Wu, N., Luu, H. H., Haydon, R. C. and He, T. C. (2013). "Wnt signaling in bone formation and its therapeutic potential for bone diseases." Therapeutic Advances in Musculoskeletal Disease **5**(1): 13-31.

Kim, J. S., Crooks, H., Dracheva, T., Nishanian, T. G., Singh, B., Jen, J. and Waldman, T. (2002). "Oncogenic beta-catenin is required for bone morphogenetic protein 4 expression in human cancer cells." Cancer Research **62**(10): 2744-2748.

Kiso, H., Takahashi, K., Saito, K., Togo, Y., Tsukamoto, H., Huang, B., Sugai, M., Shimizu, A., Tabata, Y., Economides, A. N., Slavkin, H. C. and Bessho, K. (2014). "Interactions between BMP-7 and USAG-1 (uterine sensitization-associated gene-1) regulate supernumerary organ formations." PLoS One **9**(5): e96938.

Kohli, S. S. and Kohli, V. S. (2011). "Role of RANKL-RANK/osteoprotegerin molecular complex in bone remodeling and its immunopathologic implications." The Indian Journal of Endocrinology and Metabolism **15**(3): 175-181.

Komori, T. (2006). "Regulation of osteoblast differentiation by transcription factors." Journal of Cellular Biochemistry **99**(5): 1233-1239.

Krause, C., Korchynskyi, O., de Rooij, K., Weidauer, S. E., de Gorter, D. J., van Bezooijen, R. L., Hatsell, S., Economides, A. N., Mueller, T. D., Lowik, C. W. and ten Dijke, P. (2010). "Distinct modes of inhibition by sclerostin on bone morphogenetic protein and Wnt signaling pathways." The Journal of Biological Chemistry **285**(53): 41614-41626.

Kubota, T., Michigami, T. and Ozono, K. (2009). "Wnt signaling in bone metabolism." Journal of Bone and Mineral Metabolism **27**(3): 265-271.

Kumar, D., Gittings, J. P., Turner, I. G., Bowen, C. R., Hidalgo-Bastida, L. A. and Cartmell, S. H. (2010). "Polarization of hydroxyapatite: influence on osteoblast cell proliferation." Acta Biomaterialia **6**(4): 1549-1554.

Kumegawa, M., Hiramatsu, M., Hatakeyama, K., Yajima, T., Kodama, H., Osaki, T. and Kurisu, K. (1983). "Effects of epidermal growth factor on osteoblastic cells in-vitro." Calcified Tissue International **35**(4-5): 542-548.

Kusu, N., Laurikkala, J., Imanishi, M., Usui, H., Konishi, M., Miyake, A., Thesleff, I. and Itoh, N. (2003). "Sclerostin is a novel secreted osteoclast-derived bone morphogenetic protein antagonist with unique ligand specificity." The Journal of Biological Chemistry **278**(26): 24113-24117.

Kyle, R. A. and Rajkumar, S. V. (2007). "Monoclonal gammopathy of undetermined significance and smouldering multiple myeloma: emphasis on risk factors for progression." British Journal of Haematology **139**(5): 730-743.

Kyle, R. A. and Rajkumar, S. V. (2008). "Multiple myeloma." Blood **111**(6): 2962-2972.
Laurikkala, J., Kassai, Y., Pakkasjarvi, L., Thesleff, I. and Itoh, N. (2003). "Identification of a secreted BMP antagonist, ectodin, integrating BMP, FGF, and SHH signals from the tooth enamel knot." Developmental Biology **264**(1): 91-105.

Lecka-Czernik, B., Gubrij, I., Moerman, E. J., Kajkenova, O., Lipschitz, D. A., Manolagas, S. C. and Jilka, R. L. (1999). "Inhibition of Osf2/Cbfa1 expression and terminal osteoblast differentiation by PPARgamma2." Journal of Cellular Biochemistry **74**(3): 357-371.

Lee, J. W., Chung, H. Y., Ehrlich, L. A., Jelinek, D. F., Callander, N. S., Roodman, G. D. and Choi, S. J. (2004). "IL-3 expression by myeloma cells increases both osteoclast formation and growth of myeloma cells." Blood **103**(6): 2308-2315.

Lintern, K. B., Guidato, S., Rowe, A., Saldanha, J. W. and Itasaki, N. (2009). "Characterization of wise protein and its molecular mechanism to interact with both Wnt and BMP signals." The Journal of Biological Chemistry **284**(34): 23159-23168.

Little, R. D., Recker, R. R. and Johnson, M. L. (2002). "High bone density due to a mutation in LDL-receptor-related protein 5." New England Journal of Medicine **347**(12): 943-944; author reply 943-944.

Liu, F., Chu, E. Y., Watt, B., Zhang, Y., Gallant, N. M., Andl, T., Yang, S. H., Lu, M. M., Piccolo, S., Schmidt-Ullrich, R., Taketo, M. M., Morrisey, E. E., Atit, R., Dlugosz, A. A. and Millar, S. E. (2008). "Wnt/beta-catenin signaling directs multiple stages of tooth morphogenesis." Developmental Biology **313**(1): 210-224.

Liu, Z., Tang, Y., Qiu, T., Cao, X. and Clemens, T. L. (2006). "A dishevelled-1/Smad1 interaction couples WNT and bone morphogenetic protein signaling pathways in uncommitted bone marrow stromal cells." The Journal of Biological Chemistry **281**(25): 17156-17163.

Livak, K. J. and Schmittgen, T. D. (2001). "Analysis of relative gene expression data using real-time quantitative PCR and the 2(-Delta Delta C(T)) Method." Methods **25**(4): 402-408.

Lonial, S. and Boise, L. H. (2013). "The future of drug development and therapy in myeloma." Seminars in Oncology **40**(5): 652-658.

Lyons, K. M., Hogan, B. L. and Robertson, E. J. (1995). "Colocalization of BMP 7 and BMP 2 RNAs suggests that these factors cooperatively mediate tissue interactions during murine development." Mechanisms of Development **50**(1): 71-83.

Mahindra, A., Hideshima, T. and Anderson, K. C. (2010). "Multiple myeloma: biology of the disease." Blood Reviews **24 Suppl 1**: S5-11.

Matsuo, N., Tanaka, S., Yoshioka, H., Koch, M., Gordon, M. K. and Ramirez, F. (2008). "Collagen XXIV (Col24a1) gene expression is a specific marker of osteoblast differentiation and bone formation." Connective Tissue Research **49**(2): 68-75.

Mbalaviele, G., Sheikh, S., Stains, J. P., Salazar, V. S., Cheng, S. L., Chen, D. and Civitelli, R. (2005). "Beta-catenin and BMP-2 synergize to promote osteoblast differentiation and new bone formation." Journal of Cellular Biochemistry **94**(2): 403-418.

Miller, J. R., Hocking, A. M., Brown, J. D. and Moon, R. T. (1999). "Mechanism and function of signal transduction by the Wnt/beta-catenin and Wnt/Ca2+ pathways." Oncogene **18**(55): 7860-7872.

Misra, K. and Matise, M. P. (2010). "A critical role for sFRP proteins in maintaining caudal neural tube closure in mice via inhibition of BMP signaling." Developmental Biology **337**(1): 74-83.

Miyazono, K., Kamiya, Y. and Morikawa, M. (2010). "Bone morphogenetic protein receptors and signal transduction." Journal of Biochemistry **147**(1): 35-51.

Mizuno, A., Amizuka, N., Irie, K., Murakami, A., Fujise, N., Kanno, T., Sato, Y., Nakagawa, N., Yasuda, H., Mochizuki, S., Gomibuchi, T., Yano, K., Shima, N., Washida, N., Tsuda, E., Morinaga, T., Higashio, K. and Ozawa, H. (1998). "Severe osteoporosis in mice lacking osteoclastogenesis inhibitory factor/osteoprotegerin." Biochemical and Biophysical Research Communications **247**(3): 610-615.

Morvan, F., Boulukos, K., Clement-Lacroix, P., Roman Roman, S., Suc-Royer, I., Vayssiere, B., Ammann, P., Martin, P., Pinho, S., Pognonec, P., Mollat, P., Niehrs, C., Baron, R. and Rawadi, G. (2006). "Deletion of a single allele of the Dkk1 gene leads to an increase in bone formation and bone mass." Journal of Bone and Mineral Research **21**(6): 934-945.

Munne, P. M., Felszeghy, S., Jussila, M., Suomalainen, M., Thesleff, I. and Jernvall, J. (2010). "Splitting placodes: effects of bone morphogenetic protein and Activin on the patterning and identity of mouse incisors." Evolution and Development **12**(4): 383-392.

Munne, P. M., Tummers, M., Jarvinen, E., Thesleff, I. and Jernvall, J. (2009). "Tinkering with the inductive mesenchyme: Sostdc1 uncovers the role of dental mesenchyme in limiting tooth induction." Development **136**(3): 393-402.

Muratori, M., Forti, G. and Baldi, E. (2008). "Comparing flow cytometry and fluorescence microscopy for analyzing human sperm DNA fragmentation by TUNEL labeling." Cytometry **73**(9): 785-787.

Nusse, R. (2008). "Wnt signaling and stem cell control." Cell Research **18**(5): 523-527.

Oelgeschlager, M., Larrain, J., Geissert, D. and De Robertis, E. M. (2000). "The evolutionarily conserved BMP-binding protein Twisted gastrulation promotes BMP signalling." Nature **405**(6788): 757-763.

Olson, B. J. and Markwell, J. (2007). "Assays for determination of protein concentration." Current Protocols in Protein Science **Chapter 3**: Unit 3 4.

Oshima, T., Abe, M., Asano, J., Hara, T., Kitazoe, K., Sekimoto, E., Tanaka, Y., Shibata, H., Hashimoto, T., Ozaki, S., Kido, S., Inoue, D. and Matsumoto, T. (2005). "Myeloma cells suppress bone formation by secreting a soluble Wnt inhibitor, sFRP-2." Blood **106**(9): 3160-3165.

Otto, W. R. (2005). "Fluorimetric DNA assay of cell number." <u>Methods in Molecular Biology</u> **289**: 251-262.

Oyajobi, B. O., Munoz, S., Kakonen, R., Williams, P. J., Gupta, A., Wideman, C. L., Story, B., Grubbs, B., Armstrong, A., Dougall, W. C., Garrett, I. R. and Mundy, G. R. (2007). "Detection of myeloma in skeleton of mice by whole-body optical fluorescence imaging." <u>Molecular Cancer Therapeutics</u> **6**(6): 1701-1708.

Papathanasiou, I., Malizos, K. N. and Tsezou, A. (2012). "Bone morphogenetic protein-2-induced Wnt/beta-catenin signaling pathway activation through enhanced low-density-lipoprotein receptor-related protein 5 catabolic activity contributes to hypertrophy in osteoarthritic chondrocytes." <u>Arthritis Research & Therapy</u> **14**(2): R82.

Pautke, C., Schieker, M., Tischer, T., Kolk, A., Neth, P., Mutschler, W. and Milz, S. (2004). "Characterization of osteosarcoma cell lines MG-63, Saos-2 and U-2 OS in comparison to human osteoblasts." <u>Anticancer Research</u> **24**(6): 3743-3748.

Pearce, J. J., Penny, G. and Rossant, J. (1999). "A mouse cerberus/Dan-related gene family." <u>Developmental Biology</u> **209**(1): 98-110.

Pearse, R. N. (2006). "Wnt antagonism in multiple myeloma: a potential cause of uncoupled bone remodeling." <u>Clinical Cancer Research</u> **12**(20 Pt 2): 6274s-6278s.

Pearse, R. N., Sordillo, E. M., Yaccoby, S., Wong, B. R., Liau, D. F., Colman, N., Michaeli, J., Epstein, J. and Choi, Y. (2001). "Multiple myeloma disrupts the TRANCE/ osteoprotegerin cytokine axis to trigger bone destruction and promote tumor progression." <u>Proceedings of the National Academy of Sciences of the United States of America</u> **98**(20): 11581-11586.

Pederson, L., Ruan, M., Westendorf, J. J., Khosla, S. and Oursler, M. J. (2008). "Regulation of bone formation by osteoclasts involves Wnt/BMP signaling and the chemokine sphingosine-1-phosphate." <u>Proceedings of the National Academy of Sciences of the United States of America</u> **105**(52): 20764-20769.

Philip, S., Bulbule, A. and Kundu, G. C. (2001). "Osteopontin stimulates tumor growth and activation of promatrix metalloproteinase-2 through nuclear factor-kappa B-mediated induction of membrane type 1 matrix metalloproteinase in murine melanoma cells." <u>The Journal of Biological Chemistry</u> **276**(48): 44926-44935.

Piccolo, S., Agius, E., Leyns, L., Bhattacharyya, S., Grunz, H., Bouwmeester, T. and De Robertis, E. M. (1999). "The head inducer Cerberus is a multifunctional antagonist of Nodal, BMP and Wnt signals." <u>Nature</u> **397**(6721): 707-710.

Pinzone, J. J., Hall, B. M., Thudi, N. K., Vonau, M., Qiang, Y. W., Rosol, T. J. and Shaughnessy, J. D., Jr. (2009). "The role of Dickkopf-1 in bone development, homeostasis, and disease." <u>Blood</u> **113**(3): 517-525.

Pradel, W., Mai, R., Gedrange, T. and Lauer, G. (2008). "Cell passage and composition of culture medium effects proliferation and differentiation of human osteoblast-like cells from facial bone." <u>Journal of Physiology and Pharmacology</u> **59 Suppl 5**: 47-58.

Prince, M., Banerjee, C., Javed, A., Green, J., Lian, J. B., Stein, G. S., Bodine, P. V. and Komm, B. S. (2001). "Expression and regulation of Runx2/Cbfa1 and osteoblast phenotypic markers during the growth and differentiation of human osteoblasts." Journal of Cellular Biochemistry **80**(3): 424-440.

Radl, J., Croese, J. W., Zurcher, C., Van den Enden-Vieveen, M. H. and de Leeuw, A. M. (1988). "Animal model of human disease. Multiple myeloma." The American Journal of Pathology **132**(3): 593-597.

Raggatt, L. J. and Partridge, N. C. (2010). "Cellular and molecular mechanisms of bone remodeling." The Journal of Biological Chemistry **285**(33): 25103-25108.

Rao, J. and Otto, W. R. (1992). "Fluorimetric DNA assay for cell growth estimation." Analytical Biochemistry **207**(1): 186-192.

Rawadi, G., Vayssiere, B., Dunn, F., Baron, R. and Roman-Roman, S. (2003). "BMP-2 controls alkaline phosphatase expression and osteoblast mineralization by a Wnt autocrine loop." Journal of Bone and Mineral Research **18**(10): 1842-1853.

Rijsewijk, F., Schuermann, M., Wagenaar, E., Parren, P., Weigel, D. and Nusse, R. (1987). "The Drosophila homolog of the mouse mammary oncogene int-1 is identical to the segment polarity gene wingless." Cell **50**(4): 649-657.

Robinson, J. A., Chatterjee-Kishore, M., Yaworsky, P. J., Cullen, D. M., Zhao, W., Li, C., Kharode, Y., Sauter, L., Babij, P., Brown, E. L., Hill, A. A., Akhter, M. P., Johnson, M. L., Recker, R. R., Komm, B. S. and Bex, F. J. (2006). "Wnt/beta-catenin signaling is a normal physiological response to mechanical loading in bone." The Journal of Biological Chemistry **281**(42): 31720-31728.

Robling, A. G., Castillo, A. B. and Turner, C. H. (2006). "Biomechanical and molecular regulation of bone remodeling." Annual Review of Biomedical Engineering **8**: 455-498.

Rodan, G. A. and Martin, T. J. (2000). "Therapeutic approaches to bone diseases." Science **289**(5484): 1508-1514.

Rodan, S. B., Imai, Y., Thiede, M. A., Wesolowski, G., Thompson, D., Bar-Shavit, Z., Shull, S., Mann, K. and Rodan, G. A. (1987). "Characterization of a human osteosarcoma cell line (Saos-2) with osteoblastic properties." Cancer Research **47**(18): 4961-4966.

Rodda, S. J. and McMahon, A. P. (2006). "Distinct roles for Hedgehog and canonical Wnt signaling in specification, differentiation and maintenance of osteoblast progenitors." Development **133**(16): 3231-3244.

Roodman, G. D. (2004). "Mechanisms of bone metastasis." New England Journal of Medicine **350**(16): 1655-1664.

Roodman, G. D. (2009). "Pathogenesis of myeloma bone disease." Leukemia **23**(3): 435-441.

Roodman, G. D. (2011). "Osteoblast function in myeloma." Bone **48**(1): 135-140.

Roux, S. and Mariette, X. (2004). "The high rate of bone resorption in multiple myeloma is due to RANK (receptor activator of nuclear factor-kappaB) and RANK Ligand expression." Leukemia & Lymphoma **45**(6): 1111-1118.

Roux, S. and Orcel, P. (2000). "Bone loss. Factors that regulate osteoclast differentiation: an update." Arthritis Research **2**(6): 451-456.

Russell, G., Mueller, G., Shipman, C. and Croucher, P. (2001). "Clinical disorders of bone resorption." Novartis Foundation Symposium **232**: 251-267; discussion 267-271.

Saad, F., Lipton, A., Cook, R., Chen, Y. M., Smith, M. and Coleman, R. (2007). "Pathologic fractures correlate with reduced survival in patients with malignant bone disease." Cancer **110**(8): 1860-1867.

Saldana, L., Bensiamar, F., Bore, A. and Vilaboa, N. (2011). "In search of representative models of human bone-forming cells for cytocompatibility studies." Acta Biomaterialia **7**(12): 4210-4221.

Sasse, M., Lengwinat, T., Henklein, P., Hlinak, A. and Schade, R. (2000). "Replacement of fetal calf serum in cell cultures by an egg yolk factor with cholecystokinin/gastrin-like immunoreactivity." Alternatives to Lab Animals **28**(6): 815-831.

Seidel, C., Lenhoff, S., Brabrand, S., Anderson, G., Standal, T., Lanng-Nielsen, J., Turesson, I., Borset, M. and Waage, A. (2002). "Hepatocyte growth factor in myeloma patients treated with high-dose chemotherapy." British Journal of Haematology **119**(3): 672-676.

Seki, K. and Hata, A. (2004). "Indian hedgehog gene is a target of the bone morphogenetic protein signaling pathway." The Journal of Biological Chemistry **279**(18): 18544-18549.

Sezer, O. (2009). "Myeloma bone disease: recent advances in biology, diagnosis, and treatment." Oncologist **14**(3): 276-283.

Sharma, R. P. and Chopra, V. L. (1976). "Effect of the Wingless (wg1) mutation on wing and haltere development in Drosophila melanogaster." Developmental Biology **48**(2): 461-465.

Siegel, R., Ma, J., Zou, Z. and Jemal, A. (2014). "Cancer statistics, 2014." CA: A Cancer Journal for Clinicians **64**(1): 9-29.

Sila-Asna, M., Bunyaratvej, A., Maeda, S., Kitaguchi, H. and Bunyaratavej, N. (2007). "Osteoblast differentiation and bone formation gene expression in strontium-inducing bone marrow mesenchymal stem cell." The Kobe Journal of Medical Sciences **53**(1-2): 25-35.

Silva, A. C., Filipe, M., Kuerner, K. M., Steinbeisser, H. and Belo, J. A. (2003). "Endogenous Cerberus activity is required for anterior head specification in Xenopus." Development **130**(20): 4943-4953.

Simmons, D. G. and Kennedy, T. G. (2002). "Uterine sensitization-associated gene-1: a novel gene induced within the rat endometrium at the time of uterine receptivity/sensitization for the decidual cell reaction." Biology of Reproduction **67**(5): 1638-1645.

Simonet, W. S., Lacey, D. L., Dunstan, C. R., Kelley, M., Chang, M. S., Luthy, R., Nguyen, H. Q., Wooden, S., Bennett, L., Boone, T., Shimamoto, G., DeRose, M., Elliott, R., Colombero, A., Tan, H. L., Trail, G., Sullivan, J., Davy, E., Bucay, N., Renshaw-Gegg, L., Hughes, T. M., Hill, D., Pattison, W., Campbell, P., Sander, S., Van, G., Tarpley, J., Derby, P., Lee, R. and Boyle, W. J. (1997). "Osteoprotegerin: a novel secreted protein involved in the regulation of bone density." Cell **89**(2): 309-319.

Sperisen, P., Wang, S. M., Reichenbach, P. and Nabholz, M. (1992). "A PCR-based assay for reporter gene expression." PCR Methods and Applications **1**(3): 164-170.

Standal, T., Abildgaard, N., Fagerli, U. M., Stordal, B., Hjertner, O., Borset, M. and Sundan, A. (2007). "HGF inhibits BMP-induced osteoblastogenesis: possible implications for the bone disease of multiple myeloma." Blood **109**(7): 3024-3030.

Strewler, G. J. (2001). "Local and systemic control of the osteoblast." Journal of Clinical Investigation **107**(3): 271-272.

Suda, T., Takahashi, N., Udagawa, N., Jimi, E., Gillespie, M. T. and Martin, T. J. (1999). "Modulation of osteoclast differentiation and function by the new members of the tumor necrosis factor receptor and ligand families." Endocrine Reviews **20**(3): 345-357.

Takamizawa, S., Maehata, Y., Imai, K., Senoo, H., Sato, S. and Hata, R. (2004). "Effects of ascorbic acid and ascorbic acid 2-phosphate, a long-acting vitamin C derivative, on the proliferation and differentiation of human osteoblast-like cells." Cell Biology International **28**(4): 255-265.

Talamo, G., Farooq, U., Zangari, M., Liao, J., Dolloff, N. G., Loughran, T. P., Jr. and Epner, E. (2010). "Beyond the CRAB symptoms: a study of presenting clinical manifestations of multiple myeloma." Clinical Lymphoma & Myeloma **10**(6): 464-468.

Tanaka, S., Takahashi, N., Udagawa, N., Tamura, T., Akatsu, T., Stanley, E. R., Kurokawa, T. and Suda, T. (1993). "Macrophage colony-stimulating factor is indispensable for both proliferation and differentiation of osteoclast progenitors." Journal of Clinical Investigation **91**(1): 257-263.

Dijke, P., Krause, C., de Gorter, D. J., Lowik, C. W. and van Bezooijen, R. L. (2008). "Osteocyte-derived sclerostin inhibits bone formation: its role in bone morphogenetic protein and Wnt signaling." Journal of Bone and Joint Surgery **90 Suppl 1**: 31-35.

Terpos, E., Berenson, J., Cook, R. J., Lipton, A. and Coleman, R. E. (2010). "Prognostic variables for survival and skeletal complications in patients with multiple myeloma osteolytic bone disease." Leukemia **24**(5): 1043-1049.

Terpos, E. and Dimopoulos, M. A. (2005). "Myeloma bone disease: pathophysiology and management." Journal of Bone Oncology **16**(8): 1223-1231.

Terpos, E., Roodman, G. D. and Dimopoulos, M. A. (2013). "Optimal use of bisphosphonates in patients with multiple myeloma." Blood **121**(17): 3325-3328.

Tian, E., Zhan, F., Walker, R., Rasmussen, E., Ma, Y., Barlogie, B. and Shaughnessy, J. D., Jr. (2003). "The role of the Wnt-signaling antagonist DKK1 in the development of osteolytic lesions in multiple myeloma." New England Journal of Medicine **349**(26): 2483-2494.

Tylzanowski, P., Mebis, L. and Luyten, F. P. (2006). "The Noggin null mouse phenotype is strain dependent and haploinsufficiency leads to skeletal defects." Developmental Dynamics **235**(6): 1599-1607.

Vaananen, H. K., Zhao, H., Mulari, M. and Halleen, J. M. (2000). "The cell biology of osteoclast function." Journal of Cell Science **113**(Pt 3): 377-381.

Van den Wyngaert, T., Huizing, M. T. and Vermorken, J. B. (2007). "Osteonecrosis of the jaw related to the use of bisphosphonates." Current Opinion in Oncology **19**(4): 315-322.

Vanderkerken, K., De Leenheer, E., Shipman, C., Asosingh, K., Willems, A., Van Camp, B. and Croucher, P. (2003). "Recombinant osteoprotegerin decreases tumor burden and increases survival in a murine model of multiple myeloma." Cancer Research **63**(2): 287-289.

Vanderkerken, K., De Raeve, H., Goes, E., Van Meirvenne, S., Radl, J., Van Riet, I., Thielemans, K. and Van Camp, B. (1997). "Organ involvement and phenotypic adhesion profile of 5T2 and 5T33 myeloma cells in the C57BL/KaLwRij mouse." British Journal of Cancer **76**(4): 451-460.

Varga, A. C. and Wrana, J. L. (2005). "The disparate role of BMP in stem cell biology." Oncogene **24**(37): 5713-5721.

Vinholes, J., Coleman, R. and Eastell, R. (1996). "Effects of bone metastases on bone metabolism: implications for diagnosis, imaging and assessment of response to cancer treatment." Cancer Treatment Reviews **22**(4): 289-331.

Wallner, J., Lhota, G., Jeschek, D., Mader, A. and Vorauer-Uhl, K. (2013). "Application of Bio-Layer Interferometry for the analysis of protein/liposome interactions." Journal of Pharmaceutical and Biomedical Analysis **72**: 150-154.

Walsh, D. W., Godson, C., Brazil, D. P. and Martin, F. (2010). "Extracellular BMP-antagonist regulation in development and disease: tied up in knots." Trends in Cell Biology **20**(5): 244-256.

Wang, D., Christensen, K., Chawla, K., Xiao, G., Krebsbach, P. H. and Franceschi, R. T. (1999). "Isolation and characterization of MC3T3-E1 preosteoblast subclones with distinct in-vitro and in-vivo differentiation/mineralization potential." Journal of Bone and Mineral Research **14**(6): 893-903.

Westendorf, J. J., Kahler, R. A. and Schroeder, T. M. (2004). "Wnt signaling in osteoblasts and bone diseases." Gene **341**: 19-39.

Wood, D. K., Requa, M. V. and Cleland, A. N. (2007). "Microfabricated high-throughput electronic particle detector." Review of Scientific Instruments **78**(10): 104301.

Wozney, J. M., Rosen, V., Celeste, A. J., Mitsock, L. M., Whitters, M. J., Kriz, R. W., Hewick, R. M. and Wang, E. A. (1988). "Novel regulators of bone formation: molecular clones and activities." Science **242**(4885): 1528-1534.

Xiong, J., Onal, M., Jilka, R. L., Weinstein, R. S., Manolagas, S. C. and O'Brien, C. A. (2011). "Matrix-embedded cells control osteoclast formation." Nature Medicine **17**(10): 1235-1241.

Yaccoby, S. (2010). "Osteoblastogenesis and tumor growth in myeloma." Leukemia & Lymphoma **51**(2): 213-220.

Yamaguchi, A., Komori, T. and Suda, T. (2000). "Regulation of osteoblast differentiation mediated by bone morphogenetic proteins, hedgehogs, and Cbfa1." Endocrinology Research **21**(4): 393-411.

Yanagita, M., Oka, M., Watabe, T., Iguchi, H., Niida, A., Takahashi, S., Akiyama, T., Miyazono, K., Yanagisawa, M. and Sakurai, T. (2004). "USAG-1: a bone morphogenetic protein antagonist abundantly expressed in the kidney." Biochemical and Biophysical Research Communications **316**(2): 490-500.

Yavropoulou, M. P. and Yovos, J. G. (2007). "The role of the Wnt signaling pathway in osteoblast commitment and differentiation." Hormones **6**(4): 279-294.

Yazid, M. D., Ariffin, S. H., Senafi, S., Razak, M. A. and Wahab, R. M. (2010). "Determination of the differentiation capacities of murines' primary mononucleated cells and MC3T3-E1 cells." Cancer Cell International **10**: 42.

Yeung, C. Y., Gossan, N., Lu, Y., Hughes, A., Hensman, J. J., Bayer, M. L., Kjaer, M., Kadler, K. E. and Meng, Q. J. (2014). "Gremlin-2 is a BMP antagonist that is regulated by the circadian clock." Scientific Reports **4**: 5183.

Zhang, C., Cho, K., Huang, Y., Lyons, J. P., Zhou, X., Sinha, K., McCrea, P. D. and de Crombrugghe, B. (2008). "Inhibition of Wnt signaling by the osteoblast-specific transcription factor Osterix." Proceedings of the National Academy of Sciences of the United States of America **105**(19): 6936-6941.

Zhang, M., Yan, Y., Lim, Y. B., Tang, D., Xie, R., Chen, A., Tai, P., Harris, S. E., Xing, L., Qin, Y. X. and Chen, D. (2009). "BMP-2 modulates beta-catenin signaling through

stimulation of Lrp5 expression and inhibition of beta-TrCP expression in osteoblasts." Journal of Cellular Biochemistry **108**(4): 896-905.

Zhang, R., Oyajobi, B. O., Harris, S. E., Chen, D., Tsao, C., Deng, H. W. and Zhao, M. (2013). "Wnt/beta-catenin signaling activates bone morphogenetic protein 2 expression in osteoblasts." Bone **52**(1): 145-156.

Zhang, X., Chang, C., Zhao, Y., Wu, L., Zhang, Z. and Li, X. (2012). "The effect of the combination of bisphosphonates and conventional chemotherapy on bone metabolic markers in multiple myeloma patients." Hematology **17**(5): 255-260.

Zhong, Z., Zylstra-Diegel, C. R., Schumacher, C. A., Baker, J. J., Carpenter, A. C., Rao, S., Yao, W., Guan, M., Helms, J. A., Lane, N. E., Lang, R. A. and Williams, B. O. (2012). "Wntless functions in mature osteoblasts to regulate bone mass." Proceedings of the National Academy of Sciences of the United States of America **109**(33): E2197-2204.

Zhou, S. (2011). "TGF-beta regulates beta-catenin signaling and osteoblast differentiation in human mesenchymal stem cells." Journal of Cellular Biochemistry **112**(6): 1651-1660.

Appendix

Appendix 1 - GST had no effect on Wnt or BMP-induced ALP activity and rhSOSTDC1 suppressed BMP2-induced ALP activity in differentiating OB

A

B

C
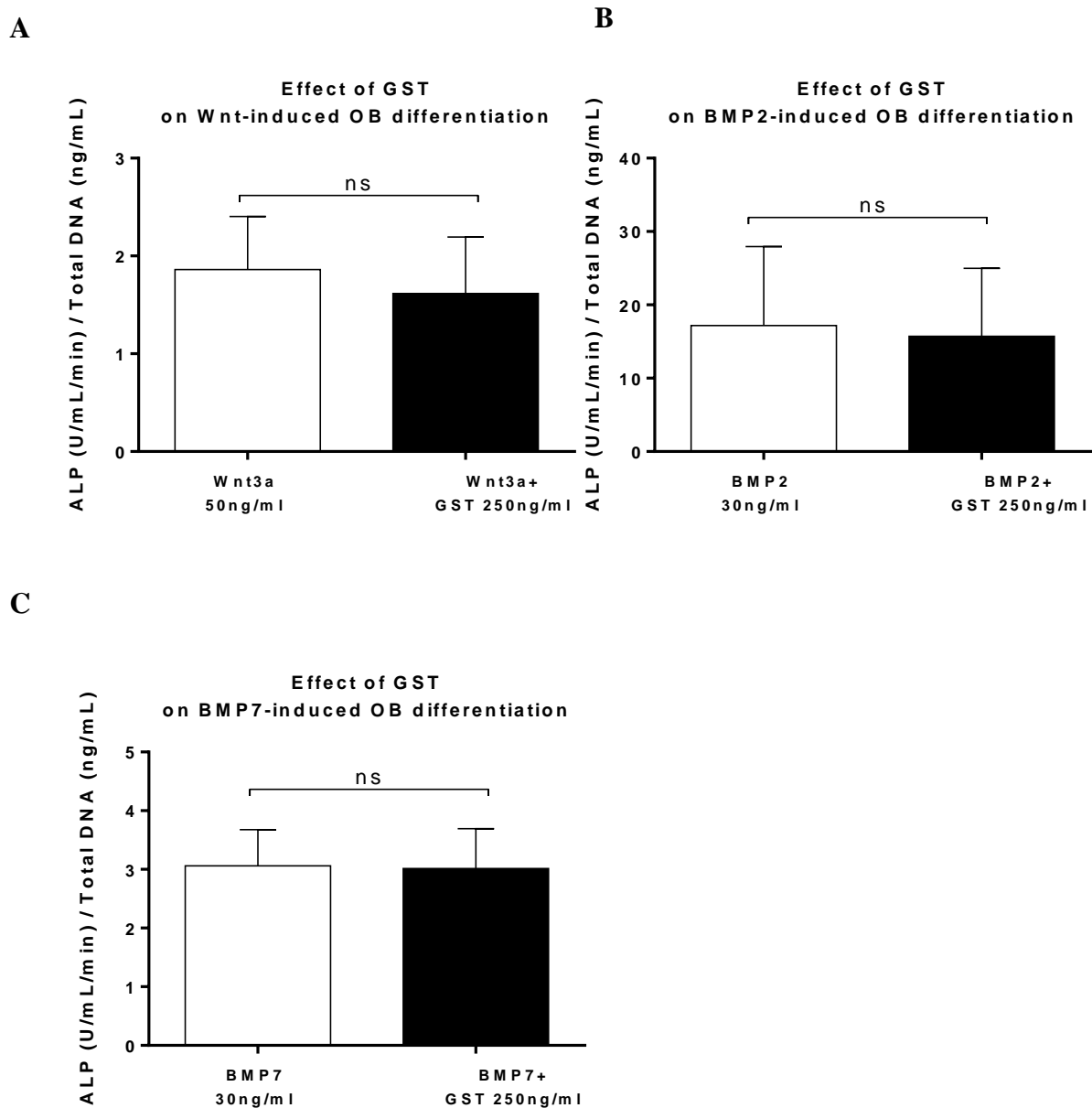
GST had no effect on Wnt or BMP-induced ALP activity in OB: *To determine whether the GST protein tag attached to the SOSTDC1 protein had any effect on OB differentiation, OB cells were treated with Wnt3a, BMP2 or BMP7 in the absence or presence of 250ng/ml GST. ALP activity of OB were determined and normalised to total DNA contents. (A, B amd C) The 250ng/ml GST, at the same concentration as SOSTDC1 used in experiments, had no effect on ALP activity of OB when in the presence of Wnt3a, BMP2 or BMP7. Unpaired t-test. Data are displayed with mean ± SEM. P=ns.*

A

B

C
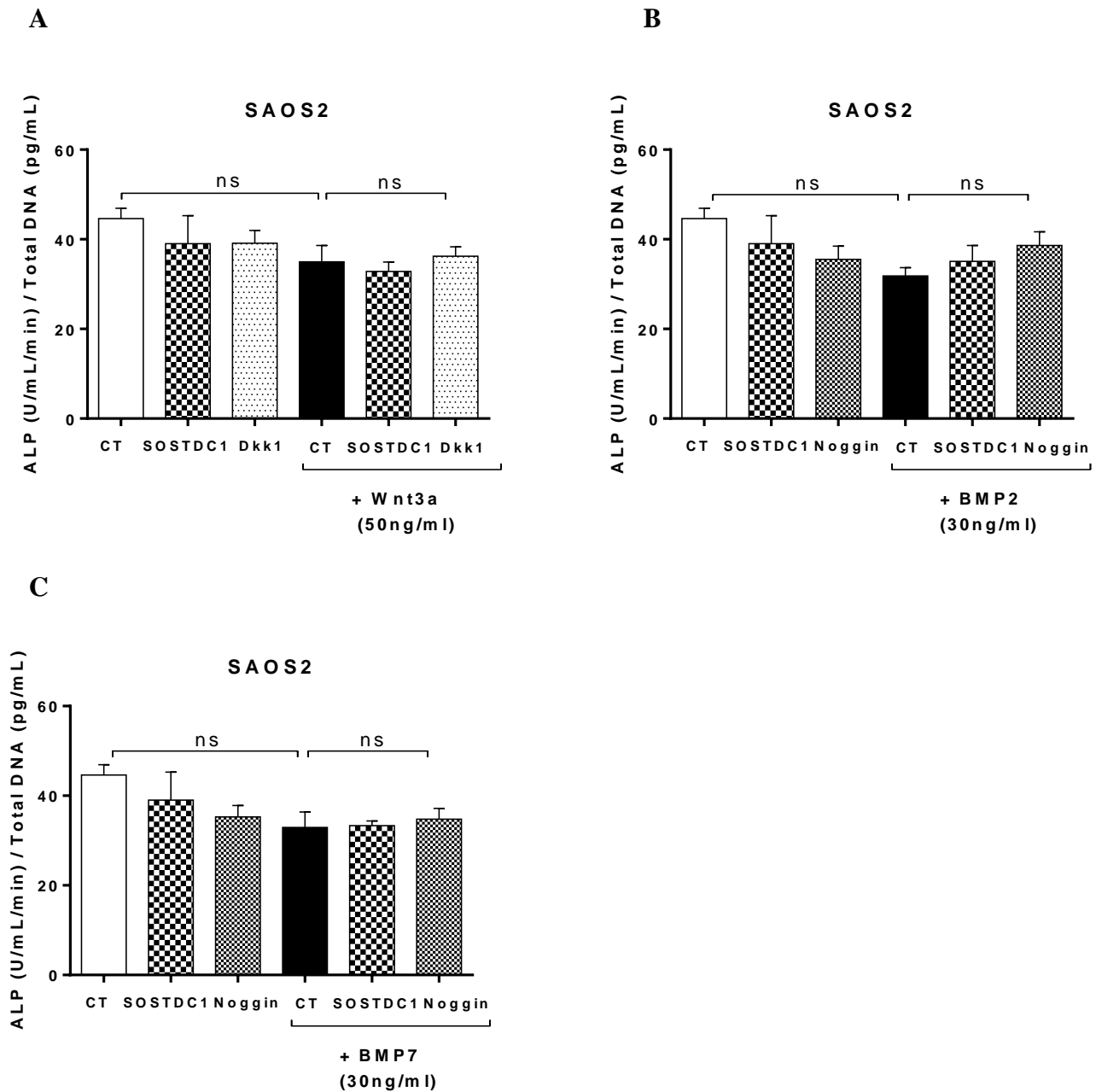
Figure 4.4.3.1 - SOSTDC1 had no effect on Wnt-induced or BMP-induced ALP activity in SAOS2 cells: *Differentiating SAOS2 cells were treated with vehicle or 250 ng/ml rhSOSTDC1 and also separately with 50ng/ml rmWnt3a, 30ng/ml rhBMP2 or 30ng/ml rhBMP7 in the presence or absence of rhSOSTDC1. (A) Wnt3a and SOSTDC1 had no effect on SAOS2 ALP activity. (B, C) BMP 2, BMP7 and SOSTDC1 had no effect on SAOS2 ALP activity. N=3 independent experiments, One way ANOVA and Holme-Sidak's post-test. Data are displayed with mean ± SEM.*

Appendix 3 - Recombinant GST protein did not bind to recombinant LRP, BMP2 and BMP7 proteins with high affinity
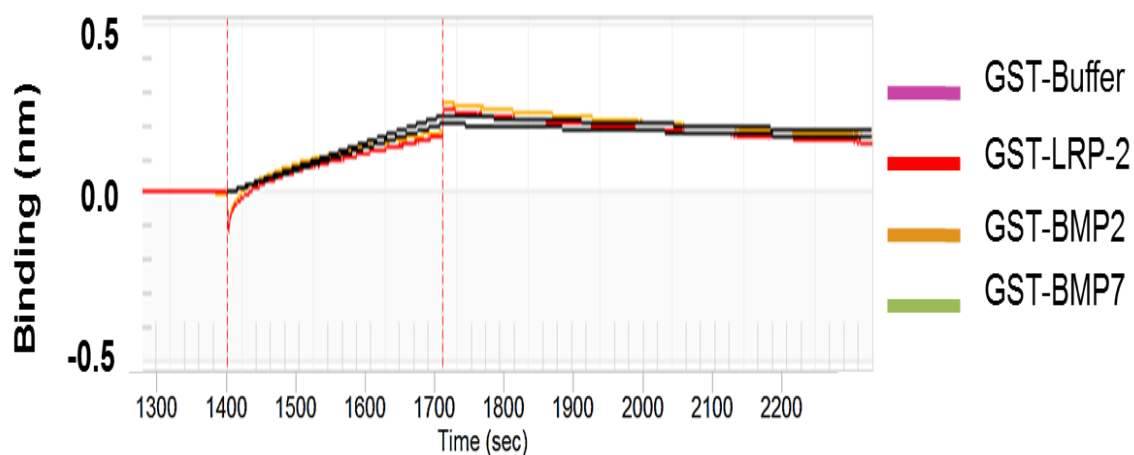
100µg/ml GST interaction with LRP-6, BMP2 and BMP7		
Sample	Concentration (µg/ml)	kD (M)
Buffer	n/a	-
LRP-6	100	-
BMP2	100	1.096e-4
BMP7	100	-

Recombinant GST protein did not bind to recombinant LRP, BMP2 and BMP7 proteins: *The affinity kD (M) of rhGST for purified carrier-free rmLRP-6, rhBMP2 and rhBMP7 proteins were determined using the Blitz Analysis system as control for the GST-tagged SOSTDC1 binding assays. Binding (nm) association showed 100ug/ml of rhGST did not bind at detectable levels to rmLRP-6 or rhBMP7 proteins. The high kD value calculated for rhGST and rhBMP2 interaction suggest any interaction would be of low affinity and not biologically relevant.*

Appendix 4 - SOSTDC1 was not upregulated in myeloma-endothelial cell co-culture
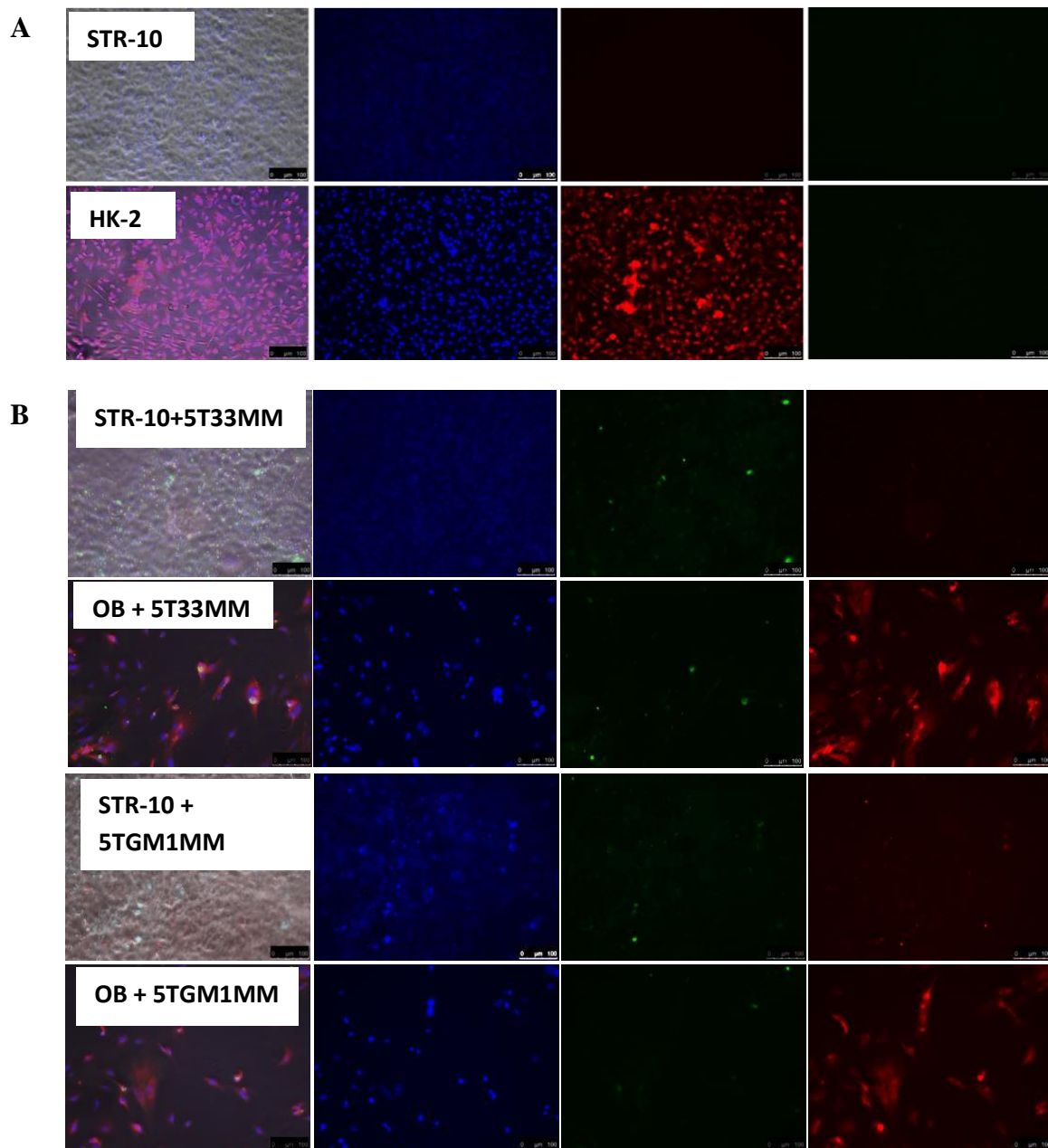
Upregulation of SOSTDC1 levels was specific to myeloma-OB progenitor co-culture and not myeloma-endothelial co-culture: *Immunofluorescent microscopy was performed to detect production of SOSTDC1 in 5T33MM/5TGM1MM-STR10 and 5T33MM/5TGM1MM-OB progenitor co-cultures. Permeabilised myeloma cells were co-cultured with endothelial cells or OB progenitors for 24 hours and stained with 1μg/ml primary anti-SOSTDC1 antibody or isotype control antibody. Co-cultures were also co-stained with anti-CD138 antibody and mounted with DAPI reagent. Images of phase contrast, DAPI, CD138 and SOSTDC1 staining were visualised simultaneously. Images are representative of at two replicates within 2 independent experiments. (A) STR10 cells did not produce detectable levels of SOSTDC1 compared to HK-2 control.(B)SOSTDC1 was upregulated in myeloma-OB progenitor co-cultures compared to myeloma-STR10 co-cultures. SOSTDC1 that was present in myeloma-STR10 co-cultures appeared to be specific to myeloma cells and not STR10 cells.*

Appendix 5 - OB progenitors did not have a SOSTDC1-specific nucleotide sequence compared to HK-2 positive control determined by sequencing

A

B

Score	Expect	Identities	Gaps	Strand
124 bits(67)	6e-26	71/74(96%)	0/74(0%)	Plus/Minus

```
Query    1    TGTCATTGACACACCGCCACTCCTGGNANCTCCTCCTGCTCCAGTACTTTGTTCCATAGC    60
              ||||||||||||||||||||||||||| | |||||||||||||||||||||||||||||||
Sbjct  600    TGTCATTGACACACCGCCACTCCTGGGAGCTCCTCCTGCTCCAGTACTTTGTTCCATAGC  541

Query   61    CTCCTCCGATCCAG    74
              |||||||| ||||||
Sbjct  540    CTCCTCCAATCCAG  527
```

SOSTDC1 cDNA sequencing of OB progenitor cells cultured alone compared to HK-2 positive control: *End-point RT-PCR products obtained from OB progenitor cells and HK-2 cells cultures were sequenced for SOSTDC1 using SOSTDC1-specific primers. (A) The OB progenitor did not have detectable SOSTDC1-specific nucleotide sequences identified by BLAST software. (B) The HK-2 cells had 97% homology with the SOSTDC1-specific sequence identified in BLAST (NCBI Reference Sequence: NM_025312.3).*

List of Abbreviations

1,25(OH)$_2$D$_3$	1,25-Dihydroxyvitamin D3
ALP	Alkaline phosphatise
APC	adenomatous polyposis coli protein
BCA	Bicinchoninic
Bcl-2	B-cell lymphoma-2
BLC	bone lining cell
BM	bone marrow
BMP	bone morphogenetic protein
BMSC	Bone Marrow Stromal Cells
BSA	Bovine serum albumin
BSP	bone sialoprotein
c-fms	colony stimulating factor
C-Smad	common mediator Smad
CBFA1	core-binding factor-1
CD138	Syndecan 1
CK1γ	serine/threonine kinase
CuSO^4	Copper II sulphate
Dkk1	Dickkopf-1
DMSO	Dimethyl Sulfoxide
dsDNA	PicoGreen® double-stranded DNA
Dsh	Dishevelled
EDTA	trypsin-ethylene-diaminetetraacetic acid
FCS	Fetal Calf Serum
FGF	fibroblast growth factors
Fz	frizzled
GAPDH	glyceraldehyde 3-phosphate dehydrogenase
GSK-3β	glycogen synthase kinase-3β
GST	Glutathione-S-transferase
HGFs	hepatocyte growth factors

HK-2	Proximal tubule epithelial cell line
HRP	Horse Radish peroxidase
HMCL	Human myeloma cell lines
I-Smads	inhibitory Smads
IFN-γ	interferon-gamma
IGF-I	insulin-like growth factor –I
IGFs	insulin-like growth factors
Ihh	Indian hedgehog
IL-11	interleukin-11
IL-1β	interleukin-1β
IL-4	interleukin-4
JNK	c-Jun N-terminal kinase
KSFM	Keratinocyte serum free medium
LEF/TCF	lymphoid enhancer-binding factor 1/T cell–specific transcription factor
LIF	leukaemia inhibiting factor
lLRP5/6	lipoprotein receptor–related protein 5/6
m-1α	macrophage inflammatory protein-1α
M-CSF	Macrophage colony-stimulating factor
MAPK	mitogen-activated protein kinase
MEM	Minimum Essential Medium
MGUS	Monoclonal Gammopathy of Undetermined Significance
MIP-β	macrophage inflammatory protein-1β
MMTV	mouse mammary tumour virus
MSC	mesenchymal stem cells
OAF	OC activating function
OB	osteoblasts
OC	osteoclasts
OPG	osteoprotegerin
PAGE	polyacrylamide gel electrophoresis
PBS	Phosphate Buffered Saline
PDGF	Platelet-derived growth factor

PenStrep	Penicillin: Streptomycin
PgE2	TNF-α or prostaglandin E2
PI3K	phosphatidylinositol-3 kinase
PIC	protease inhibitor cocktail
PMSF	Phenylmethylsulfonyl Fluoride
pNPP	p-Nitrophenyl phosphate
PVDF	Polyvinylidene fluoride
R-Smads	Regulatory Smads
RANK	Receptor Activator of Nuclear Factor κ B
RANKL	receptor activator of nuclear factor-κB ligand
RUNX2	Runt-related transcription factor 2
SDF-α	stromal derived factor-1α
SDS	sodium dodecyl sulfate
sFRPs	secreted Frizzled-related proteins
SMM	Smouldering Multiple Myeloma
SOSTDC1	Sclerostin Domain Containing 1
Src	tyrosine kinase
TGF-β	Transforming growth factor β
TNF	Tumour Necrosis Factor
TRAFs	TNFR-associated factors
TRAIL	Tumour necrosis factor-related apoptosis inducing ligand
USAG-1	uterine sensitisation-associated gene-1
VCAM-1	vascular cell adhesion molecule-1
VEGF	vascular endothelial growth factor
Wg	Wingless
Wnt	Wingless-type